

**THE APPLICATION OF NEW METHODS TO THE SYNTHESIS OF CONSTRAINED  
PROLINE DERIVATIVES, (+)-SERRATEZOMINE A, AND HAPALINDOLES A, G, I,  
AND K**

**(CHAPTER I. RESULTS AND DISCUSSION)**

By

**Aroop Chandra**

Dissertation

Submitted to the Faculty of the  
Graduate School of Vanderbilt University  
in partial fulfillment of the requirements

for the degree of

DOCTOR OF PHILOSOPHY

in

Chemistry

May, 2011

Nashville, TN

Approved

Professor Jeffrey N. Johnston

Professor Gary A. Sulikowski

Professor Ned A. Porter

Professor Lawrence J. Marnett

To My Parents,  
Dawn, and  
My Brother

## ACKNOWLEDGEMENTS

It is my greatest pleasure to thank all the people who have helped and supported me as I worked towards the completion of this thesis. As I write this acknowledgement, I cherish the unforgettable moments and memories of my graduate school life.

I would first like to thank my advisor, Dr. Jeffrey N. Johnston. I still vividly remember my initial days of graduate school life in the United States as an international student. While getting adjusted to the graduate school at Indiana University Bloomington (where I began my graduate studies), I also had the difficult task of choosing a graduate mentor in my first semester, as the rotation policy for first year graduate students was nonexistent at IUB. After meeting with Jeff, I was so impressed by his enthusiasm and passion for the subject that I joined his group even being aware of the possibility of a move to Vanderbilt University. It was probably one of the best decisions I have made in my life. He has expertly guided my growth in this field of research and beyond, and set targets for me to accomplish, which galvanized me to improve my thought process and work attitude. He has been a source of inspiration throughout my graduate life. I would never have accomplished so much without his motivation and encouragement, and I deeply acknowledge him for my development as a research scientist.

The completion of this journey would not have been possible without the help of the friends and great scientists from whom I received incredible advice, help, company and friendship at different stages of my graduate school. To past members, Dr. Jeremy Wilt, Dr. Julie Pigza, Dr. Anand Singh, thank you for being such great role models, mentors and friends. To current lab members, Tyler Davis, Hubert Muchalski, Priya

Matthew, Mark Dobish, Amanda Doody, and Jessica Shackleford, thank you for everything – for all of your science input and camaraderie.

Finally, I would like to give special recognition to Dawn Makley. Without her support and encouragement, much of this work would have been impossible. Thank you for enduring all my scientific frustrations and successes and being there for me. I would also like to thank Dawn's parents, Mr. and Mrs. Makley, Nick, and Trisha for treating me like family.

In the end, I want to thank my Mummy and Papa, Mr. Kaushal Kumar Singh and Mrs. Suman Singh, as well as my brother, for being there for me in my life, helping me and encouraging me in the struggling and difficult days of my graduate school. I will never forget the sacrifices they made that allowed me to reach for my dreams and goals, and I cannot thank them enough for it. The completion of this dissertation is as much their success as my own.



## Table of Contents

DEDICATION .....	i
ACKNOWLEDGEMENTS .....	ii
LIST OF FIGURES .....	ix
LIST OF SCHEMES .....	xii
LIST OF TABLES .....	xxii

Chapter1. Synthetic Conserved and Nonconserved Proline Derivatives from a Single Amino Acid Template.....	1
1.1. Introduction and Background.....	1
1.2. Conformational Analysis of Proline Containing Peptides .....	5
1.2.1. X-ray Diffraction Analysis .....	6
1.2.2. Nuclear Magnetic Resonance (NMR) .....	6
1.2.3. Infrared (IR) Evidence for Reverse Turns in Peptides .....	7
1.3. Proline Peptidomimetics .....	7
1.4. Applications of $\beta$ -turn .....	15
1.4.1. Pharmaceuticals .....	15
1.4.2. Organocatalysis .....	21
1.5. Synthesis of Indoline and Azaindoline Amino Acids .....	23
1.6. Synthesis and Conformational Analyses of Indoline and Azaindoline Amino Acid-Containing Dipeptides.....	26

1.7. Synthesis of Ind and <sup>N7</sup> Ind $\alpha$ -Amino Acid-Containing Tetrapeptides .....	31
1.8. Conformational Analyses of <sup>N7</sup> Ind-Containing Tetrapeptides .....	35
1.9. Conformational Analyses of Ind-Containing Tetrapeptides .....	41
1.10. Conclusions .....	43
Chapter 2. Total Synthesis of (+)-Serratezomine A.....	45
2.1. Background .....	45
2.1.1. Introduction to <i>Lycopodium</i> Alkaloids and (+)-Serratezomine A.....	45
2.1.2. Biosynthesis of the <i>Lycopodium</i> Alkaloids .....	47
2.2. Approaches to the Synthesis of <i>Lycopodium</i> Alkaloids.....	51
2.2.1. Lycopodine Class .....	51
2.2.2. Miscellaneous Class .....	53
2.2.3. Fawcettimine Class.....	62
2.2.4. Lycodine Class .....	75
2.3. Retrosynthetic Analysis of Serratezomine A .....	84
2.4. Results and Discussion.....	86
2.4.1. Synthesis of the Vinylogous Amide .....	86
2.4.2 Ester Reduction and Advancement of <b>222</b> .....	92
2.4.3 Secondary Alcohol Protection and Optimization of Hydroboration Step .....	102
2.4.4. Advancement of the $\alpha$ -alcohol ( <b>245</b> ).....	106
2.4.5. Advancement of the $\alpha$ -alcohol ( <b>279</b> ).....	110
Chapter 3. Total Synthesis of Chlorinated Hapalindoles (K, A, G) and Progress towards the Total Synthesis of (+)-Ambiguine G Nitrile.....	122

3.1. Background .....	122
3.1.1. Introduction to Indole Marine Alkaloids and (+)-Ambiguine G Nitrile.....	122
3.1.2. Biosynthesis of Indole Marine Alkaloids and (+)-Ambiguine G Nitrile.....	123
3.2. Approaches towards the Synthesis of Nitrile- and Isonitrile-Containing Indole Marine Alkaloids.....	126
3.2.1. Synthetic Studies towards Hapalindoles.....	126
3.2.2. Synthetic Studies towards Welwitindolinones .....	137
3.2.3. Synthetic Efforts towards Fischerindoles .....	150
3.2.4. Synthetic Efforts towards Ambiguines.....	153
3.3. Retrosynthetic Analysis of Ambiguine G .....	156
3.4. Results and Discussion of First/Second Generation Synthetic Endeavours .....	157
3.4.1. C-Ring Construction through Enolate C-Arylation Attempts .....	157
3.4.2. C-Ring Construction through Rh(II) Catalyzed Intramolecular C-H Insertion Reaction .....	161
3.4.3. Advancement of the $\beta$ -Tetralone to Tricyclic Core of Ambiguine G.....	163
3.4.4. Synthetic Strategy towards Prenylated Tricyclic Diene .....	166
3.4.5. Elaboration of the Aryl Amination Product ( <b>474</b> ).....	172
3.4.6. A tandem Friedel-Crafts Acylation/Alkylation Sequence to Access the ABC- ring System of Ambiguine G.....	179
3.4.7. Friedel-Crafts Acylation Utilizing 2,3,3-Trimethylacrylic Acid.....	191
3.4.8. Dienophile Synthesis .....	195
3.4.9. Attempted Diels-Alder Reaction with $\beta$ -Chloro- $\alpha$ -methyl acrolein.....	197
3.4.10. Towards the synthesis and Attempted Diels-Alder Reaction with Various Dienophiles under Thermal Conditions.....	199
3.4.11. Lewis Acid Mediated Diels-Alder Reaction of Silyldienol Ether <b>553</b> with <b>562</b> .....	203

3.4.12. Cyclohexene Ring Functionalization.....	206
3.4.13. Appending the C11-N Bond Using an Established S <sub>N</sub> 2 Reaction Protocol	208
3.4.14. Total Synthesis of Hapalindole K.....	211
3.4.15. Total Synthesis of Hapalindole A.....	215
3.4.16. Formal Synthesis of hapalindole G .....	218
3.4.17. Summary.....	221

## List of Figures

<b>Figure</b>	<b>Page</b>
<i>Figure 1.</i> Motif elements in proteins .....	1
<i>Figure 2.</i> Peptide Turn Structures.....	3
<i>Figure 3.</i> <i>trans-cis</i> Equilibrium in Peptides.....	4
<i>Figure 4.</i> <i>trans-cis</i> Equilibrium in Peptides N-terminal to Proline Derivatives .....	5
<i>Figure 5.</i> Dihedral Angles in Proline-Incorporated Peptides .....	5
<i>Figure 6.</i> <i>cis-</i> and <i>trans-</i> <sup>t</sup> Butyl Prolines.....	9
<i>Figure 7.</i> X-ray Crystal Structure of Ac-L-Tyr- <sup>t</sup> BuPro-NHMe .....	11
<i>Figure 8.</i> Influence of Sequence on the Amide Equilibrium.....	11
<i>Figure 9.</i> Tetrazoles and Azaprolines as Mimics .....	13
<i>Figure 10.</i> Mutter's Oxazolidines and Thiazolidines as Proline Mimics .....	14
<i>Figure 11.</i> Singly and Doubly H-bonded Mimics .....	15
<i>Figure 12.</i> Peptidic and Peptidomimetic ligands .....	16
<i>Figure 13.</i> Peptidic and Peptidomimetic ACE Inhibitor .....	19
<i>Figure 14.</i> Prolyl Amide Isomers of Oxytocin and Analogues .....	20
<i>Figure 15.</i> Epoxidation Catalysis by an Acid/Peracid Pair .....	21
<i>Figure 16.</i> Asymmetric Epoxidation of Olefins in the Presence of the Peptide Catalyst. 22	
<i>Figure 17.</i> <i>cis-trans</i> Isomerism in Indoline Containing Peptides .....	23
<i>Figure 18.</i> Amide Coupling Reagents .....	26
<i>Figure 19.</i> Equilibrium Constant Measurements of Ind- Dipeptides .....	28
<i>Figure 20.</i> NOESY Correlations of L-Phe-L-Ind-OMe .....	29
<i>Figure 21.</i> Variable Temperature Experiment of <b>23a</b> .....	29

<i>Figure 22.</i> Dihedral Angles in Proline-Incorporated Peptides .....	30
<i>Figure 23.</i> NOESY Analysis of Dipeptide <b>25b</b> .....	31
<i>Figure 24.</i> Equilibrium Constant Measurements of <sup>N7</sup> Ind-tripeptides.....	32
<i>Figure 25.</i> Equilibrium Constant Measurements of Ind-Tripeptides.....	35
<i>Figure 26.</i> Conformational Depiction of Boc-L-Ala-D-Phe-L- <sup>N7</sup> Ind-L-Ala-NHMe ( <b>33aa</b> ) .....	36
<i>Figure 27.</i> Observed Regional (a-c) and Long Range (d) NOESY Correlations for Tetrapeptide <b>33aa</b> .....	36
<i>Figure 28.</i> Effect of Solvent on the NH Amide Protons in <b>33aa</b> .....	37
<i>Figure 29.</i> Conformational Depiction of Boc-L-Ala-L-Phe-L- <sup>N7</sup> Ind-L-Ala-NHMe ( <b>33ab</b> ) .....	38
<i>Figure 30.</i> Observed Regional (a-c) and Long Range (d) NOESY Correlations for Tetrapeptide <b>33ab</b> .....	39
<i>Figure 31.</i> Effect of Solvent on the NH Amide Protons in <b>33ab</b> .....	40
<i>Figure 32.</i> Conformational Depiction of D- <sup>N7</sup> Ind-Containing Tetrapeptides ( <b>33ba</b> and <b>33bb</b> ).....	40
<i>Figure 33.</i> Conformational Depiction of Boc-L-Ala-L-Phe-L-Ind-L-Ala-NHMe (36ab)	41
<i>Figure 34.</i> Observed Regional (a-c) and Long Range (d) NOESY Correlations for Tetrapeptide <b>36ab</b> .....	42
<i>Figure 35.</i> Structure of Serratezomine A.....	45
<i>Figure 36.</i> <i>Lycopodium</i> Alkaloids Containing N-C4 Bond .....	49
<i>Figure 37.</i> Cernuane Alkaloids.....	60
<i>Figure 38.</i> Structure of (+)-Lycoposerramine C.....	72

<i>Figure 39.</i> Structure of (+)-Lycoflexine .....	74
<i>Figure 40.</i> Structure of (+)-Fastigiatine.....	79
<i>Figure 41.</i> Hydroboration Byproducts.....	88
<i>Figure 42.</i> Side Product in the CAN Promoted Cyclization Step.....	91
<i>Figure 43.</i> Rationale for the Undesired Retro-Aldol Reaction of <b>255</b> .....	99
<i>Figure 44.</i> Crystal Structure of $\beta$ -diol .....	103
<i>Figure 45.</i> Structure of (+)-Ambiguine G Nitrile and Chlorinated Hapalindoles (A, G, K) .....	122
<i>Figure 46.</i> Proposed Biosynthesis of Hapalindoles and Ambiguines.....	125
<i>Figure 47.</i> Structures of Members of Hapalindole Family of Indole Alkaloids.....	127
<i>Figure 48.</i> Structures of the Members of the Welwitindolinone Family.....	141
<i>Figure 49.</i> Structures of the Members of Fischerindole and Related Class of Indole Alkaloids.....	151
<i>Figure 50.</i> Members of the Ambiguine Family .....	154

## List of Schemes

<i>Scheme</i>	<b>Page</b>
<i>Scheme 1.</i> Retrosynthetic Analysis of Indoline and Azaindoline Amino Acid .....	24
<i>Scheme 2.</i> Enantioselective Alkylation.....	25
<i>Scheme 3.</i> Synthesis of Azaindoline Amino Acids.....	26
<i>Scheme 4.</i> Synthesis of L-Ind-OMe Containing Dipeptides.....	27
<i>Scheme 5.</i> Synthesis of D-Ind-OMe Containing Dipeptides .....	27
<i>Scheme 6.</i> Synthesis of the Dipeptide Fragment Ala-Phe ( <b>27</b> ).....	31
<i>Scheme 7.</i> Mechanism for the racemization of Phe-C <sub>α</sub> stereocenter .....	32
<i>Scheme 8.</i> Synthesis of Indoline Amino Acid Containing Model Tetrapeptide System ..	34
<i>Scheme 9.</i> Proposed Biosynthetic Pathway to Lycopodine .....	48
<i>Scheme 10.</i> Biosynthesis of N-C4 Containing Lycopodium Alkaloids.....	50
<i>Scheme 11.</i> Polonovski-Potier Rearrangement.....	51
<i>Scheme 12.</i> Carter's Enantioselective Synthesis of Lycopodine .....	52
<i>Scheme 13.</i> Synthesis of (+)-Lyconadin A and (-)-Lyconadin B.....	53
<i>Scheme 14.</i> Synthesis of (+)-Lyconadin A and (-)-Lyconadin B.....	54
<i>Scheme 15.</i> Sarpong's Synthesis of (±)-Lyconadin A .....	56
<i>Scheme 16.</i> Sarpong's Synthesis of (±)-Lyconadin A .....	56
<i>Scheme 17.</i> Overman's Synthesis of (+)-Nankakurine A and B.....	58
<i>Scheme 18.</i> Water's Synthesis of (±)-Nankakurine A and B.....	59
<i>Scheme 19.</i> Takayama's Synthesis of Cernuine and Cermizine D.....	60
<i>Scheme 20.</i> Takayama's Syntheses of Cernuine and Cermizine D (Completion).....	61
<i>Scheme 21.</i> Inubushi's Synthesis of (±)-Fawcettimine.....	62



<i>Scheme 22.</i> Inubushi's Synthesis of (±)-Fawcettimine and 8-Deoxyserratenine .....	64
<i>Scheme 23.</i> Heathcock's Synthesis of (±)-Fawcettimine.....	65
<i>Scheme 24.</i> Toste's Synthesis of (+)-Fawcettimine .....	66
<i>Scheme 25.</i> Toste's Synthesis of (+)-Fawcettimine (Completion) .....	66
<i>Scheme 26.</i> Mukai's Synthesis of (+)-Fawcettimine .....	67
<i>Scheme 27.</i> Dake's Synthesis of (+)-Fawcettidine .....	69
<i>Scheme 28.</i> Dake's Synthesis of (+)-Fawcettidine (Completion).....	69
<i>Scheme 29.</i> Inubushi's Synthesis of (±)-Serratinine .....	70
<i>Scheme 30.</i> Inubushi's Synthesis of (±)-Serratinine (Completion) .....	71
<i>Scheme 31.</i> Takayama's Asymmetric Synthesis of Lycoposerramine C.....	72
<i>Scheme 32.</i> Takayama's Asymmetric Synthesis of Lycoposerramine C (Completion) ...	73
<i>Scheme 33.</i> Takayama's Biomimetic Synthesis of Phlegmariurine A.....	73
<i>Scheme 34.</i> Mulzer's Asymmetric Synthesis of (+)-Lycoflexine.....	74
<i>Scheme 35.</i> Fukuyama's Asymmetric Synthesis of (-)-Huperzine A .....	77
<i>Scheme 36.</i> Fukuyama's Asymmetric Synthesis of (-)-Huperzine A (Completion).....	78
<i>Scheme 37.</i> Shair's Asymmetric Synthesis of (+)-Fastigiatine.....	80
<i>Scheme 38.</i> Sarpong's Asymmetric Synthesis of (+)-Complanadine A .....	81
<i>Scheme 39.</i> Siegel's Asymmetric Synthesis of (+)-Complanadine A .....	83
<i>Scheme 40.</i> Siegel's Asymmetric Synthesis of (+)-Complanadine A (Completion) .....	84
<i>Scheme 41.</i> Retrosynthetic Analysis of (+)-Serratezomine A .....	85
<i>Scheme 42.</i> Synthesis of the Key Carboxylic Acid Fragment ( <b>235</b> ).....	86
<i>Scheme 43.</i> Synthesis of Imine .....	89
<i>Scheme 44.</i> Synthesis of β-Stannyl Enamine .....	89

<i>Scheme 45.</i> Synthesis of Vinylogous Amide <b>127</b> .....	90
<i>Scheme 46.</i> Rationale for Observed Diastereoselectivity in the Cyclization Step.....	91
<i>Scheme 47.</i> Formation of the Undesired Cyclized Product ( <b>239</b> ).....	92
<i>Scheme 48.</i> Reduction of the Ester Functionality in <b>222</b> .....	93
<i>Scheme 49.</i> Attempts towards Appending the 3-Carbon Fragment.....	93
<i>Scheme 50.</i> CAN Mediated Allylation Step .....	94
<i>Scheme 51.</i> Substrate Controlled Reduction.....	95
<i>Scheme 52.</i> Attempted Lactonization of <b>249</b> .....	96
<i>Scheme 53.</i> Attempted Lactonization of <b>251</b> .....	96
<i>Scheme 54.</i> Attempted Synthesis of Piperidine Ring.....	97
<i>Scheme 55.</i> Mechanism of the Undesired Retro-Aldol reaction of <b>254</b> .....	98
<i>Scheme 56.</i> The Metal Catalyzed Reduction of <b>254</b> .....	100
<i>Scheme 57.</i> Attempted Piperidine Ring Formation from the Primary Alcohol ( <b>260</b> ) ....	100
<i>Scheme 58.</i> Efforts towards Protecting the Diol ( <b>244</b> ) .....	101
<i>Scheme 59.</i> Attempted Silylation of the Diol ( <b>246</b> ).....	102
<i>Scheme 60.</i> Efforts towards Protecting the Alcohol ( <b>245</b> ).....	102
<i>Scheme 61.</i> Mesylation of Alcohol <b>244</b> .....	104
<i>Scheme 62.</i> Formation of Undesired Cyclic Ether <b>266</b> .....	104
<i>Scheme 63.</i> Optimization of Hydroboration Step .....	105
<i>Scheme 64.</i> Alternate Strategy to Access Piperidine Ring .....	106
<i>Scheme 65.</i> Advancement of the $\alpha$ -alcohol ( <b>245</b> ).....	107
<i>Scheme 66.</i> Substrate Controlled Reduction of Iminium <b>272</b> .....	107
<i>Scheme 67.</i> Failed Attempts towards Oxidation of Alcohol <b>274</b> .....	108

<i>Scheme 68.</i> Alternate Synthetic Plan to Access Serratezomine A from Alcohol <b>274</b> ....	109
<i>Scheme 69.</i> Failed Attempts towards the Synthesis of Ether <b>276</b> .....	109
<i>Scheme 70.</i> Synthetic Plan to Access <b>277</b> from <b>274</b> .....	109
<i>Scheme 71.</i> Attempted S <sub>N</sub> 2 Displacement of Mesylate by an Oxygen Nucleophile .....	110
<i>Scheme 72.</i> Modified Synthetic Plan to Access Serratezomine A.....	110
<i>Scheme 73.</i> Advancement of the $\alpha$ -alcohol ( <b>279</b> ).....	111
<i>Scheme 74.</i> Synthesis of Alcohol <b>183</b> .....	112
<i>Scheme 75.</i> Effect of Temperature on the Ketone ( <b>238</b> ) Reduction .....	113
<i>Scheme 76.</i> Undesired Formation of Enamides <b>283</b> and <b>282</b> .....	114
<i>Scheme 77.</i> Hydroboration of <b>280</b> under Optimized Conditions.....	115
<i>Scheme 78.</i> Undesired Formation of Vinylogous Amide <b>190</b> .....	116
<i>Scheme 79.</i> Mechanism for the Undesired Formation of Vinylogous Amide <b>286</b> .....	116
<i>Scheme 80.</i> Leaving Group Effect on Vinylogous Amide <b>286</b> Formation.....	118
<i>Scheme 81.</i> Substrate Controlled Reduction of Iminium <b>290</b> .....	118
<i>Scheme 82.</i> Successful Lactonization of <b>291</b> .....	119
<i>Scheme 83.</i> Completion of the Total Synthesis of (+)-Serratezomine A.....	120
<i>Scheme 84.</i> Total Synthesis of (+)-Serratezomine A.....	121
<i>Scheme 85.</i> Proposed Biogenesis of Hapalindoles, Ambiguines, Welwitindolinones and Fischerindoles .....	124
<i>Scheme 86.</i> Natsume's Synthesis of ( $\pm$ )-Hapalindoles J and M.....	128
<i>Scheme 87.</i> Natsume's Synthesis of ( $\pm$ )-Hapalindoles U and H .....	130
<i>Scheme 88.</i> Natsume's Enantioselective Synthesis of Hapalindole O .....	131
<i>Scheme 89.</i> Fukuyama's Enantioselective Synthesis of (-)-Hapalindole G .....	132

<i>Scheme 90.</i> Fukuyama's Enantioselective Synthesis of (-)-Hapalindole G (Completion)	133
<i>Scheme 91.</i> Albizati's Enantioselective Synthesis of (+)-Hapalindole Q	134
<i>Scheme 92.</i> Radical Coupling of Indole and (R)-Carvone Fragment	135
<i>Scheme 93.</i> Baran's Enantioselective Synthesis of (+)-Hapalindole Q	135
<i>Scheme 94.</i> Organomediated Diels-Alder Reaction	136
<i>Scheme 95.</i> Kerr's Enantioselective Synthesis of (+)-Hapalindole Q	137
<i>Scheme 96.</i> Proposed Biosynthesis of Welwitindolinones	138
<i>Scheme 97.</i> Baran's Attempted Biomimetic Synthesis of Welwitindolinone B from Welwitindolinone A	138
<i>Scheme 98.</i> Baran's Biomimetic Enantioselective Synthesis of (+)-Welwitindolinone A	139
<i>Scheme 99.</i> Mechanism of Xenon Fluoride Mediated Ring Contraction Process	140
<i>Scheme 100.</i> Wood's Enantioselective Synthesis of (+)-Welwitindolinone A	142
<i>Scheme 101.</i> Wood's Enantioselective Synthesis of (+)-Welwitindolinone A (Completion)	143
<i>Scheme 102.</i> Shea's Diels-Alder Approach towards Welwistatin	144
<i>Scheme 103.</i> Trost's Diels-Alder Approach towards Welwistatin/Welwitindolinone	145
<i>Scheme 104.</i> Funk's Synthetic Approach towards Welwistatin/Welwitindolinone	146
<i>Scheme 105.</i> Jung's C-H Insertion Approach towards Welwistatin/Welwitindolinone	147
<i>Scheme 106.</i> Jung's C-H Insertion Approach towards Welwistatin/Welwitindolinone	148
<i>Scheme 107.</i> Avendanö's C-H Insertion Approach	148

<i>Scheme 108.</i> Successful Application of C-H Insertion Reaction to Secure the ABCD-Ring System of Welwistatin .....	149
<i>Scheme 109.</i> Rawal's Approach to the Synthesis of ABC-Ring system of Welwistatin	150
<i>Scheme 110.</i> Baran's Enantioselective Synthesis of (-)-12- <i>epi</i> -Fischerindole U .....	152
<i>Scheme 111.</i> Baran's Enantioselective Synthesis of (+)-Fischerindole I .....	153
<i>Scheme 112.</i> Baran's Enantioselective Synthesis of (-)-Fischerindole G .....	153
<i>Scheme 113.</i> Baran's Protecting Group Free Synthesis of (+)-Ambiguine H and (-)-Hapalindole U .....	155
<i>Scheme 114.</i> Retrosynthetic Analysis of (+)-Ambiguine G Nitrile .....	157
<i>Scheme 115.</i> Retrosynthetic Disconnections for Tricyclic Ketone <b>450</b> .....	157
<i>Scheme 116.</i> Synthesis of Ketone-Imine <b>455</b> .....	158
<i>Scheme 117.</i> Synthesis of the Indoline ( <b>451</b> ) .....	159
<i>Scheme 118.</i> Attempted bis-Radical Cyclization .....	160
<i>Scheme 119.</i> Revised Retrosynthetic Strategy to Access Tricyclic Ketone <b>448</b> .....	161
<i>Scheme 120.</i> AC-Ring Construction Utilizing C-H Insertion Method .....	162
<i>Scheme 121.</i> Intramolecular Buchner Reaction .....	163
<i>Scheme 122.</i> PTC Catalyzed Alkylation .....	164
<i>Scheme 123.</i> ABC-Ring Construction .....	165
<i>Scheme 124.</i> Stereocontrolled [4+2] Cycloaddition .....	166
<i>Scheme 125.</i> Outline of the Synthetic Plan towards C2 <i>tert</i> -Prenyl Tricyclic Diene <b>480</b> .....	166
<i>Scheme 126.</i> Synthesis of <i>tert</i> -Prenylated Schiff Base <b>478</b> .....	167
<i>Scheme 127.</i> Michael Addition of Enone <b>463</b> with Schiff Base <b>478</b> .....	168

<i>Scheme 128.</i> Model Substrate to Install the C2 <i>tert</i> -Prenyl Functionality.....	169
<i>Scheme 129.</i> Attempted Michael Addition with Nitroalkane .....	170
<i>Scheme 130.</i> Attempted Double Conjugate Addition Approach to Access <b>488</b> .....	170
<i>Scheme 131.</i> Attempted Conjugate Addition with Acid <b>486</b> .....	171
<i>Scheme 132.</i> Elaboration of the Ester Side Chain of <b>474</b> .....	172
<i>Scheme 133.</i> Dunkerton's Claisen-Ireland Approach to Install C2 <i>tert</i> -Prenyl Group in Indole .....	173
<i>Scheme 134.</i> Attempted Saponification of Indoline <b>474</b> .....	174
<i>Scheme 135.</i> Attempted Synthesis of Claisen-Ireland Rearrangement Precursor .....	174
<i>Scheme 136.</i> Synthesis of Alcohol <b>504</b> .....	175
<i>Scheme 137.</i> Revised Strategy to Access Ireland-Claisen Rearrangement Precursor ....	175
<i>Scheme 138.</i> Preparation of Ireland-Claisen Rearrangement Precursor .....	176
<i>Scheme 139.</i> Attempted Ireland-Claisen Rearrangement with <b>505</b> .....	177
<i>Scheme 140.</i> Attempted Ireland-Claisen Rearrangement with Indoline <b>509</b> .....	178
<i>Scheme 141.</i> Attempted Ireland-Claisen Rearrangement of bis-Silyl Enol Ether <b>515</b> ...	179
<i>Scheme 142.</i> Tandem Friedel-Crafts Acylation/Alkylation Sequence to Access ABC-Ring System of Hapalindoles and Ambiguines .....	180
<i>Scheme 143.</i> Optimization of C2 <i>tert</i> -Prenyl Indole Synthesis .....	181
<i>Scheme 144.</i> Undesired Retro Friedel-Crafts Reaction .....	182
<i>Scheme 145.</i> Effect of Electronics and Sterics on the Friedel-Crafts Alkylation Step...	183
<i>Scheme 146.</i> Literature Precedence for a Novel Molten AlCl <sub>3</sub> -NaCl Solution Mediated C-4 Alkylation of Indoles .....	184
<i>Scheme 147.</i> AlCl <sub>3</sub> -NaCl Solution-Mediated C-4 Alkylation of Model Compounds ....	185

<i>Scheme 148.</i> Revised Friedel-Crafts Acylation/Alkylation Sequence to Access Diene <b>529</b>	185
<i>Scheme 149.</i> Synthesis of Tricyclic Ketone <b>530</b>	186
<i>Scheme 150.</i> Attempts at Appending the C-2 tert-Prenyl Group in Tricyclic Ketone <b>530</b> by Oxy-Cope Rearrangement Protocol	187
<i>Scheme 151.</i> Attempts at Appending a C14 Methyl Group in Tricyclic Ketone <b>530</b>	188
<i>Scheme 152.</i> Construction of Enone <b>535</b>	189
<i>Scheme 153.</i> Unsuccessful Attempts at Masking the C14-C15 Double Bond of Enone <b>535</b>	190
<i>Scheme 154.</i> Synthesis of the $\alpha,\beta$ -Unsaturated Nitrile	191
<i>Scheme 155.</i> Tandem Friedel-Crafts Acylation/Alkylation Using 2,3,3-Trimethylacryloyl Chloride	191
<i>Scheme 156.</i> Synthesis of Tricyclic Ketone <b>547</b>	193
<i>Scheme 157.</i> Synthesis of $\alpha,\beta$ -Unsaturated Nitrile <b>549</b> Using $\text{Et}_2\text{AlCN}$	194
<i>Scheme 158.</i> Synthesis of $\alpha,\beta$ -Unsaturated Nitrile <b>549</b> Using TMS-CN	194
<i>Scheme 159.</i> Optimized Conditions for the Synthesis of $\alpha,\beta$ -Unsaturated Nitrile <b>549</b>	195
<i>Scheme 160.</i> Synthesis of Diene <b>553</b>	195
<i>Scheme 161.</i> Synthesis of $\beta$ -Chloro- $\alpha$ -Methyl Acrolein <b>475</b>	196
<i>Scheme 162.</i> Diels-Alder Cycloadditions of <b>553</b> with $\alpha$ -Methyl Acrolein and $\beta$ -Chloro- $\alpha$ - Methyl Acrolein	198
<i>Scheme 163.</i> Formal Synthesis of ( $\pm$ )-Hapalindole U	198
<i>Scheme 164.</i> Attempted Diels-Alder Reaction with <b>562</b> under Thermal Conditions	199

<i>Scheme 165.</i> Attempted Diels-Alder with Dienol Ether <b>568</b> , Dienol Acetate <b>566</b> and Dienol Triflate <b>569</b> .....	201
<i>Scheme 166.</i> Attempted Synthesis of Various Dienamines .....	202
<i>Scheme 167.</i> Structure Elucidation of Diels-Alder and Mukaiyama Aldol Adduct .....	205
<i>Scheme 168.</i> Elaboration of the the Central Cyclohexene Core .....	206
<i>Scheme 169.</i> Attempts at Optimizing the Elimination Reaction.....	207
<i>Scheme 170.</i> Mechanism of the TBAF Mediated Rearrangement Step.....	207
<i>Scheme 171.</i> Alternate Attempted Strategy to Circumvent the Formation of Undesired Tetracycle <b>580</b> .....	208
<i>Scheme 172.</i> First Generation Synthetic Strategy towards Hapalindole K.....	209
<i>Scheme 173.</i> First Generation Synthetic Strategy towards Hapalindole K.....	210
<i>Scheme 174.</i> Proposed Mechanism of Elimination/Rearrangement Reaction Side Product .....	211
<i>Scheme 175.</i> Second Generation Synthetic Strategy towards Hapalindole K .....	212
<i>Scheme 176.</i> Application of an S <sub>N</sub> 1 Process to Construct the Desired C11-N Bond .....	212
<i>Scheme 177.</i> Unsuccessful Attempt at Using a Carbon Nucleophile to Trap the Intermediate Carbocation <b>594</b> .....	213
<i>Scheme 178.</i> A Solvolysis product with Acetic Acid as the Nucleophile .....	214
<i>Scheme 179.</i> A Ritter Reaction with TMS-CN as the Nucleophile .....	214
<i>Scheme 180.</i> Total Synthesis of Hapalindole K (Completion) .....	215
<i>Scheme 181.</i> Appending the cis-Decalin Ring System of Hapalindole A .....	216
<i>Scheme 182.</i> Structural Elucidation and Proposed Mechanism for the Formation of Formamide <b>604</b> .....	217



<i>Scheme 183.</i> Total Synthesis of Hapalindole A.....	218
<i>Scheme 184.</i> Synthetic Strategy towards the Formal Synthesis of Hapalindole G.....	218
<i>Scheme 185.</i> LiAlH <sub>4</sub> -Mediated Diastereoselective Reduction of Allylic Alcohol <b>579</b> ..	219
<i>Scheme 186.</i> Proposed Mechanism of LiAlH <sub>4</sub> Mediated Diastereoselective Reduction of <b>579</b> .....	219
<i>Scheme 187.</i> Formal Synthesis of Hapalindole G.....	220
<i>Scheme 188.</i> Total Synthesis of Hapalindole A and K.....	222
<i>Scheme 189.</i> Formal Synthesis of Hapalindole G.....	223

## List of Tables

<i>Table</i>	<b>Page</b>
<i>Table 1.</i> Influence of Solvent on Amide Isomer Equilibrium .....	10
<i>Table 2.</i> Optimization of Ketone Reduction .....	111
<i>Table 3.</i> Solvent Screen for the Reduction of <b>238</b> .....	114
<i>Table 4.</i> Lewis Acid Screen to Effect the Diels-Alder Reaction .....	204

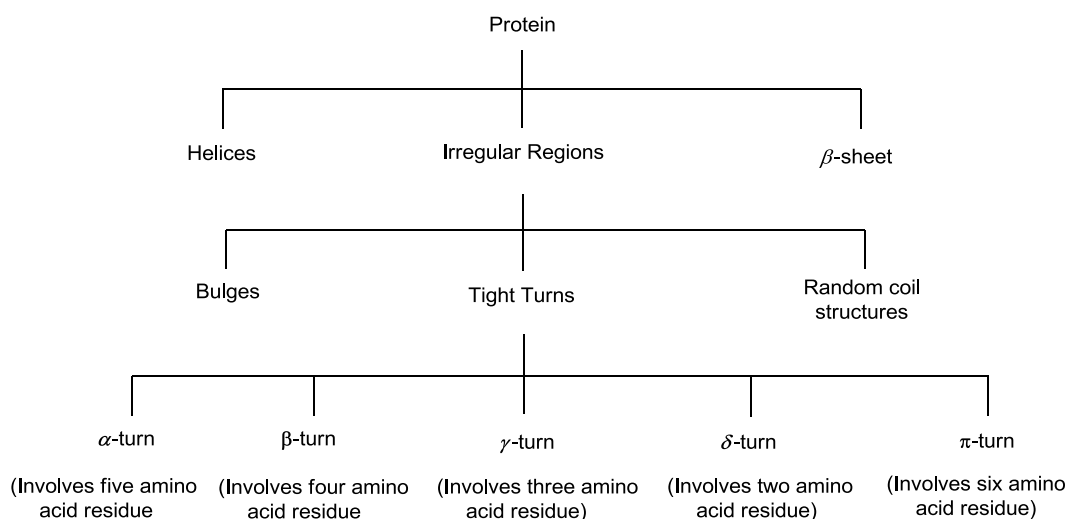
# Chapter1

## Synthetic Conserved and Nonconserved Proline Derivatives from a Single Amino Acid Template

### 1.1. Introduction and Background

Proteins are built up of long-chain polymers of amino acids, called polyamino acids or polypeptide chains. Polypeptide chains formed by upto 20 different amino acids are more versatile because of the great number of different side chains that may be present. Driven by a variety of interaction forces, polypeptide chains are folded into many different three-dimensional structures. The protein architecture is characterized by repetitive motif elements such as  $\alpha$ -helices and  $\beta$ -sheets, as well as nonrepetitive motif elements such as tight turns, bulges, and random coil structures (Figure 1).<sup>1</sup>

Figure 1. Motif elements in proteins



From both structural and functional points of view, tight turns play an important role, as reflected by the following facts: (i) a polypeptide chain cannot fold into a

<sup>1</sup> Richardson, J. S. *Adv. Protein Chem.* **1981**, 34, 167.

compact globular structure without the element of tight turns; (ii) tight turns usually occur on the exposed surface of proteins and hence are likely involved in molecular recognition processes between proteins and in interactions between peptide substrates and receptors; (iii) tight turns provide very useful information for defining template structures in the design of new molecules such as drugs, pesticides, and antigens. Accordingly, tight turns have long been recognized as one of the three most important features of proteins with the other two being the  $\alpha$ -helix and  $\beta$ -sheet.

The smallest tight turn is a  $\delta$ -turn. It involves only two amino acid residues, and is also referred to as 1 $\rightarrow$ 2 type, 2 $\rightarrow$ 3 type, or C<sub>8</sub> form.<sup>2</sup> The intra-turn hydrogen bond for a  $\delta$ -turn is formed between the backbone NH(*i*) and the backbone CO(*i*+1). The possible angles ( $\phi$ ,  $\psi$ ) for hydrogen-bonded  $\delta$ -turns were determined by Nagarajaram, *et al.*<sup>3</sup>

The second smallest tight turn is a  $\gamma$ -turn, which involves three amino acid residues (Figure 2). The intra-turn hydrogen bond for a  $\gamma$ -turn is formed between the backbone CO(*i*) and the backbone NH(*i*+2). The possible angles ( $\phi$ ,  $\psi$ ) for hydrogen-bonded  $\gamma$ -turns were determined by Nemethy and Printz. An inverse  $\gamma$ -turn is a mirror image  $\gamma$ -turn.<sup>4</sup>

A  $\beta$ -turn simply involves the arrangement of four amino acids, such that the polypeptide backbone undergoes a 180 °C change in direction. The  $\beta$ -turns, originally recognized by Venkatachalam, is stabilized by a hydrogen bond between the backbone

---

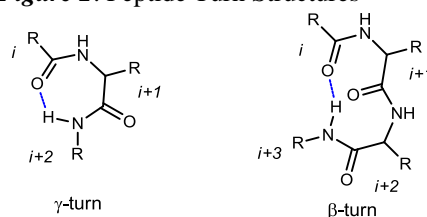
<sup>2</sup> Toniolo, C.; *Crit. Rev. Biochem.* **1980**, *9*, 1.

<sup>3</sup> Nagarajaram, H. A.; Paul, P. K. C.; Ramanarayanan, K.; Soman, K. V.; Ramakrishnan, C. *Int. J. Peptide Protein Res.* **1992**, *40*, 383.

<sup>4</sup> Nemethy, G.; Printz, M. P. *Macromolecules.* **1972**, *5*, 755.

CO(*i*) and the backbone NH(*i*+3). However, Lewis *et al.*,<sup>5</sup> found that 25% of  $\beta$ -turns are “open,” meaning they have no intra-turn hydrogen bond at all.<sup>6</sup> Open turns do not lend themselves to classification by dihedral angles. Therefore, the definition widely accepted for  $\beta$ -turns is four consecutive residues in which the distance between C <sup>$\alpha$</sup> (*i*) and C <sup>$\alpha$</sup> (*i*+3) is less than 7 Å (1 Å = 0.1 nm) and the tetrapeptide chain is not in a helical conformation.<sup>7</sup>

**Figure 2.** Peptide Turn Structures



An  $\alpha$ -turn involves five amino acid residues, where the distance between C <sup>$\alpha$</sup> (*i*) and C <sup>$\alpha$</sup> (*i*+4) is less than 7 Å,<sup>8</sup> and the pentapeptide chain is not in a helical conformation. An energy minimization study on  $\alpha$ -turns was conducted by Ramakrishnan and Nataraj.<sup>9</sup> The largest tight turn is a  $\pi$ -turn, which involves six amino acid residues.<sup>10</sup> A turn formed by seven or more amino acids is not considered a tight turn, but rather a “loose turn” or loop.

Proline is the only naturally occurring amino acid that is a secondary amine. Proline markedly influences protein architecture because its ring structure makes it more conformationally restricted than the other amino acids. This otherwise subtle difference in the substitution of the amine results in an increased propensity to form turn motifs, and

<sup>5</sup> Lewis, P. N.; Momany, F. A.; Scheraga, H. A. *Biochem. Biophys. Acta.* **1973**, *303*, 211.

<sup>6</sup> Venkatachalam, C. M. *Biopolymers.* **1968**, *6*, 1425.

<sup>7</sup> Rose, G. D., Gierasch, L. M., Smith, J. A. *Adv. Protein Chem.* **1985**, *37*, 1.

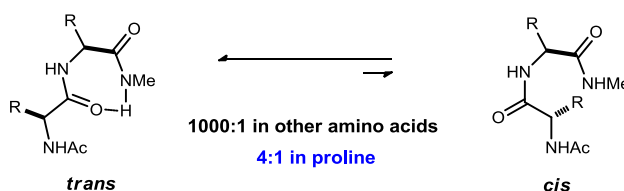
<sup>8</sup> a) Pavone, V., Gaeta, G., Lombardi, A., Nastri, F., Maglio, O. *Biopolymers.* **1996**, *38*, 705–721. b) Chou, K. C. *Biopolymers.* **1996**, *42*, 837.

<sup>9</sup> Ramakrishnan, C., Nataraj, D. V. *J. Peptide Sci.* **1988**, *4*, 239.

<sup>10</sup> Kim, S. H., Sussman, J. S. *Nature.* **1976**, *260*, 645.

it is therefore often exposed on the protein surface.<sup>11</sup> The tertiary nature of the amide nitrogen in proline means that the preceding peptide bond in a protein can adopt either the *cis* or *trans* conformation almost isoenergetically. The activation energy barrier for *cis-trans* isomerization of Xaa-Pro peptide bonds has been well characterized, with values ranging from 80 to 100 kJ mol<sup>-1</sup> (20–25 Kcal mol<sup>-1</sup>) in model peptides and proteins. Generally, *cis* amide bond conformers are relatively scarce in natural peptides (Figure 3).<sup>12,13</sup>

**Figure 3.** *trans-cis* Equilibrium in Peptides



The cyclic nature of the proline residue confers unique conformational properties to the peptide or protein backbone when compared to other common protein-genic amino acids.<sup>7,14</sup> Conformationally rigid surrogates of *cis* and *trans* isomers of X-Pro amide bonds have emerged as important tools for studying the relationship between isomer geometry and peptide bioactivity (Figure 4).<sup>15,16</sup>

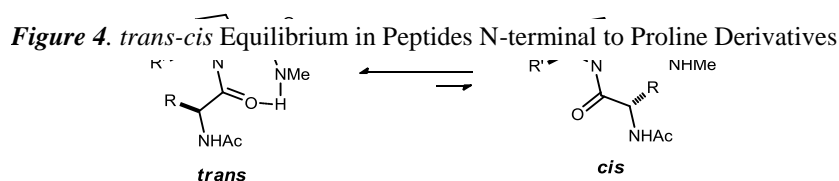
<sup>11</sup> a) Werner, M. H.; Wemmer, D. E. *Biochemistry* **1992**, *31*, 999. b) Kim, E. E.; Varadarajan, R.; Wyckoff, H. W.; Richards, F. M. *Biochemistry* **1992**, *31*, 12304. c) Epp, O.; Lattman, E. E.; Schiffer, M.; Huber, R.; Palm, W. *Biochemistry* **1975**, *14*, 4943.

<sup>12</sup> Fersht, A. *Structure and Mechanism in Protein Science: A Guide to Enzyme Catalysis and Protein Folding*; W. H. Freeman and Company, **1999**, p 9.

<sup>13</sup> Richardson, J. S.; Richardson, D. C. *Principles and Patterns of Protein Conformation. In Prediction of Protein Structure and the Principles of Protein Conformation*, G. D. Fasman, Ed.; Plenum Press; New York, **1989**, p 1-98.

<sup>14</sup> Müller, G.; Gurrath, M.; Kurz, M.; Kessler, H. *Proteins: Struct. Funct., Genet.* **1993**, *15*, 235.

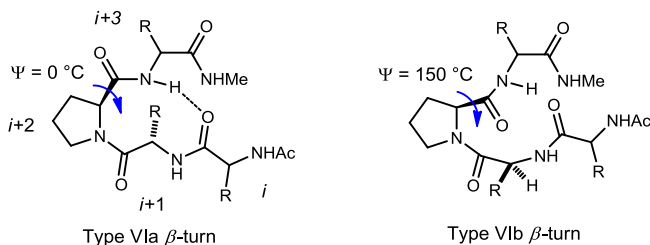
<sup>15</sup> a) Brady, S. F.; Paleveda, W. J., Jr.; Arison, B. H.; Saperstein, R.; Brady, E. J.; Raynor, K.; Veber, D. F.; Freidinger, R. M. *Tetrahedron* **1993**, *49*, 3449. b) Cumberbatch, S.; North, M. Zagotta, G. *Tetrahedron* **1993**, *49*, 9049. c) Cumberbatch, S.; North, M. Zagotta, G. *J. Chem. Soc. Chem. Commun.* **1993**, 641. d) Horne, A.; North, M.; Parkinson, J. A.; Sadler, I. H. *Tetrahedron* **1993**, *49*, 5891.



## 1.2. Conformational Analysis of Proline Containing Peptides

As a result of its unique *trans-cis* isomerization profile, proline can assist the formation of  $\beta$ -turns. The type VI  $\beta$ -turn is a unique member of the  $\beta$ -turn family, since it is the only turn that adopts an *s-cis* peptide bond.<sup>17</sup> Type VI  $\beta$ -turns are classified into two sub-types based on the dihedral angle values of their central  $i + 1$  and  $i + 2$  residues (Figure 5).<sup>14</sup> In type VIa  $\beta$ -turn, the proline  $\Psi$ -dihedral angle is equal to  $0^\circ$ , and a 10-membered intramolecular hydrogen bond exists between the carbonyl oxygen of the  $i$  residue and the amide hydrogen of the  $i+3$  residue. This intramolecular hydrogen bonding is absent in type VIb  $\beta$ -turn in which the proline  $\Psi$ -dihedral angle is equal to  $150^\circ$ .

**Figure 5.** Dihedral Angles in Proline-Incorporated Peptides



<sup>16</sup> Azabicycloalkane Gly-Pro type VI  $\beta$ -turn peptidomimetics are described in: a) Dumas, J.-P.; Germanas, J. P. *Tetrahedron Lett.* **1994**, 35, 1493. b) Gramberg, D.; Robinson, J. A. *Tetrahedron Lett.* **1994**, 35, 861. c) Kim, K.; Dumas, J.-P.; Germanas, J. P. *J. Org. Chem.* **1996**, 61, 3138.

<sup>17</sup> a) Wilmot, C. M.; Thornton, J. *J. Mol. Biol.* **1988**, 203, 221.

Several physical techniques are used to study the conformational parameters and the turn motif in peptides.

### ***1.2.1. X-ray Diffraction Analysis***

X-ray diffraction analysis of peptide crystal structures provides an unequivocal determination of peptide conformation, albeit in the solid state. The structure observed in a crystal is of lowest energy only in the given crystal environment, dominated by intermolecular interactions. The crystal conformation of a peptide may not be identical to its solution conformation. However, the molecular conformation observed for a peptide in a crystal is likely to be among possible the low energy structures.

### ***1.2.2. Nuclear Magnetic Resonance (NMR)***

$^1\text{H}$  and  $^{13}\text{C}$  spectroscopy are among the foremost methods utilized in determining peptide conformations.  $^1\text{H}$  NMR spectroscopy identifies the peptide backbone N-H protons participating in intramolecular hydrogen bonding by observing: (a) the temperature dependence of the N-H chemical shifts ( $\Delta d/\Delta T$ ); (b) the solvent dependence of the N-H chemical shifts; (c) the concentration dependence of N-H chemical shifts in non-polar solvents; (d) deuterium exchange kinetics; and (e) sensitivity of N-H chemical shifts to addition of reagents acting as perturbants.

The existence of an intermolecular hydrogen bond is signaled by a large dependence on temperature of the proton resonance involved in the hydrogen bond. This reflects a perturbation in equilibrium between a free proton and its hydrogen bonded states with increased temperature. The N-H resonance is shifted upfield with increasing temperature as a consequence of the low field position of a hydrogen bonded N-H



resonance. On the other hand, a small temperature dependence implies either intramolecular hydrogen bonding or a “buried” N-H resonance, which is not exposed to the solvent and which does not participate in intramolecular hydrogen bonding.

The extent of perturbation of N-H resonances during a solvent titration, or comparison of the resonances in different solvents, is also informative. As expected, intermolecular hydrogen bonding will be favored in solvents that interact weakly with the peptide. A concentration dependence of N-H resonances that participate in intermolecular hydrogen bonding is significant. Again, a buried N-H proton or an intramolecularly hydrogen bonded proton would show no concentration dependence.

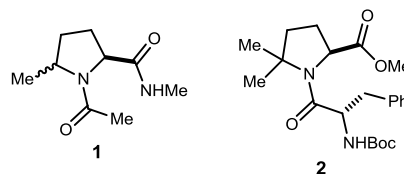
### ***1.2.3. Infrared (IR) Evidence for Reverse Turns in Peptides***

IR has been extensively employed in the conformational analysis of model amides and polypeptides. The characteristic amide frequencies are sensitive to hydrogen bonding. The absence of such shifts in IR is attributed to either the lack of any hydrogen bonds or bond angle distortions. The vibrational bands involving the amide hydrogen bond and their overtones occur between 3300 and 3500  $\text{cm}^{-1}$ . Although these bands do not show any dependence on the peptide conformation, they are markedly affected by hydrogen bonding.

### ***1.3. Proline Peptidomimetics***

Variation of the *trans/cis* ratio can be used to further understand the behavior of peptides and proteins. Over the years a number of proline analogues have been developed to study the structural and biological properties of proline surrogates in peptides. This is done by controlling prolyl *N*-terminal bond isomerization, leading to reverse turn

formation. Study of the factors that control rotation around this bond therefore has relevance not only to protein ground state structure, but also to various rates related to peptide folding, degradation, and dynamics. The barrier to amide isomerization in proline is critical to the rate-determining step in the protein-folding phenomenon. Because of the importance of  $\beta$ -turns in protein folding and recognition,<sup>18</sup> considerable efforts have focused on developing conformationally rigid backbone mimics. Several approaches have been made to selectively destabilize the *trans* isomer, thereby increasing the amount of the *cis* isomer. These strategies are largely based on the application of conformational constraints using structural links and steric interactions. The employment of alkylprolines and their steric interactions to control amide isomer



geometry is a useful method to prepare conformationally rigid amide isomers. A single methyl substituent at the proline 5-position was shown to have a subtle influence on the X-Pro amide isomer equilibrium of *N*-(acetyl)proline *N'*-methylamide (**1**).<sup>19</sup> A 5% increase in the amide *cis*-isomer population was observed in water for the 5-methyl *trans*-diastereomer. The combined effect of two methyl groups at the proline 5-position was studied by Moore<sup>20</sup> in *N*-Boc-phenylalanyl-5,5-dimethylproline methylester (**2**), which was reported to exist as a 9:1 mixture of amide *cis-trans* isomers.

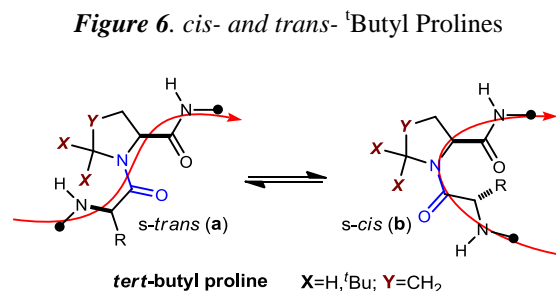
Secondary amides exhibit  $A^{1,3}$ -strain between the nitrogen and  $\alpha$ -carbon substituents, destabilizing the *s-trans* amide bond conformation relative to the remaining natural amino acids. This feature has been exaggerated by proline derivatives bearing

<sup>18</sup> a) Mehta, A.; Jaouhari, R.; Benson, T.; Douglas, K. *Tetrahedron Lett.* **1992**, *33*, 5441. b) Conley, J.; Kohn, H. *J. Med. Chem.* **1987**, *30*, 567. c) Pangborn, A. B.; Giardello, M. A.; Grubbs, R. H.; Rosen, R. K.; Timmers, F. J. *Organometallics* **1996**, *15*, 1518.

<sup>19</sup> Delaney, N. G.; Madison, V. *Int. J. Peptide Protein Res.* **1982**, *19*, 543.

<sup>20</sup> Maggaard, V. W.; Sanchez, R. M.; Bean, J. W.; Moore, M. L. *Tetrahedron Lett.* **1993**, *34*, 381.

large substituents at the 5-position, and was exploited by Lubell,<sup>21</sup> who found that introduction of a sterically demanding *tert*-butyl group at the 5-position of proline disfavored the amide *trans*-isomer and magnified the *cis*-isomer population (Figure 6).<sup>22</sup>

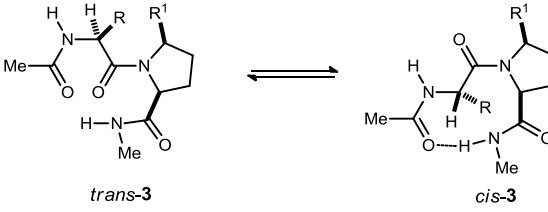


Lubell *et al.* prepared a series of dipeptides containing various amino acid residues attached to the *N*-terminus of the prolyl residue (Table 1). The major conformer of peptides **3f** and **3g** possessed *trans*-amide geometry at the *N*-terminus of the prolyl residue, whereas the peptides **3a-e** adopted *cis*-amide geometry at the *N*-terminus of the 5-*tert*-butyl prolyl residue, with the *cis*-isomer predominant in CDCl<sub>3</sub>. The *N'*-methylamide proton signal appeared between 8.27 and 8.48 ppm, whereas the acetamide signal appeared between 5.97 and 6.41 ppm. They attributed the downfield shift to the existence of hydrogen bonding between the *N'*-methylamide proton and the acetamide carbonyl in a type VI b-turn conformation.<sup>23</sup> This evidence was supported by the fact that the *N'*-methylamide proton signal was much less affected by change of solvent than the acetamide proton, indicating that the *N'*-methylamide proton was involved in an intramolecular hydrogen bond.

<sup>21</sup> a) Halab, L.; Lubell, W. D. *J. Am. Chem. Soc.* **2002**, *124*, 2474. b) Halab, L. Lubell, W. D. *J. Org. Chem.* **1999**, *64*, 3312.

<sup>22</sup> Beausoleil, E.; Lubell, W. D. *J. Am. Chem. Soc.* **1996**, *118*, 12902.

<sup>23</sup> Reviewed in: Dyson, H. J.; Wright, P. E. *Annu. Rev. Biophys. Biophys. Chem.* **1991**, *20*, 519.

**Table 1.** Influence of Solvent on Amide Isomer Equilibrium

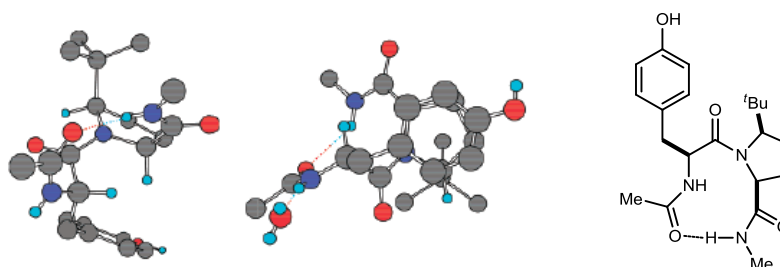
Entry	R	R <sup>1</sup>	% <i>cis</i> -isomer ± 3%		
			D <sub>2</sub> O	DMSO	CDCl <sub>3</sub>
<b>3a</b>	CH <sub>3</sub>	<i>t</i> -Bu	79	79	83
<b>3b</b>	CH <sub>2</sub> CH <sub>2</sub> SCH <sub>3</sub>	<i>t</i> -Bu	74	72	73
<b>3c</b>	CH <sub>2</sub> CH(CH <sub>3</sub> ) <sub>2</sub>	<i>t</i> -Bu	81	67	85
<b>3d</b>	CH(CH <sub>3</sub> ) <sub>2</sub>	<i>t</i> -Bu	81	73	89
<b>3e</b>	CH <sub>2</sub> Ph	<i>t</i> -Bu	90	79	89
<b>3f</b>	CH <sub>3</sub>	H	14	30	19
<b>3g</b>	CH <sub>2</sub> CH(CH <sub>3</sub> ) <sub>2</sub>	H	19	17	20

They also presented evidence for the twisted amide geometry, due to steric interactions between 5-*tert*-butyl substituent and the *N*-terminal residue, using <sup>13</sup>C chemical shift. The carbonyl carbon chemical shift for the *N*-terminal residue of **3a** was 3.1 ppm farther downfield relative to that of **3f**. Because inhibition of amide resonance by factors that distort the N-C(O) bond deshields the carbonyl carbon,<sup>24</sup> the downfield shift is consistent with steric strain that disfavors a planar, resonance-delocalized amide. This twisting resulted in the energy barrier for the *trans-cis* amide isomerization of 5-*tert*-butyl proline to be 3.9 kcal/mol lower in energy than that of proline. X-ray crystallographic analysis revealed dihedral angles of peptide **3c** resembling those of central, *i*+1 and *i*+2 residues of a type VIa β-turn. X-ray analysis of Ac-L-Tyr-*t*-BuPro-NHMe (Figure 7) demonstrated the presence of an amide *cis*-isomer at the *N*-terminus of the 5-*tert*-butylprolyl residue. The sterically bulky 5-*tert*-butyl group influenced the prolyl amide

<sup>24</sup> a) Bennet, A. J.; Somayaji, V.; Brown, R. S.; Santarsiero, B. D. *J. Am. Chem. Soc.* **1991**, *113*, 7563. b) Shao, H.; Jiang, X.; Gantzel, P.; Goodman, M. *Chem. Biol.* **1994**, *1*, 231. c) Bennet, A. J.; Wang, Q.-P.; Slebocka-Tilk, H. Somayaji, V.; Brown, R. S. *J. Am. Chem. Soc.* **1990**, *112*, 6383. d) Kirby, A. J.; Komarov, I. V.; Feeder, N. *J. Am. Chem. Soc.* **1998**, *120*, 7101.

bond and distorted it from planarity. The X-ray structure also illustrated the stabilization of the prolyl *cis*-isomer by stacking interaction between the aromatic and proline rings. An intramolecular hydrogen bond was inferred to exist between *N'*-methyleamide proton and the acetamide carbonyl oxygen from the interatomic distances (2.08 and 2.18 Å).

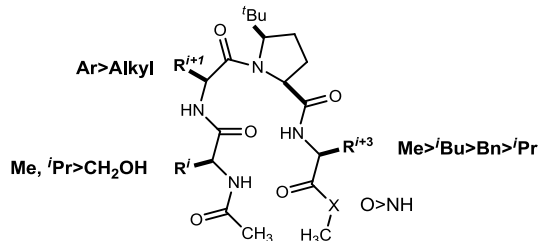
**Figure 7.** X-ray Crystal Structure of Ac-L-Tyr-<sup>t</sup>BuPro-NHMe



Circular Dichroism (CD) spectra were measured for **3a**, **3c**, **3f**, and **3g** in both water and acetonitrile. Peptides **3a** and **3c** exhibited a strong negative peak at 188 nm, a positive band at 209 nm and a weak negative band at 227 nm, and were assigned to a  $\beta$ -turn conformation.<sup>25</sup>

In addition to the dipeptides, Lubell also synthesized a series of tetrapeptides (Ac-Xaa-Yaa-5-<sup>t</sup>BuPro-Zaa-XMe) to examine the influence of the sequence on the amide equilibrium and the turn geometry (Figure 8).<sup>26</sup>

**Figure 8.** Influence of Sequence on the Amide Equilibrium



<sup>25</sup> Deslaurieirs, R.; Evans, D. J.; Leach, S. J.; Meinwald, Y. C.; Minasian, E.; Némethy, G.; Rae, I. D.; Scheraga, H. A.; Somorjai, R. L.; Stimson, E. R.; Van Nispen, J. W.; Woody, R. W. *Macromolecules* **1981**, *14*, 985.

<sup>26</sup> Halab, L.; Lubell, W. D. *J. Am. Chem. Soc.* **2002**, *124*, 2474.

The relative population of *cis* and *trans*-proline amide isomers was determined by integrating the *tert*-butyl singlets and the *N'*-methanamide or methyl ester signals in the <sup>1</sup>H NMR spectroscopy. The *cis*-isomer geometry was stabilized by aliphatic residues, such as alanine and valine in the *i* position (Table 2). A significant augmentation of the *cis*-isomer was observed when an aromatic residue was placed at the *N*-terminus of proline (*i*+1 residue). At the *i*+3 position of the peptide, alanine and lysine were more likely than other amino acid residues to favor a higher *cis*-isomer population. Also, when the *N'*-methanamide was replaced by a methylester, a significant increase in the *cis*-isomer population was observed.

**Table 2.** Amide Isomer Equilibrium of Tetrapeptides Ac-Xaa-Yaa-5-<sup>t</sup>BuPro-Zaa-XMe

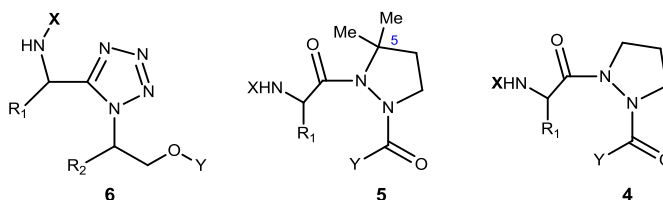
entry	Xaa ( <i>i</i> )	Yaa( <i>i</i> +1)	( <i>i</i> +2)	Zaa ( <i>i</i> +3)	X	% <i>cis</i> -isomer
1	Ala	Ala	5- <sup>t</sup> BuPro	Ala	NH	49
2	Ala	Ala	5- <sup>t</sup> BuPro	Leu	NH	44
3	Ala	Ala	5- <sup>t</sup> BuPro	Phe	NH	47
4	Ala	Ala	5- <sup>t</sup> BuPro	Phe	O	73
5	Ala	Leu	5- <sup>t</sup> BuPro	Leu	NH	50
6	Ala	Leu	5- <sup>t</sup> BuPro	Phe	NH	43
7	Ala	Phe	5- <sup>t</sup> BuPro	Phe	NH	62
8	Ala	Phe	5- <sup>t</sup> BuPro	Leu	NH	65
9	Ala	Phe	5- <sup>t</sup> BuPro	Val	NH	52
10	Ala	Phe	5- <sup>t</sup> BuPro	Val	O	68
11	Ala	Phe	5- <sup>t</sup> BuPro	Lys	O	79
12	Ala	Phe	5- <sup>t</sup> BuPro	Ala	NH	68
13	Ala	Phe	5- <sup>t</sup> BuPro	Ala	O	84
14	Ser	Phe	5- <sup>t</sup> BuPro	Ala	NH	70
15	Ser	Phe	5- <sup>t</sup> BuPro	Ala	O	73
16	Val	Phe	5- <sup>t</sup> BuPro	Ala	O	80
17	Ala	Phe	Pro	Ala	NH	22
18	Ala	Phe	Pro	Ala	O	9

When the 5-*tert*-butyl group was replaced by hydrogen, the *cis*-isomer population decreased from 68-84% to 9-22% (entries 17 and 18), indicating that the steric interaction between the bulky 5-*tert*-butyl group and the side chain of the residue attached to the *N*-terminus of proline disfavored the *trans*-isomer, thereby enhancing the *cis*-isomer population.

The coupling constant values ( $^3J_{\text{NH-C}\alpha\text{H}}$ ) for the  $i+1$  and  $i+2$  residues of tetrapeptides (entries 13 and 16, 3.7 Hz) exhibiting the highest *cis*-isomer populations are characteristic of a turn structure with a dihedral angle of  $-60^\circ$  for the  $i+1$  residue in a type VIa  $\beta$ -turn.<sup>27</sup>

In an aza-amino acid, the  $\alpha$ -carbon is replaced by a nitrogen. Incorporation of such residues into biologically active peptides was pioneered by Dutta and Morley.<sup>28</sup> Additionally, Marshall has studied peptides containing tetrazoles and azaprolines (Figure 9).<sup>29</sup> The probability of the occurrence of a *cis*- $\alpha$  conformation in an azaPro-containing peptide was almost 100%. The conformational preference in **4** was mainly due to an unfavorable lone-pair/lone-pair repulsion between the preceding carbonyl oxygen and the  $\alpha$ -nitrogen in the *trans*-amide conformer. Installation of alkyl substituents at C5 of azPro-containing peptides (**5**) further augments the *cis*-amide conformer population. The 1,5-tetrazole ring **6** also fixes the amide bond in a *cis* geometry.

**Figure 9.** Tetrazoles and Azaprolines as Mimics



Oxaproline and thioproline are often referred to as pseudoprolines due to their structural similarities to the naturally occurring amino acid proline. A modest increase in preference for the *cis*-amide conformation was observed for **7** and **8**. This is probably due

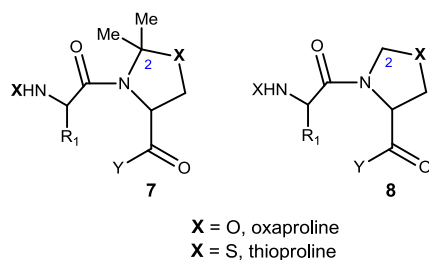
<sup>27</sup> a) Valdeavella, C. V.; Blatt, H. D.; Pettitt, B. M. *Int. J. Peptide Protein Res.* **1995**, *46*, 372. b) Wang, Y.; Scott, P. G.; Sejbál, J.; Kotovych, G. *Can. J. Chem.* **1996**, *74*, 389.

<sup>28</sup> Dutta, A. S.; Morley, J. S. *J. Chem. Soc., Perkin Trans. 1*, **1975**, 1712.

<sup>29</sup> a) Zabrocki, J.; Smith, G. D.; Dunbar, J. B., Jr.; Iijima, H.; Marshall, G. R.; *J. Am. Chem. Soc.* **1988**, *110*, 5875. b) Zhang, W. J.; Berglund, A.; Cao, J. L.-F.; Couty, J.-P.; Gershengorn, M. C.; Marshall, G. R. *J. Am. Chem. Soc.* **2003**, *125*, 1221.

to the induced dipole of the C<sub>δ</sub>-X<sub>γ</sub> bond, which interacts with the preceding carbonyl group, containing a partial negative charge in the *cis* conformation rather than in the *trans* conformation. Mutter's synthesis of pseudo-prolines (oxazolidines and thiazolidines) as molecular hinges revealed a pronounced effect of the 2-C substituents on the *cis* to *trans* ratio of the amide bond in solution.<sup>30</sup> 2,2-Dimethylated derivatives adopted the *cis* amide conformation with high preference (Figure 10). These results were supported by conformational energy calculations.

**Figure 10.** Mutter's Oxazolidines and Thiazolidines as Proline Mimics



The bicyclic analog is also a surrogate for *cis*-peptidyl proline, and forming a lactam-bridged type VI turn mimetic. The bicyclic approach incorporates a second ring in the opposite direction of the pyrrolidine ring to further constraint the *cis*-amide bond. Many different types of bicyclic analogs are possible depending upon the size of the constraint and the chemical characteristics of linker groups. Germanas prepared and characterized an extensive series of bis-amino acid conjugates of a novel  $\beta$ -turn mimic.<sup>31</sup> These peptidomimetics had the ability to form either singly or doubly hydrogen-bonded

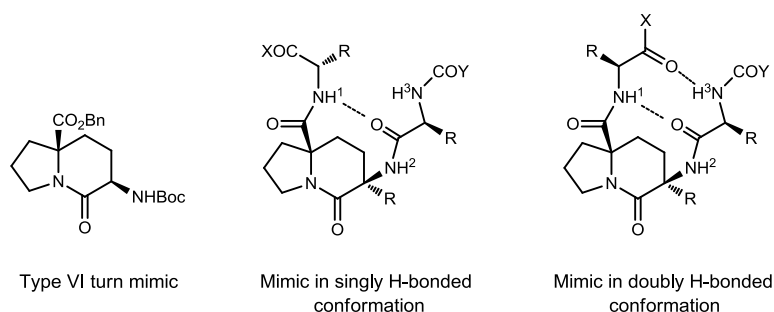
<sup>30</sup> a) Wittelsberger, A.; Keller, M.; Scarpellino, L.; Acha-Orbea, H.; Mutter, M. *Angew. Chem. Int. Ed.* **2000**, *39*, 1111. b) Dumy, P.; Keller, M.; Ryan, D. E.; Rohwedder, B.; Wöhr, T.; Mutter, M. *J. Am. Chem. Soc.* **1997**, *119*, 918. c) Keller, M.; Sager, C.; Dumy, P.; Schutkowski, M.; Fischer, G.; Mutter, M. *J. Am. Chem. Soc.* **1998**, *120*, 2714.

<sup>31</sup> a) Kim, K.; Germanas, J. P. *J. Org. Chem.* **1997**, *62*, 2847. b) Kim, K.; Germanas, J. P. *J. Org. Chem.* **1997**, *62*, 2853.



conformations, to represent  $\beta$ -turn or antiparallel  $\beta$ -ladder structures respectively (Figure 11).

**Figure 11.** Singly and Doubly H-bonded Mimics



## 1.4. Applications of $\beta$ -turn

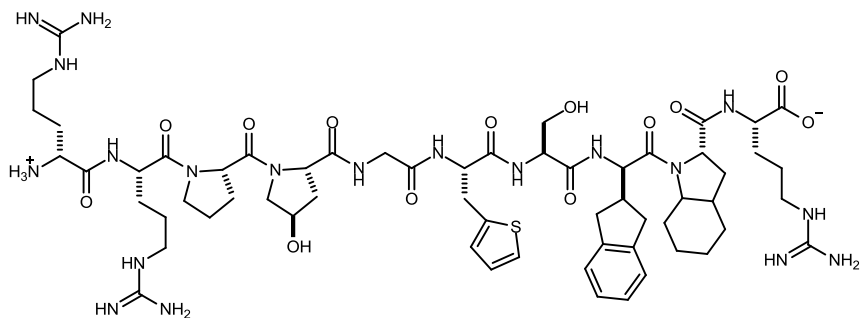
### 1.4.1. Pharmaceuticals

As a result of its unique *trans-cis* isomerization profile, proline can assist the formation of  $\beta$ -turns. The type VI  $\beta$ -turn is a unique member of the  $\beta$ -turn family of peptides, since it is the only turn that adopts an *s-cis* peptide bond.<sup>14,17</sup> Type VI  $\beta$ -turns have been shown to be the recognition sites for peptidyl prolyl isomerases (PPIases) which can accelerate protein folding by catalyzing the interconversion of *cis* and *trans* amide bond conformers.<sup>32</sup> Type VI  $\beta$ -turn conformations play important roles in the recognition and reactivity of bioactive peptides and proteins. For example, a type VI  $\beta$ -turn is required for thrombin-catalyzed cleavage of the V<sub>3</sub> loop of HIV gp120, a prerequisite to viral infection.<sup>33</sup> Natural-type VI  $\beta$ -turns always contain a proline amino acid as the *i*+2<sup>th</sup> residue since peptides incorporating this amino acid are the only ones that can substantially exhibit an *s-cis* configuration.

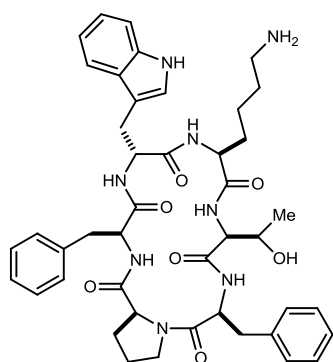
<sup>32</sup> Fischer, S.; Michnick, S.; Karplus, M. *Biochemistry* **1993**, 32, 12830.

<sup>33</sup> Johnson, M. E.; Lin, Z.; Padmanabhan, K.; Tulinsky, A.; Kahn, M. *FEBS Lett.* **1994**, 337, 4.

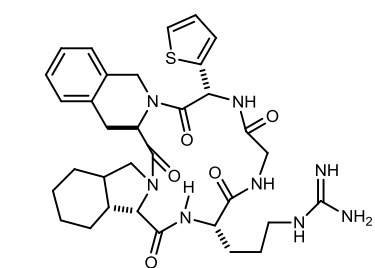
**Figure 12.** Peptidic and Peptidomimetic ligands



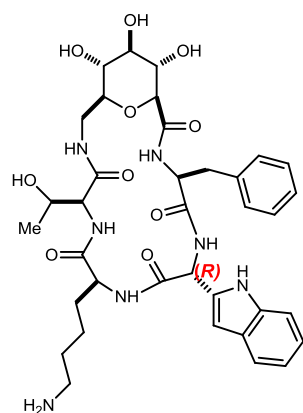
**Bradykinin antagonist B-9340 (two  $\beta$ -turn)**



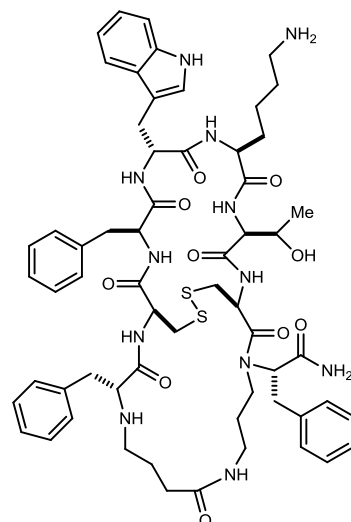
**Cyclic hexapeptide analogue of Somatostatin (Type II'  $\beta$ -turn conformation)**



**Bradykinin receptor antagonist (pA<sub>2</sub> 7.4) (Type II'  $\beta$ -turn conformation)**



**Glucose scaffold containing analogue of Somatostatin (Type II'  $\beta$ -turn conformation)**



**A bicyclic analogue of Somatostatin (Type II'  $\beta$ -turn conformation)**

G protein-coupled receptors (GPCRs) are seven transmembrane helical bundle proteins found on the surface of all cells. They mediate cellular responses to a diverse range of extracellular stimuli, including both endogenous chemical signals and

exogenous environmental agents (e.g. light, amino acids, peptides, proteins, small organic molecules such as amines and lipids, nucleosides, nucleotides, metal ions, and pharmaceuticals). Once activated by an extracellular signal, GPCRs activate heterotrimeric G proteins that interact promiscuously with multiple receptors including guanine nucleotides GTP and GDP, and with the GPCR itself. Of the several hundred GPCRs known to be activated by peptide or protein hormones, only peptide-activated GPCRs for angiotensin, endothelin, oxytocin, neurokinin, and somatostatin have been successfully targeted by small molecule pharmaceuticals.<sup>34</sup> A large number of synthetic non-peptidic and peptidomimetic ligands have been developed as GPCR agonists or antagonists (Figure 12). A general “turn” motif is adopted by these peptidic and peptidomimetic ligands (small molecule) in solution and is likely associated with binding to, and mediating bioactivity through, GPCRs. There is a growing collection of turn-inducing constraints that are now available for fixing  $\beta$ -turns in peptides and cyclic peptides and many such constraints have become useful as scaffolds for constructing nonpeptidic ligands for GPCRs.<sup>35</sup>

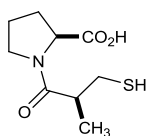
Recognition of a turn conformation normally only involves interactions between side chain residues of the ligand with the receptor, and thus the peptide turn can be considered to be a scaffold, which could potentially be either conformationally constrained or entirely replaced by an alternative rigid non-peptidic scaffold designed to support moieties that may mimic peptide side chains.

---

<sup>34</sup> Tyndall, J. D. A.; Pfeiffer, B.; Abbenante, G.; Fairlie, D. P. *Chem. Rev.* **2005**, *105*, 793.

<sup>35</sup> a) Fairlie, D. P.; Abbenante, G.; March, D. R. *Curr. Med. Chem.* **1995**, *2*, 654. b) Fairlie, D. P.; West, M. L.; Wong, A. K. *Curr. Med. Chem.* **1998**, *5*, 29. c) Andrews, M. J. I.; Tabor, A. B. *Tetrahedron* **1999**, *55*, 11711. d) Hruby, V. J.; al-Obeidi, F.; Kazmierski, W. *Biochem. J.* **1990**, *268*, 249. e) Hruby, V. J.; Sharma, S. D. *Curr. Opin. Biotechnol.* **1991**, *2*, 599. f) Stradley, S. J.; Rizo, J.; Bruch, M. D.; Stroup, A. N.; Gierasch, L. M. *Biopolymers.* **1990**, *29*, 263. g) Toniolo, C. *Int. J. Pept. Protein Res.* **1990**, *35*, 287. h) Giannis, A. *Angew. Chem. Int. Ed.* **1993**, *32*, 1244.

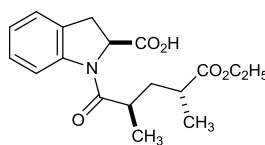
Angiotensin I-converting enzyme is a zinc metallopeptidase that catalyzes the proteolysis of angiotensin I to the vasopressor angiotensin II.<sup>36</sup> ACE inhibitors are widely used to treat cardiovascular diseases, including high blood pressure, heart failure, coronary artery disease, and kidney failure. Due to the critical role of ACE in



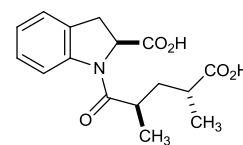
**Captopril**

cardiovascular and renal diseases, it has been an attractive target for drug design. Captopril was the first marketed orally active ACE inhibitor approved for treatment of human hypertension.<sup>37</sup> Cocrystallization studies

have shown that the *trans*-amide rotamer is the biologically active form of captopril. Captopril lowers arterial pressure effectively in renovascular hypertension and essential hypertension. However, clinically, captopril occasionally produces adverse effects that may be related to the presence of a thiol group in the molecule. This initiated a search for nonthiol ACE inhibitors. These efforts resulted in identification of pentopril as a nonthiol ACE inhibitor. Pentopril<sup>38</sup> is the ethyl ester derivative of the dicarboxylic acid CGS 13934, which is believed to be the biologically active form. The observed rotamer around the proline amide bond is *trans* in Pentopril. Structural studies have shown that bulky hydrophobic group in Pentopril enhances the enzyme-substrate interaction, and



**Pentopril**



**CGS 13934**

a thiol group in the molecule. This initiated a search for nonthiol ACE inhibitors. These efforts resulted in identification of pentopril as a nonthiol ACE inhibitor. Pentopril<sup>38</sup> is the ethyl ester derivative of the dicarboxylic acid CGS 13934, which is believed to be the biologically active form. The observed rotamer around the proline amide bond is *trans* in Pentopril. Structural studies have shown that bulky hydrophobic group in Pentopril enhances the enzyme-substrate interaction, and

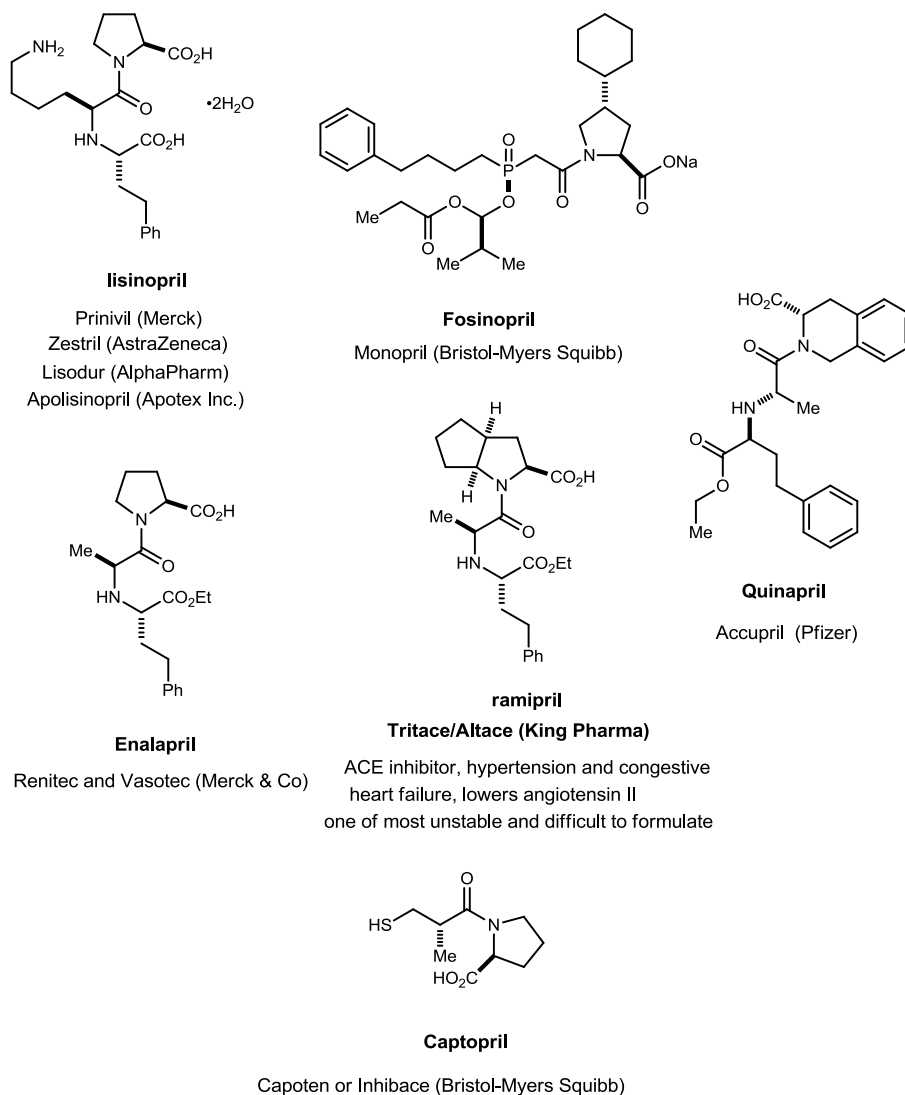
<sup>36</sup> a) Ehlers, M. R. W.; Fox, E. A.; Strydom, D. J.; Riordan, J. F. *Proc. Natl. Acad. Sci.* **1989**, *86*, 7741. b) Turner, A. J.; Hooper, N. M. *Trends Pharmacol. Sci.* **2002**, *23*, 177. c) Eriksson, U.; Danilczyk, U.; Penninger, J. M. *Curr. Biol.* **2002**, *12*, 745. d) Acharya, K. R.; Sturrock, E. D.; Riordan, J. F.; Ehlers, M. R. W. *Nat. Drug Discov.* **2003**, *2*, 891.

<sup>37</sup> a) Cushman, D. W.; Cheung, H. S.; Sabo, E. F.; Ondetti, M. A. *Biochemistry.* **1977**, *16*, 5484. b) Ondetti, M. A.; Rubin, B.; Cushman, D. W. *Science.* **1977**, *196*, 441.

<sup>38</sup> Goodman, F. R.; Weiss, G. B.; Hurley, M. E. *New Drugs Annual: Cardiovascular Drugs.* **1985**, *3*, 1985.

thus making it more potent than Captopril.<sup>39</sup> In last two decades, several other peptidic and peptidomimetic ACE inhibitor have been synthesized (Figure 13).

**Figure 13.** Peptidic and Peptidomimetic ACE Inhibitor



Lubell *et al.* employed 5-*tert*-butylproline to explore the conformational requirements for prolyl peptide bioactivity in oxytocin.<sup>40</sup> Due to the steric interaction of

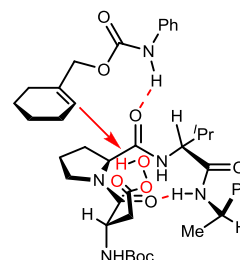
<sup>39</sup> a) Thorsett, E. D.; Harris, E. E.; Aster, S. D.; Petersen, E. R.; Snyder, J. P.; Springer, J. P.; Hirsfield, J.; Tristram, E. E.; Patchett, A. A.; Ulm, E. H.; Vassil, T. C. *J. Med. Chem.* **1986**, 29, 251. b) Ksander, G. M.; Yuan, A. M.; Diefenbacher, C. G.; Stanten, J. L. *J. Med. Chem.* **1985**, 28, 1606.





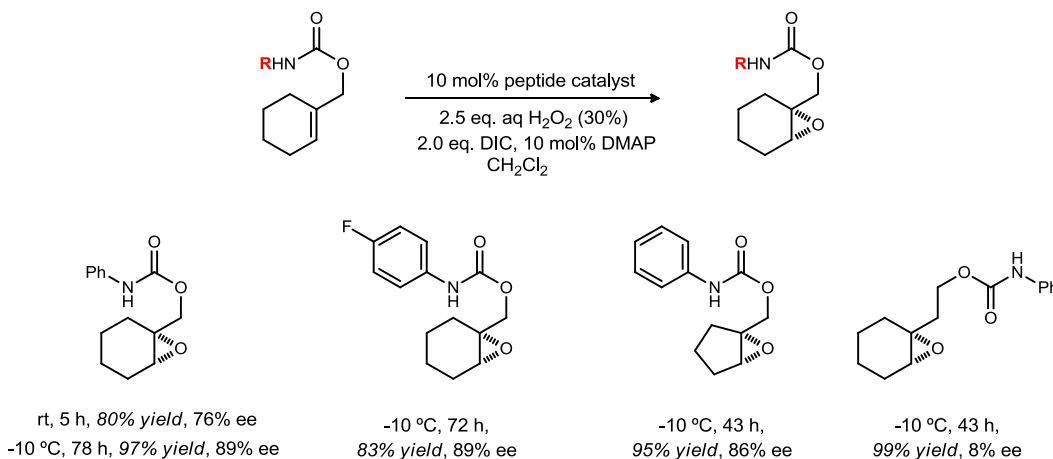
Only olefin tethered carbamate substrates gave promising results in the epoxidation reactions (Figure 16). Good epoxide yields and remarkable enantioselectivities were achieved, and lower reaction temperatures generally led to increased enantioselectivity. Elongation of the tether by only one methylene group is deleterious for stereoselectivity, leading to lower diastereo- and enantioselection.

The need for a hydrogen-bonding substituent (such as the tethered carbamate) and the high sensitivity of the enantioselectivity to the distance between the hydrogen-bonding moiety and the double bond to be epoxidized points to hydrogen



bonding as the crucial feature of catalyst-substrate interaction. A hypothetical hydrogen-bonded transition state proposed by Miller *et al.* shows that the carbamate group of the substrate is the hydrogen bond donor and the proline carboxamide group of the catalyst is the acceptor.

**Figure 16.** Asymmetric Epoxidation of Olefins in the Presence of the Peptide Catalyst

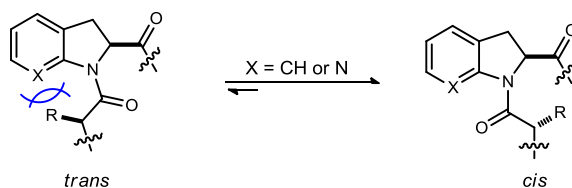




## 1.5. Synthesis of Indoline and Azaindoline Amino Acids<sup>44,45</sup>

While all the proline analogues discussed in the previous section have proven useful for inducing specific constraints on prolyl *N*-terminal bond isomerization, no one template can lay claim on the ability to shift the prolyl amide equilibrium toward both the *cis* and *trans* isomers. This is in part because none of these analogues have strategically positioned functional groups to alter the amide equilibrium. We investigated the effect of a fused aromatic ring (indoline and azaindoline) on prolyl *N*-terminal bond isomerization. It was hypothesized that the steric interactions between the proline aromatic ring and C $\alpha$  substituents would disfavor the *trans*-isomer, thereby promoting the prolyl *cis*-amide population (Figure 17).

Figure 17. *cis-trans* Isomerism in Indoline Containing Peptides



In order to determine the energy barrier for the *cis-trans* isomerization of peptides showing an equilibrium between the two conformations at room temperature, we constructed model dipeptides incorporating the indoline amino acid. Both enantiomers of the carboxyl terminus of the indoline amino acid were also easily synthesized, enabling the effect of this chiral center on the protein structure to be evaluated.

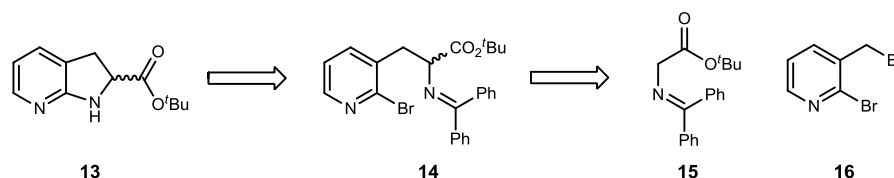
From the retrosynthetic perspective, we proposed that the protected indoline (**13**) would be accessed from a free radical mediated aryl amination of **14**, utilizing tributyl

<sup>44</sup> Srinivasan, J. M. Ph. D. Dissertation, Indiana University Bloomington, IN, **2008**.

<sup>45</sup> Srinivasan, J. M.; Burks, H. E.; Smith, C. R.; Viswanathan, R.; Johnston, J. N. *Synthesis*, **2005**, 330.

tinhydride and AIBN.<sup>46</sup> The Schiff base would be formed via enantioselective alkylation of O'Donnell's glycine Schiff base (**15**)<sup>47</sup> with alkylbromide **16**, using cinchona alkaloids and utilizing Corey's improved protocol (Scheme 1).<sup>48</sup>

**Scheme 1.** Retrosynthetic Analysis of Indoline and Azaindoline Amino Acid



The enantioselective synthesis of the azaindoline amino acids commences with the formation of glycine Schiff base **15**. Treatment of *tert*-butyl chloroacetate with sodium azide produced the corresponding azide, which was then reduced by hydrogenolysis to afford the glycine *tert*-butyl ester. The amine was then transiminated with benzophenone imine to form the Schiff base (**15**) in 85% yield (Scheme 2).

The pyridyl dibromide (**16**) was synthesized in three steps from commercially available 2-bromopyridine. Directed metalation and formylation of 2-bromopyridine using LDA and DMF, followed by reduction of the resulting aldehyde afforded the primary alcohol (**17**). Treatment of the alcohol with PBr<sub>3</sub> provided the primary bromide (**16**) in good yield.

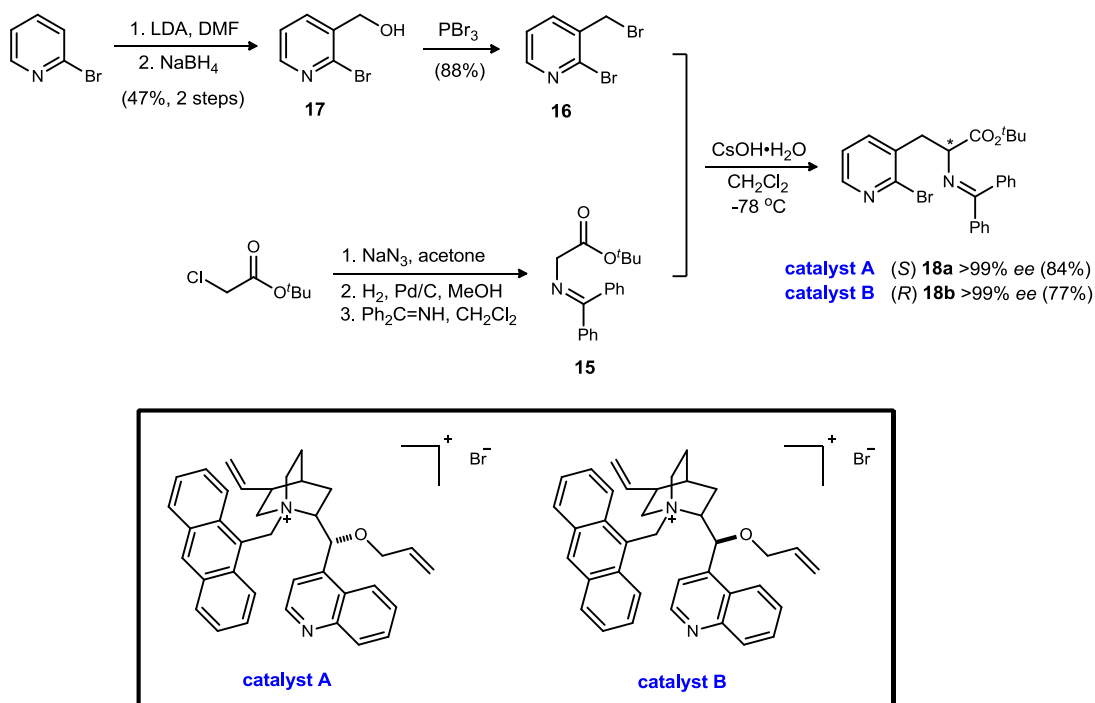
<sup>46</sup> a) Viswanathan, R.; Plotkin, M. A.; Prabhakaran, E. N.; Johnston, J. N. *J. Am. Chem. Soc.* **2003**, *125*, 163. b) Viswanathan, R.; Mutnick, D.; Johnston, J. N. *J. Am. Chem. Soc.* **2003**, *125*, 7266. c) Johnston, J. N.; Plotkin, M. A.; Viswanathan, R.; Prabhakaran, E. N. *Org. Lett.* **2001**, *3*, 1009. d) Viswanathan, R.; Smith, C. R.; Prabhakaran, E. N.; Johnston, J. N. *J. Org. Chem.* **2008**, *73*, 3040.

<sup>47</sup> a) O'Donnell, M. J. *Catalytic Asymmetric Synthesis*, 2<sup>nd</sup> ed.; Ojima, I., Ed.; Wiley-VCH: NY, **2000**, Chap. 10. b) Maruoka, K.; Ooi, T. *Chem. Rev.* **2003**, *103*, 3013. c) O'Donnell, M. J. *Aldrichimica Acta* **2001**, *34*, 3.

<sup>48</sup> a) Corey, E. J.; Xu, F.; Noe, M. C. *J. Am. Chem. Soc.* **1997**, *119*, 12414. b) Lygo, B.; Wainwright, P. G. *Tetrahedron Lett.* **1997**, *38*, 8595. c) Lygo, B.; Andrews, B. I. *Acc. Chem. Res.* **2004**, *37*, 518.

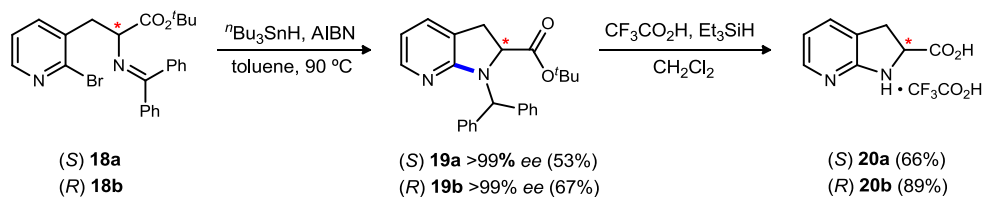
With the imine (**15**) and the pyridyl dibromide (**16**) electrophile in hand, an enantioselective glycine Schiff base alkylation<sup>48</sup> was effected under phase transfer catalyzed conditions to afford **18a** using cinchonidine derived catalyst A, and **18b** using cinchonine derived catalyst B (Scheme 2) in 3 days at -60 °C. Following the purification, the resulting white solid was triturated with hexanes to afford **18a** and **18b** in >99% ee.

**Scheme 2.** Enantioselective Alkylation

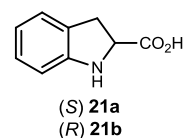


The stage was now set to examine the radical mediated aryl amination<sup>1</sup> reaction to form the indoline ring. Treatment of the Schiff base (**18a** and **18b**) with <sup>n</sup>Bu<sub>3</sub>SnH and AIBN in benzene at 90 °C provided the two individual indoline enantiomers (**19a** and **19b**) in >99% ee after trituration with hexanes (Scheme 3). Global deprotection of the protected indoline (**19a** and **19b**) utilizing trifluoroacetic acid and triethylsilane, provided L-<sup>N7</sup>Ind amino acid (66%) and D-<sup>N7</sup>Ind amino acid (89%), as their trifluoroacetate salts.

**Scheme 3.** Synthesis of Azaindoline Amino Acids



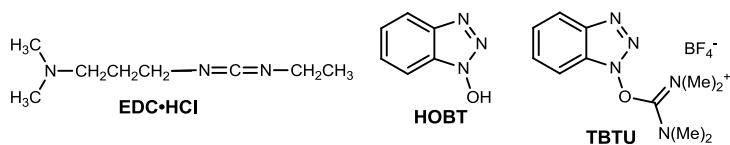
The corresponding indoline amino acids L-Ind amino acid and D-Ind amino acid were similarly synthesized starting from the commercially available 2-bromobenzyl bromide via enantioselective alkylation using catalysts A and B, followed by the radical amination reaction and subsequent global deprotection step to afford the indoline amino acids (**21a** and **21b**) as the free base.



**1.6. Synthesis and Conformational Analyses of Indoline and Azaindoline Amino Acid-Containing Dipeptides**

In order to determine the energy barrier for the *cis-trans* isomerization of peptides showing an equilibrium between the two conformations at room temperature, model dipeptides incorporating the indoline and azaindoline amino acids were synthesized. Also, various combinations of peptide coupling reagents were investigated (TBTU and HOBT, and EDC·HCl and HOBT), but they consistently failed to yield the desired product (Figure 18) in significant yield.<sup>44,49</sup>

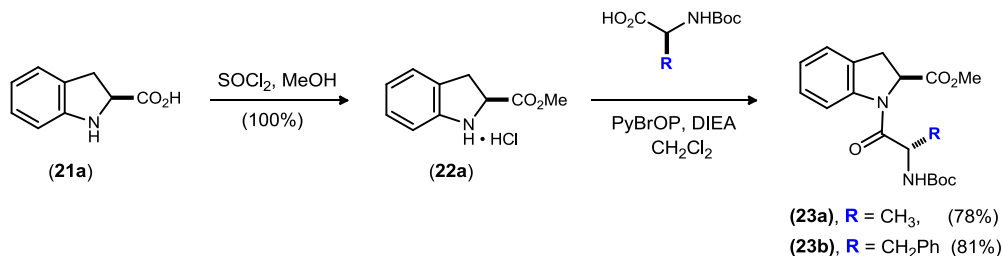
**Figure 18.** Amide Coupling Reagents



<sup>49</sup> Heather Burks, B. S. Thesis, Department of Chemistry, Indiana University, May 2003.

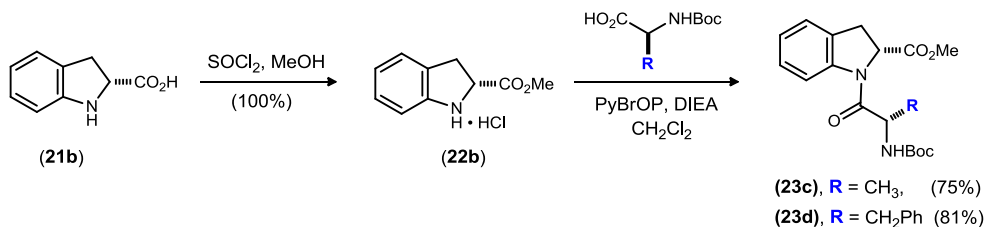
The attention was then focused on the protection of the amino acid as its ester. Treatment of **21a** with thionyl chloride afforded the methyl ester (**22a**) in quantitative yield (Scheme 4). The methyl ester amino acid was treated with Boc-L-alanine in the presence of BOPCl for the construction of the dipeptide containing the sequence Boc-L-Ala-L-Ind-OMe (**23a**).<sup>44</sup> The reaction proceeded to yield only 34% of the dipeptide, and no further extension of the reaction time improved the yield. However, a substantial increase in the yield (78%) was observed when PyBroP<sup>50</sup> was used as the peptide coupling reagent (Scheme 4). Substituting Boc-L-alanine with Boc-L-phenylalanine in the above reaction afforded Boc-L-Phe-L-Ind-OMe (**23b**) in good yield as well.

**Scheme 4.** Synthesis of L-Ind-OMe Containing Dipeptides



Substitution of (*R*)-indoline amino acid into the above procedure furnished the desired dipeptides (Scheme 5).

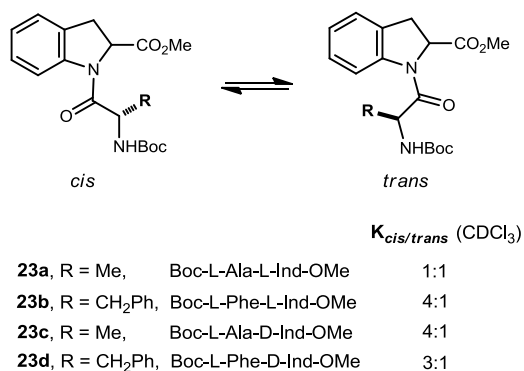
**Scheme 5.** Synthesis of D-Ind-OMe Containing Dipeptides



<sup>50</sup> a) Coste, J.; Frérot, E.; Jouin, P.; Castro, B. *Tetrahedron Lett.* **1991**, 32, 1967. b) Coste, J.; Frérot, E.; Patrick, J. J. *Org. Chem.* **1994**, 59, 2437.

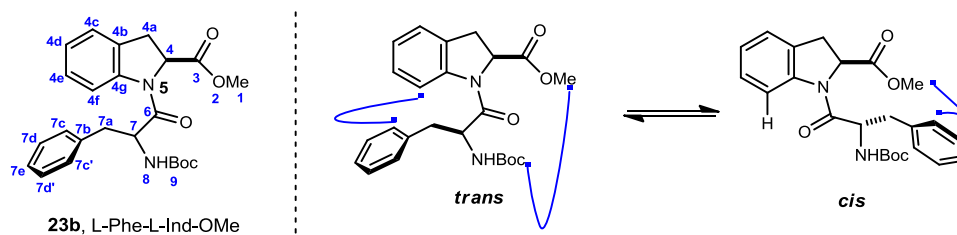
$^1\text{H}$  NMR analysis of the dipeptide **23a** showed a mixture of *cis-trans* isomers about the amide bond (1:1 in  $\text{CDCl}_3$ , and  $\sim 2:1$  in  $d_8$ -toluene), whereas the dipeptide **23b** showed 4:1 *cis:trans* ratio in  $\text{CDCl}_3$  (Figure 19). This observation was in perfect agreement with our original hypothesis that the  $\text{A}^{1,3}$ -strain developed by incorporating a fused aromatic ring to proline would disfavor the *trans* conformation, thereby promoting the *cis*-population. However surprisingly, incorporation of (*R*)-indoline amino acid promoted the *N*-prolyl-*cis*-rotamer population for both the dipeptides (**23c** and **23d**).

**Figure 19.** Equilibrium Constant Measurements of Ind- Dipeptides



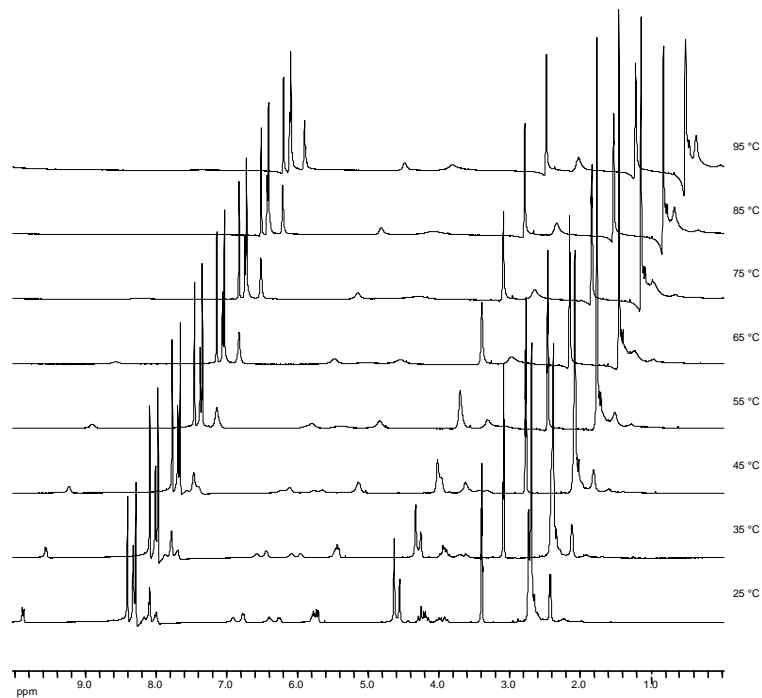
The *cis*-isomer was assigned based on the 2D NMR analysis.  $\text{H}7\text{c}/\text{H}4\text{f}$  and  $\text{H}9/\text{H}1$  NOESY correlations confirmed the presence of *trans*-rotamer. A strong  $\text{H}7\text{c}/\text{H}1$  correlation was observed, which was consistent with the *cis*-amide bond (Figure 20). Also, a downfield shift for  $\text{H}4\text{f}$  (8.12 ppm) was observed in the *cis*-rotamer, probably due to the deshielding effect by  $\text{O}6$ . This uncharacteristic downfield shift of  $\text{H}4\text{f}$  was utilized in determining the *trans-cis* isomer population for the rest of the (*R*)- and (*S*)-indoline amino acid containing peptides

**Figure 20.** NOESY Correlations of L-Phe-L-Ind-OMe



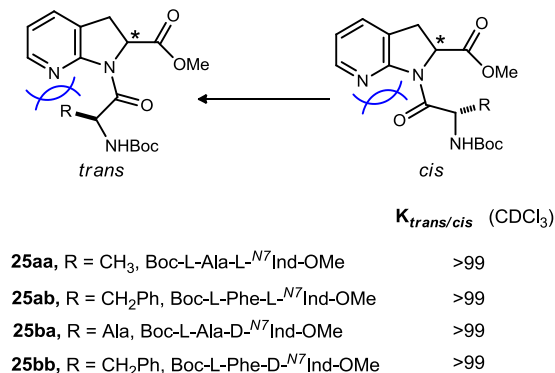
A variable temperature experiment (in  $d_8$ -toluene from 25 °C to 95 °C) was conducted for **23a** (Figure 21), and the energy barrier was calculated to be 36 kJ/mol from an Eyring plot (rate constant vs. temperature). The temperature of coalescence of the two isomers was determined to be 75 °C.

**Figure 21.** Variable Temperature Experiment of **23a**



Analogous to the Ind-dipeptides,  $^{N7}$ Ind-dipeptides were synthesized, and investigated for the *cis-trans* rotamer population. Contrary to the Ind amino acid containing dipeptides, the  $^{N7}$ Ind amino acid incorporated dipeptides showed only one set of peaks in  $^1\text{H}$  NMR. This observation was consistent with the presence of just one of the *cis/trans* amide rotamers, offering a rigid system for the type II and II' peptidomimetics. The equilibrium constant measurements for the di and tripeptide systems are presented in Figure 22.

**Figure 22.** Dihedral Angles in Proline-Incorporated Peptides

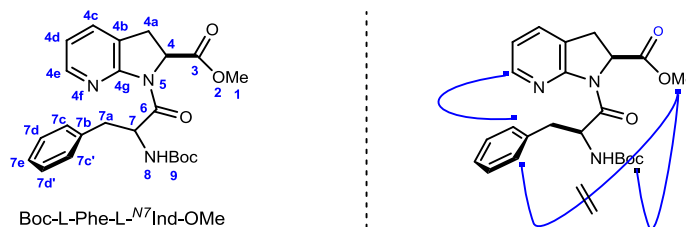


Unlike the Ind-incorporated dipeptides, the  $^{N7}$ Ind-containing di- and tri- peptides predominantly existed in the *trans* conformation. We believe that the lone pair-lone pair repulsion between N4f and O6 overrides the steric repulsion between the  $^{N7}$ Ind aromatic ring and the residue *N*-terminus to the  $^{N7}$ Ind residue (Phe in this case).

For the dipeptide Boc-L-Phe-L- $^{N7}$ Ind-OMe (**25b**), a NOESY correlation between H4e/H7c and H9/H1 were observed, consistent with a prolyl *trans*-amide bond geometry (Figure 23). No such correlation between H7c'/H1 was observed confirming that the dipeptide existed exclusively as the *trans*-amide rotamer.



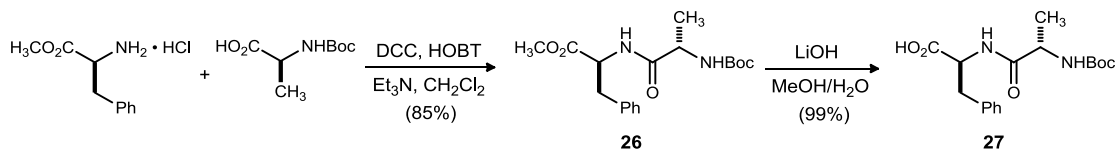
**Figure 23.** NOESY Analysis of Dipeptide **25b**



### 1.7. Synthesis of Ind and <sup>N7</sup>Ind $\alpha$ -Amino Acid-Containing Tetrapeptides

To examine the influence of indoline and azaindoline amino acids on turn geometry, we have introduced these synthetically conserved and noconserved amino acids into a model tetrapeptide, which was reported earlier by Lubell *et al.*<sup>21a</sup> The synthesis commences with the coupling of methyl esters **24a** and **24b** with the dipeptide fragment (**27**). The dipeptide fragment was synthesized from the commercially available Boc-protected alanine and phenyl alanine methyl ester using DCC as the coupling reagent, followed by saponification of the resulting ester (**26**) using lithium hydroxide (Scheme 6).

**Scheme 6.** Synthesis of the Dipeptide Fragment Ala-Phe (**27**)<sup>49</sup>

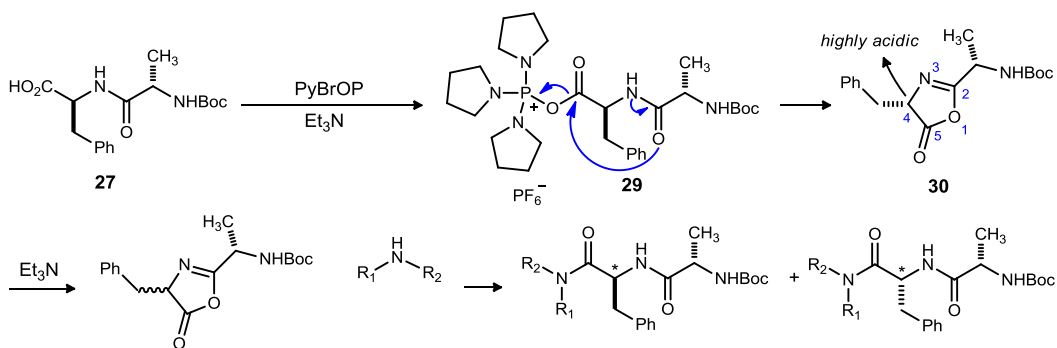


The amine salt (**24a**) was treated with the Ala-Phe dipeptide fragment (**27**) in the presence of PyBroP for the construction of the tripeptide containing the sequence Boc-L-Ala-Phe-L-<sup>N7</sup>Ind-OMe (**28aa** and **28ab**) (eq 1). The reaction proceeded smoothly to provide the desired tripeptides as an inseparable 3:1 mixture of diastereomers in 70%

yield. Substitution of the enantiomeric amine salt (**24b**) into the above procedure furnished the corresponding tripeptides in 69% yield. The tripeptides (**28ba** and **28bb**) were characterized as an inseparable 10:9 mixture of diastereomers.

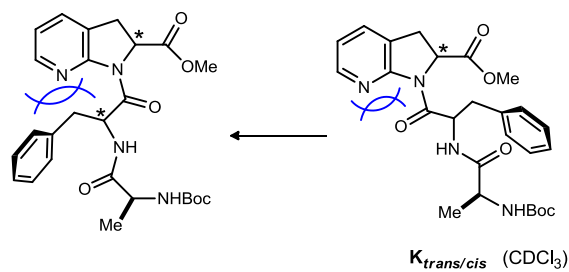
A partial racemization of the Phe- $C_{\alpha}$  stereocenter was observed during the peptide coupling reaction. The carboxylic acid (**27**) is converted to an activated ester **29**, which undergoes an intramolecular cyclization step to form an oxazolone intermediate **30**, with the concomitant release of phosphine oxide. Ionization of the acidic H4 in presence of  $\text{Et}_3\text{N}$  followed by the attack of a secondary amine at C5 leads to the two corresponding diastereomers (Scheme 7).

**Scheme 7.** Mechanism for the racemization of Phe- $C_{\alpha}$  stereocenter



Analogous to the  $N^7$ Ind-incorporated dipeptides, the  $N^7$ Ind-containing tripeptides

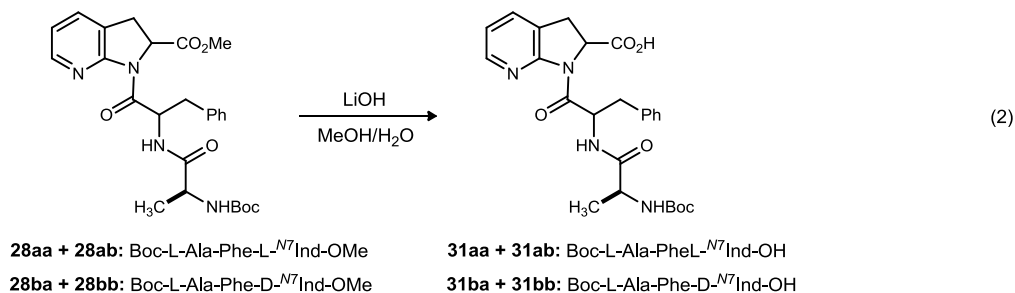
**Figure 24.** Equilibrium Constant Measurements of  $N^7$ Ind-tripeptides



Structure	$K_{trans/cis}$ ( $\text{CDCl}_3$ )
<b>28aa</b> , Boc-L-Ala-D-Phe-L- $N^7$ Ind-OMe	>99
<b>28ab</b> , Boc-L-Ala-L-Phe-L- $N^7$ Ind-OMe	>99
<b>28ba</b> , Boc-L-Ala-D-Phe-D- $N^7$ Ind-OMe	>99
<b>28bb</b> , Boc-L-Ala-L-Phe-D- $N^7$ Ind-OMe	>99

predominantly existed in the *trans* conformation (Figure 24).

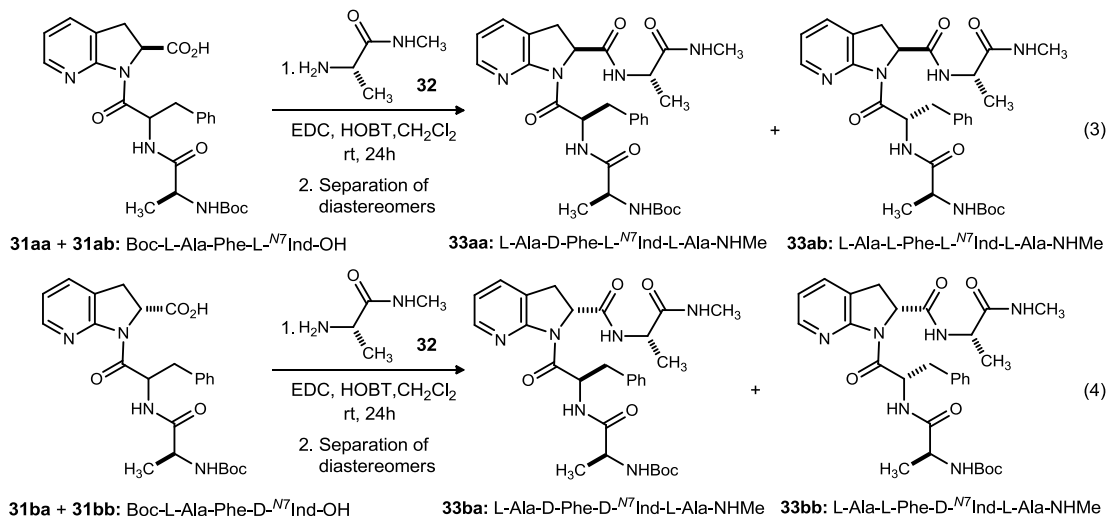
The diastereomeric mixture of the tripeptide methyl esters (**28aa** and **28ab**) was saponified using lithium hydroxide to yield an inseparable mixture of carboxylic acids **31aa** and **31ab** in 85% yield (eq 2). In a similar way, the Boc-L-Ala-Phe-D-<sup>N7</sup>Ind-OMe (**28ba** and **28bb**) tripeptides were also saponified to provide their respective carboxylic acids **31ba** and **31bb**.



The C-terminal alanine fragment was incorporated by coupling the diastereomeric mixture of tripeptides **31aa** and **31ab** with the alanine fragment **32** (eq 3) to afford the desired tetrapeptide with the sequence Boc-L-Ala-Phe-<sup>N7</sup>Ind-Ala-NHMe (analogous to Lubell's peptide sequence Boc-L-Ala-L-Phe-5-*tert*-butylPro-Ala). The two diastereomers showed significant difference in their R<sub>f</sub> values on TLC which enabled their separation by silica column chromatography. The more polar diastereomer was determined to be **33aa** (Boc-L-Ala-D-Phe-L-<sup>N7</sup>Ind-L-Ala-NHMe) and was obtained in 22% yield. The less polar diastereomer was found to be **33ab** (Boc-L-Ala-L-Phe-L-<sup>N7</sup>Ind-L-Ala-NHMe) and was obtained in 44% yield.

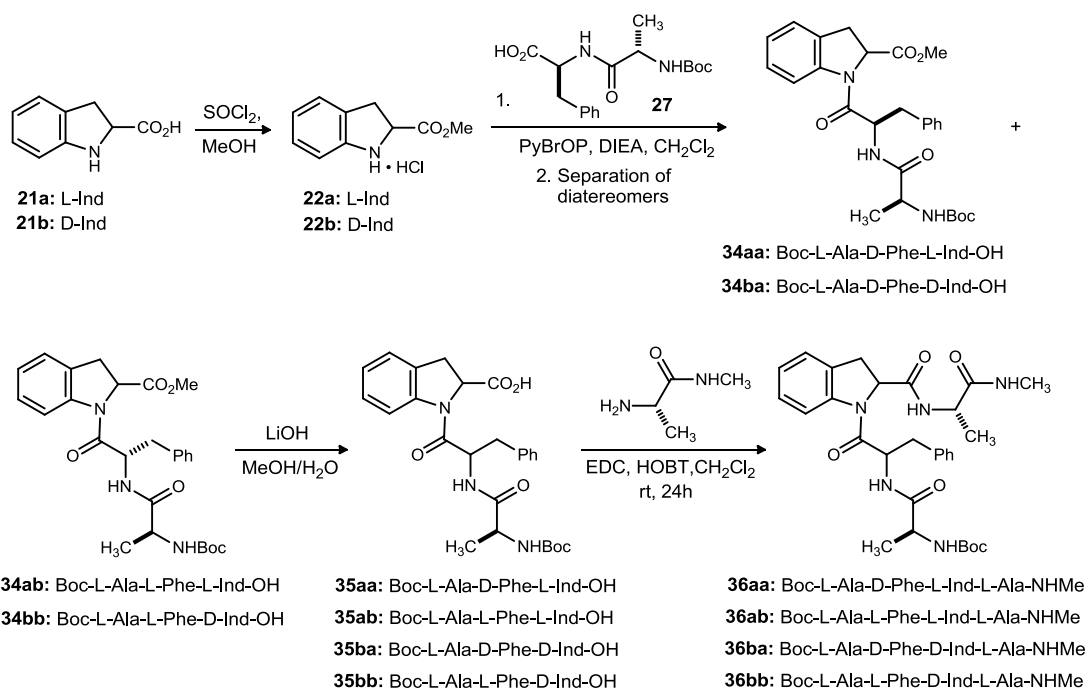
Substitution of D-<sup>N7</sup>Ind tripeptides (**31ba** and **31bb**) in place of L-<sup>N7</sup>Ind peptides also afforded two separable diastereomeric tetrapeptides (more polar: Boc-L-Ala-D-Phe-

D-<sup>N7</sup>Ind-L-Ala-NHMe, **33ba**, 22%; less polar: Boc-L-Ala-L-Phe-D-<sup>N7</sup>Ind-L-Ala-NHMe, **33bb**, 35%) in a similar way (eq 4).



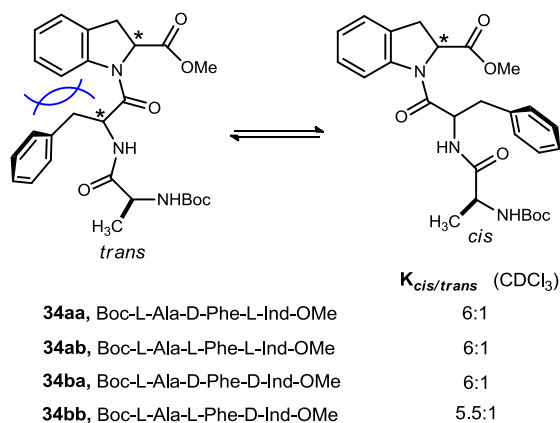
In a manner analogous to the synthesis of azaindoline peptides, the corresponding indoline amino acid-containing tetrapeptides were synthesized from **21a** and **21b** to afford two diastereomers in each case **36aa** (Boc-L-Ala-D-Phe-L-Ind-L-Ala-NHMe), **36ab** (Boc-L-Ala-L-Phe-L-Ind-L-Ala-NHMe), and **36ba** (Boc-L-Ala-D-Phe-D-Ind-L-Ala-NHMe), **36bb** (Boc-L-Ala-L-Phe-D-Ind-L-Ala-NHMe), respectively (Scheme 8).

**Scheme 8.** Synthesis of Indoline Amino Acid Containing Model Tetrapeptide System



The NOESY correlations of the indoline amino acids-containing tripeptides were also evaluated for their equilibrium constants (Figure 25).

**Figure 25.** Equilibrium Constant Measurements of Ind-Tripeptides

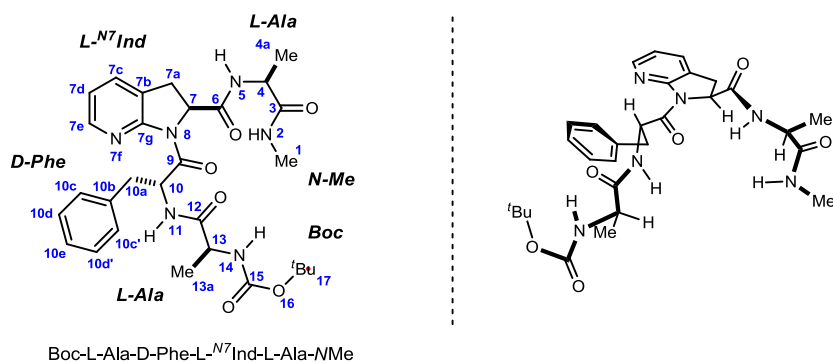


### 1.8. Conformational Analyses of <sup>N7</sup>Ind-Containing Tetrapeptides

The azaindoline tetrapeptides were evaluated by NMR (1D and 2D) experiments for the turn structures and the amide conformations. From the <sup>1</sup>H, <sup>13</sup>C and HSQC (<sup>1</sup>J<sub>CH</sub>), and NOESY NMR experiments, all the proton and carbon chemical shifts of the <sup>N7</sup>Ind tetrapeptides were assigned. Lubell<sup>26</sup> had observed a sequential H $\alpha$ N (*i*, *i*+1) NOEs for all the residues in his tetrapeptides and an additional H $\alpha$ N (*i*, *i*+2) NOE was observed between the  $\alpha$ -hydrogen of Phe and the amide proton of the C-terminal Ala, characteristic of a  $\beta$ -turn.

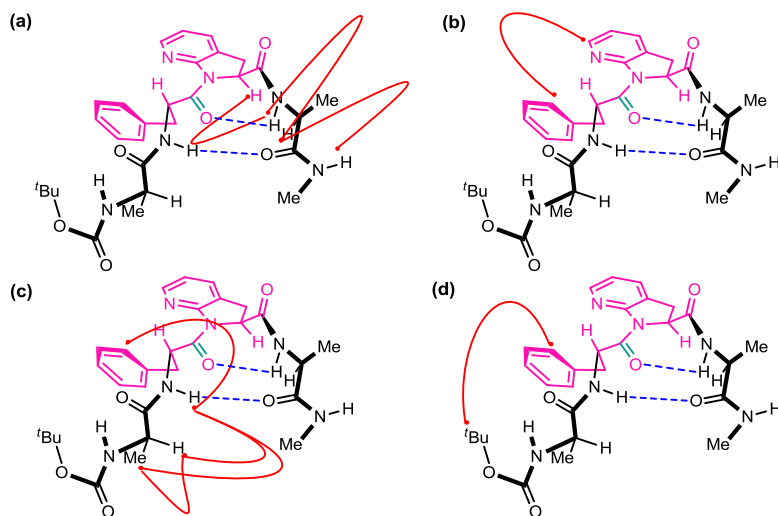
The conformational analysis of the tetrapeptide Boc-L-Ala-D-Phe-L-<sup>N7</sup>Ind-L-Ala-NHMe (**33aa**) is depicted in Figure 26.

**Figure 26.** Conformational Depiction of Boc-L-Ala-D-Phe-L-<sup>N7</sup>Ind-L-Ala-NHMe (**33aa**)



Assignment of both phenylalanine configuration (as D-Phe) and tetrapeptide conformation were made using NOESY data. The crosspeaks could be separated into three local regions (Figure 27, *a-c*) and a long-range correlation (Figure 27, *d*). Beginning from the C-terminal methyl amide, crosspeaks for H2/H4 and H2/H5 defined the *s-trans* conformation of the methyl amide. However a weaker NOESY correlation for H2/H4 suggests that the peptide chain C-terminal to <sup>N7</sup>Ind does not fold back upon itself by 180°. A similar *s-trans* assignment for the alanine amide could be made by observation of a H5/H7 cross peak (Figure 27, *a*).

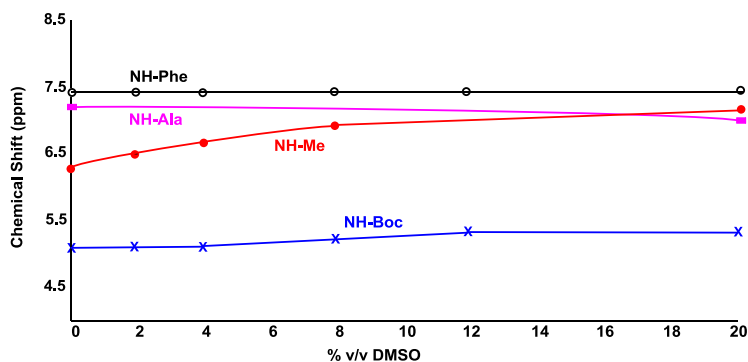
**Figure 27.** Observed Regional (*a-c*) and Long Range (*d*) NOESY Correlations for Tetrapeptide **33aa**



The *s-trans* conformation of the azaindoline amide bond was determined by observation of crosspeaks between H10/H10c and H10c/H7e (Figure 27). Complementary to these are crosspeaks for H10/H11 and H11/H10c', though crosspeaks could not be observed to definitively assign the local conformation of the alanine amide bond as *trans*. Long range crosspeak H17/H10c is consistent with *syn* conformation of the *tert*-butyl group such that it is positioned at the exterior of the turn. Absence of crosspeak H10/H5 confirms the configuration of phenylalanine as (*R*). Absence of H17/H1, H17/H2, H13a/H2 or H13a/H1 crosspeaks are also indicative of the fact that the peptide chain does not fold back on itself by 180°.

Intramolecular hydrogen bonding in **33aa** was evaluated by plotting the change in the chemical shift value of the amide proton as a function of DMSO-*d*<sub>6</sub> added to the peptide in CDCl<sub>3</sub> because exchangeable protons engaged in intramolecular hydrogen bonds are not influenced by strong hydrogen-bonding solvents, such as DMSO- *d*<sub>6</sub>,

**Figure 28.** Effect of Solvent on the NH Amide Protons in **33aa**



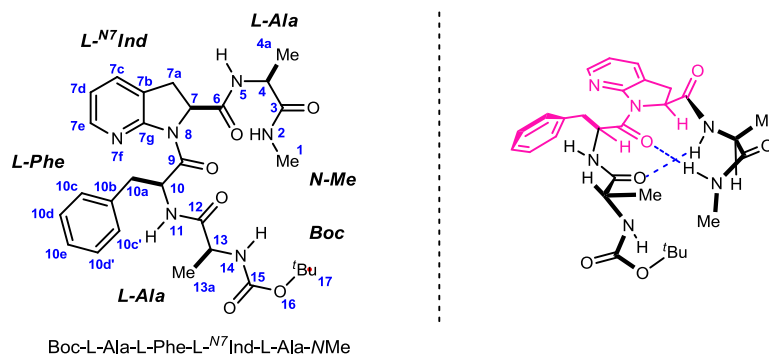
relative to exposed protons.<sup>51</sup> The experiment clearly showed the presence of three NH signals (NH11, NH5, NH14) that were affected minimally by the increasing addition of DMSO-*d*<sub>6</sub>. This study indicated the presence of a hydrogen bond between NH11 and O3

<sup>51</sup> Awasthi, S. K.; Raghothama, S.; Balaram, P. *Biochem. Biophys. Res. Commun.* **1995**, 216, 275.

to form an 11-membered ring and a hydrogen bond between NH5 and O9 to form a 7-membered ring ( $\delta$ -turn) (Figure 28). In contrast, NH2 shifted appreciably with increasing amounts of DMSO- $d_6$  indicating that this hydrogen was solvent exposed and not involved in hydrogen bonding.

The attention then focused on the structural elucidation of Boc-L-Ala-L-Phe-L- $^{N7}$ Ind-L-Ala-NHMe (**33ab**) (Figure 29).

**Figure 29.** Conformational Depiction of Boc-L-Ala-L-Phe-L- $^{N7}$ Ind-L-Ala-NHMe (**33ab**)



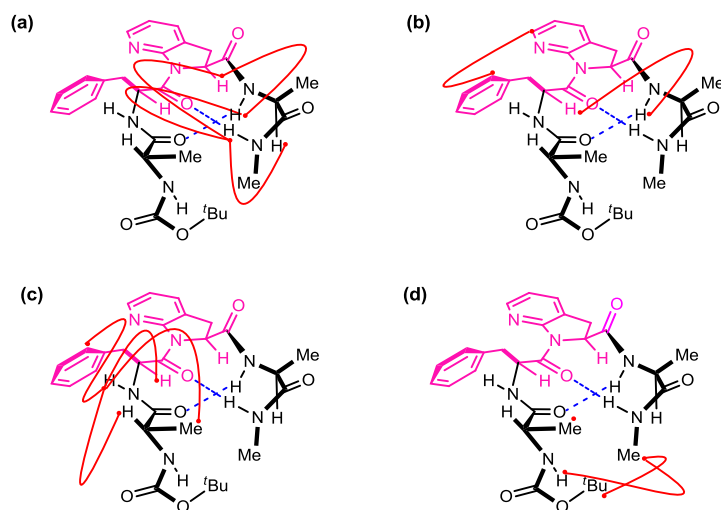
Beginning from the C-terminal methyl amide, crosspeaks for H2/H4 and H2/H5 defined the *s-trans* conformation of this functionality. A long range weak correlation between H7/H2 (Figure 30, a) suggests the folding of C-terminal peptide chain (L-Ala) such that a 10-membered hydrogen bond exists between H2/O9. A similar *s-trans* assignment for the alanine amide could be made by observation of an H5/H7 crosspeak (Figure 30).

The *s-trans* conformation of the azaindoline amide bond was determined by observation of crosspeaks between H10/H10c and H10c/H7e (Figure 30). Complementary to these are crosspeaks for H10/H11 and H11/H10c', though crosspeaks could not be observed to definitively assign the local conformation of the alanine amide



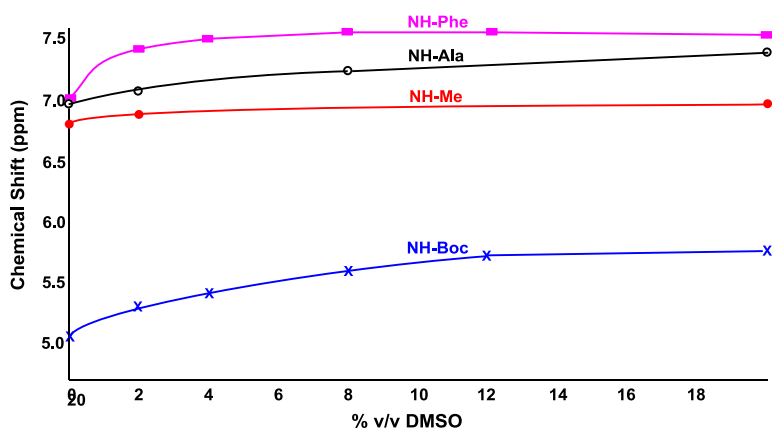
bond as *trans*. This assignment is supported, however, by a long range crosspeak H1/H13a for which such a geometry would be necessary. Additional long range crosspeaks H14/H1 and H1/H17 are consistent with an *anti* conformation of the *tert*-butyl group such that it is positioned at the interior of the turn. The presence of crosspeak H10/H5 confirms the configuration of phenylalanine as (*S*).

**Figure 30.** Observed Regional (a-c) and Long Range (d) NOESY Correlations for Tetrapeptide **33ab**



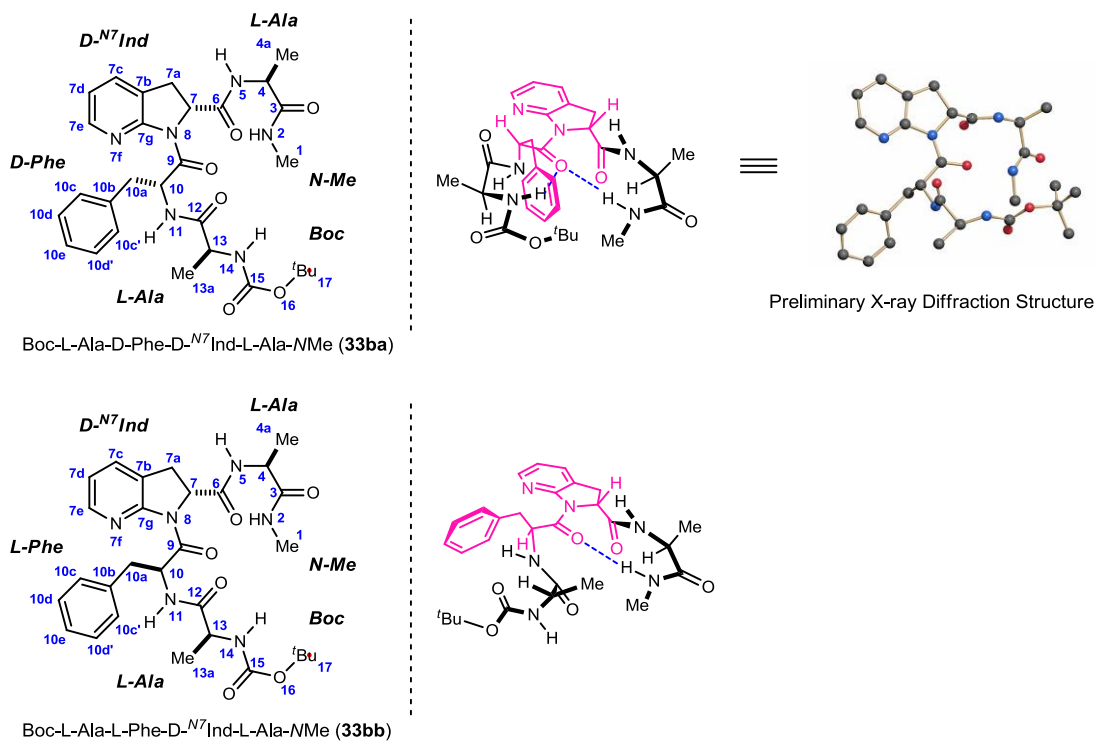
A DMSO- $d_6$  titration experiment, analogous to the one carried out for the D-Phe incorporated peptide revealed the presence of a hydrogen bond between NH5 and O12 to form a 10-membered ring ( $\beta$ -turn) and another hydrogen bond between NH2 and O9 to form a 10-membered ring ( $\beta$ -turn). The experiment showed the presence of two NH signals (NH5 and NH2) that were affected minimally by the increasing DMSO- $d_6$  concentration. In contrast, NH11 and NH14 shifted appreciably with increasing amounts of DMSO- $d_6$  indicating that these hydrogens were solvent exposed, which is also consistent with the  $\beta$ -turn conformation (Figure 31).

**Figure 31.** Effect of Solvent on the NH Amide Protons in **33ab**



Similar experiments with Boc-L-Ala-D-Phe-D-<sup>N7</sup>Ind-L-Ala-NHMe (**33ba**) and Boc-L-Ala-L-Phe-D-<sup>N7</sup>Ind-L-Ala-NHMe (**33bb**) suggested a *trans* configuration about all the

**Figure 32.** Conformational Depiction of D-<sup>N7</sup>Ind-Containing Tetrapeptides (**33ba** and **33bb**)



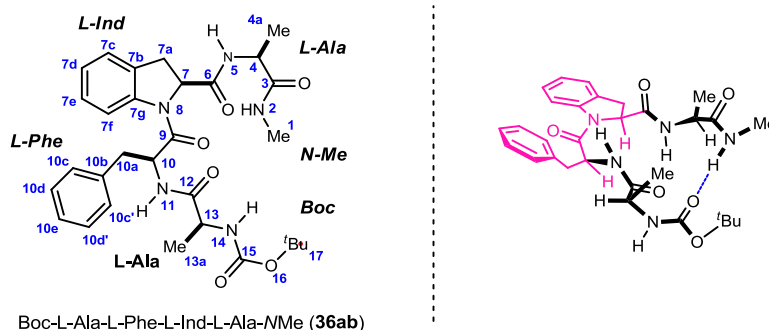
amide bonds as well as a  $\beta$ -turn configuration (Figure 32). We were successful in obtaining small and fine crystals of the peptide derived from (D-<sup>N7</sup>Ind) amino acid (Boc-L-Ala-D-Phe-D-<sup>N7</sup>Ind-L-Ala-NHMe, **33ba**) in CDCl<sub>3</sub>, which were examined by X-ray diffraction using synchrotron radiation. The raw crystal structure data (Figure 32) was in agreement with the NMR results, and identified a *trans*-conformation about the azaindoline amide bond. It also supported the NMR result that the Phe C<sub>α</sub> stereocenter was epimerized.

### 1.9. Conformational Analyses of Ind-Containing Tetrapeptides

The influence of the conserved and nonconserved indoline amino acid on the model tetrapeptide secondary structure was then examined next. The two Ind-incorporated peptides were analyzed by 2D NMR experiments for their conformational geometry. During the NMR analyses it was observed that diastereomers Boc-L-Ala-D-Phe-L-Ind-L-Ala-NHMe (**36aa**) and Boc-L-Ala-D-Phe-D-Ind-L-Ala-NHMe (**36ba**) resulted in poorly resolved broad peaks, implying that the peptides might have aggregated in solution.

The analyses of Boc-L-Ala-L-Phe-L-Ind-L-Ala-NHMe (**36ab**) showed results that were contradictory to what was observed for the corresponding L-<sup>N7</sup>Ind incorporated

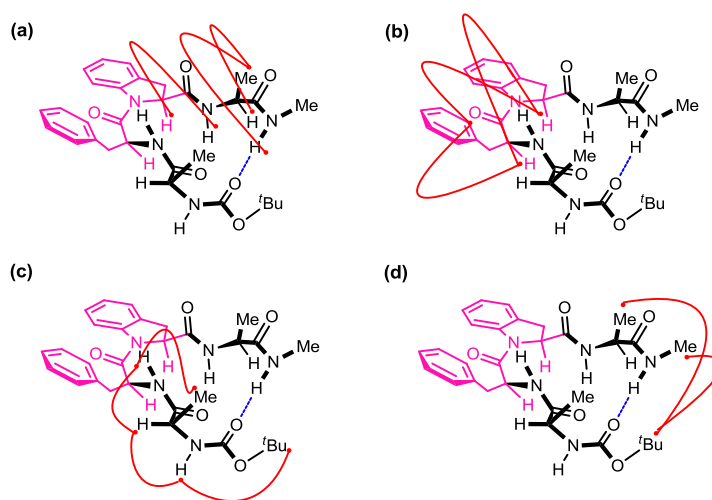
**Figure 33.** Conformational Depiction of Boc-L-Ala-L-Phe-L-Ind-L-Ala-NHMe (**36ab**)



tetrapeptides, but were consistent with our original hypothesis about the design of our peptides (Figure 33).

The crosspeaks were separated into three local regions (Figure 34, a-c) and a long range correlation (Figure 34, d). Beginning from the C-terminal methyl amide, crosspeaks for H2/H4 and H2/H3 defined the *s-trans* conformation. A similar *s-trans* assignment for the alanine amide could be made by observation of a H5/H7 cross peak.

**Figure 34.** Observed Regional (a-c) and Long Range (d) NOESY Correlations for Tetrapeptide **36ab**

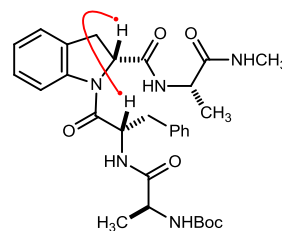


However, importantly, the indoline amide bond was found to possess a *s-cis* conformation with its *N*-terminal Phe residue. This was confirmed by crosspeaks between H10/H10c, H7/H10 and H10c/H7 (Figure 34, b). Complementary to these are crosspeaks for H10/H11 and H11/H10c', though crosspeaks could not be observed to definitively assign the local conformation of the alanine amide bond as *trans*. This assignment is supported, however, by a long range crosspeak H17/H1 and H17/H14a for which such geometry would be necessary. Additional long range crosspeaks H11/H13, H13/H15, H15/H17 are consistent with *syn* conformation of the *tert*-butyl group such that it is

positioned at the exterior of the turn (Figure 34, d). Assignment of phenylalanine configuration as (*S*) was made by the observation of H7/H10 crosspeak (Figure 34, b).

Introspection of the amide protons upon titration with DMSO-*d*<sub>6</sub> provided the following results: the experiments suggested the presence of a hydrogen bond between NH2 and O15, to form a 16-membered ring, and another weak hydrogen bond between NH5 and O12, to form a ten membered ring ( $\beta$ -turn).

A NOESY cross peak between the Phe-C $\alpha$  and indoline-C $\alpha$  protons was observed for the peptide derived from (*R*)-indoline amino acid (**36bb**), indicating that the tetrapeptide had a *cis*-configuration at the amide bond between the prolyl and the Phe



Boc-L-Ala-L-Phe-D-Ind-L-Ala-NMe (**36bb**)

residue. A complete structural elucidation of **36bb** could not be accomplished as the tetrapeptide exhibited only 75% *cis*-isomer.

### 1.10. Conclusions

We have determined, by NMR spectroscopy, the effects of each of the indoline and azaindoline amino acids on prolyl *N*-terminal *cis-trans* amide isomer population. A series of di, tri, and tetrapeptides containing indoline amino acids with or without a nitrogen mutation at C7 were synthesized and evaluated. Because of A<sup>1,3</sup>-strain between the fused aromatic group (indoline) and prolyl *N*-terminal residue in unmutated indoline amino acids, the *cis*-amide bond geometry about the L-Ind fragment was able to be favored. However, all the peptides incorporating the <sup>N7</sup>Ind mutations resulted in exclusive formation of the *trans*-rotamer about the Phe-<sup>N7</sup>Ind amide bond. This conformation

preference for <sup>N7</sup>Ind containing peptides was due to an unfavorable lone-pair/lone-pair repulsion between the preceding carbonyl oxygen and azaindoline nitrogen in *s-cis* conformation. The synthetic access to both indoline and azaindoline  $\alpha$ -amino acids and their enantiomers that we have accomplished here might allow the development of novel immunogenic peptides.

## Chapter 2

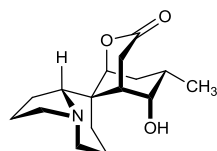
### Total Synthesis of (+)-Serratezomine A

#### 2.1. Background

##### 2.1.1. Introduction to *Lycopodium* Alkaloids and (+)-Serratezomine A

The *Lycopodium* alkaloids are a structurally related, yet diverse group of compounds, originally identified in *Lycopodium* (sensu lato).<sup>52,53</sup> They are isolated from a variety of club moss (*Lycopodium*), which are low, mossy evergreen branches. These alkaloids usually contain a skeleton comprised of 16 carbons, although sometimes they can contain as many as 32 carbons (apparent dimers) or less than 16 carbons (likely resulting from bond cleavage). Serratezomine A (**37**) was isolated from the club moss *L. serratum* var. *serratum* in 2000 by Kobayashi.<sup>54</sup> Serratezomine A displayed moderate

Figure 35. Structure of Serratezomine A



(+)-serratezomine A (**37**)

cytotoxicity<sup>55</sup> against murine lymphoma L1210 cells ( $IC_{50} = 9.7 \mu\text{g/mL}$ ) and human epidermoid carcinoma KB cells ( $IC_{50} >10 \mu\text{g/mL}$ ) and exhibited strong acetyl-choline esterase (AChE) inhibition. Serratezomine A is an inspiring synthetic target containing a *seco*-serratinine-type skeleton containing six contiguous stereocenters and an all-carbon spirocyclic center embedded within four connected ring systems. The structure of

<sup>52</sup> For a review of the *Lycopodium* alkaloids see: Ayer, W. A.; Trifonov, L. S. in *The Alkaloids*; Cordell, G. A.; Brossi, A. Academic Press: New York, 1994; Vol. 45, 233-266 and Maclean, D. B. in *The Alkaloids*; Brossi, A. Academic Press: New York, 1985, Vol. 26, 241-296.

<sup>53</sup> Ma, X.; Gang, D. R. *Nat. Prod. Rep.* **2004**, *21*, 752.

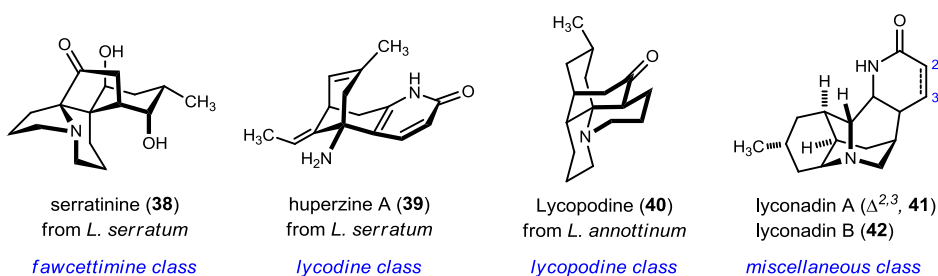
<sup>54</sup> Morita, H.; Arisaka, M.; Yoshida, N.; Kobayashi, J. *J. Org. Chem.* **2000**, *65*, 6241.

<sup>55</sup> An  $IC_{50}$  value of less than  $4 \mu\text{g/mL}$  is required by the National Cancer Institute for classification as a potential anti-cancer drug.

serratezomine A was determined by  $^1\text{H}$  and  $^{13}\text{C}$  NMR as well as 2D NMR techniques including COSY, HOHAHA, HMQC, and HMBC in  $\text{CD}_3\text{OD}$ .

To date, over 200 *Lycopodium* alkaloids have been identified from different species of *Lycopodium*.<sup>53</sup> A. W. Ayer<sup>52</sup> separated the *Lycopodium* alkaloids into four structural classes: the lycopodine class, the lycodine class, the fawcettimine class and the miscellaneous class. Representative compounds for these structural classes are represented in Chart 1.<sup>56</sup> Serratezomine A, a  $\text{C}_{16}\text{N}$  alkaloid, belongs to the fawcettimine class.

**Chart 1.** Structure of some *Lycopodium* Alkaloids



Various species of Huperziaceae and Lycopodiaceae (club mosses) have a long history of use in Chinese folk medicine for the treatment of contusions, strains, swellings, schizophrenia and organophosphate poisoning. In addition, *in vitro* and *in vivo* pharmacological studies have demonstrated that *Lycopodium* alkaloids produce definite effects in the treatment of diseases that affect the cardiovascular or neuromuscular

<sup>56</sup> Isolation/structure references for the compounds in: a) serratinine - Inubushi, Y.; Ishii, H.; Yasui, B.; Hashimoto, M.; Harayama, T. *Tetrahedron Lett.* **1966**, *8*, 1537 and later structural revision: Nishio, K.; Ishii, H.; Inubushi, Y.; Harayama, T. *Tetrahedron Lett.* **1969**, *11*, 861. b) huperzine A: Liu, - J.-S.; Zhu, Y.-L.; Yu, C.-M.; Zhou, Y.-Z.; Han, Y.-Y.; Wu, F.-W.; Qi, B.-F. *Can J. Chem.* **1986**, *64*, 837; NMR assignment: Zhou, B.-N.; Zhu, D.Y.; Huang, M.-F.; Lin, L.-J.; Lin, L.-Z.; Han, X.-Y.; Cordell, G. A. *Phytochemistry* **1993**, *34*, 1425. c) lycopodine - Bödeker, K. *Justus Liebigs Ann. Chem.* **1881**, 208, 363. d) lyconadin A - Kobayashi, J.; Hirasawa, Y.; Yoshida, N.; Morita, H. *J. Org. Chem.* **2001**, *66*, 5901.



systems, or that are related to cholinesterase activity.<sup>57</sup> *Lycopodium* alkaloids have been shown to have positive effects on learning and memory. Of the alkaloid family, huperzine A, a constituent alkaloid isolated from the club moss *L. serratum*, has the most relevant biological activity. HupA has been found to be a potent, reversible and selective acetylcholinesterase inhibitor (AChEI).<sup>58</sup> HupA crosses the blood–brain barrier smoothly, and shows high specificity for acetylcholinesterase (AChE) with a prolonged biological half-life.<sup>59</sup> However, all of the other *Lycopodium* alkaloids identified so far have either not shown any AChE inhibition activity or have possessed activity that is significantly lower than that of HupA.<sup>60</sup>

### **2.1.2. Biosynthesis of the *Lycopodium* Alkaloids**

Spenser et al. conducted the feeding experiments that sought to identify biosynthetic pathway intermediates to *Lycopodium* alkaloids.<sup>61</sup> In these experiments, <sup>14</sup>C and <sup>13</sup>C labeled precursors were fed to shoots of *Lycopodium* species growing in their natural habitat. A few days after application of the radio- or stable isotope labeled putative precursor, the shoots of the plant were harvested and these tissues were then analyzed for the incorporation of label into end product alkaloids or into potential pathway intermediates. Feeding studies with lysine demonstrated that the entry point into the pathway is through the decarboxylation of lysine (by lysine decarboxylase) to form

---

<sup>57</sup> a) Kozikowski, A. P.; Tuckmantel, W. *Acc. Chem. Res.* **1999**, *32*, 641. b) Liu, J. S.; Zhu, Y. L.; Yu, C. M.; Zhou, Y. Z.; Han, Y. Y.; Wu, F. W.; Qi, B. F. *Can. J. Chem.* **1986**, *64*, 837.

<sup>58</sup> a) Tang, X. C.; Han, Y. F.; Chen, X. P.; Zhu, X. D. *Acta. Pharmacol. Sin.* **1986**, *7*, 507. b) Tang, X. C.; Sarno, P. D.; Sugaya, K.; Giacobini, E. *J. Neurosci. Res.* **1989**, *24*, 276.

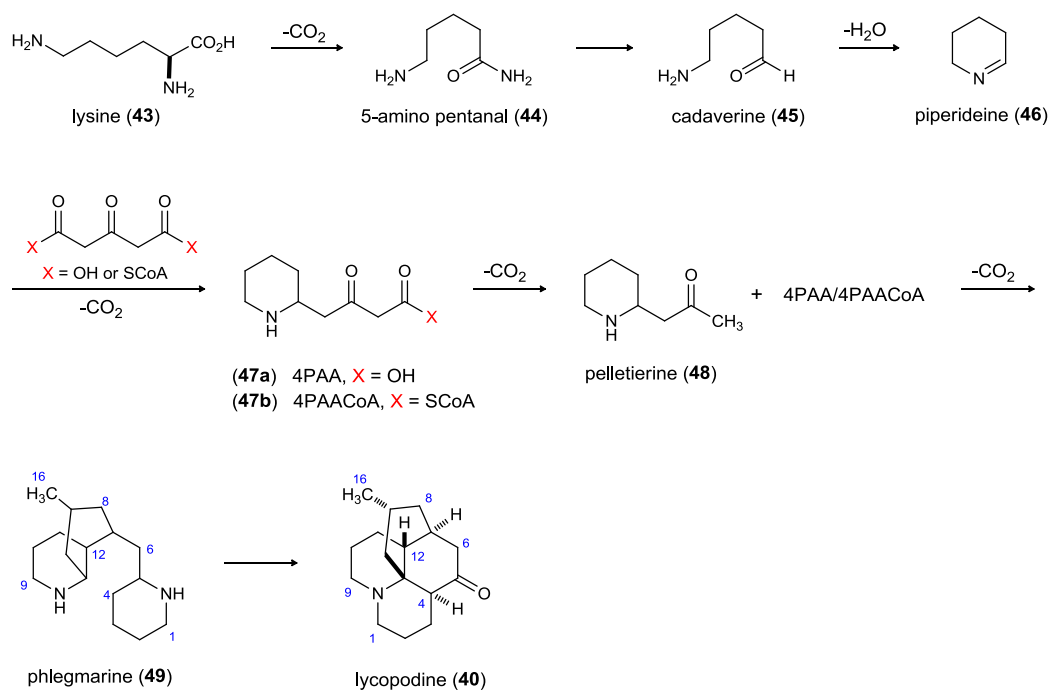
<sup>59</sup> Jiang, H. L.; Luo, X. M.; Bai, D. L. *Curr. Med. Chem.* **2003**, *10*, 2231.

<sup>60</sup> Tori, M.; Shimoji, T.; Shimura, E.; Takaoka, S.; Nakashima, K.; Sono, M.; Ayer, W. A. *Phytochemistry*. **2000**, *53*, 503.

<sup>61</sup> a) Castillo, M.; Gupta, R. N.; Ho, Y. K.; MacLean, D. B.; Spenser, I. D. *J. Am. Chem. Soc.* **1970**, *92*, 1074. b) Gupta, R. N.; Ho, Y. K.; MacLean, D. B.; Spenser, I. D. *J. Chem. Soc. D Chem. Comm.* **1970**, 409. c) Hemscheidt, T.; Spenser, I. D. *J. Am. Chem. Soc.* **1993**, *115*, 3020.

cadaverine (**44**) (Scheme 9). Cadaverine is then transformed *via* 5-aminopentanal (**45**) to piperidine (**46**) by the enzyme diamine oxidase. Piperidine is then coupled to acetonedicarboxylic acid (or its bisCoA ester), formed by the condensation of two molecules of malonyl-CoA by a ketosynthase-type enzyme, to form 4-(2-piperidyl) acetoacetate (**47a**) or 4-(2-piperidyl) acetoacetyl-CoA, 4PAACoA (**47b**) *via* the action of an unknown enzyme. 4PAA/4PAACoA is then decarboxylated by unknown decarboxylase enzyme to form pelletierine (**48**), the first general intermediate to *Lycopodium* alkaloids. Pelletierine and 4PAA/4PAACoA are then coupled, with

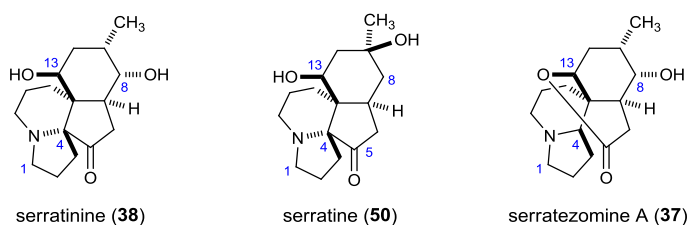
**Scheme 9.** Proposed Biosynthetic Pathway to Lycopodine



concomitant decarboxylation, to form phlegmarine (**49**), the second general intermediate to all *Lycopodium* alkaloids. A series of oxidations and reductions result in lycopodine

(40). Phlegmarine and lycopodine are the main intermediates in the biosynthesis of other *Lycopodium* alkaloids.<sup>62</sup> In a series of oxidative steps, phlegmarine (49) can be transformed to huperzine A. From lycopodine (40), the entire fawcettimine structural class of *Lycopodium* alkaloids can be established, including the target molecule serratezomine A (37).

**Figure 36.** *Lycopodium* Alkaloids Containing N-C4 Bond



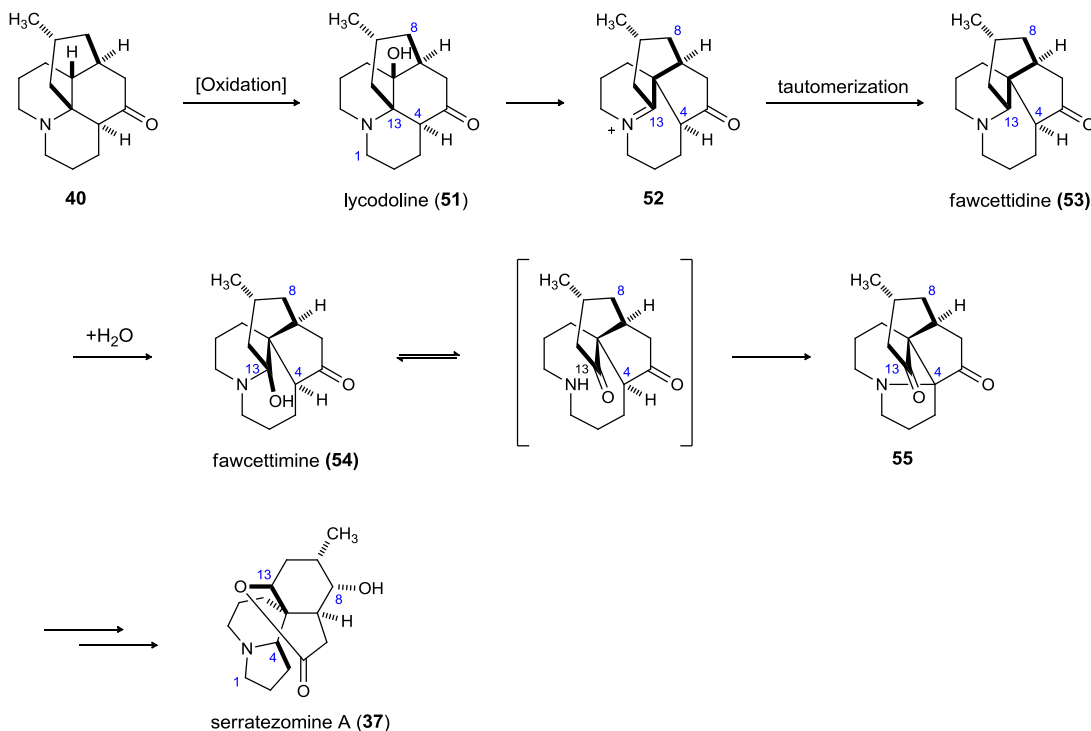
Lycopodine undergoes an oxidation at C12 to install a tertiary hydroxyl group, forming lycodoline (51, Scheme 10). Lycodoline undergoes a 1,2-carbon bond shift, initiated by the lone pair of electrons on the nitrogen, displacing the hydroxyl group. The resulting iminium (52) tautomerizes to provide more stable enamine 53. The C13–C14 double bond of fawcettidine, being an enamine, is easily hydrated to give a hemiaminal (*i.e.* fawcettimine), which can then lead to C13–N bond-cleavage to form a carbonyl group. This has been confirmed by demonstration of equilibrium between the carbinolamine form of 54 and the keto-amine form.<sup>63</sup> Once the N-C13 bond is cleaved, a subclass of the fawcettimine group is observed, containing a new N-C4 bond. This subclass encompasses serratezomine A (37) and the structurally related serratinine (38) and serratine (50) (Figure 36). Based on the structure of serratinine (38), serratezomine A

<sup>62</sup> For more background information and proposals of the biosynthesis of lycopodine see: Blumenkopf, T. A.; Heathcock, C. H. in *Alkaloids: Chemical and Biological Perspectives*. Pelletier, S. W., Ed.; John Wiley & Sons, Inc.: New York, 1985; vol. 3, pp 185-240 and MacLean, D. B. in *The Alkaloids*; Brossi, A.; Ed.; Academic Press: New York, 1985; vol. 26, pp 241-298.

<sup>63</sup> Ayer, W. A. *Nat. Prod. Rep.* **1991**, 8, 455.

(37) has a lactone ring formed by cleavage of the C4–C5 bond and then attachment of the C13 hydroxyl to the C5 carbonyl group. This gives a spiro structure, which is very unusual in the *Lycopodium* alkaloids. Inubushi *et al* has also proposed a biogenetic pathway from a lycopodine derivative to serratinine.<sup>64</sup>

**Scheme 10.** Biosynthesis of N-C4 Containing *Lycopodium* Alkaloids



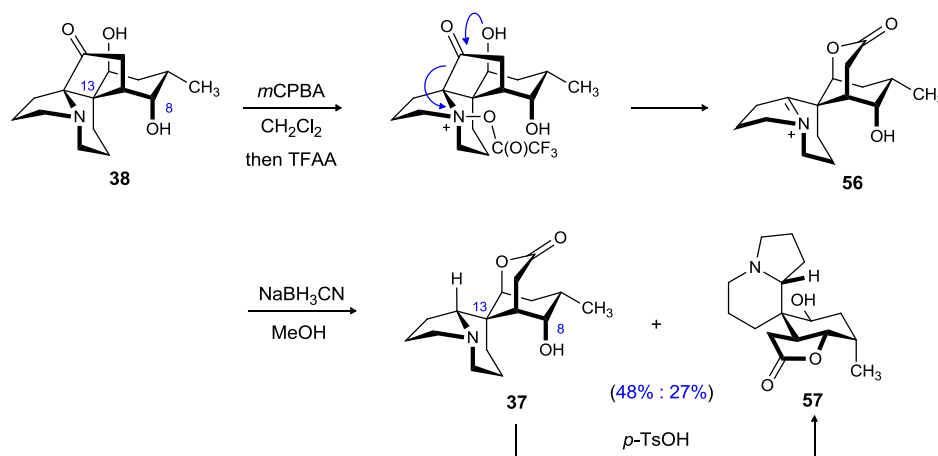
As a further proof serratinine (**38**) is a biogenetic precursor of serratezomine A, Kobayashi *et al.* reported a biomimetic interconversion of serratinine to serratezomine A via a modified Polonovski rearrangement.<sup>65</sup> In this one-pot transformation (Scheme 11), treatment of serratinine (**38**) with *m*CPBA resulted in formation of the *N*-oxide (serratezomine B), which then was treated with trifluoroacetic anhydride to induce the Polonovski-Potier rearrangement. The free alcohol attacks the ketone resulting in a lactone ring with subsequent loss of the trifluoroacetate anion. The resulting iminium ion

<sup>64</sup> Inubushi, Y.; Ishii, H.; Yasui, B.; Hashimoto, M.; Harayama, T. *Tetrahedron Lett.* **1966**, 7, 1537.

<sup>65</sup> Morita, H.; Kobayashi, J. *J. Org. Chem.* **2002**, 67, 5378.

(**56**) was reduced by NaCNBH<sub>3</sub> in the same pot to give serratezomine A (**37**) in 48% yield as a colorless solid. A by-product of *trans*-lactonization (**57**, 27%) formed during the one-pot sequence can be made exclusively from **37** upon treatment with *p*-TsOH.

**Scheme 11.** Polonovski-Potier Rearrangement



## 2.2. Approaches to the Synthesis of Lycopodium Alkaloids

### 2.2.1. Lycopodine Class

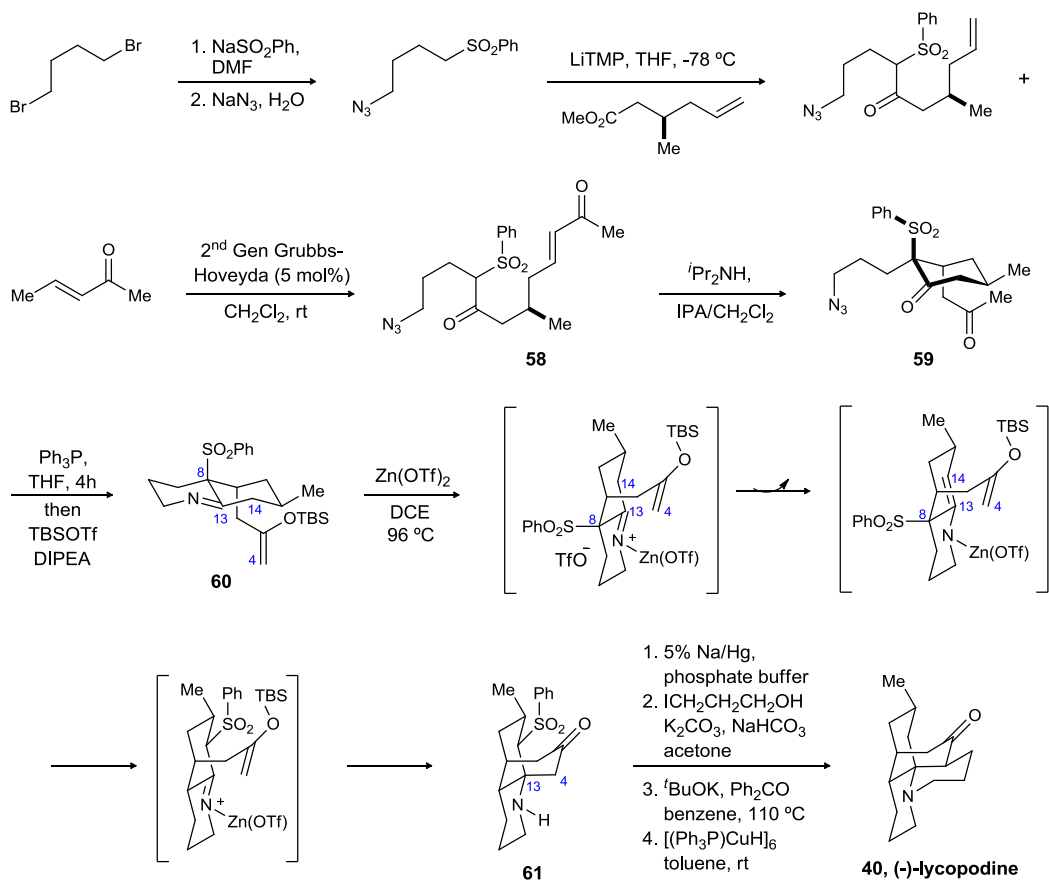
Lycopodine is the largest group of known *Lycopodium* alkaloids, and appears to be the most widely distributed. The first *Lycopodium* alkaloid to be identified (lycopodine) belongs to this group.<sup>56c,66</sup> To date, seven racemic total syntheses and two racemic formal syntheses of lycopodine have been reported.<sup>67</sup> Recently, Carter *et al.* reported the first enantioselective synthesis of lycopodine.<sup>68</sup>

<sup>66</sup> (a) Achmatowicz, O.; Uzieblo, W. *Rocz. Chem.* **1938**, *18*, 88. (b) Ayer, W. A.; Iverach, G. G. *Tetrahedron Lett.* **1962**, 87. (c) Rogers, D.; Quick, A.; Hague, M. *Acta Crystallogr.* **1974**, *B30*, 552. (d) Hague, M.; Rogers, D. *J. Chem. Soc., Perkin Trans 2.* **1975**, 93–98.

<sup>67</sup> (a) Stork, G.; Kretchmer, R. A.; Schlessinger, R. H. *J. Am. Chem. Soc.* **1968**, *90*, 1647. (b) Ayer, W. A.; Bowman, W. R.; Joseph, T. C.; Smith, P. *J. Am. Chem. Soc.* **1968**, *90*, 1648. (c) Kim, S.; Bando, Y.; Horii, Z. *Tetrahedron Lett.* **1978**, 2293. (d) Heathcock, C. H.; Kleinman, E. F.; Binkley, E. S. *J. Am. Chem. Soc.* **1982**, *104*, 1054. (e) Schumann, D.; Mueller, H. J.; Naumann, A. *Liebigs Ann. Chem.* **1982**, 1700. (f) Kraus, G. A.; Hon, Y. S. *Heterocycles* **1987**, *25*, 377. (g) Grieco, P. A.; Dai, Y. *J. Am. Chem. Soc.* **1998**, *120*, 5128. Formal syntheses of lycopodine: (h) Padwa, A.; Brodney, M. A., Jr.; Sheehan, S. M. *J. Org. Chem.* **1997**, *62*, 78. (i) Mori, M.; Hori, K.; Akashi, M.; Hori, M.; Sato, Y.; Nishida, M. *Angew. Chem. Int. Ed.* **1998**, *37*, 637.

<sup>68</sup> Yang, H.; Carter, R. G.; Zakharov, L. N. *J. Am. Chem. Soc.* **2008**, *130*, 9238.

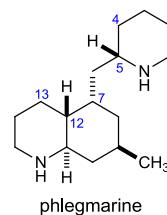
**Scheme 12.** Carter's Enantioselective Synthesis of Lycopodine



The key step in their route was the intramolecular Michael addition of keto sulfone **58**, itself prepared in 4 steps from commercially available 1,4-dibromobutane (Scheme 12). The Michael adduct **59** was isolated as a single product in 89% yield. The methyl ketone was converted to **60** in one pot reaction featuring the Staudinger reaction followed by *tert*-butyldimethylsilyl enol ether formation. The key Mannich cyclization of imine **60** afforded the rearranged tricyclic **61** as a result of net 1,3-rearrangement of the sulfone moiety from the expected C8 position to the C14 position. Desulfurization of sulfone **61** using Na/Hg amalgam and annulation of the piperidine ring onto the tricyclic ketone in a three step sequence afforded (-)-lycopodine (**40**) in 11 steps from 1,4-dibromobutane.<sup>67e</sup>

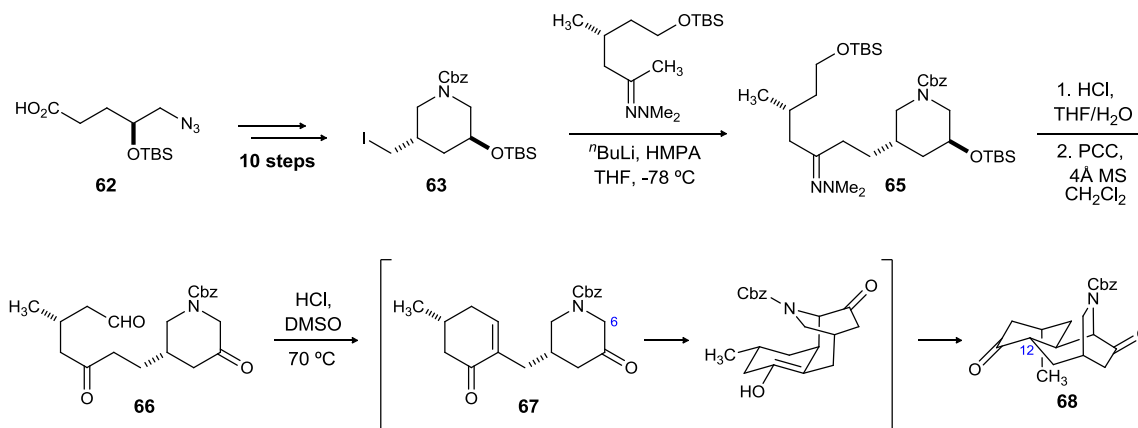
### 2.2.2. Miscellaneous Class

The miscellaneous class consists of more than 40 *Lycopodium* alkaloids. This group includes all of the *Lycopodium* alkaloids that do not belong to the lycopodine, lycodine or fawcettimine class, and represent quite a diversity of structural motifs. All of the compounds in this group are derived from phlegmarine. In all of the miscellaneous class compounds, C4 remains unconnected to C12 or C13. In the other three classes, C4 of phlegmarine invariably forms a C-C bond with either C13 or C12.



The first enantioselective synthesis of lyconadin A and lyconadin B was accomplished by Smith and coworkers.<sup>69</sup> The synthesis commenced with the known acid **62** (Scheme 13). In ten synthetic operations, the acid was converted to iodide **63** in 61% overall yield.

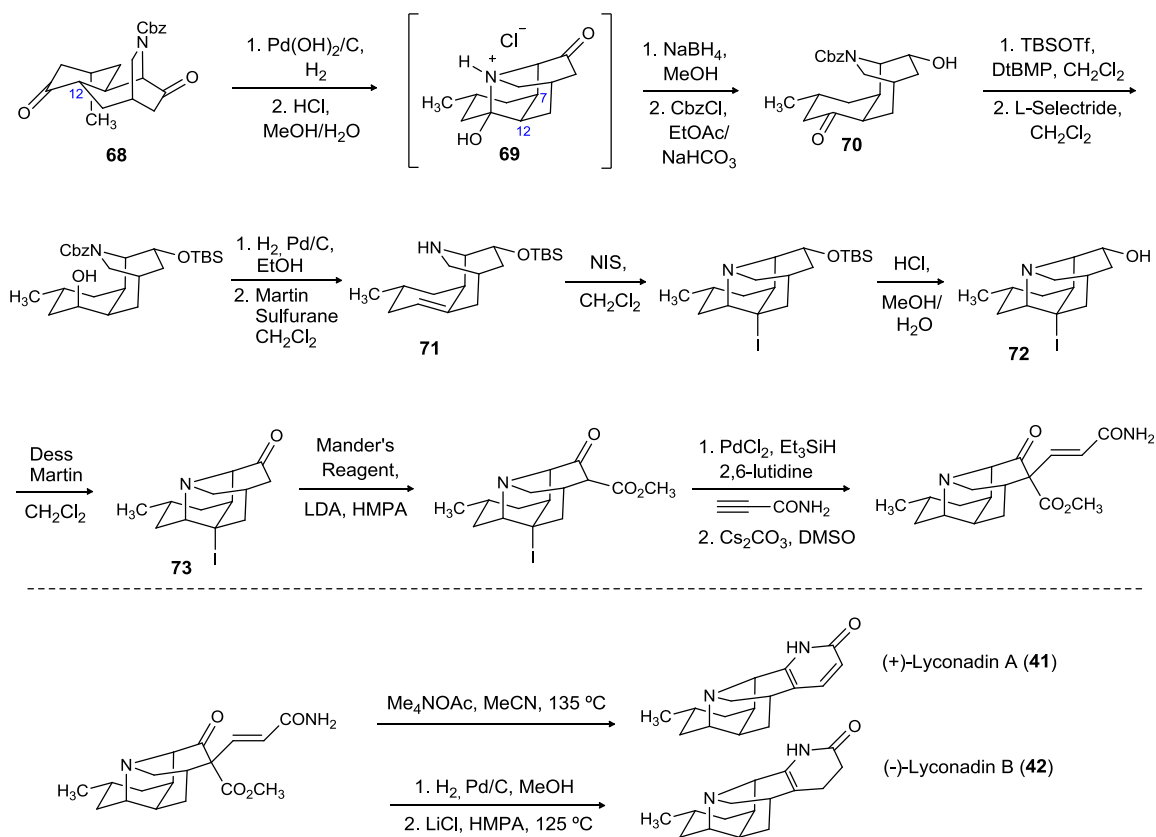
**Scheme 13.** Synthesis of (+)-Lyconadin A and (-)-Lyconadin B



<sup>69</sup> Beshore, D. C.; Smith, A. B. *J. Am. Chem. Soc.* **2007**, *129*, 4148. Beshore, D. C.; Smith, A. B. *J. Am. Chem. Soc.* **2008**, *130*, 13778.

The union of the iodide and hydrazone **64**, prepared in seven steps from commercially available (-)-methyl (*R*)-3-methylglutarate, furnished **65**. Acid promoted unmasking of the carbonyl and hydroxyl group followed by oxidation of the free alcohol provided unstable diketoaldehyde **66**. Intramolecular aldol condensation of **66** employing hydrochloric acid furnished enone **67** *in situ*. The enone underwent a favorable 7-*endo-trig* intramolecular conjugate addition, presumably of the C6 enol *anti* to the cyclohexenone group, to provide the key tricyclic ketone **68**. The Cbz group was removed to provide the free amine, and the forced epimerization at C12 was effected by trapping the desired *cis* C7-C12 epimer as a stable hemiaminal salt **69**.

**Scheme 14.** Synthesis of (+)-Lyconadin A and (-)-Lyconadin B





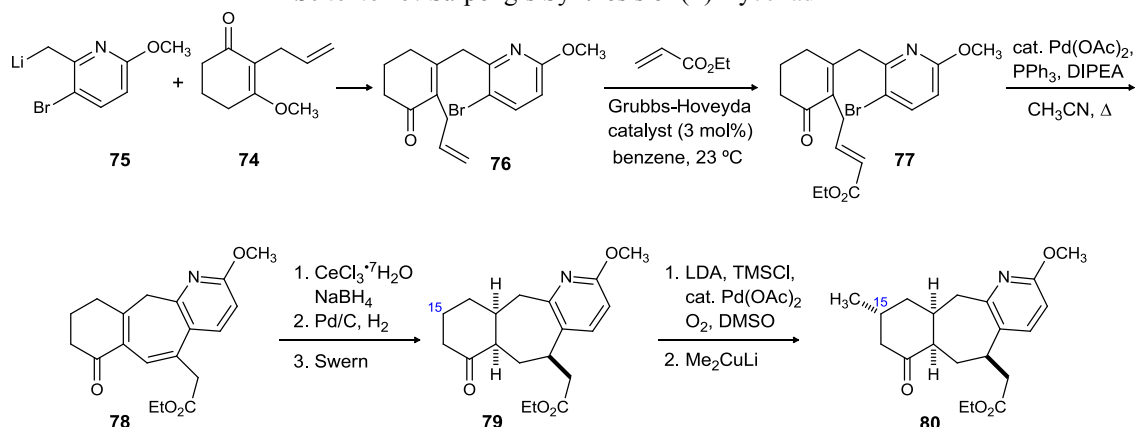
However, all attempts to form the iminium by either removal or derivatization of the hydroxyl group were unprofitable. Aminoiodination of the alkene (**71**) was then considered to be a viable strategy for constructing the central pyrrolidine ring. To this end, reduction of **69** and Cbz protection of amine afforded hydroxyketone **70**. A four step sequence converted the hydroxyketone into alkene **71**, setting the stage for aminoiodination with NIS to furnish key intermediate **72**. Acid mediated desilylation followed by oxidation of the resulting alcohol afforded highly advanced intermediate **73**. Finally, annulation of the  $\alpha$ -pyridinone or dihydropyridinone ring onto the tetracyclic ketone provided lyconadin A and B.

In their synthesis of racemic lyconadin A (Scheme 15),<sup>70</sup> the Sarpong group started from the enone **76**, which was synthesized by the coupling of anion **75** and vinylogous ester **74**. The enone was transformed to ketoester **77** utilizing Grubbs-Hoveyda metathesis condition. Heck cyclization of the enolate with subsequent isomerization of the resulting exocyclic double bond into cross conjunction with the enone moiety, provided cycloheptadiene **78**. In a three step sequence of reduction and oxidation, the first three stereocenters in the seven-membered ring were introduced. The C16 methyl substituent was introduced in a highly diastereoselective way by employing a Saegusa-Ito oxidation of **79** followed by conjugate addition to the resultant enone using the Gilman reagent to provide **80**. To prevent the epimeriation of C12 under saponification condition, the C13 carbonyl group was reduced and protected. Curtius rearrangement of the acid and subsequent protection of the amine followed by reinstallation of the carbonyl functionality afforded **81** (Scheme 16).

---

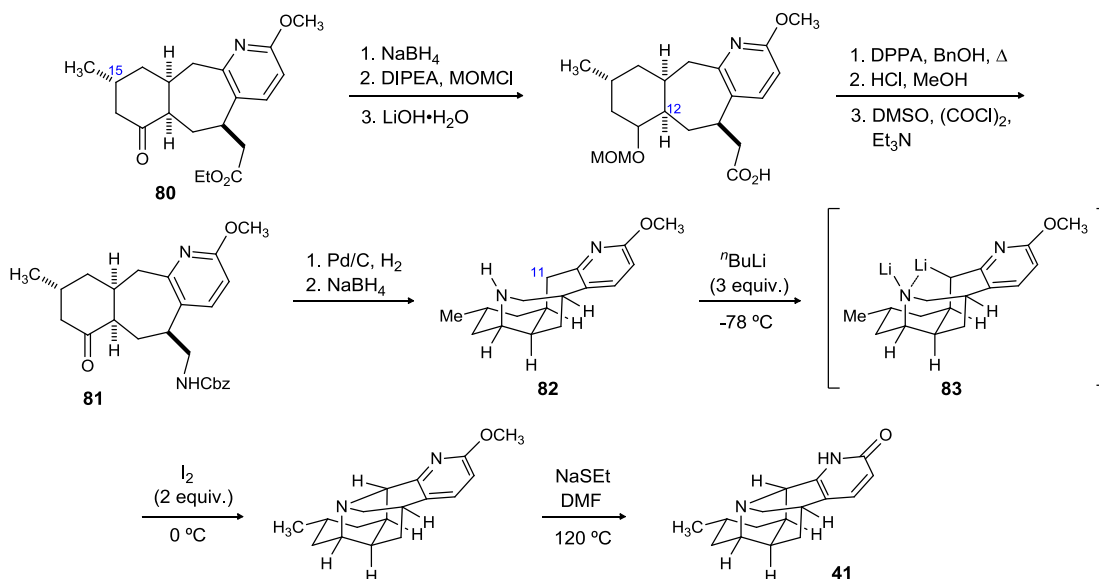
<sup>70</sup> Bisai, A.; West, S. P.; Sarpong, R. *J. Am. Chem. Soc.* **2008**, *130*, 7222.

**Scheme 15.** Sarpong's Synthesis of (±)-Lyconadin A

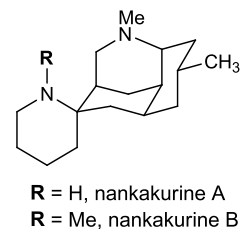


Hydrogenolysis of the Cbz group and  $\text{NaBH}_4$  reduction of the resulting hemiaminal afforded the tetracyclic intermediate (**82**). To elicit the desired C11-N bond formation, the secondary amine (**82**) was treated with  $n\text{BuLi}$  and the resulting dianion was **83** was oxidized by  $\text{I}_2$  to afford (±) lyconadin A in 18 steps from commercially available picoline derivative.

**Scheme 16.** Sarpong's Synthesis of (±)-Lyconadin A



Two beautiful syntheses of other architecturally complex molecules of this class of *Lycopodium* alkaloids, Nankakurine A and B, have been completed by Overman and Waters group.<sup>71</sup> The tetracyclic alkaloids Nankakurine A and Nankakurine B were isolated from the club moss *Lycopodium hamiltonii* by Kobayashi and coworkers in



2004.<sup>72</sup> Nankakurine A induces the secretion of neurotrophic factors and promote neuronal differentiation.<sup>73</sup>

The key step in the first syntheses of Nankakurine A and of Nankakurine B, reported by Overman and coworkers utilized a novel intramolecular aza-Prins cyclization to form the tetracyclic core of nankakurines. The synthesis commenced with easily accessible 5-methyl cyclohexenone **84**, prepared from (*R*)-pulegone (Scheme 17). The diene **85** was prepared from the alkyne **84**, following the procedure developed by Diver. One of the earlier difficulty encountered in the Diels-Alder reaction was the epimerization adduct under the Diels-Alder reaction condition. This was overcome by utilizing the activation method devised by Gassman *et al.* The modified reaction condition utilized the condensation of diene and dienophile in the presence of bis-silyl ether and TMSOTf as the Lewis acid provided the adduct **86** with the protected ketone functionality. Hydrolysis off the Diels-Alder adduct under mild condition, utilizing FeCl<sub>3</sub>, followed by reductive amination of the resulting hydrazide **87** provided the aza-Prins cyclization precursor in high diastereoselection. With the hydrazide **87** in hand, the

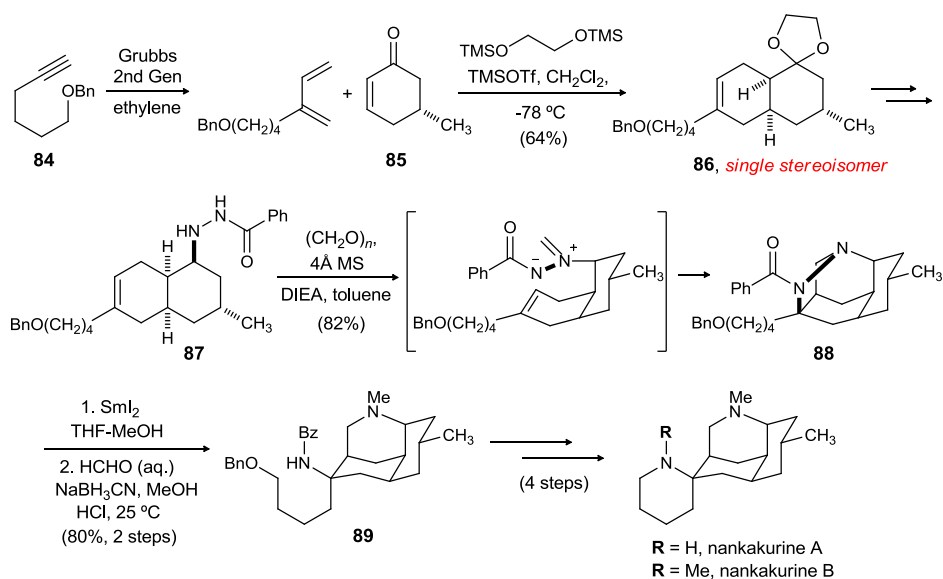
<sup>71</sup> a). Nilsson, B. L.; Overman, L. E.; Read de Alaniz, J.; Rohde, J. M. *J. Am. Chem. Soc.* **2008**, *130*, 11297. b) Cheng, X.; Water, S. P. *Org. Lett.* **2010**, *12*, 205.

<sup>72</sup> Hirasawa, Y.; Morita, H.; Kobayashi, J. *Org. Lett.* **2004**, *6*, 3389.

<sup>73</sup> Hirasawa, Y.; Kobayashi, J.; Obara, Y.; Nakahata, N.; Kawahara, N.; Goda, Y.; Morita, H. *Heterocycles* **2006**, *68*, 2357.

key aza-Prins reaction was performed to provide the desired tetracycle **88**. A sequence of two synthetic operations, including a)  $\text{SmI}_2$  induced reductive ring opening reaction and b) reductive methylation of the resulting tricyclic product provided the advanced intermediate **89**. A sequence of 4 and 5 straightforward synthetic transformations were utilized to complete the syntheses of (+)-nankakurine A and B.

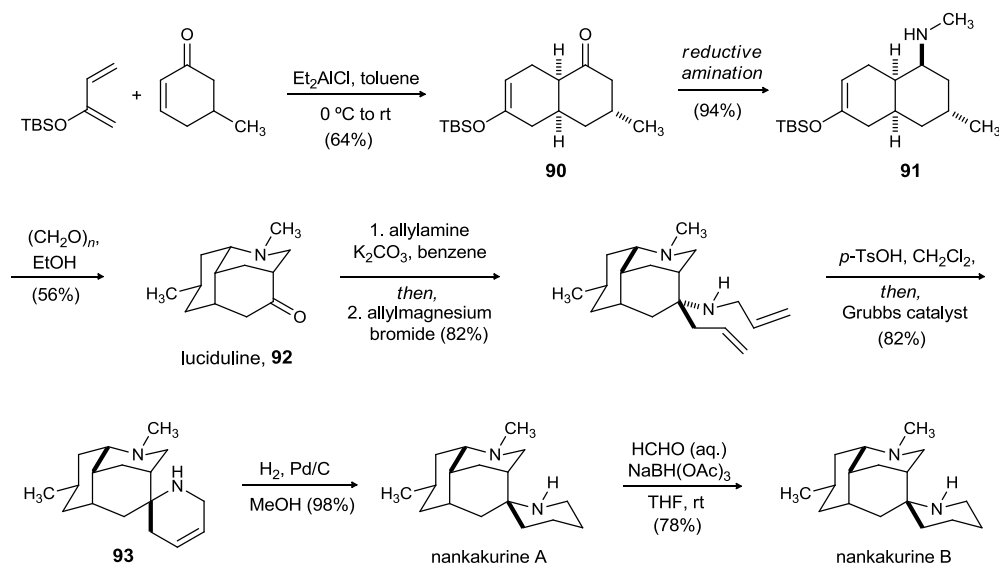
**Scheme 17.** Overman's Synthesis of (+)-Nankakurine A and B



Two years later, Waters and coworkers reported a racemic synthesis of nankakurines A and B from luciduline, utilizing a key aminoallylation/ring-closing metathesis sequence.<sup>71b</sup> Water's synthesis commences with a Diels-Alder reaction to fashion the core bicyclic system **90** in high diastereoselection (d.r 12:1) (Scheme 18). A highly diastereoselective reductive amination provided the amine **91** which was treated with aqueous formaldehyde to give luciduline (**92**). A sequence of a substrate controlled diastereoselective aminoallylation, followed by a ring-closing metathesis reaction, were utilized to give the highly advanced tetracyclic core **93**. Hydrogenation of the alkene in spiroamine **93** provided ( $\pm$ )-nankakurine A. Reductive methylation of ( $\pm$ )-nankakurine A

furnished ( $\pm$ )-nankakurine B. In summary, the syntheses of Nankakurines A and B required only 7 and 8 steps, respectively, from commercially available starting material.

**Scheme 18.** Water's Synthesis of ( $\pm$ )-Nankakurine A and B



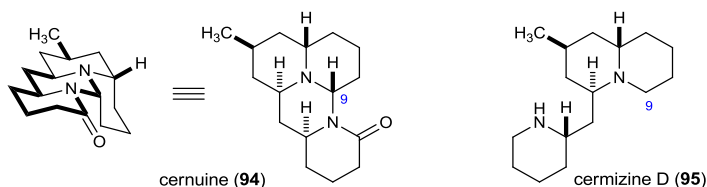
Takayama *et al.* has reported an enantioselective synthesis of two cernuane-type *Lycopodium* alkaloids, cernuine **94** and cermizine D **95**, in 2008.<sup>74</sup> Although cernuine was isolated in 1948 by Manske and coworkers,<sup>75</sup> the synthesis of this alkaloid has remained elusive to the synthetic community. The isolation of cermizine D was reported in 2004 by Kobayashi and coworkers.<sup>76</sup> Cermizine D, a molecule possessing a N-C<sub>9</sub> *seco*-cernuane skeleton, exhibited cytotoxicity against murine lymphoma L1210 cells with an IC<sub>50</sub> of 7.5  $\mu\text{g/mL}$ . The key step in Takayama's syntheses of these two alkaloids was a late stage stereoselective aminoallylation step to set the key C-N bond in the molecule.

<sup>74</sup> Nishikawa, Y.; Kitajima, M.; Takayama, H. *Org. Lett.* **2008**, *10*, 1987.

<sup>75</sup> Marion, L.; Manske, R. H. F. *Can. J. Res.* **1948**, *26*, 12

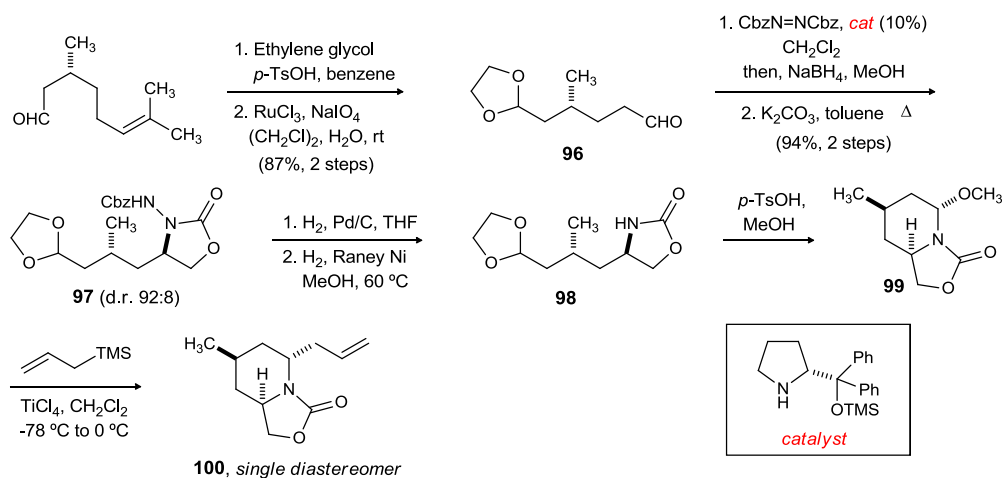
<sup>76</sup> Morita, H.; Hirasawa, Y.; Shinzato, T.; Kobayashi, J. *Tetrahedron.* **2004**, *60*, 7023.

**Figure 37.** Cernuane Alkaloids



The synthesis begins with the elaboration of oxazolidinone **97**. Required aldehyde **96**, for the organocatalytic  $\alpha$ -amination, was accessed from (+)-citronellal. Acetylation of aldehyde functionality in citronellal was followed by oxidative cleavage of the residual olefin function (Scheme **19**). The enantioselective amination of **96** could be achieved by treatment of aldehyde this compound with dibenzyl azidocarboxylate in the presence of a proline derived catalyst. Reduction of the resulting intermediate was followed by treatment with  $K_2CO_3$  to provide the desired oxazolidinone **97**. Reductive cleavage of the N-N bond in hydrazide **97** was achieved by a sequential reduction protocol, utilizing  $H_2/Pd$  followed by Raney Nickel, to provide oxazolidinone **98**. The oxazolidinone was then treated with *p*-TsOH to effect the desired cyclization. Treatment of the resulting aminoacetal **99** with allyl trimethylsilane and  $TiCl_4$  provided allylated aminoacetal **100** as

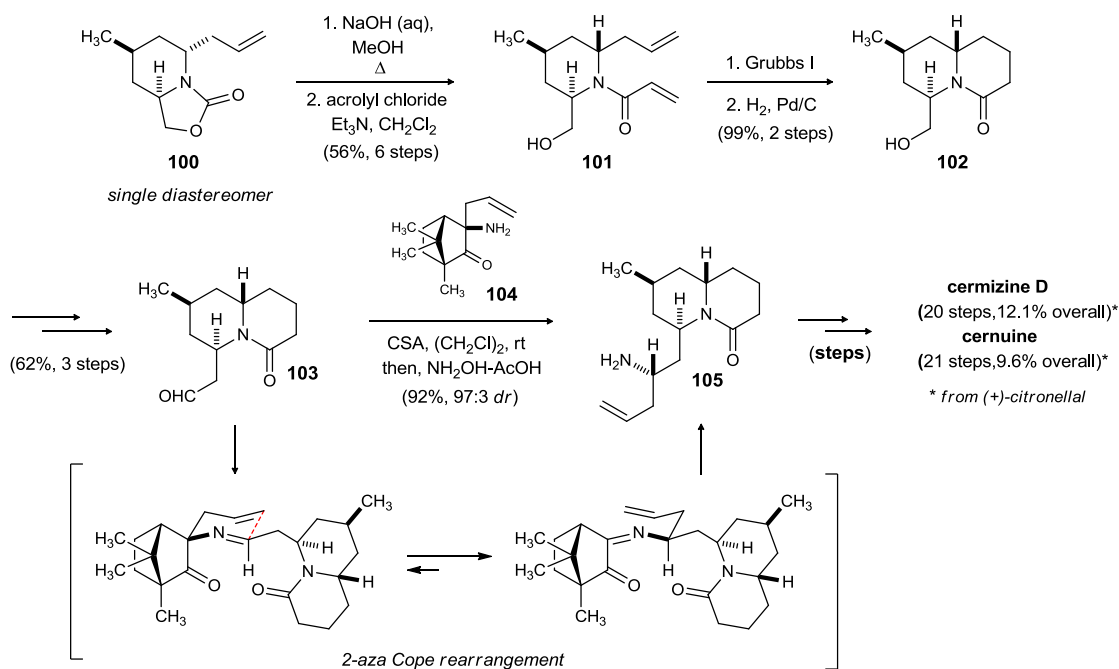
**Scheme 19.** Takayama's Synthesis of Cernuine and Cermizine D



a single diastereomer.

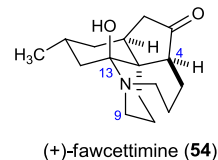
Hydrolysis of oxazolidinone **100** and acrolylation of the resulting amine provided acrylamide **101**. Ring closing methasis of **101** utilizing a Grubbs I generation catalyst provided the intermediate enone which was reduced to yield the bicyclic skeleton (**102**) of ceruine and cermizine D. The terminal alcohol in **102** was elaborated to the aldehyde (**103**) by implementing a standard one carbon homologation protocol. The aldehyde was then subjected to the key stereoselective transfer aminoallylation protocol. Treatment of the aldehyde with (1*R*)-camphor quinone derived catalyst **104** provided homoallylamine **105**. High diastereoselection (97:3) in transfer aminoallylation could be attributed to the formation of a six-membered transition state in the 2-*aza* Cope rearrangement step. **105** was then subjected to a sequence of straightforward synthetic transformations to provide (-)-ceruine and (+)-cermizine D. In summary, (-)-ceruine and (+)-cermizine D were synthesized in 19 steps (11% yield) and 21 steps (13.9%) respectively.

**Scheme 20.** Takayama's Syntheses of Ceruine and Cermizine D (Completion)



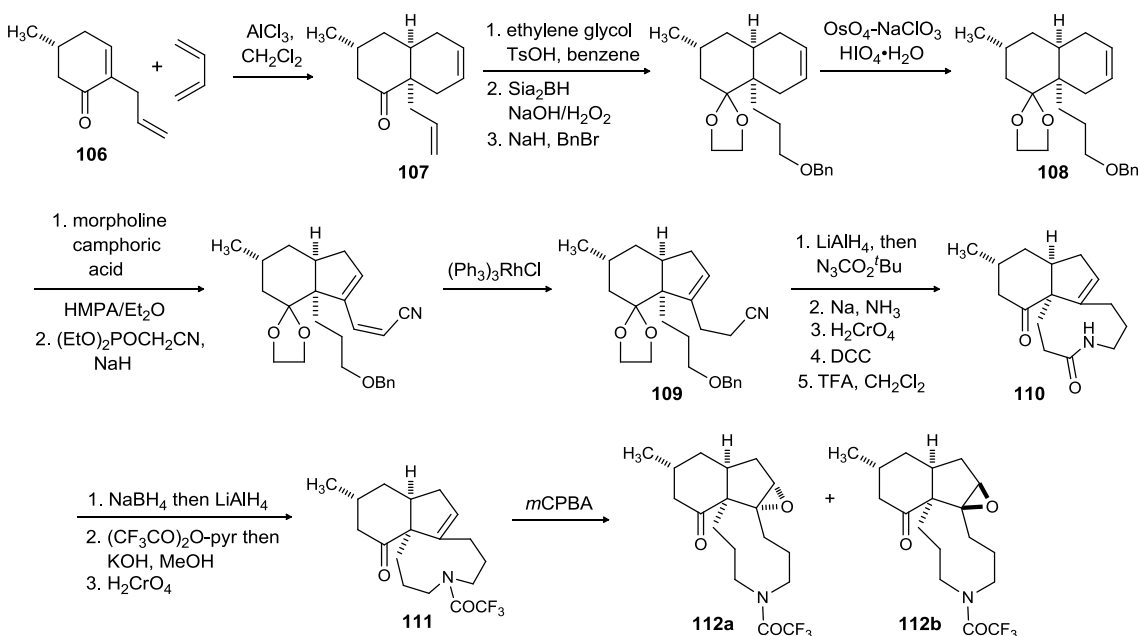
### 2.2.3. Fawcettimine Class

The fawcettimine class of Lycopodium alkaloids consists of over 60 natural products. In 1959, the first member of this class, fawcettimine (**54**), was isolated by Burnell.<sup>77</sup> Inubushi and co-workers later confirmed the structure by chemical correlation through X-ray crystallography.<sup>78</sup> Syntheses of *rac*-fawcettimine,<sup>79</sup> as well as three enantioselective synthesis of fawcettimine have been reported so far.<sup>80</sup>



Inubushi's synthesis of (±)-fawcettimine and 8-deoxyserratinine commences with a Diels-Alder reaction of butadiene with substituted quinone derivative **106** to provide **107**

**Scheme 21.** Inubushi's Synthesis of (±)-Fawcettimine



<sup>77</sup> Burnell, R. H. *J. Chem. Soc.* **1959**, 3091.

<sup>78</sup> Nishio, K.; Fujiwara, T.; Tomita, K.; Ishii, H.; Inubushi, Y.; Harayama, T. *Tetrahedron Lett.* **1969**, *10*, 861.

<sup>79</sup> a) Harayama, T.; Takatani, M.; Inubushi, Y. *Tetrahedron Lett.* **1979**, *44*, 4307; *Chem. Pharm. Bull.* **1980**, *28*, 2394; b) Heathcock, C. H.; Smith, K. M.; Blumenkopf, T. A. *J. Am. Chem. Soc.* **1986**, *108*, 5022; full paper - Heathcock, C. H.; Blumenkopf, T. A.; Smith, K. M. *J. Org. Chem.* **1989**, *54*, 1548.

<sup>80</sup> a) Liu, K.-M.; Chau, C.-M.; Sha, C.-K. *Chem. Commun.* **2008**, 91. b) Linghu, X.; Kennedy-Smith, J. J.; Toste, F. D. *Angew. Chem. Int. Ed.* **2007**, *46*, 1. c) Otsuka, Y.; Inagaki, F.; Mukai, C. *J. Org. Chem.* **2010**, *75*, 3420.

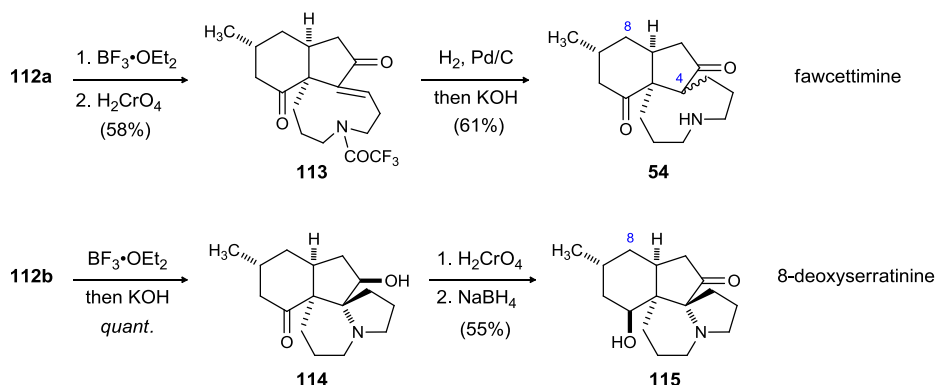


(Scheme 21). The Michael adduct was converted to **108** by executing the following operations: (i) acetalization of the carbonyl group; (ii) hydroboration of the terminal alkene; (iii) protection of the resulting alcohol; and (iv) dihydroxylation of the doubly substituted alkene followed by periodate cleavage of the resulting diol. Regioselective intramolecular aldol condensation of the dialdehyde (**108**) and subsequent functionalization of the resulting aldehyde afforded nitrile **109**. To form the nine-membered lactam ring, the nitrile was reduced and protected as the Boc-amine. Liquid ammonia benzyl amine deprotection and oxidation to the carboxylic acid was carried out, which also effected cleavage of the acetal to form **110**. In a three step reaction sequence, the amide was converted to **111**. Subsequent epoxidation afforded epoxide **112** as a mixture of diastereomers.

On treatment with  $\text{BF}_3 \cdot \text{OEt}_2$ , the  $\alpha$ -epoxide (**112a**) underwent an elimination and epoxide ring opening sequence to afford the allylic alcohol (Scheme 22). The alcohol was then oxidized to form enone **113**. Alkene reduction followed by amine deprotection furnished ( $\pm$ )-fawcettimine and *epi*-fawcettimine in 27 steps from commercially available 5-methyl-1,3-cyclohexenedione.  $\beta$ -epoxide (**112b**) was converted to 8-deoxyserratinine in a 4-step sequence (Scheme 22). Intramolecular epoxide ring opening by nitrogen and treatment of the intermediate with KOH to effect the trifluoroacetate deprotection, afforded tetracyclic compound **114**. Oxidation of the alcohol and selective reduction of the six-membered ring ketone provided 8-deoxyserratinine **115**. The configuration of fawcettimine (**54**) was not well established at the C4 center due to inconclusive data from previous IR studies. The ability of the amine to cyclize onto either ketone is directly related to the C4 configuration: condensation onto the six-membered ring ketone would

require a (4*S*) configuration while condensation onto the five-membered ring ketone would require (4*R*). Synthesis of *rac*-fawcettimine by the Heathcock group helped to elucidate the exact configuration of fawcettimine as (4*S*).

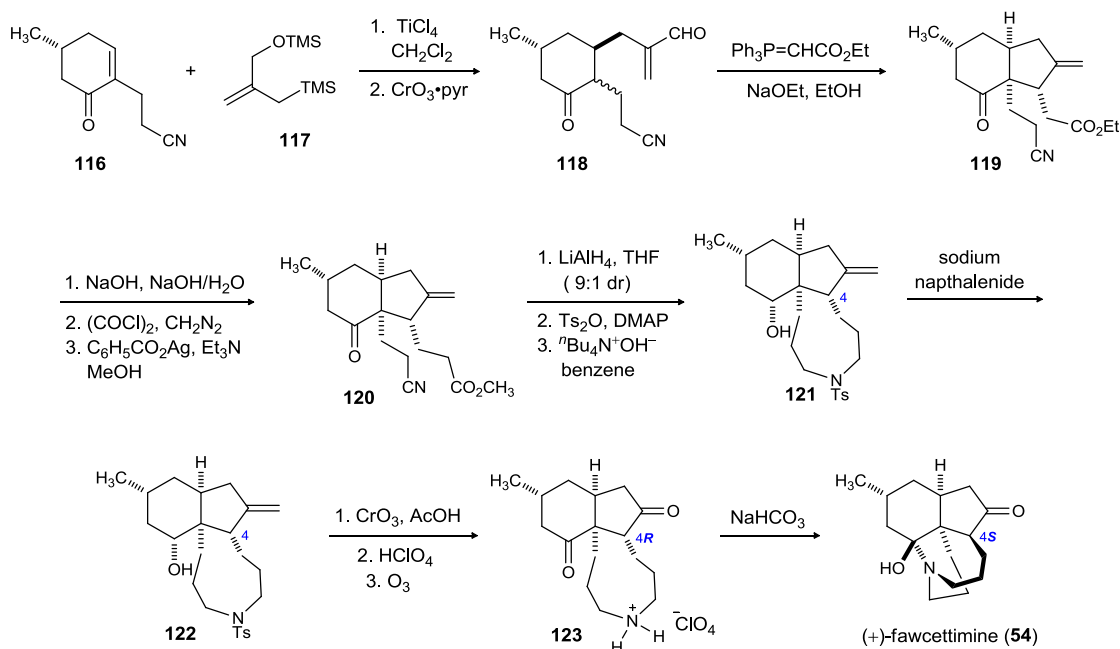
**Scheme 22.** Inubushi's Synthesis of (±)-Fawcettimine and 8-Deoxyserratenine



The Heathcock synthesis starts with nitrile **116** (Scheme 23).<sup>79b</sup> A Sakurai reaction with substituted allylsilane **117** and oxidation of the resulting alcohol employing modified Sarratt procedure, provided aldehyde **118** as a mixture of diastereomers. Wittig reaction of the aldehyde, and an intramolecular Michael addition of the resulting conjugated nitrile in a *5-exo-trig* fashion, provided ester **119**. This intermediate contains all but one carbon necessary for completion of the fawcettimine skeleton. This additional carbon was added by an Arndt-Eistert homologation of the acetic acid side chain, obtained by saponification of the ethyl ester (**119**). The Arndt-Eistert homologation product **120** was converted to the nine-membered ring **121** by executing the following operations: (i) global reduction with  $LiAlH_4$  to provide the amino diol as a 9:1 mixture of alcohol diastereomers; (ii) tosylation of the resulting primary alcohol and amine; and (iii) amine displacement of the tosylate using  $^tBu_4N^+OH^-$ . The amine was deprotected and the secondary alcohol was oxidized to provide a keto-amine intermediate, however, the amine did not cyclize onto the ketone carbonyl, providing support for the assignment of

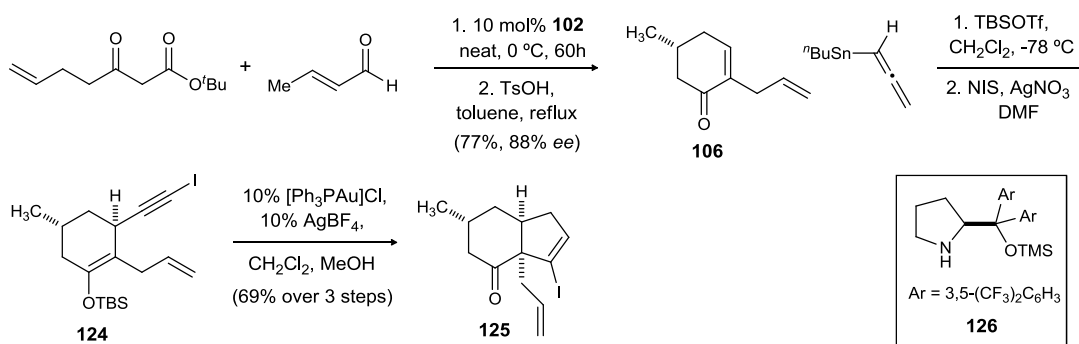
the *C4* stereochemistry as (*R*). The amine was protected as the perchlorate salt and ozonolysis of the exocyclic double bond provided amine **123**, which upon standing cyclized to ( $\pm$ )-fawcettimine. A crystal structure of the HBr salt of ( $\pm$ )-fawcettimine demonstrated that the *C4* stereocenter was now epimerized to *S* – leading to 4*S* stereochemical assignment for the natural product.

**Scheme 23.** Heathcock's Synthesis of ( $\pm$ )-Fawcettimine



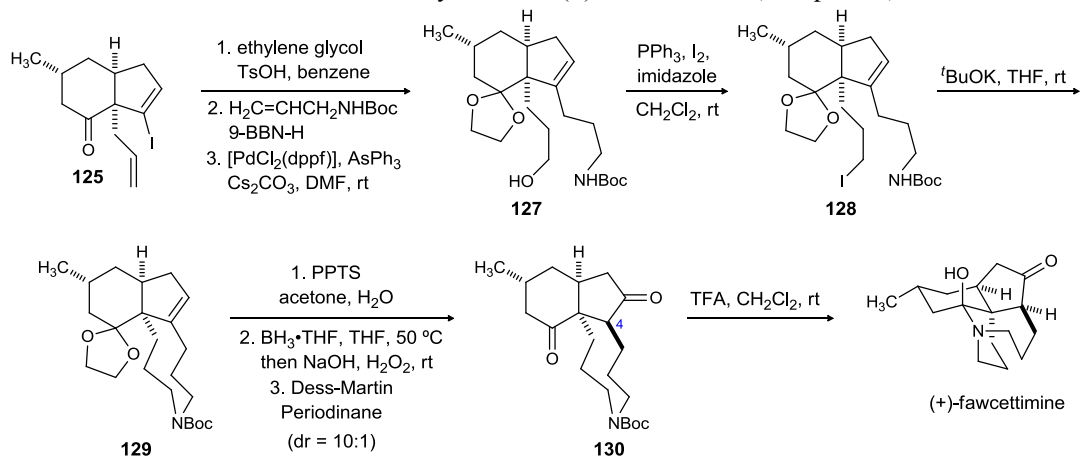
The key step in Toste synthesis of (+)-fawcettimine is a transition-metal-catalyzed *5-endo-dig* cyclization to form the *cishydrindanone* core (**125**).<sup>80b</sup> The first step utilizes an organocatalytic, asymmetric Robinson annulation to form enone **106** in 88% ee (Scheme 24). The enone was converted to the *cis*-hydrindanone core (**125**) using the following synthetic operations (Scheme 24): (i) conjugate propargylation with allenyl tin in the presence of TBSOTf; (ii) treatment with NIS to form alkynyl iodide; and (iii) gold(I)-mediated *5-endo-dig* cyclization of **124**.

**Scheme 24.** Toste's Synthesis of (+)-Fawcettimine



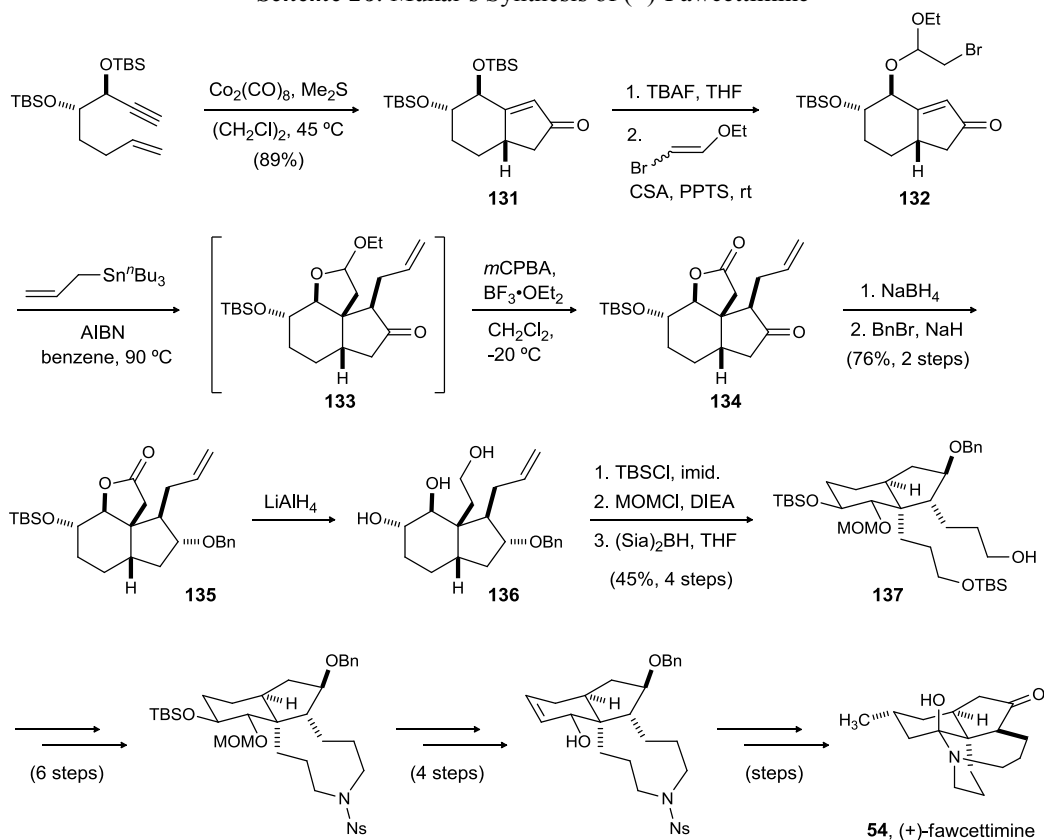
Protection of ketone as acetonide and hydroboration of the terminal alkene followed by cross coupling of the vinyl iodide with allyl amine afforded the primary alcohol (**127**) (Scheme 25). The alcohol was converted to iodide **128** and the subsequent base mediated cyclization provided the desired nine-membered ring (**129**). Several transformations including deprotection of the carbonyl group and alkene functionalization resulting the ketone, were carried out to provide the azepine ring (**130**) as a mixture (10:1) of diastereomers favoring the the *trans* epimer. Acid mediated deprotection of the Boc-amine provided (+)-fawcettimine in 13 steps from crotonaldehyde. The C4 *cis*-epimer was also isolated which isomerized to the natural product over time.

**Scheme 25.** Toste's Synthesis of (+)-Fawcettimine (Completion)



An efficient synthetic approach to (+)-fawcettimine and (+)-lycoserramine-B was demonstrated by Mukai and coworkers which utilizes a Pauson-Khand reaction for the rapid assembly of central bicyclic skeleton (**131**).<sup>80c</sup> TBAF mediated selective silyl deprotection followed by treatment of the resulting alcohol with bromo ethylvinylether furnished ketal (**132**). **132** underwent free radical mediated intramolecular cyclization, in presence of AIBN and allylstannane, to provide the allylated tricycle **133** which was oxidized *in situ* to provide **134** (Scheme 26).

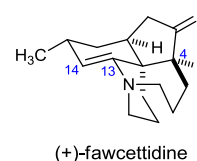
**Scheme 26.** Mukai's Synthesis of (+)-Fawcettimine



Substrate controlled reduction of **134**, followed by protection of the resulting alcohol provided **135**.  $\text{LiAlH}_4$  mediated reduction of **135** led to triol **136** (Scheme 26). Chemoselective -TBS protection of two alcohols and MOM protection of the third

alcohol in **136** was followed by hydroboration of the terminal alkene to provide the advanced intermediate **137**. **137** was finally converted to (+)-fawcettimine utilizing a strategy which was similar to the earlier reported synthesis of fawcettimine by Heathcock *et al.*<sup>79b</sup>

Fawcettidine (**53**) is proposed to be a biogenetic precursor to fawcettimine. The C13–C14 double bond of fawcettidine is hydrated to afford fawcettimine. Fawcettidine was isolated by Burnell *et al.* in

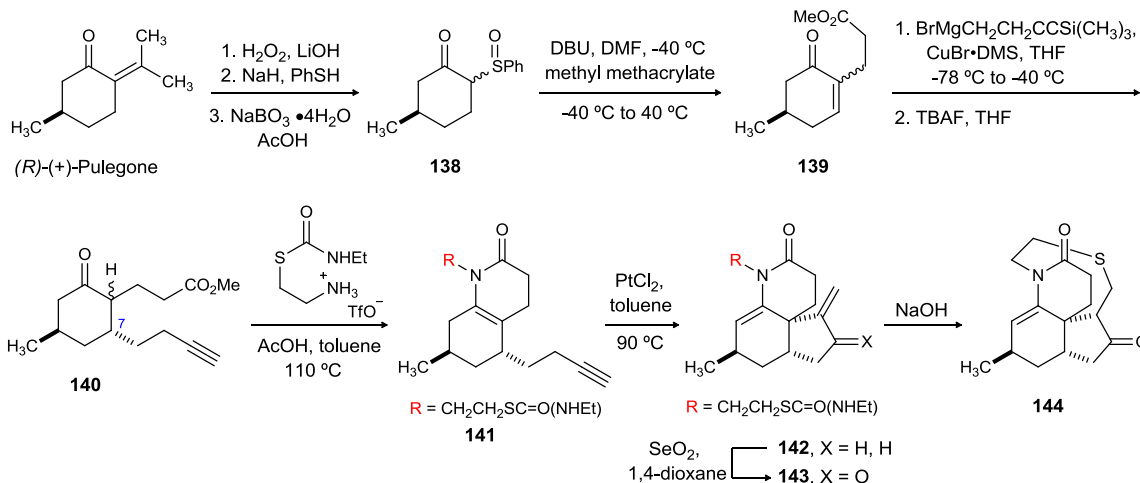


the late 1950's from *Lycopodium fawcetti*.<sup>77</sup> The structure of fawcettidine was established based on its semisynthesis from other members of the *Lycopodium* family.<sup>81</sup> The first total synthesis of (+)-fawcettidine was recently reported by Dake and coworkers.<sup>82</sup> The Dake group recognized that the key all-carbon quaternary center in fawcettidine could be prepared by an intramolecular platinum(II)-catalyzed annulation using enamide as a nucleophile (Scheme 27). To this end, (*R*)-(+)-Pulegone was elaborated to give sulfoxide **138** in three steps. Michael addition with methyl methacrylate followed by unsaturation afforded the enone (**139**). A cuprate addition followed by desilylation afforded **140** as a mixture of diastereomers, which was then elaborated to a 10:1 mixture of enamide isomers **141**. The key platinum(II)-catalyzed annulation step underwent smoothly to afford the tricycle **142** as a single product. Chemoselective allylic oxidation to form **142** followed by the conjugate addition of thiolate, resulting from the deprotection of the carbamate group, afforded sulfide **143**.

<sup>81</sup> a) Ishii, H.; Yasui, B.; Nishino, R. –I.; Harayama, T.; Inubushi, Y. *Chem. Pharm. Bull.* **1970**, *18*, 1880. b) Inubushi, Y.; Harayama, T.; Yamaguchi, K.; Ishii, H. *Chem. Pharm. Bull.* **1981**, *29*, 3418. c) Inubushi, Y.; Ishii, H.; Harayama, T.; Burnell, R. H.; Ayer, W. A.; Altenkirk, B. *Tetrahedron Lett.* **1967**, *8*, 1069.

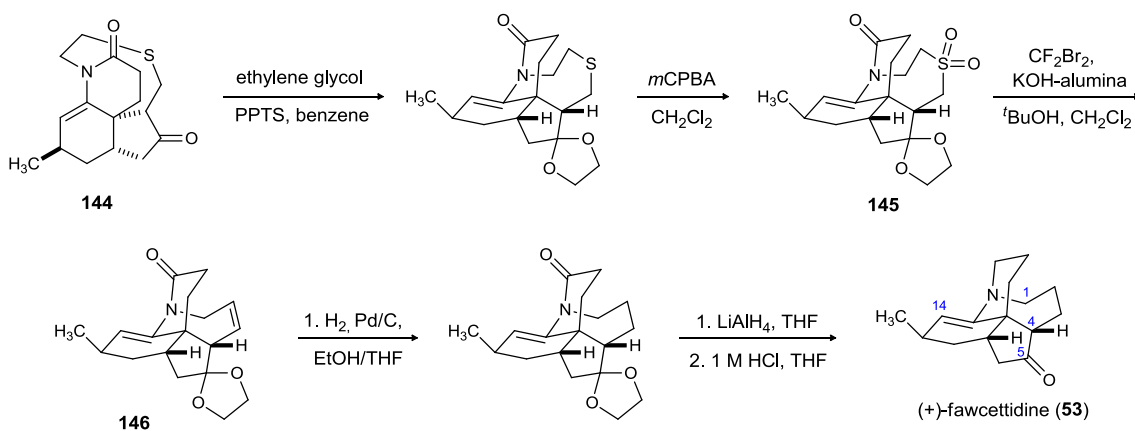
<sup>82</sup> Kozak, J. A.; Dake, G. R. *Angew. Chem. Int. Ed.* **2008**, *47*, 4221.

**Scheme 27.** Dake's Synthesis of (+)-Fawcettidine



The protection of the carbonyl group followed by sulfide oxidation afforded the sulfone **145**. The Ramberg-Bäcklund reaction was utilized to elicit the desired C2-C3 bond formation (Scheme 23). The resulting alkene **146** was then converted to (+)-fawcettidine in a three step sequence including alkene and amide reduction, and acetone deprotection.

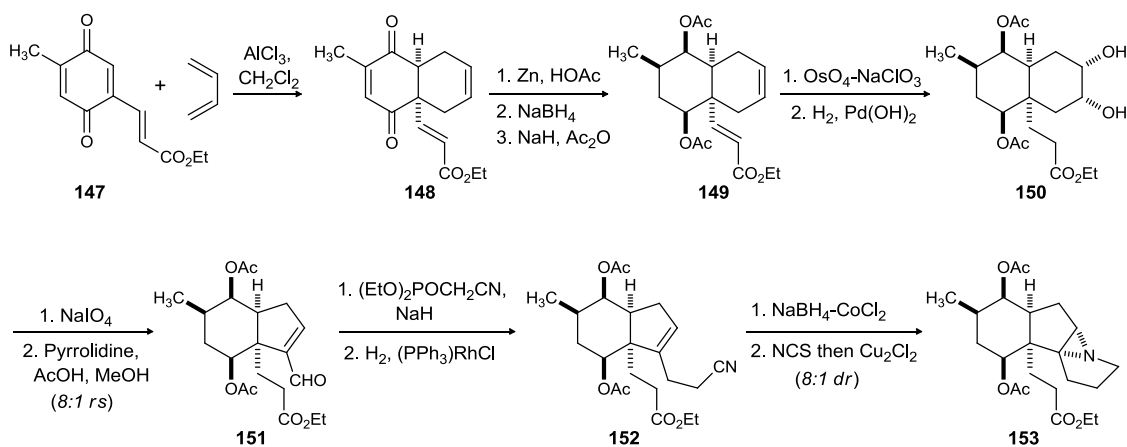
**Scheme 28.** Dake's Synthesis of (+)-Fawcettidine (Completion)



To date, there are no total syntheses of serratezomine A. However, there has been a total synthesis of racemic serratinine (**38**), a biogenetic precursor to serratezomine A,

accomplished by Inubushi.<sup>83</sup> The synthesis begins with the Diels-Alder reaction of the quinone derivative (**147**) with butadiene to afford **148** (Scheme 29). Zinc reduction of the doubly-unsaturated alkene and then NaBH<sub>4</sub> mediated ketone reduction followed by acetylation resulted in the unsaturated ester (**149**). Dihydroxylation of the electron-rich alkene followed by hydrogenation of the conjugated alkene led to the diol **150**. The diol was cleaved with sodium periodate and the resulting dialdehyde was treated with pyrrolidine to afford the aldehyde (**151**) as a 9:1 ratio of regioisomers. The aldehyde was elaborated, utilizing a Wittig reaction and reduction, to the alkyl nitrile side chain (**152**). The nitrile was selectively reduced in the presence of the ester using NaBH<sub>4</sub>/CoCl<sub>2</sub>, and the resulting amine was chlorinated using NCS. Treatment with Cu<sub>2</sub>Cl<sub>2</sub> led to *in situ* aziridination via a nitrene intermediate to afford a 8:1 diastereomeric mixture of aziridine **153**, resulting from addition to the less hindered, convex face of the cyclopentene.

**Scheme 29.** Inubushi's Synthesis of (±)-Serratinine



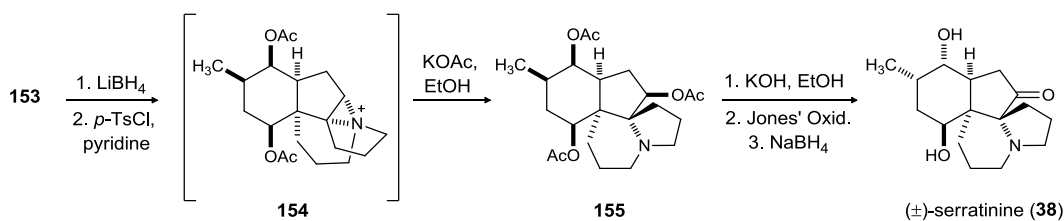
Reduction of the ester, tosylate formation, and displacement with the aziridine nitrogen formed an aziridinium ion **154** in which the aziridine nitrogen is part of three

<sup>83</sup> a) Harayama, T.; Ohtani, M.; Oki, M.; Inubushi, Y. *J. Chem. Soc. Chem. Commun.* **1974**, 827. b) Harayama, T.; Ohtani, M.; Oki, M.; Inubushi, Y. *Chem. Pharm. Bull.* **1975**, 23, 1511. c) reviewed in: Inubushi, Y.; Harayama, T. *Heterocycles* **1981**, 15, 611.



ring systems (Scheme 30). This intermediate was treated with KOAc to afford the serratinine skeleton (**124**). Global acetate deprotection was accomplished with KOH and the three alcohols were oxidized with H<sub>2</sub>CrO<sub>4</sub>, which also caused epimerization of the methyl group to the correct configuration. Treatment with NaBH<sub>4</sub> provided reduction of the two six-membered ring ketones in preference to the five-membered ring ketone, providing *rac*-serratinine (**38**) in 17 steps from **147** in less than 1% yield

**Scheme 30.** Inubushi's Synthesis of (±)-Serratinine (Completion)



In addition to the total synthesis of *rac*-Serratinine described above, a total synthesis of the closely related 13-deoxyserratinine<sup>84</sup> has also been accomplished, as well as two syntheses of the framework contained within serratinine.<sup>85</sup>

An elegant synthesis of (+)-lycoposerramine C has recently been reported by Takayama and coworkers.<sup>86</sup> The isolation of this molecule was reported by the same group in 2002.<sup>87</sup> (+)-Lycoposerramine C is a fawcettimine-type *Lycopodium* alkaloid possessing a double bond at the C6–C7 positions of fawcettimine (Figure 38). Preliminary screening has indicated that this natural product exhibits strong acetylcholine esterase (AChE) inhibition. This is the only synthesis of this natural product reported till date.

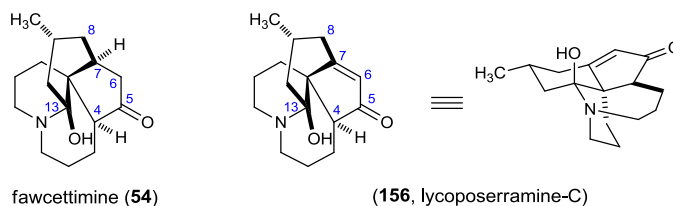
<sup>84</sup> Cassayre, J.; Gagosz, F.; Zard, S. Z. *Angew. Chem. Int. Ed.* **2002**, *41*, 1783.

<sup>85</sup> a) Mehta, G.; Reddy, M. S.; Radhakrishnan, R.; Manjula, M. V.; Viswamitra, M. A. *Tetrahedron Lett.* **1991**, *32*, 6219; b) Luedtke, G.; Livinghouse, T. *J. Chem. Soc. Perkin Trans. I.* **1995**, 2369.

<sup>86</sup> Nakayama, A.; Kogure, N.; Kitajima, M.; Takayama, H. *Org. Lett.* **2009**, *11*, 5554.

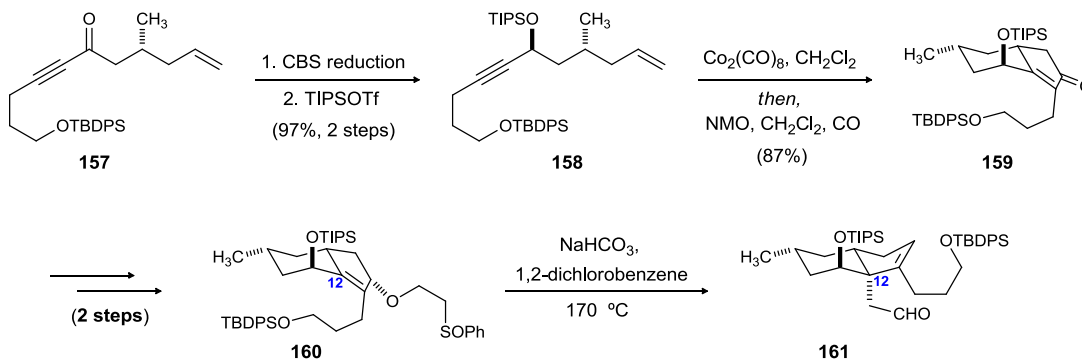
<sup>87</sup> Takayama, H.; Katakawa, K.; Kitajima, M.; Yamaguchi, K.; Aimi, N. *Tetrahedron Lett.* **2002**, *43*, 8307.

**Figure 38.** Structure of (+)-Lycoposerramine C



Like the Mukai's synthesis of fawcettimine,<sup>80c</sup> Takayama's synthesis relies on the Pauson-Khand reaction to construct the bicyclic core (**159**) of lycoposerramine C. The substrate for this transformation was synthesized in two steps from easily accessible **157**. To prepare the sulfoxide (**160**), the Pauson-Khand adduct was subjected to Mandai's conditions. Employment of a Claisen rearrangement led to the elegant construction of the rather difficult angular quaternary center. 2D NMR analysis indicated that C12 in **161** had the expected (*S*) configuration.

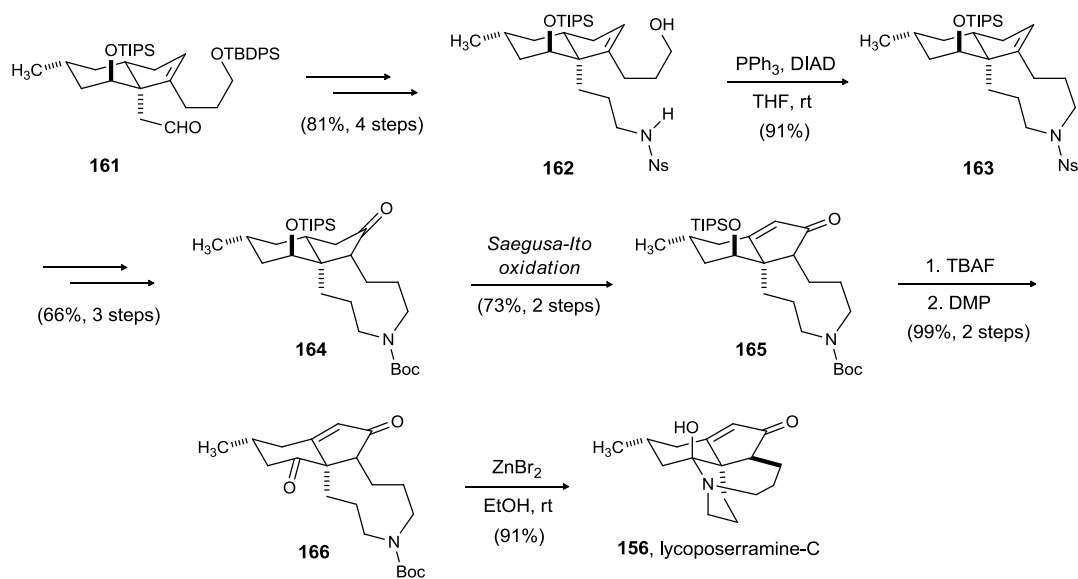
**Scheme 31.** Takayama's Asymmetric Synthesis of Lycoposerramine C



The aldehyde (**161**) was elaborated to provide aminoalcohol **162** in 4 steps and 81% overall yield (Scheme 32). **161** was subjected to an intramolecular Mitsunobu reaction to forge the azepine ring (**163**). Straightforward synthetic operations were then employed to synthesize **164**. The requisite C6-C7 double bond was formed by utilizing a Saegusa-Ito oxidative protocol. Desilylation followed by oxidation of the resulting

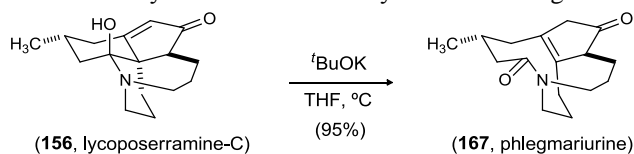
alcohol provided keto-enone **165**. ZnBr<sub>2</sub> mediated BOC deprotection revealed a keto-amine intermediate which underwent spontaneous hemiaminal formation to provide (+)-lycoposerramine C.

**Scheme 32.** Takayama's Asymmetric Synthesis of Lycoposerramine C (Completion)



In a biomimetic synthesis of phlegmariurine A, a tricyclic *Lycopodium* alkaloid, Takayama and coworkers treated (+)-lycoposerramine with NaOMe to form phlegmariurine A.

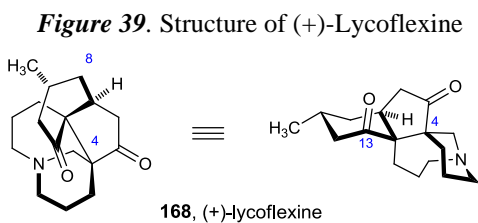
**Scheme 33.** Takayama's Biomimetic Synthesis of Phlegmariurine A



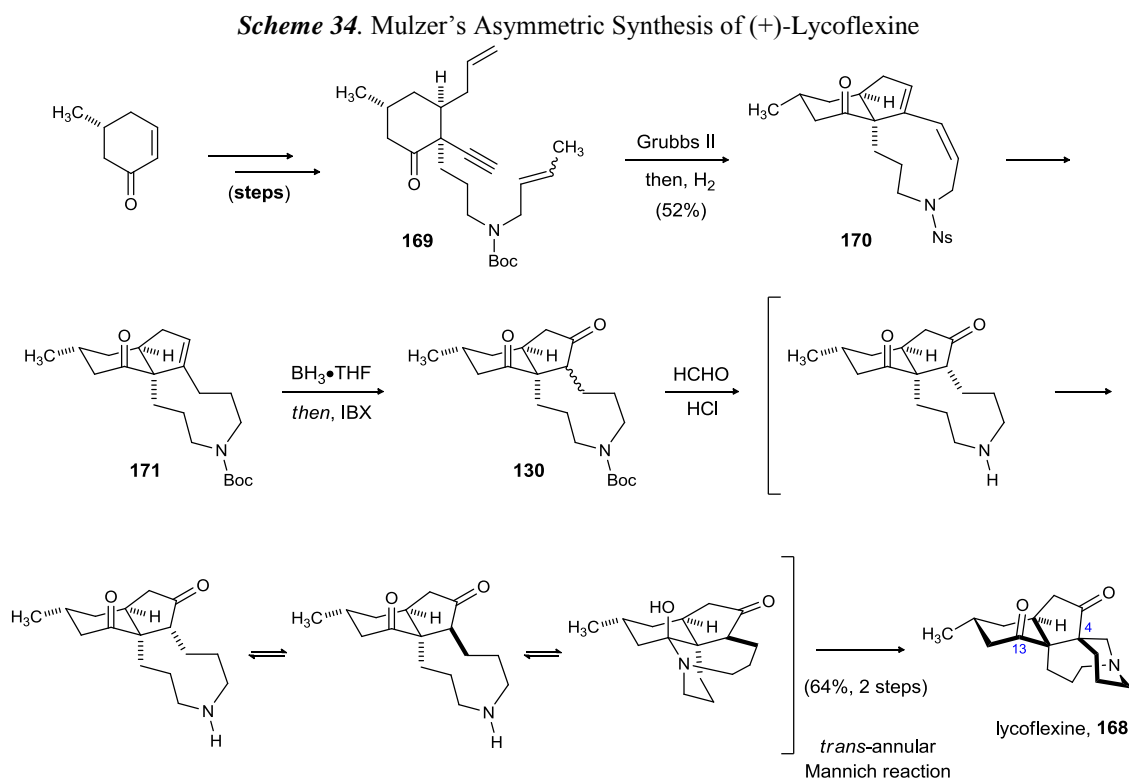
The synthesis of (+)-lycoflexine, a biogenetic precursor of serratezomine, has recently been reported by Mulzer and coworkers.<sup>88</sup> (+)-Lycoflexine belongs to a sub class of the fawcettimine alkaloids. Lycoflexine has been proposed to be biosynthetically

<sup>88</sup> Ramharter, J.; Weinstabl, H.; Mulzer, J. *J. Am. Chem. Soc.* **2010**, *132*, 14438.

derived from fawcettimine by the cleavage of the *N*-C13 bond followed by formation of a new *N*-C4 bond (Figure 39).



Mulzer's synthesis commences with dienyne **169** which is accessible from a known optically-active cyclohexenone derivative in 5 steps and 40% overall yield (Scheme 34). The azepine ring in lycoflexine was synthesized in a two-step one-pot sequence which included a ring-closing metathesis step followed by reduction of the resulting tricyclic carbamate **170** *in situ*. The cyclopentene derivative (**171**) was elaborated to cyclopentanone derivative **130** by utilizing two sequential oxidative steps.



To validate the biosynthetic proposal of lycoflexine by Ayers *et al.*,<sup>89</sup> the advanced intermediate (**130**) was sequentially treated with HCl and aqueous formaldehyde. In this tandem reaction, unmasking of the secondary amine was followed by spontaneous cyclization to provide fawcettimine which then underwent a transannular Mannich reaction, through the formation of an intermediate iminium species, to provide (+)-lycoflexine. The Mulzer's synthesis of (+)-lycoflexine **168** is noteworthy due to its conciseness and efficiency.

These syntheses of the fawcettimine class of *Lycopodium* alkaloids provide the synthetic community with novel strategies to assemble the highly condensed and complex natural products with relative ease and efficiency.

#### 2.2.4. Lycodine Class

The lycodine class of *Lycopodium* alkaloids is the smallest subclass of *Lycopodium* alkaloid, consisting of 26 natural products. In contrast to other subclasses of *Lycopodium* alkaloids, the lycodine subclass is rarely hydroxylated. Variations in structures are mainly due to dehydrogenation, skeletal additions (methylation), acetylation or other substitutions. The lycodine subclass of *Lycopodium* alkaloids possesses 4 rings, including a pyridine or pyridine ring.

Huperzine A (HupA), which was isolated from the Chinese folk medicinal herb *Qian Ceng Ta* by Liu and coworkers<sup>56b</sup> is the most well-known, and appears to be the most potent member of this family of alkaloids. Huperzine A possesses a bicyclo[3.3.1] skeleton fused with a pyridone and ethylidene moiety. Due to its fascinating structure and

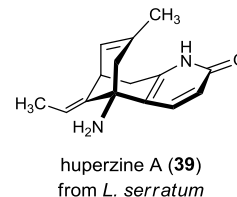
---

<sup>89</sup> Ayer, W. A.; Fukazawa, Y.; Singer, P. P. *Tetrahedron Lett.* **1973**, *14*, 5045.

potent biological activity, huperzine has attracted a considerable attention from the synthetic community<sup>90</sup> since its first synthesis by Kozlowski<sup>91</sup> and Qian *et al.*<sup>92</sup>

Fukuayama *et al.* has recently reported a novel and efficient synthesis of (-)-huperzine A.<sup>93</sup> The key step in this synthesis was a cation-olefin cyclization to forge the tricyclic skeleton (**179**). The precursor for the cyclization step

was synthesized from easily accessible anhydride **172**. The synthesis commences with the desymmetrization of the aldehyde, using Bolm's protocol, to provide **173**.<sup>94</sup> Selective reduction of



the carboxylic acid functionality followed by lactonization under the reductive conditions provided **174**. The lactone was converted to the key hydroxyenone **178** by using the following synthetic operations (Scheme 35): (a) a KHMDS promoted ring opening of the furan, and treatment of the resulting dianion (**175**) with methallyl bromide, to provide **176**; (ii) stereoselective epoxidation of the homoallylic alcohol to provide epoxy alcohol **177**; and (iii) conversion to the hydroxyenone by epoxide cleavage under Swern reaction conditions. With the requisite hydroxyketone in hand, various methods to forge the bicycle[3.3.1] skeleton were investigated. During the course of this investigation, it was fortuitously found that the desired tricyclic skeleton (**179**) could be accessed by TfOH

<sup>90</sup> Asymmetric syntheses using the tandem Michel-aldol reaction: a) Yamada, F.; Kozikowski, A. P.; Reddy, E. R.; Pang, Y.-P.; Miller, J. H.; McKinney, M. *J. Am. Chem. Soc.* **1991**, *113*, 4695. b) Kaneko, S.; Yoshino, T.; Katoh, T.; Terashima, S. *Heterocycles* **1997**, *46*, 27. c) Kaneko, S.; Yoshino, T.; Katoh, T.; Terashima, S. *Tetrahedron* **1998**, *54*, 5471. d) Pan, Q.-B.; Ma, D.-W. *Chin. J. Chem.* **2003**, *21*, 7. Asymmetric syntheses using the palladium-catalyzed annulation: e) Kaneko, S.; Yoshino, T.; Katoh, T.; Terashima, S. *Tetrahedron: Asymmetry* **1997**, *8*, 829. f) Chassaing, C.; Haudrechy, A.; Langlois, Y. *Tetrahedron Lett.* **1999**, *40*, 8805. g) Haudrechy, A.; Chassaing, C.; Riche, C.; Langlois, Y. *Tetrahedron* **2000**, *56*, 3181. h) He, X.-C.; Wang, B.; Yu, G.; Bai, D. *Tetrahedron: Asymmetry* **2001**, *12*, 3213.

<sup>91</sup> a) Xia, Y.; Kozikowski, A. P. *J. Am. Chem. Soc.* **1989**, *111*, 4116. b) Kozikowski, A. P.; Campiani, G.; Aagaard, P.; McKinney, M. *J. Chem. Soc., Chem. Commun.* **1993**, 860.

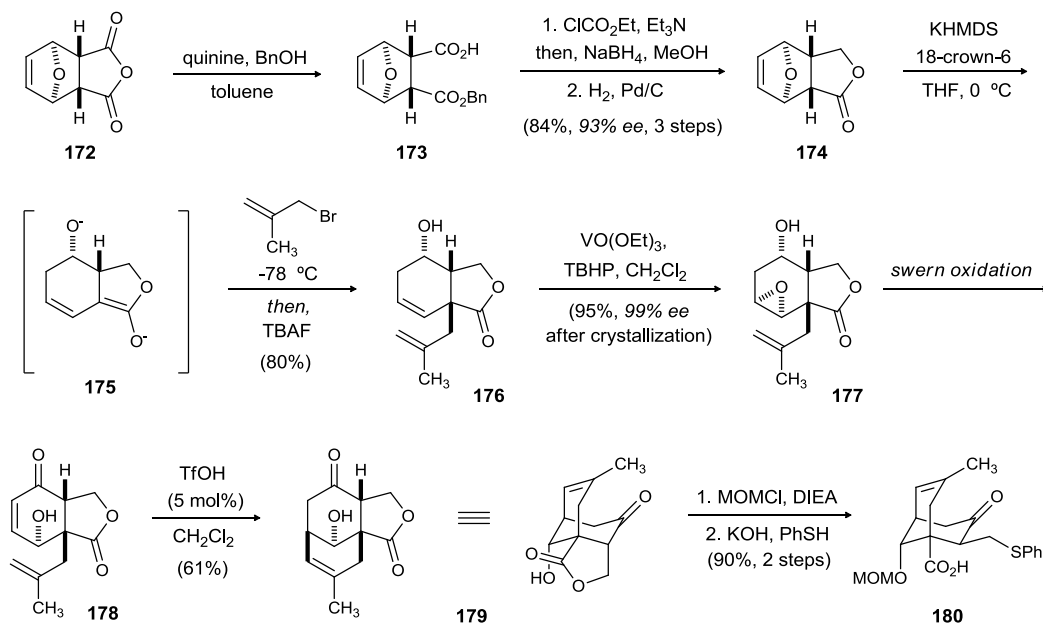
<sup>92</sup> Qian, L.; Ji, R. *Tetrahedron Lett.* **1989**, *30*, 2089.

<sup>93</sup> Koshiba, T.; Yokoshima, S.; Fukuyama, T. *Org Lett.* **2009**, *11*, 5354.

<sup>94</sup> Bolm, C.; Atodiresei, I.; Schiffrers, I. *Org. Synth.* **2005**, *82*, 120.

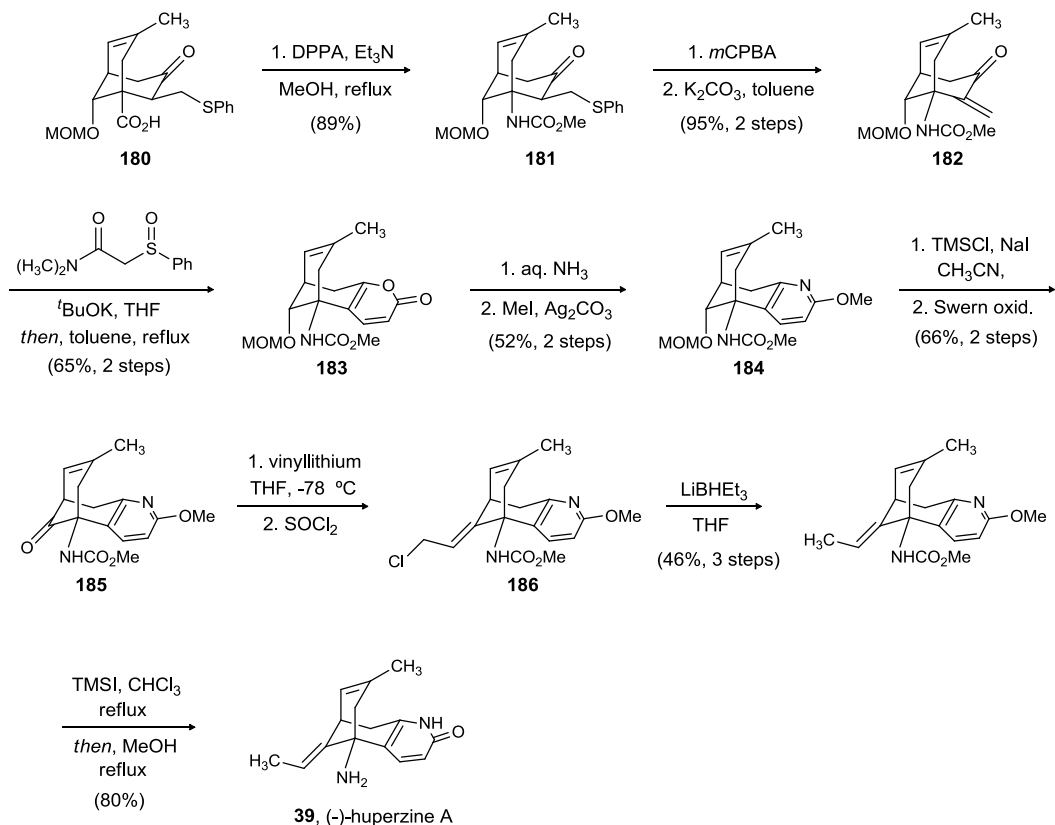
mediated cation-olefin cyclization. Tertiary alcohol protection in **179** followed by PhSH mediated ring cleavage of the fused lactone ring provided **180**.

**Scheme 35.** Fukuyama's Asymmetric Synthesis of (-)-Huperzine A



Tertiary amine functionality in the natural product was installed by employing Curtius rearrangement protocol to provide **181**. Simultaneous oxidation and elimination steps were required to form the enone functionality in **182**. The enone (**182**) was elaborated to provide the 2-methoxypyridine derivative (**184**) in 4 synthetic operations. With the amine and the pyridone functionality in place, the only missing piece in the synthesis was the installation of the ethylidene functionality. To this end, the protected secondary alcohol in **184** was unmasked and the resulting alcohol was oxidized to provide ketone **185**. The ketone was then elaborated to provide allylic chloride **186** in two steps. Reduction of the allylic chloride, followed by global deprotection, led to huperzine A in 23 overall steps.

**Scheme 36.** Fukuyama's Asymmetric Synthesis of (-)-Huperzine A (Completion)

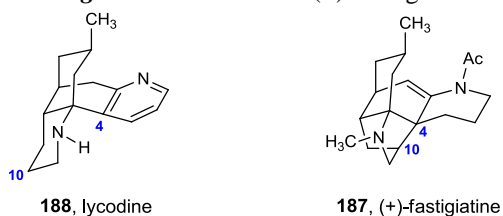


Some other complex molecules belonging to the lycodine subclass of *Lycopodium* alkaloids have been recently reported.<sup>95</sup> In 2010, Shair and coworkers developed a highly convergent strategy to assemble the lycodine framework in their synthesis of fastigiatine **187**.<sup>95a</sup> Fastigiatine possesses an unprecedented pentacyclic skeleton with added complexity in the form of a C4-C10 bond, a feature missing in other members of lycodine family. In addition to the highly strained cage-like structure, fastigiatine is adorned with five contiguous chiral centers including two vicinal quaternary centers (Figure 40).

<sup>95</sup> a) Liau, B. B.; Shair, M. D. *J. Am. Chem. Soc.* **2010**, *132*, 9594. b) Yuan, C.; Chang, C. -T.; Axelrod, A.; Siegel, D. *J. Am. Chem. Soc.* **2010**, *132*, 5924. c) Fischer, D. F.; Sarpong, R. *J. Am. Chem. Soc.* **2010**, *132*, 5926.

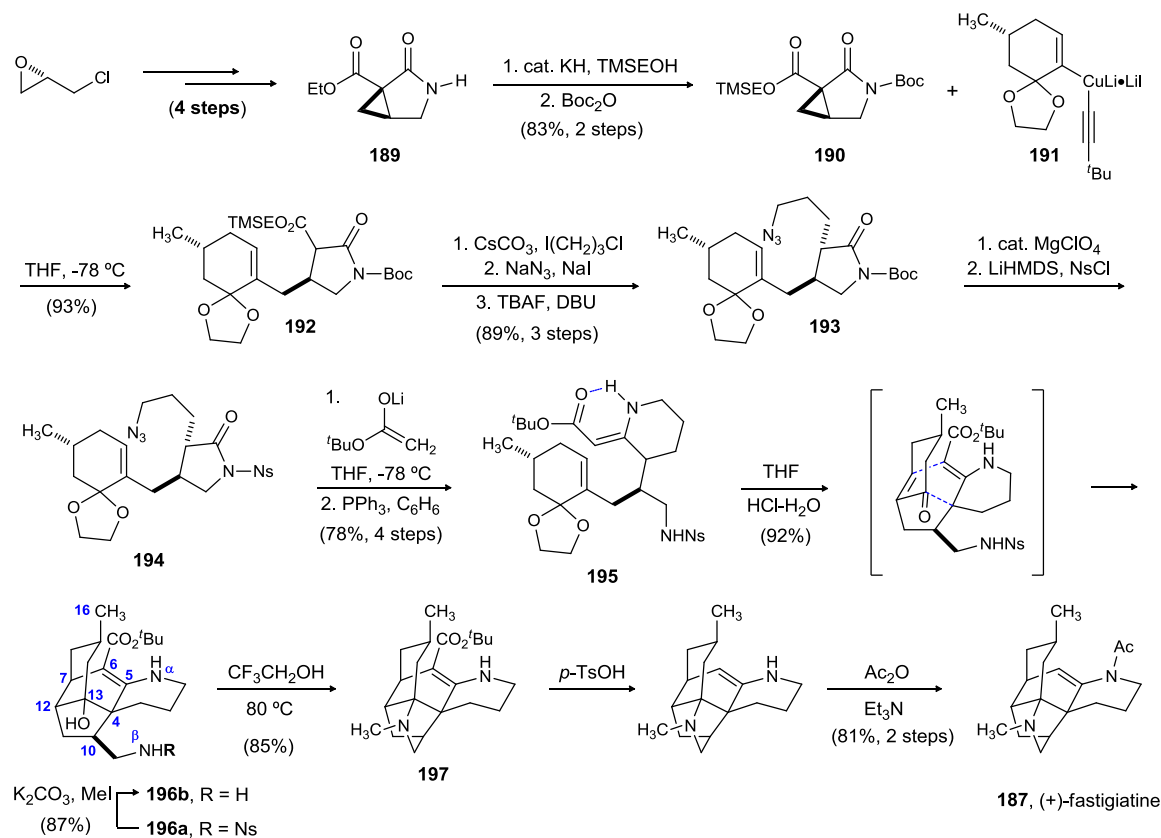


**Figure 40.** Structure of (+)-Fastigiatine



Shair's biosynthetically inspired synthesis commences with the elaboration of (*S*)-epichlorohydrin to provide cyclopropane (**189**). Adequate protection of the reactive functionalities led to the cyclopropane (**190**), which engages in a regioselective epoxide ring opening upon exposure to mixed cuprate **191**. The adduct (**192**) was then elaborated, by implementing a tandem alkylation/substitution sequence followed by a base promoted decarboxylation step, to provide *N*-Boc-2-pyrrolidinone **193**. Addition of the lithium enolate of *tert*-butylacetate to activated amide **194**, and subjection of the resulting  $\beta$ -ketoester to aza-Wittig reaction conditions afforded vinylogous urethane **195** as an inconsequential mixture of diastereomers. In an effort to secure the tetracyclic core of fastigiatine, the research group fortuitously discovered that the desired formal [3+3]-cycloaddition could be achieved in excellent diastereoselection by exposure of **195** to aqueous HCl. Shair *et al.* proposes that this noteworthy transformation occurs via initial C13-dioxolane cleavage, a 7-*endo-trig* intramolecular conjugate addition to form the C6–C7 bond, tautomerization to secure the C12 stereocenter, and finally a transannular aldol reaction to form the C4–C13 bond. The construction of the fifth ring (**197**) was achieved by heating the hydroxylamine (**196b**) in trifluoroethanol. This domino reaction is believed to occur by a tandem retro aldol reaction/iminium ion formation followed by a transannular Mannich reaction. Implementation of decarboxylation and acylation steps led to (+)-fastigiatine in 19 steps and 15% overall yield

**Scheme 37.** Shair's Asymmetric Synthesis of (+)-Fastigiatine



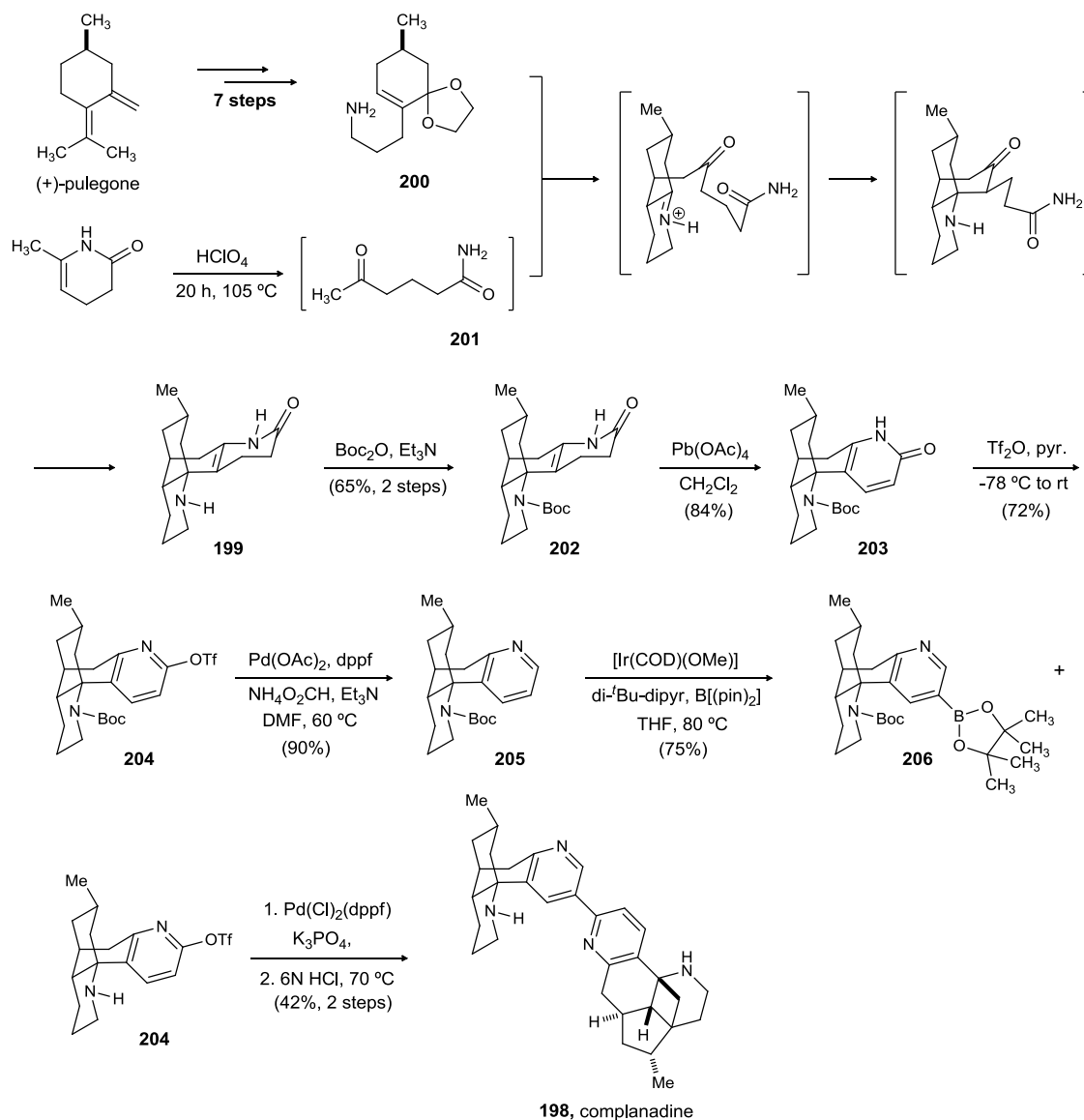
Two synthetic strategies towards complanadine **198**, a dimer of lycodine, have recently been reported.<sup>96</sup> Sarpong and coworkers reported a concise and efficient synthesis of complanadine A.<sup>96a</sup> As complanadine is an unsymmetrical dimer of lycodine, Sarpong's synthetic plan relied on the introduction of position-control elements in a common intermediate (**199**) prior to their coupling. Synthesis of **199** was achieved by following a procedure reported earlier by Schumann *et al.*<sup>97</sup> The strategy utilizes an acid-promoted formal cycloaddition of **200** and **201**; and the highly advanced intermediate (**199**) could be isolated after a cascade cyclization process (Scheme 38).

<sup>96</sup> a) Fischer, D. F.; Sarpong, R. *J. Am. Chem. Soc.* **2010**, *132*, 5926. b) Yuan, C.; Chang, C., -T, Axelrod, A.; Siegel, D. *Am. Chem. Soc.* **2010**, *132*, 5924.

<sup>97</sup> Schumann, D.; Naumann, A. *Liebigs Ann. Chem.* **1983**, 220.

The first half required for the final coupling step could be synthesized in three steps from **199** by performing the following synthetic operations: (i) Boc protection of **199** to provide **202**; (ii)  $\text{Pb}(\text{OAc})_4$  mediated oxidation of **202**; and (iii) conversion of resulting pyridone **203** to **204** by treatment with triflic anhydride.

*Scheme 38.* Sarpong's Asymmetric Synthesis of (+)-Complanadine A

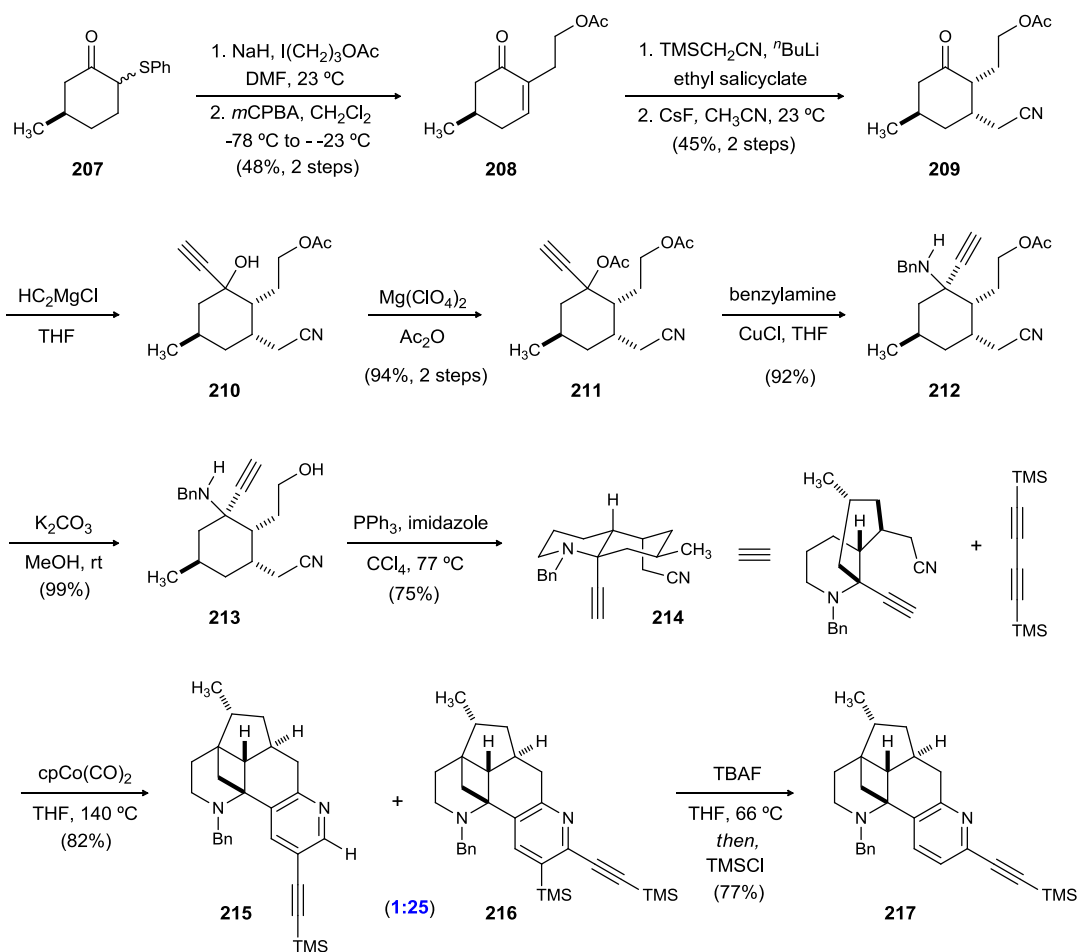


The synthesis of the second half could be accomplished in 2 steps (Scheme 38). This included the removal of triflate in **204** under Pd-catalyzed reducing conditions and

the desired functionalization of resulting pyridine derivative **205** to provide boronic ester **206**. The crucial Suzuki cross-coupling of boronic ester **206** and triflate **204** underwent uneventfully to provide the Boc protected complanadine. Acid catalyzed removal of the Boc group led to (+)-complanadine A. The utility of this synthetic strategy was later demonstrated by the same group in preparing analogues of lycodine.

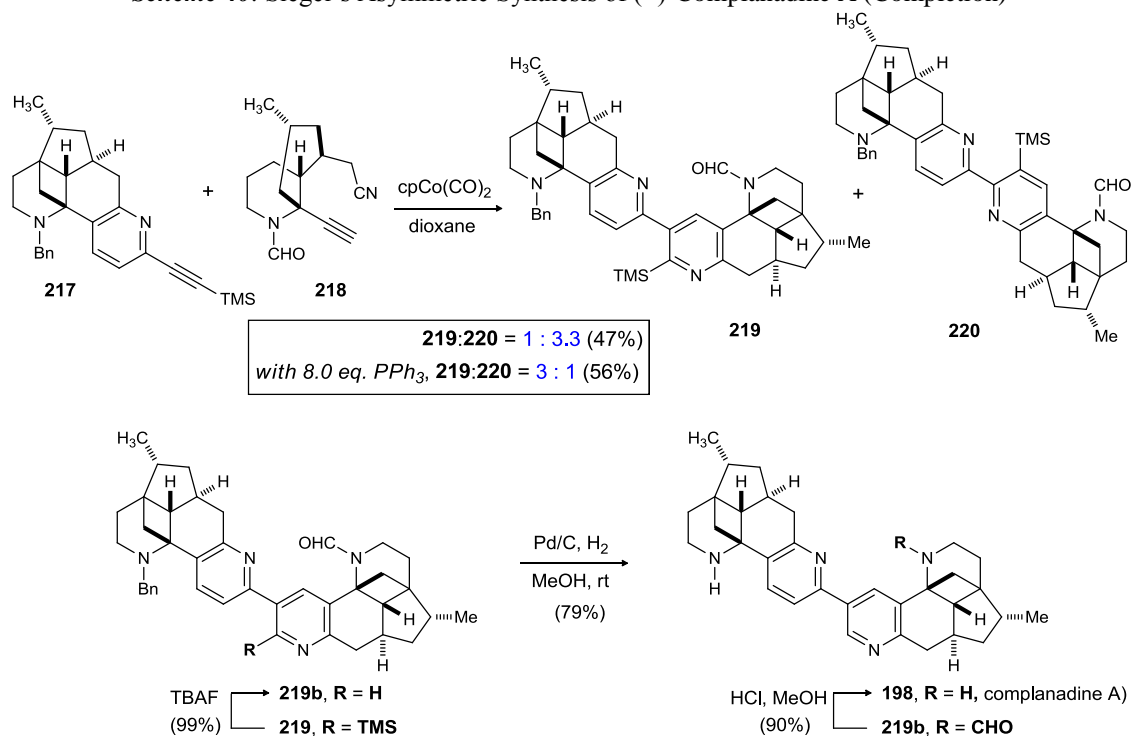
Siegel's key step in the synthesis of (+)-complanadine A involved a metal catalyzed [2+2+2] cyclization of a substituted diyne with its corresponding alkyne-nitrile to construct the bispyridine core. The synthesis commenced with readily available functionalized cyclohexanone **209**, which was synthesized in 4 steps from thioether **207** (Scheme 39). Treatment of **209** with ethylmagnesium bromide provided propargyl alcohol **210** as a single diastereomer. The acetate (**211**), synthesized by the acylation of tertiary alcohol **210**, was subjected to a Cu (I) mediated amination protocol to provide propargyl amine **212**. Unmasking of the primary alcohol under mild basic conditions, followed by cyclization using PPh<sub>3</sub>/imidazole, provided alkene-nitrile **214**. The desired [2+2+2] cycloaddition of alkyne-nitrile **214** and bis(trimethylsilyl)butadiyne proceeded smoothly under thermal conditions using CpCo(CO)<sub>2</sub> to afford the adduct **215** in excellent regioselection. The stage was then set to construct the second pyridine core by engaging pyridyl-alkyne **216** and alkyne-nitrile **214** in an another metal catalyzed [2+2+2] cycloaddition reaction. However, the pyridyl-alkyne **216** was found to be recalcitrant to effect this reaction under a variety of catalysts and conditions. After an exhaustive investigation, a solution to this problem was found. This included a global silyl deprotection of **216** followed by selective TMS protection of the resulting alkyne.

**Scheme 39.** Siegel's Asymmetric Synthesis of (+)-Complanadine A



The desired metal catalyzed [2+2+2] cycloaddition was achieved by heating **217** and **214** under the optimized reaction conditions (Scheme 40). The adduct **219** could be isolated in modest regioselectivity. The use of a formyl group in place of the benzyl group in **218** was required as **217** and **214** failed to react in the presence of PPh<sub>3</sub>. Completion of the total synthesis was accomplished by executing the following synthetic operations (Scheme 40): (i) fluoride mediated removal of the aryl-trimethylsilyl group in **219**; (ii) debenzoylation of **219b** by hydrogenation; and (iii) conversion to (+)-complanadine by deformylation of **219b**.

**Scheme 40.** Siegel's Asymmetric Synthesis of (+)-Complanadine A (Completion)

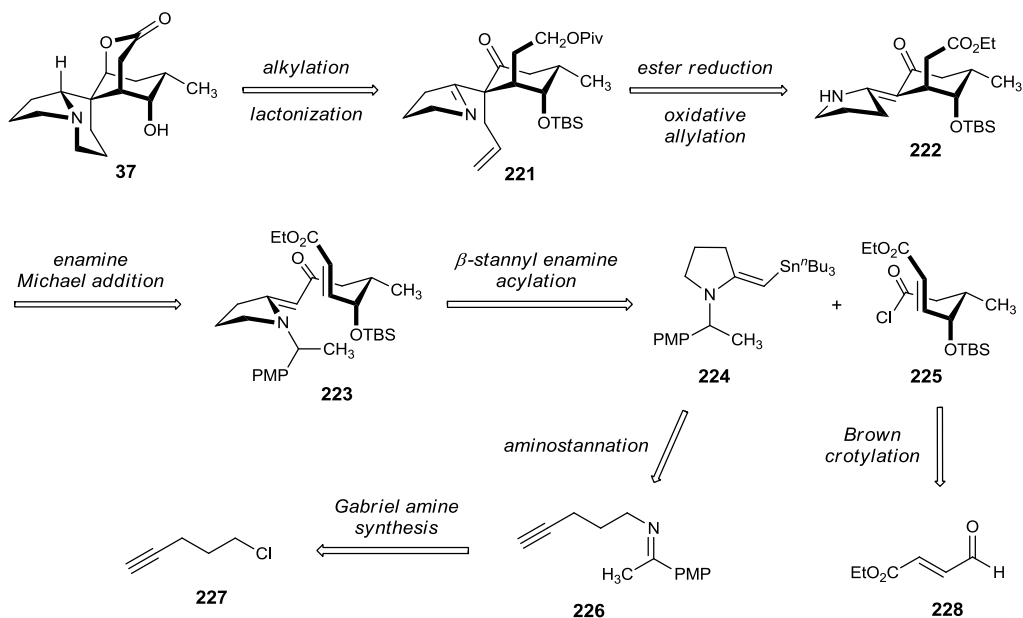


### 2.3. Retrosynthetic Analysis of Serratezomine A

From a retrosynthetic perspective, we proposed that the potentially unstable bridged lactone functionality in **37** would be constructed in the final stages of synthesis, by oxidation of the diol, resulting from ketone reduction to the  $\beta$ -OH and removal of the pivalate protecting group from the primary alcohol (Scheme 41). The late-stage annulation of the piperidine ring onto the pyrroline ring would be realized by elaboration of the terminal alkene in **221**. Therefore, **221** was considered to be a key intermediate as it contained all of the required carbons of the natural product. Installation of the allyl group would result from a cerium-mediated diastereoselective allylation of vinylogous amide **222**. The cyclohexane ring in the vinylogous amide **222** would be formed via a

tandem *N*-deprotection/enamine Michael addition onto the  $\alpha,\beta$ -unsaturated ester of **223**. The *N*-protected vinylogous amide would be formed via an acylation of  $\beta$ -stannyleneamine **224** with acid chloride **225**. The  $\beta$ -stannyleneamine was synthesized by methodology developed within our group, involving a radical-mediated *5-exo-trig* cyclization of a vinyl radical onto the nitrogen of an imine.<sup>98</sup> The imine (**226**) would be accessed from the commercially available alkynyl chloride **227**. The acid chloride would be accessed from the commercially available aldehyde **228**, by utilizing a Brown crotylation reaction to install the first two stereocenters in the molecule. These two stereocenters would in turn direct the installation of remaining four stereocenters in serratezomine A.

**Scheme 41.** Retrosynthetic Analysis of (+)-Serratezomine A



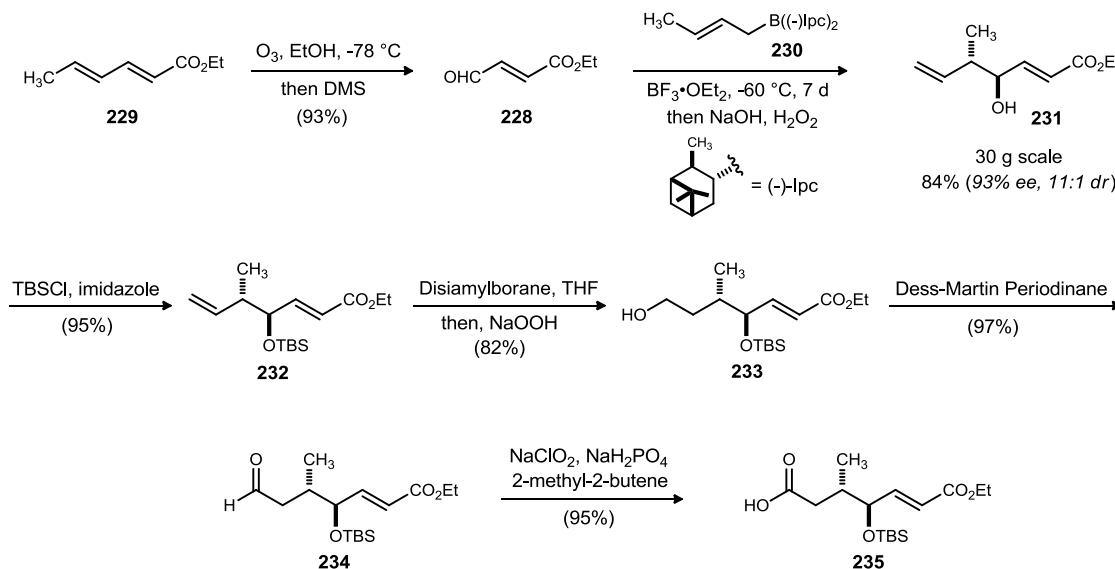
<sup>98</sup> For development of the  $\beta$ -stannyleneamine methodology see: a) Nugent, B. M.; Williams, A. L.; Prabhakaran, E. N.; Johnston, J. N. *Tetrahedron* **2003**, *59*, 8877; b) Prabhakaran, E. N.; Nugent, B. M.; Williams, A. L.; Nailor, K. E.; Johnston, J. N. *Org. Lett.* **2002**, *4*, 4197.

## 2.4. Results and Discussion

### 2.4.1. Synthesis of the Vinylogous Amide<sup>99</sup>

The synthesis of the vinylogous amide was already accomplished in the Johnston group. The synthesis commences with the commercially available ethyl sorbate **229**.<sup>100</sup> Ozonolysis of the terminal alkene using Sudan Red 7B as the indicator provided  $\alpha,\beta$ -unsaturated aldehyde **228**, after vacuum distillation, in 93% yield (Scheme 42). On a larger scale (> 50 g), the reaction yield dropped marginally to 70-75%. The  $\alpha,\beta$ -unsaturated aldehyde can also be obtained directly from the commercial sources.<sup>101</sup>

**Scheme 42.** Synthesis of the Key Carboxylic Acid Fragment (**235**)



<sup>99</sup> a) Milligram scale: Mutnick, Daniel M. M.S. Thesis, Indiana University, Bloomington, IN, 2003.

b) Scale up (gram scale): Pigza, Julie A. Ph. D. Dissertation, Indiana University, Bloomington, IN, 2008; and (c) Jeong-seok Han.

<sup>100</sup> Ethyl sorbate (sorbic acid ethyl ester) was purchased from TCI Chem. Co. 500 mL/\$128.74 and distilled before use.

<sup>101</sup> Commercially available from TCI



To install the first two stereocenters, a brown crotylation strategy was employed.<sup>102</sup> On small scale, the reaction was run for three days at -78 °C to provide the desired product in 53% yield (92% ee, 10:1 dr). The structure of the major diastereomer was confirmed by formation of both the (*R*)- and (*S*)-Mosher esters<sup>103</sup> in which NMR analysis supported assignment of the compound as alcohol **231**. On larger scale (~30g scale), reaction setup required a 3 L, 3-necked round bottom flask fitted with a mechanical stirrer and pressure addition funnel. It was determined that the reaction temperature needed to be maintained around -60 °C with dry ice/acetone. Lower reaction temperatures adversely affected the yield. Running the reaction at -78 °C resulted in 40-45% yield of the crotylation product. Optimal conditions were found to be stirring for 7 days at -60 °C, which required a large insulated box to hold temperature constant. With these optimized conditions in place, on a 30 g to 50 g scale, the aldehyde was converted to alcohol **231** in 70-85% yield. The workup of the crotylation also required modification from small scale due to the close elution by column chromatography of the product alcohol and the byproduct terpene alcohol (from the (-)-Ipc reagent, **230**). A distillation could be performed on the crude product mixture in which the terpene alcohol was distilled selectively, leaving behind the distillate with a ratio of terpene alcohol to desired alcohol as ~2:1. The mixture of alcohols were treated with TBSCl in DMF for 10 hours to afford the TBS protected alcohols, allowing the desired TBS alcohol (**232**) to be purified by column chromatography.

After successfully installing the first two stereocenters, the attention was focused on elaboration of the terminal alkene **232**. Treatment of the alkene with disiamylborane

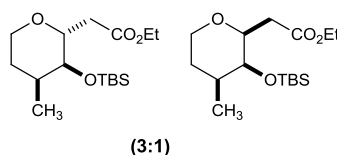
---

<sup>102</sup> For addition to  $\alpha,\beta$ -unsaturated aldehydes see: Toshima, K. et al. *J. Org. Chem.* **2001**, *66*, 1708. For a general reference see: Brown, H. C.; Bhat, K. S. *J. Am. Chem. Soc.* **1986**, *108*, 293.

<sup>103</sup> Ohtani, I.; Kusumi, T.; Kashman, Y.; Kakisawa, H. *J. Am. Chem. Soc.* **1991**, *113*, 4092.

for 4 hours followed by oxidative work up afforded primary alcohol **233** in decent yields (70-85%). A side product (mixture of diastereomers, Figure 41) resulting from the conjugate addition of the alkoxide formed during the work up process with the enoate, was also observed in varying amounts. Maintaining the reaction temperature at 0 °C during the oxidative work up step was necessary to minimize the amount of byproducts.

**Figure 41.** Hydroboration Byproducts

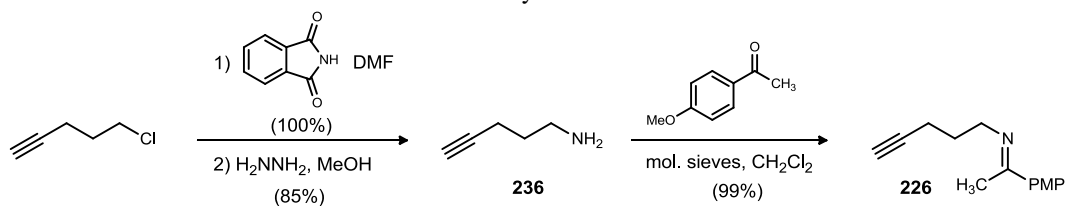


Subsequent oxidation of the primary alcohol using the Dess-Martin Periodinane<sup>104</sup> gave the desired aldehyde **234** in quantitative yields. The Pinnick oxidation of the aldehyde afforded the carboxylic acid **235** in 95% yield. Careful monitoring of these oxidation reactions was necessary on large scale.

With carboxylic acid **235** in hand, the convergent coupling step was carried out with  $\beta$ -stannyl enamine **224**. The enamine was formed in three steps from pentynyl chloride via a Gabriel amine synthesis (Scheme 43). The chloride was converted to phthalimide and subsequent deprotection of the phthalimide afforded the primary amine (**236**) in 85% yield. Condensation of the amine with *p*-methoxy acetophenone provided the imine (**226**).

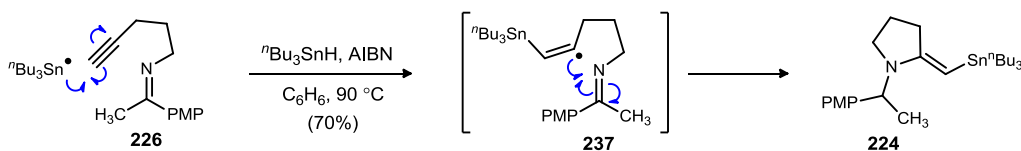
<sup>104</sup> IBX was prepared according to: Frigerio, M.; Santagostino, M.; Sputore, S. *J. Org. Chem.* **1999**, *64*, 4537. Dess-Martin was prepared from IBX using (step B only): Boeckman, R. K.; Shao, P.; Mullins, J. J. *Org. Syn., Coll. Vol. 10*, p.696 (2004); *Vol. 77*, p.141 (2000).

**Scheme 43.** Synthesis of Imine



Free radical-mediated aminostannation of imine **226** was carried out using <sup>n</sup>Bu<sub>3</sub>SnH and AIBN in refluxing benzene.<sup>98</sup> The <sup>n</sup>Bu<sub>3</sub>Sn radical adds to the terminal position of the alkyne, forming a vinyl radical **237** (Scheme 44). The 5-*exo-trig* cyclizations of the vinyl radical to the azomethine nitrogen provides a stabilized tertiary carbon radical adjacent to *para*-methoxy phenyl group.<sup>105</sup> This radical is subsequently quenched by excess <sup>n</sup>Bu<sub>3</sub>SnH to form β-stannyleneamine **224**, which is used crude for the subsequent reaction. Careful slow addition of a solution of <sup>n</sup>Bu<sub>3</sub>SnH and AIBN in degassed benzene via syringe pump over 4 hours to the imine **226** in refluxing benzene (90-95 °C) afforded β-stannyl enamine in yields ranging from 65-70%. The nucleophilicity of β-stannyleneamine was then tapped by acylation, to provide the key vinylogous amide **223**.

**Scheme 44.** Synthesis of β-Stannyl Enamine

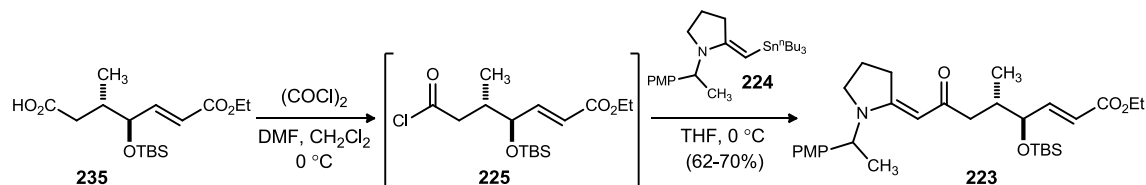


The acid chloride portion of the desired coupling reaction was made by treatment of acid **235** with oxalyl chloride in CH<sub>2</sub>Cl<sub>2</sub> at 0 °C. After removal of all volatiles, the crude acid chloride **225** was dissolved in THF, cooled to 0 °C and added dropwise via

<sup>105</sup> At least one radical-stabilizing group is required, either an aromatic ring or a trifluoromethyl group

cannula to the  $\beta$ -stannyl enamine (**224**) in THF at 0 °C. The resulting crude oil was chromatographed to provide the coupled product (**223**) in yields ranging from 62-70%.

**Scheme 45.** Synthesis of Vinylogous Amide **127**

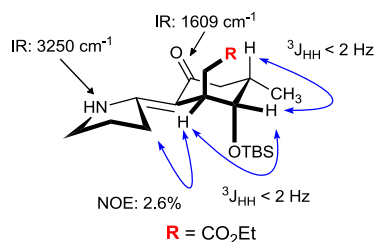


With vinylogous amide **223** in hand, the tandem amine deprotection/intramolecular Michael addition was attempted. To this end, treatment of the vinylogous amide (**223**) with ceric ammonium nitrate (CAN)<sup>106</sup> resulted in the desired cyclized product **222**. One possible explanation for this diastereoselectivity may be a

A<sup>1,3</sup>-strain between the large ethyl ester side chain and the nitrogen protecting group in transition state **a**, a feature that would disfavor the ethyl ester substituent in the equatorial position (Scheme 46).

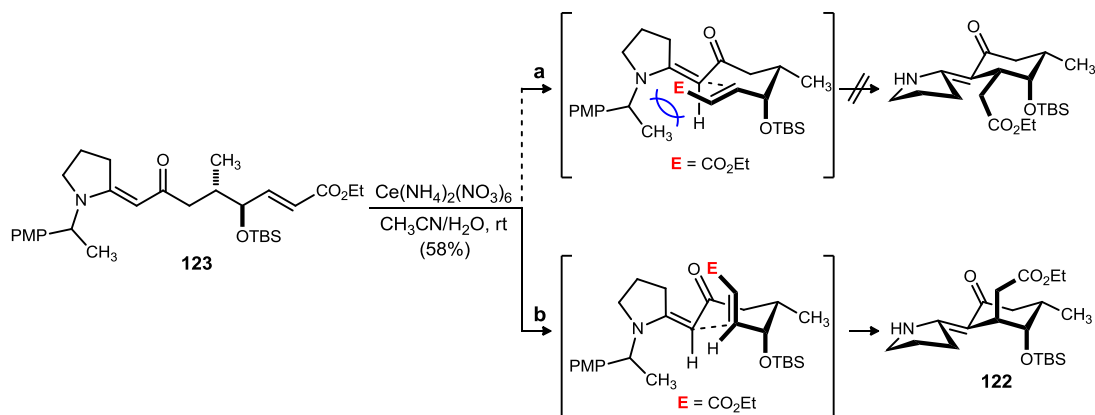
Alternatively, transition state **b** contains the

hydrogen substituent in the equatorial position, minimizing the developing interactions with the pyrrolidine ring. NOE studies were performed which not only confirmed the stereochemistry of the ester side chain and chair conformation of the cyclohexanone ring, but also showed that the vinylogous amide was *cis*.<sup>99b</sup> This was also evident by a downfield shift of the NH hydrogen at 10.7 ppm in the <sup>1</sup>H NMR, most likely due to internal hydrogen bonding with the carbonyl functionality.



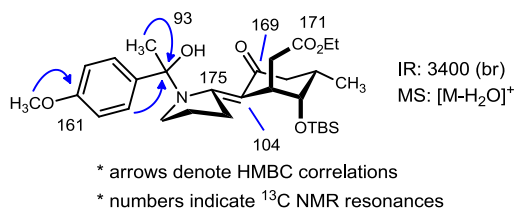
<sup>106</sup> a) Maulide, N.; Vanherck, J.; Gautier, A.; Markó, I. E. *Acc. Chem. Res.* **2007**, *40*, 381; b) Nair, V.; Balagopal, L.; Rajan, R.; Mathew, J. *Acc. Chem. Res.* **2004**, *37*, 21; c) Wright, J. A.; Jinqun, Y.; Spencer, J. B. *Tetrahedron Lett.* **2001**, *42*, 4033; d) Molander, G. A. *Chem. Rev.* **1992**, *92*, 29

**Scheme 46.** Rationale for Observed Diastereoselectivity in the Cyclization Step



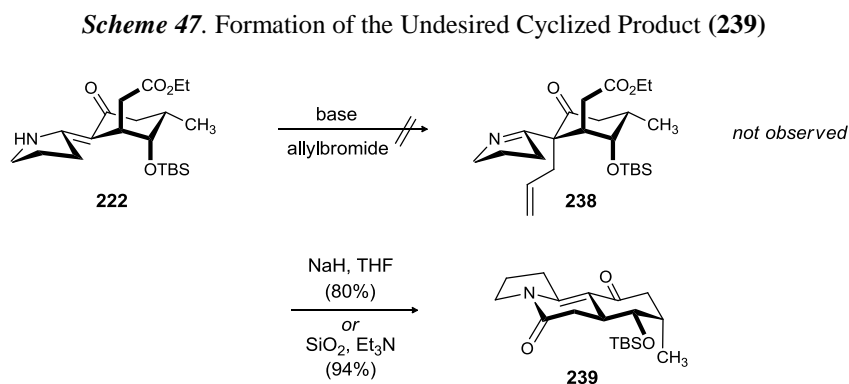
A side product (Figure 42) in varying yields of 15-25% was also observed in the CAN promoted cyclization step.<sup>99b</sup>

**Figure 42.** Side Product in the CAN Promoted Cyclization Step



The next desired step was the installation of an allyl group which provide the carbons that would be contained in the piperidine ring of the natural product. However, exposure of vinylogous amide **222** to a variety of bases (LDA, KO<sup>t</sup>Bu, KHMDS, <sup>n</sup>BuLi) with different temperatures and alkylating agents did not provide any of the desired allylated substrate (**238**).<sup>99b</sup> Instead, under all conditions, either starting material was recovered or a new product was formed containing a strongly UV active  $\pi$ -system. Full characterization utilizing 2D NMR, COSY and NOESY led to assignment of the new product as vinylogous amide **239** (Scheme 47). The reaction could be optimized using

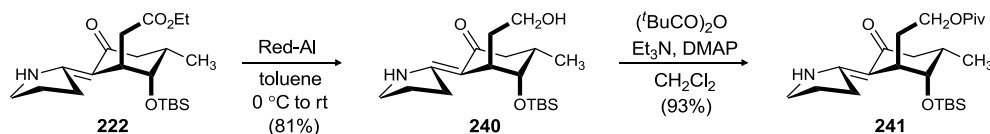
NaH and THF to furnish **239** as a solid (80%). The vinylogous amide (**222**) could also be quantitatively converted to the tricyclic compound (**239**) upon treatment with SiO<sub>2</sub> for 24 h (Scheme 47). To prevent the cyclization of **222** to the tricyclic compound (**239**), the ethyl ester functionality was reduced.



#### 2.4.2 Ester Reduction and Advancement of **222**<sup>99b,c</sup>

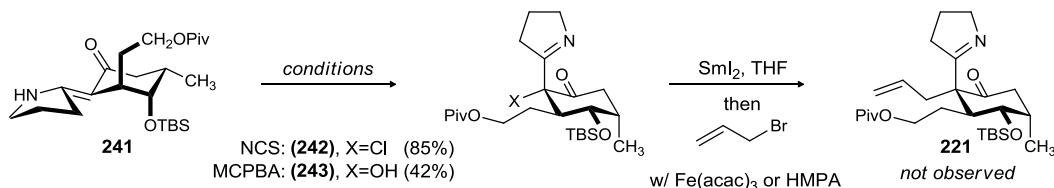
After a range of alkylation/allylation attempts to establish the desired configuration at the central carbon of the  $\beta$ -imino ketone failed, attention was then focused on the reduction of the ester functionality to render a more stable substrate for further annulation of the piperidine ring onto the bicyclic compound (**241**). Initial efforts to bring about the selective reduction of the ester, using NaBH<sub>4</sub> and DIBAL-H, promoted the undesired intramolecular lactamization to afford the tricyclic compound (**139**). The inability to reduce **222** was fortunately overcome by using Red-Al in toluene to afford the primary alcohol (**238**) in moderate to good yields (Scheme 48). Use of three equivalents of Red-Al provided complete consumption of starting material, and the resulting alcohol was isolated as a white solid in yields ranging from 70-82%. The alcohol was then protected as pivaloate **241** in good yield.

**Scheme 48.** Reduction of the Ester Functionality in **222**



With the stable pivaloate protected compound **241** in hand, different *N*- alkylation were attempted next to install the three carbon chain necessary to form the piperidine ring. No desired alkylation product was ever observed and the unreacted starting compound **241** was isolated in all these cases. However, exposing the pivaloate protected vinylogous amide **241** to oxidants gave promising results.<sup>107,108</sup> Treatment of **241** with NCS and *m*CPBA provided  $\alpha$ - chloroketoimine **242** and  $\alpha$ - hydroxyketoimine **243** respectively in moderate to good yields (Scheme 34). The ketoimine **242** and **243** were then subjected to a variety of allylation conditions. Unfortunately, all these allylation efforts proved fruitless, as the only product observed was **241**.<sup>109</sup> Exposure of either **242** or **243** to SmI<sub>2</sub> and allyl bromide provided complex reaction mixtures by <sup>1</sup>H NMR.

**Scheme 49.** Attempts towards Appending the 3-Carbon Fragment



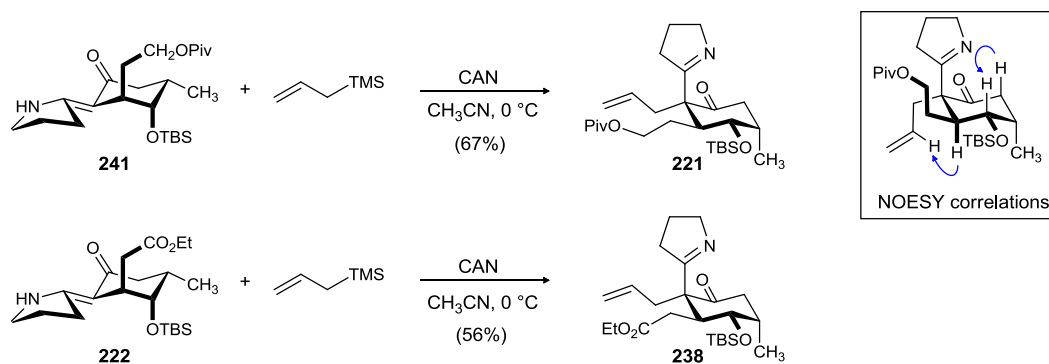
<sup>107</sup> For chlorination/bromination of vinylogous amides in a similar fashion see: a) Pierron, C.; Garnier, J.; Levy, J.; LeMen, J. *Tetrahedron Lett.* **1971**, *12*, 1007. b) Jirkovsky, I. *Can. J. Chem.* **1974**, *52*, 55.

<sup>108</sup> The  $\alpha$ -chloroketone is proposed as an intermediate in the NaOCl oxidation of a vinylogous amide: Staskun, B. *J. Org. Chem.* **1988**, *53*, 5287.

<sup>109</sup> a) Molander, G.; McKie, J. A. *J. Org. Chem.* **1991**, *56*, 4112; b) Inanaga, J. Ishikawa, M.; Yamaguchi, M. *Chem. Lett.* **1987**, 1485.

The desired allylation was finally effected by utilizing the cerium-mediated oxidative allylation<sup>110</sup> methodology developed by Flowers, *et al.*<sup>111</sup> Cerium ammonium nitrate and allyl trimethyl silane combine with the vinylogous amide **241** to deliver **221**, as a result of ring flip, in 56% yield and 23:1 dr (Scheme 50). Substituting Cerium *tert*-butylammonium nitrate in place CAN also afforded the product in decent yields. Exposing ester **222** to this oxidative allylation reaction condition also led to the allylated  $\beta$ -imino ketone **238** in high diastereoselectivity.

**Scheme 50.** CAN Mediated Allylation Step



After establishing the all carbon quaternary center, the attention turned to accessing the piperidine ring by functionalizing terminal alkene. Hydroboration attempts were thwarted by the simultaneous ketone reduction and low yields. As a result, ketone was reduced prior to hydroboration. Reduction with  $\text{NaBH}_4$  in THF at room temperature provided the undesired  $\alpha$ -alcohol **245** in the yields ranging from 45-58% yield (Scheme 51). However, employing  ${}^n\text{Bu}_3\text{SnH}$  as a reducing agent (added over 45 minutes) in the presence of a bidentate Lewis acid  $\text{Et}_2\text{AlCl}$  afforded the desired  $\beta$ -alcohol (**244**, 10:1 *dr*)

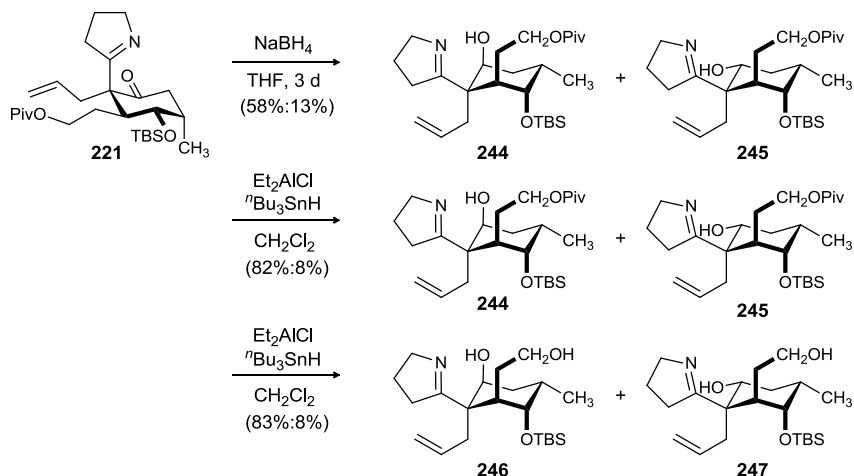
<sup>110</sup> Pioneering work on  $\beta$ -diketone allylations with CAN: Hwu, J. R.; Chen, C. N.; Shiao, S.-S. *J. Org. Chem.* **1995**, *60*, 856.

<sup>111</sup> Zhang, Y.; Raines, A. J.; Flowers II, R. A. *J. Org. Chem.* **2004**, *69*, 6267.

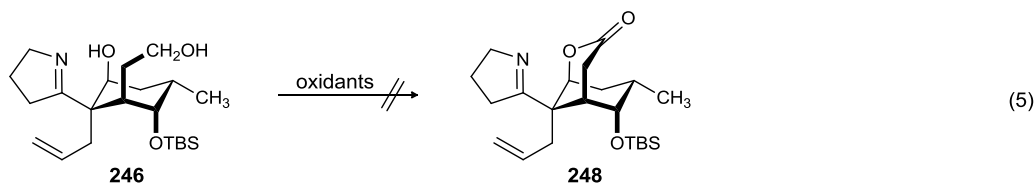


in good yield. Rapid addition of  ${}^n\text{Bu}_3\text{SnH}$  resulted in the concomitant reduction of ester to afford the diol (**246**).

**Scheme 51.** Substrate Controlled Reduction



At this stage, 5 stereocenters in the natural product were installed. Investigations turned toward installation of first the lactone ring, followed by piperidine ring construction in separate synthetic operations (eq 5). However, subjecting the diol (**246**) to a variety of oxidation conditions including  $\text{Ag}_2\text{CO}_3/\text{C}_6\text{H}_6$  (Fetizon oxidation),<sup>112</sup> Dess-Martin, PCC, and TEMPO proved fruitless, as no oxidation products were observed

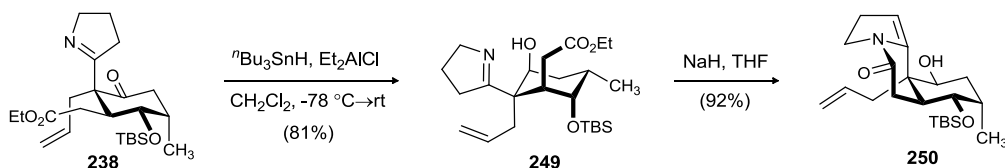


Attention then focused on using keto ester **238** as a starting material for the production of lactone **248**. Directed reduction of the ketone in **238** with  ${}^n\text{Bu}_3\text{SnH}$  and AIBN furnished the  $\beta$ -alcohol (**249**) in good yield (Scheme 52). Attempts to form the

<sup>112</sup> For examples see: a) “Silver(I) Carbonate on Celite”, Fetizon, M. *Electronic Encyclopedia of Reagents for Organic Synthesis*, Crich, D.; Fuchs, P. L.; Molander, G.; Paquette, L. A. Eds.; John Wiley & Sons Ltd.: Sussex, 2005; b) Lafontaine, J. A.; Provencal, D. P.; Gardelli, C.; Leahy, J. W. *J. Org. Chem.* **2003**, *68*, 4215.

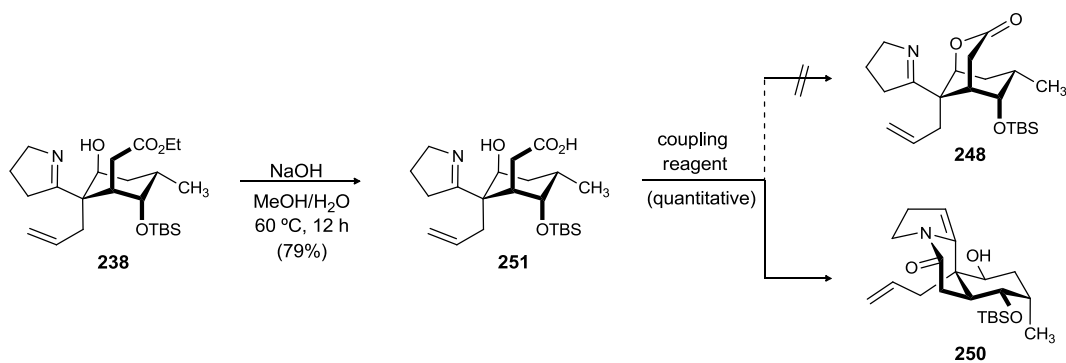
lactone ring with base were instead found to promote intramolecular lactamization with the terminal ester, resulting in enamide **250**.<sup>113</sup> The NMR peaks of **250** were all very broad, suggesting two interconverting chair conformations.

**Scheme 52.** Attempted Lactonization of **249**



At this stage, an intramolecular lactonization strategy to install the lactone ring was also investigated (Scheme 53). It was postulated that the mild conditions required for the lactonization might overcome the competing enamide formation. To this end, the ester **238** was subjected to the saponification condition to afford hydroxyl ester **251** in 79% yield. However, acid activation by a variety of coupling reagents including DCC, PyBroP and EDC initiated the undesired lactamization to provide enamide **250**.

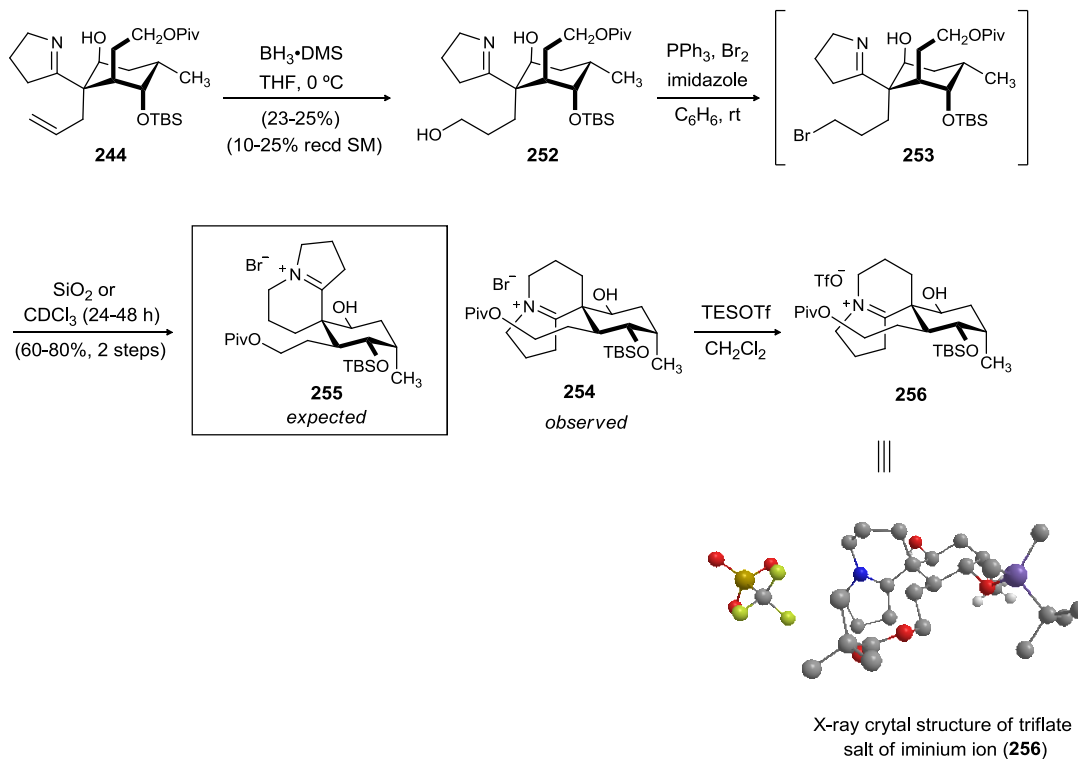
**Scheme 53.** Attempted Lactonization of **251**



<sup>113</sup> The cyclization to the enamide rather than the lactone occurred upon standing of the alcohol (**249**). This same pattern was not found with ketone **238**, which may indicate the chair conformation in **238** prevents cyclization.

Failure to convert diol **246** or the hydroxyester (**238**) to the lactone **248** necessitated yet another synthetic re-evaluation. Therefore, piperidine ring construction via terminal alkene functionalization was investigated. Treatment of the alkene (**244**) with  $\text{BH}_3 \cdot \text{THF}$  or  $\text{BH}_3 \cdot \text{DMS}$  followed by oxidative work-up provided the desired primary alcohol **252** in low yields (23-35%). Screening a variety of boron reagents, including 9-BBN, disiamyl borane, or catechol borane with Wilkinson's catalyst ( $\text{RhCl}(\text{PPh}_3)_3$ ) proved fruitless, as no hydroboration product was isolated. Increasing the borane amount (2 equivalents), reaction time and temperature proved to be detrimental to the yield. The primary alcohol **252** was treated with excess  $\text{Br}_2$ ,  $\text{PPh}_3$  and imidazole to afford the primary bromide (**253**), which cyclized slowly upon standing.

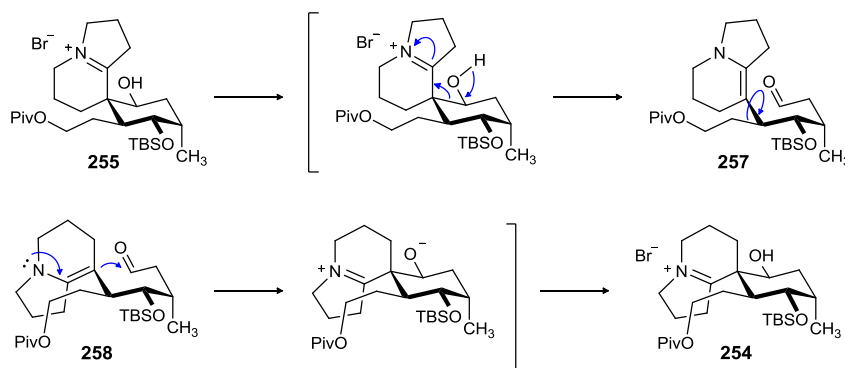
*Scheme 54.* Attempted Synthesis of Piperidine Ring



This cyclized product was identified as iminium ion **254**, having the epimeric spirocyclic stereocenter instead of the expected epimer (**255**, Scheme 54). The tandem bromination/cyclization step proceeded smoothly to afford the iminium ion (**254**) in 60-80% yield, as well as a side product that co-eluted with iminium ion **254** (in 0-10%). Upon stirring **254** in CH<sub>2</sub>Cl<sub>2</sub> with excess TESOTf, the bromide counterion could be exchanged for a triflate counterion. A crystal structure of the triflate salt **256** was obtained which supported the expected epimerization (Scheme 54).

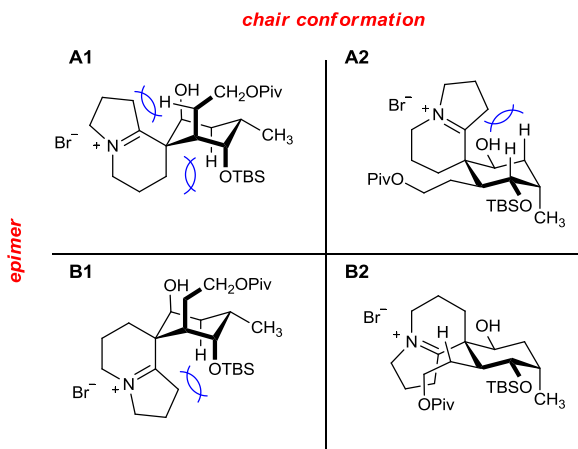
The epimerization was expected to occur through an enamine retro-aldol reaction of the expected cyclized product (**255**) (Scheme 55). **255** undergoes a ring opening phenomenon, which is promoted by donation of electrons of the O-H bond into the C-O bond, to form an enamine-aldehyde (**257**). Rotation about the C-C  $\sigma$ -bond in **257** provides an intermediate such as **258**, where the indolizidine ring has effectively rotated 180° about the single bond. Enamine addition to the aldehyde results in **254** after protonation, with overall epimerization of the spirocyclic carbon. 2D NMR analysis revealed that the alcohol configuration (equatorial) did not change during the ring opening.

**Scheme 55.** Mechanism of the Undesired Retro-Aldol reaction of **254**



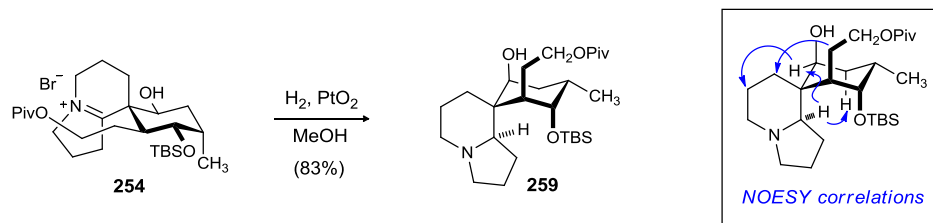
Based on the model study, it was hypothesized that the epimerization of the quaternary carbon seems to relieve strain associated with the pyrrolidine CH<sub>2</sub> interactions within the various intermediates (Figure 43). Before epimerization, structure **A1** has a severe 1,3-diaxial interaction with the pyrrolidine ring methylene and the OTBS. If it undergoes a chair flip to **A2**, it then encounters a more severe 1,3-diaxial interactions due to the pyrrolidine ring position in the β-plane of the cyclohexane ring. Epimer **B1** may likely be the highest in energy since like **A2**, the pyrrolidine ring is forced toward the cyclohexane ring and additionally encounters the large OTBS. However, once it undergoes a chair flip to **B2**, it only encounters 1,3-diaxial interactions with the hydrogens and the piperidine ring. Of all four possible conformations, **B2** seems to result in the least severe non-bonding interactions which may explain why **B2** is the only observed product after cyclization.

**Figure 43.** Rationale for the Undesired Retro-Aldol Reaction of **255**



The metal catalyzed reduction of **254** provided the tertiary amine (**259**) in good yield (Scheme 56). 2D NMR analysis revealed that the reduction has taken from the back face, as the front face is blocked by pivaloate side chain.

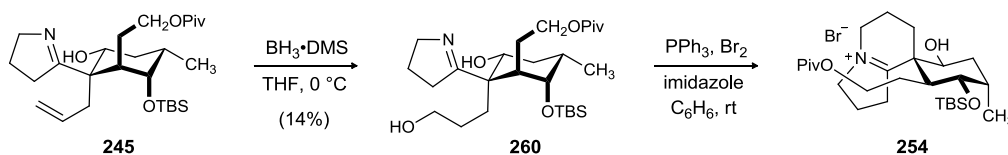
**Scheme 56.** The Metal Catalyzed Reduction of **254**



The fact that alcohol configuration did not change during the epimerization of iminium (**254**) made  $\alpha$ -alcohol **245** an appealing substrate for effecting the cyclization step. The  $\alpha$ -alcohol may not undergo the epimerization at the spirocyclic center as was the case previously with the  $\beta$ -alcohol (**244**).

The hydroboration of **245** provided even lower yields of the primary alcohol than was previously found with the  $\beta$ -alcohol. The primary alcohol (**260**) was then subjected to the tandem bromination/cyclization condition to afford the cyclized product. The cyclized product was identified to be **254**, as a result of double epimerization at both the spirocycle and the alcohol stereocenter (Scheme 57). At this point, it became clear that the protection of secondary alcohol was necessary to prevent the epimerization of the iminium salt (**254**).

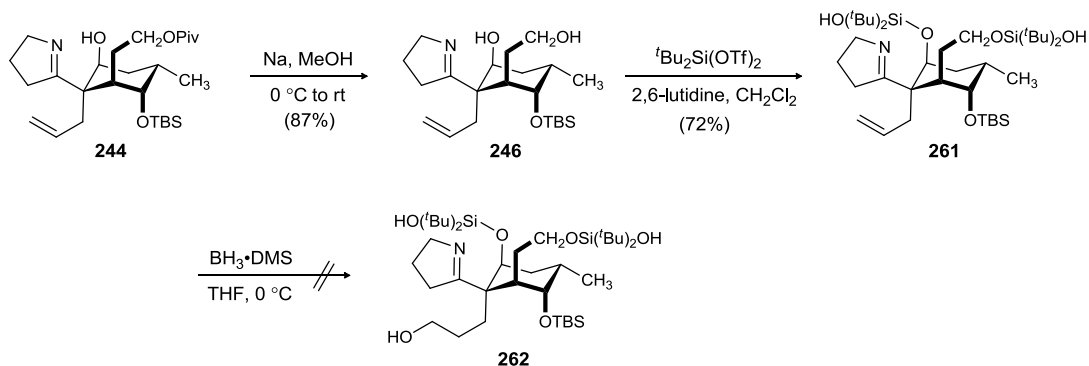
**Scheme 57.** Attempted Piperidine Ring Formation from the Primary Alcohol (**260**)



After a few failed trials with common alcohol protecting groups, such as benzyl, MOM, and acetyl derivatives, it was realized that the task of  $\beta$ -alcohol (**244**) protection would not be straightforward. After more protecting group screening, it was found that



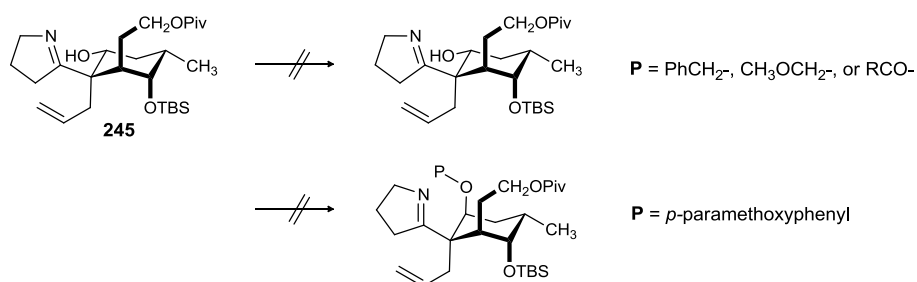
**Scheme 59.** Attempted Silylation of the Diol (**246**)



### 2.4.3 Secondary Alcohol Protection and Optimization of Hydroboration Step

Although non-productive, our efforts to convert the  $\beta$ -alcohol (**244**) to the desired iminium salt (**255**) did illustrate the need to protect the  $\beta$ -alcohol prior to iminium salt **255** formation (Scheme 54 and 57). After the initial failures to protect the  $\beta$ -alcohol, methods to elicit the protection of  $\alpha$ -alcohol (**245**) were evaluated. To this end, the  $\alpha$ -alcohol (**245**) was subjected to various protecting group reaction conditions. However, the unreacted starting material was isolated in all cases. Employing Mitsunobu reaction conditions to protect the alcohol, with inversion of stereochemistry was unsuccessful as well (Scheme 60).

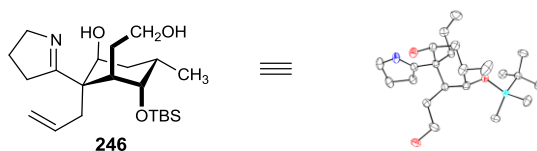
**Scheme 60.** Efforts towards Protecting the Alcohol (**245**)





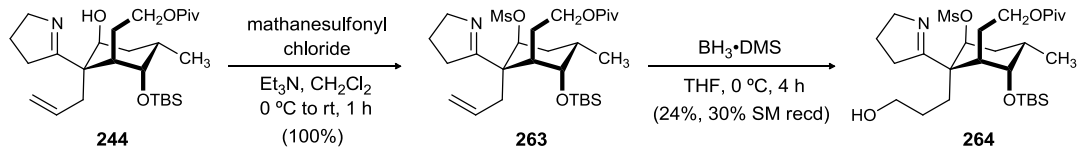
In the event, a crystal structure of diol (**246**) was obtained, which revealed that a 6-membered hydrogen bond existed between the imine nitrogen and alcohol proton (Figure 44). This could explain the observed unreactivity of the  $\beta$ -alcohol towards protecting group reaction conditions. The unreactivity of  $\alpha$ -alcohol **245** could be accounted for by the same reasoning.

**Figure 44.** Crystal Structure of  $\beta$ -diol



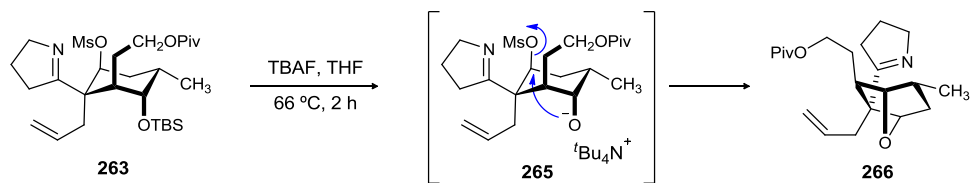
We then turned our attention towards sulfonation of  $\beta$ -alcohol **244**. Though tosylation and triflation conditions were unsuccessful and led to the decomposition of starting material, we were pleased to find out that alcohol could be protected as mesylate **263** in quantitative yield.  $^1\text{H}$  NMR analysis revealed the desired chair conformation for the mesylated compound (**263**). The mesylate was then carried on to the hydroboration step. It was thought that the mesylate group, being a good leaving group, might undergo elimination in the oxidative work-up step of hydroboration reaction. Therefore, even though the secondary mesylate functionality in (**263**) was hindered, the hydroboration step was approached with some trepidation. However, these fears proved to be unfounded as subjecting **263** to the hydroboration condition provided the primary alcohol (**264**), albeit in low yields (Scheme 61).

**Scheme 61.** Mesylation of Alcohol **244**



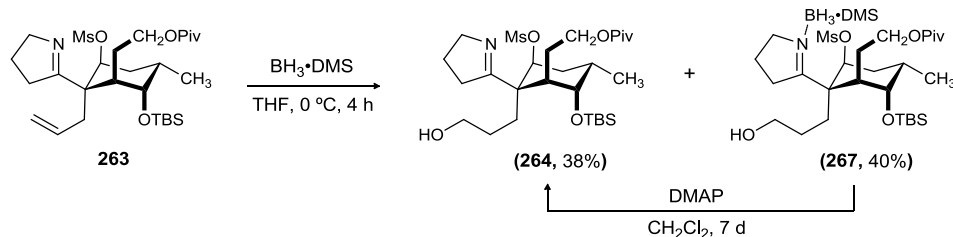
In an effort to increase the yield of hydroboration step, the deprotection of TBS group was attempted next. It was speculated that the terminal alkene is sterically hindered by the bulky *tert*-butyl silyl group, thus leading to low yields of primary alcohol **264**. Treatment of **263** with TBAF at 66 °C for 2 h provided a yellow oil. This compound could be fully characterized by 2D NMR as **266**. The cyclic ether (**266**) was formed as a result of  $\text{S}_{\text{N}}2$  displacement of the mesylate by an intermediate alkoxide (**265**) (Scheme 62).

**Scheme 62.** Formation of Undesired Cyclic Ether **266**



Despite the low yield of hydroboration step, the initial results appeared promising (Scheme 63). In an effort to further improve the yield of primary alcohol, the alkene (**263**) was treated with a variety of borane reagents. Treatment with 9-BBN and disiamyl borane only afforded trace amounts of primary alcohol **264**. Increasing the reaction time to 5 h, and utilizing  $\text{BH}_3\cdot\text{DMS}$  as borane reagent provided primary alcohol **264** in moderate yields (35-40%).

**Scheme 63.** Optimization of Hydroboration Step



More polar fractions were also obtained from column chromatography which provided a colorless viscous oil accounting for 35-40% of material.  $^1\text{H}$  NMR analysis revealed a set of broad peaks different from the primary alcohol (**264**). Upon storage of this viscous oil for long duration of time, a new set of peaks were observed in  $^1\text{H}$  NMR analysis which matched the  $^1\text{H}$  NMR spectral data for primary alcohol **264**. It was speculated that the broadness of the peaks maybe a result of  $\text{BH}_3 \cdot \text{DMS}$  binding with the electron rich imine. Furthermore, it has been reported in literature that amine-borane complexes are stable and isolable compounds at room temperature.<sup>115,116</sup> To test this hypothesis, a solution of the colorless viscous oil **267** in  $\text{CH}_2\text{Cl}_2$  was treated with an excess of 4-dimethylamino pyridine (DMAP) for 7 days. DMAP, an electron rich tertiary amine, was expected to bind more strongly to borane than to the imine functionality in **267**, and thus would act as a “borane scavenger”. Indeed, purification of the reaction mixture afforded the pure primary alcohol (Scheme 63). Interestingly, the hydroboration product of the imine group was not observed under these reaction conditions.

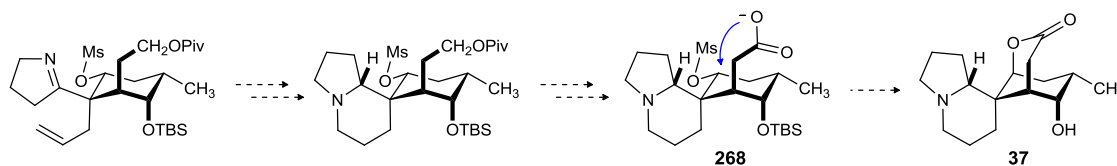
<sup>115</sup> a) Dewar, M. J. S.; Gleicher, G. J.; Robinson, B. P. *J. Am. Chem. Soc.* **1964**, *86*, 5698. b) Dewar, M. J. S.; Rona, P. *J. Am. Chem. Soc.* **1967**, *89*, 6294. c) Polívka, Z.; Ferles, M. *Collect. Czech. Chem. Commun.* **1969**, *34*, 3009. d) Polívka, Z.; Kubelka, V.; Holubová, N.; Ferles, M. *Collect. Czech. Chem. Commun.* **1970**, *35*, 1131. e) Wille, H.; Goubeau, J. *Chem. Ber.* **1972**, *105*, 2156. f) Baboulene, M.; Torregrosa, J.-L.; Speziale, V.; Lattes, A. *Bull. Chim. Soc. Fr.* **1980**, II-565. g) Midland, M, M.; Kazubski, A. *J. Org. Chem.* **1992**, *57*, 2953.

<sup>116</sup> For intramolecular hydroboration of homoallylic and bishomoallylic amine boranes by activation of  $\text{I}_2$  at elevated temperatures, see: a) Scheideman, M.; Wang, G.; Vedejs, E. *J. Am. Chem. Soc.* **2008**, *130*, 8669. b) Scheideman, M.; Shapland, P.; Vedejs, E. *J. Am. Chem. Soc.* **2003**, *125*, 10502. c) Wang, G.; Vedejs, E. *Org. Lett.* ASAP.

#### 2.4.4. Advancement of the $\alpha$ -alcohol (**245**)

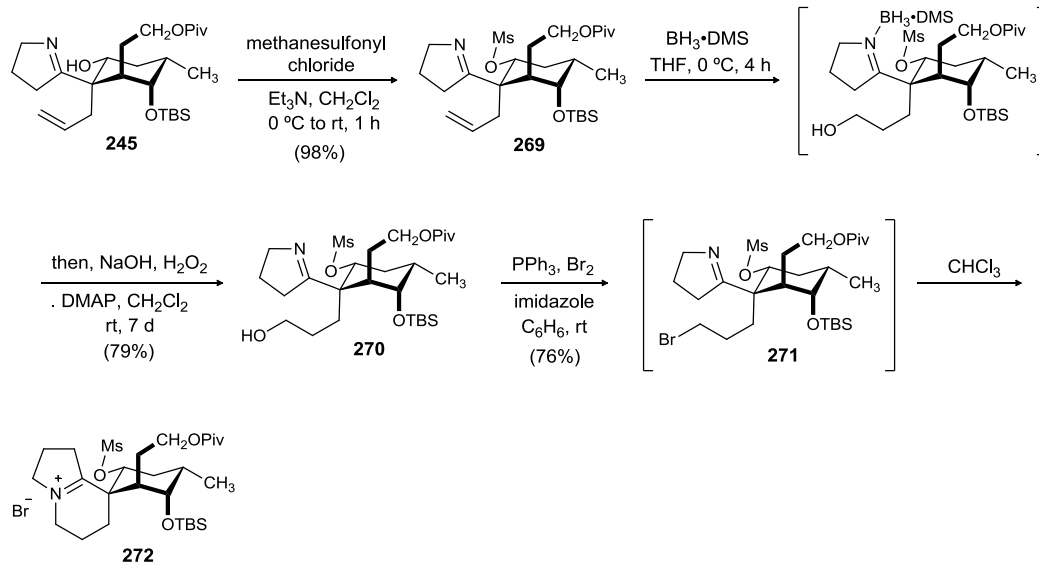
Having solved the issues related with the secondary alcohol protection and hydroboration steps, synthetic strategies for constructing the lactone ring were evaluated next. Considering the difficulties associated with deprotection of the methane sulfonyl group to provide the free alcohol necessary for constructing the bridged lactone, we decided to take advantage of the fact that the mesylate functionality is a good leaving group.  $\alpha$ -alcohol **245** emerged as a viable substrate to test this hypothesis. The  $\alpha$ -stereocenter is opposite to that required in serratezomine A, However; the lactone ring can be formed via displacement of mesylate with a carboxylate on the side chain (**268**, Scheme 64).

*Scheme 64.* Alternate Strategy to Access Piperidine Ring



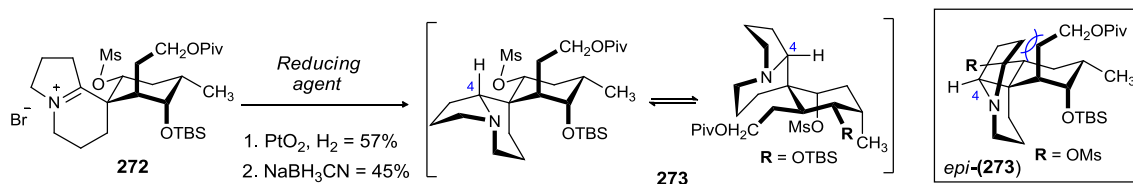
The  $\alpha$ -alcohol (**245**) was treated with methanesulfonyl chloride to provide the  $\alpha$ -mesylate (**269**) in excellent yield. The mesylate was subjected to the hydroboration conditions, and the resulting crude oil was treated with DMAP for 7 days at room temperature. Upon purification, the desired primary alcohol (**270**) was isolated as a viscous oil in 79% yield. The alcohol was treated with bromine,  $\text{PPh}_3$  and imidazole for 10 minutes to afford the primary bromide (**271**), which cyclized slowly upon standing to afford the iminium salt (**272**) (Scheme 65). The coupling constants observed by  $^1\text{H}$  NMR were consistent with the chair conformer depicted for **272**. The iminium salt was found to be stable upon storage for long duration of time.

**Scheme 65.** Advancement of the  $\alpha$ -alcohol (**245**)



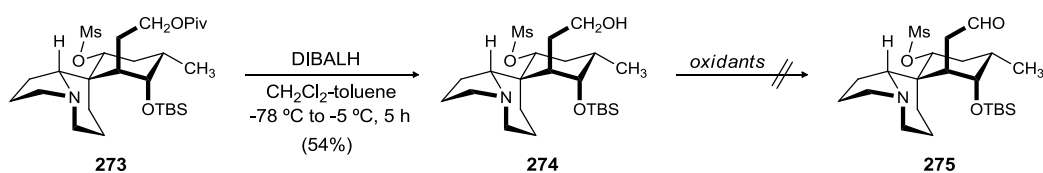
The subsequent reduction of the iminium ion **272** was then investigated by utilizing both reducing agents and metal-catalyzed hydrogenation. The latter case proved superior in providing the amine (**273**, Scheme 66). The NMR peaks of **273** were all very broad, suggesting two interconverting chair conformations, and as a result 2D NMR analysis to determine the facial selectivity of the reduction step could not be conducted. However, the presence of only one set of peaks in NMR analysis strongly suggested the reduction was highly stereoselective in nature. Based on the model studies, it was also hypothesized that the reduction takes place from the  $\beta$ -face, as interactions between the pyrrolidine and the cyclohexane rings in **273** are considerably less than in *epi*-**273** (at C4) (Scheme 66).

**Scheme 66.** Substrate Controlled Reduction of Iminium **272**



With tertiary amine **273** in hand, attention turned towards the installation of the carboxylic acid functionality, which first required deprotection of the pivaloate protecting group (Scheme 67). Treatment of **273** with DIBAL afforded the desired primary alcohol (**274**) in good yield. NMR analysis revealed the presence of both chair conformers for the alcohol (**274**). The alcohol was then subjected to a variety of oxidation conditions including, Dess Martin Periodinane, Parikh-Doering oxidation and Swern oxidation. In all these cases, decomposition of the starting material was observed and no oxidation product **275** could ever be isolated (Scheme 67). It was believed that lone pair of electrons on the nitrogen was donating into the aldehyde (**275**), and that the resulting strained hemiaminal underwent a variety of fragmentation pathway, leading to the decomposition of **274**. In their synthesis of (-)-Sarain A, Overman *et al.* reported a similar difficulty in the oxidation of an alcohol proximal to a tertiary amine in the molecule.<sup>117</sup> Difficulties encountered during the oxidation of the alcohol (**274**) prompted us to consider other ways to construct the bridged lactone ring.

**Scheme 67.** Failed Attempts towards Oxidation of Alcohol **274**

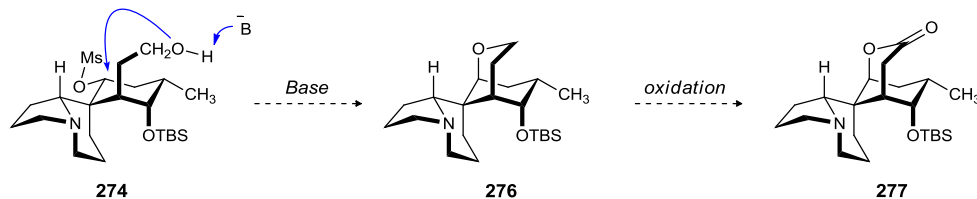


Two strategies were investigated for the construction of desired lactone ring. Initially, it was reasoned that **37** could be accessed by a RuO<sub>4</sub> mediated oxidation of cyclic ether **276**.<sup>118</sup> The cyclic ether could be accessed from primary alcohol **274**, via S<sub>N</sub>2 displacement of the mesylate by an alkoxide (Scheme 68).

<sup>117</sup> Garg, N. K.; Hiebert, S.; Overman, L. E. *Angew. Chem. Int. Ed.* **2006**, *45*, 2912.

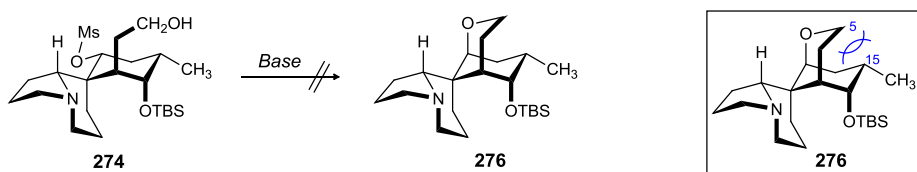
<sup>118</sup> Schuda, P.; Cichowicz, M. B.; Heimann, M. R. *Tetrahedron Lett.* **1983**, *24*, 3829.

**Scheme 68.** Alternate Synthetic Plan to Access Serratezomine A from Alcohol **274**



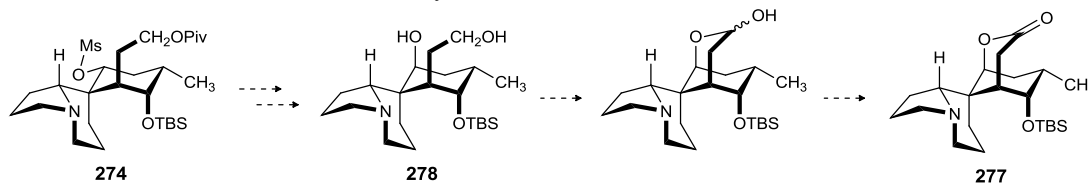
Surprisingly, the primary alcohol **274** was inert to most basic reaction conditions including, potassium *tert*-butoxide, sodium hydride, LiHMDS and LDA (Scheme 69). Exposure to <sup>n</sup>BuLi and <sup>t</sup>BuLi led to complete decomposition of the starting material. Based on the model studies, it was believed that the steric interactions between C5 and C15 in too high to overcome in the cyclic ether (**276**).

**Scheme 69.** Failed Attempts towards the Synthesis of Ether **276**



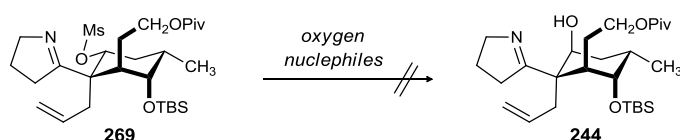
Another strategy investigated was an S<sub>N</sub>2 displacement of mesylate by an oxygen nucleophile to provide β-alcohol **278**. It was hypothesized that the presence of the β-alcohol in diol **278** would lead to the formation of the lactone **277**, via a lactol intermediate. The lactol formation should be favored over a strained hemiaminal formation (Scheme 70).

**Scheme 70.** Synthetic Plan to Access **277** from **274**



The  $\alpha$ -mesylate (**269**) was chosen as a model substrate to investigate this strategy (Scheme 71). The mesylate was treated with a variety of oxygen nucleophiles including, CsOAc,<sup>119</sup>  $n\text{Bu}_4\text{N}^+\text{NO}_3^-$ ,<sup>120</sup> and  $\text{KNO}_2$ <sup>121</sup> at elevated temperatures (>100 °C) and for long duration of time (10-20 hours). However, the starting material was recovered in all cases. The unreactivity of mesylate **269** could be due to the sterically hindered environment of the *C13* neopentyl mesylate.

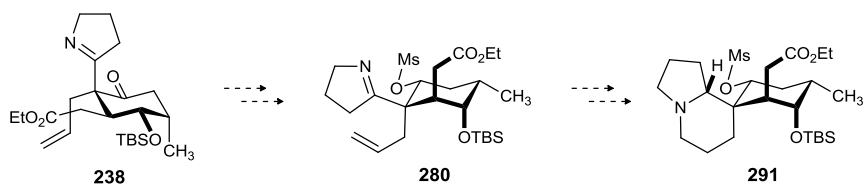
**Scheme 71.** Attempted  $\text{S}_{\text{N}}2$  Displacement of Mesylate by an Oxygen Nucleophile



#### 2.4.5. Advancement of the $\alpha$ -alcohol (**279**)

Unable to advance alcohol **245** to **277** (presumably due to steric and electronic factors), we turned to an alternate strategy wherein the required carboxylic acid **291**, necessary for the construction of lactone ring, would be accessed from **238**. The ester was envisioned to arise in a straightforward manner by elaboration of the terminal alkene of  $\alpha$ -mesylate **280**. The desired  $\alpha$ -mesylate could in turn be accessed from ketone **238** (Scheme 72).

**Scheme 72.** Modified Synthetic Plan to Access Serratezomine A



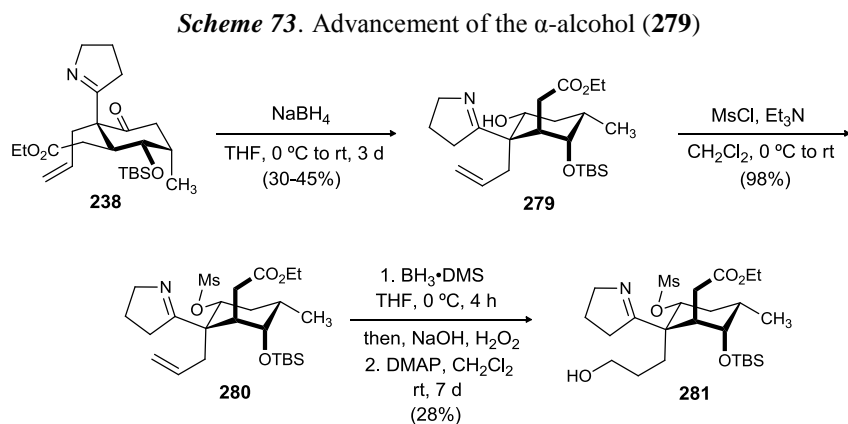
<sup>119</sup> Li, Z.; Mintzer, E.; Bittman, R. *J. Org. Chem.* **2006**, *71*, 1718.

<sup>120</sup> Cainelli, G.; Manescalchi, F.; Martelli, G.; Panunzio, M.; Plessi, L. *Tetrahedron Lett.* **1985**, *26*, 3369.

<sup>121</sup> Moriarty, R. M.; Zhuang, R.; Penmasta, R.; Liu, K.; Awasthi, A. K.; Tuladhar, S. M.; Singh, V. K. *Tetrahedron Lett.* **1993**, *34*, 8029.



To prepare the desired  $\alpha$ -alcohol (**279**), the ketone was treated with an excess of NaBH<sub>4</sub> in THF. The reaction was sluggish, but ultimately provided the alcohol (**279**) in high diastereoselectivity (>20:1), albeit in low yields (30-45%). Treatment of the alcohol (**279**) with methanesulfonyl chloride provided  $\alpha$ -mesylate **280** in excellent yield. Subjecting the mesylate **280** to hydroboration conditions resulted in low yields of primary alcohol **281** (Scheme 73).



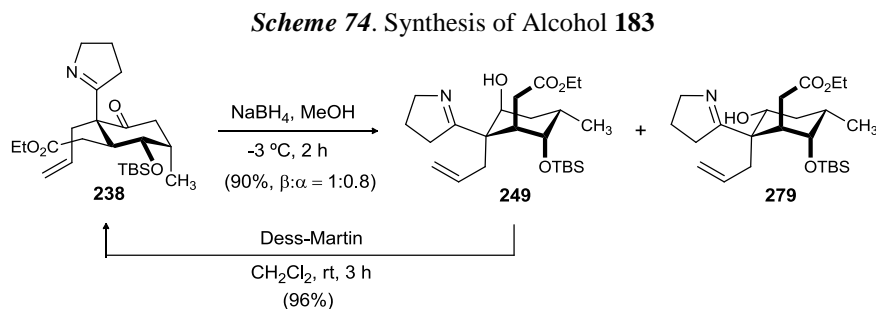
In an attempt to increase the yield of the reduction step, a variety of reducing agents and reaction conditions were evaluated (Table 2).

**Table 2.** Optimization of Ketone Reduction

entry <sup>a</sup>	Reducing agent <sup>b</sup>	solvent	time	$\alpha$ : $\beta$	Conversion <sup>c</sup>
1 <sup>d</sup>	NaBH <sub>4</sub>	THF	3 d	>20:1	30-45%
2	NaBH <sub>4</sub>	MeOH	1.5 h	0.8:1	100%
3 <sup>d</sup>	LiBH <sub>4</sub>	THF	2 d	>5:1	25%
4	L-selctride	THF	2 d	-	5%
5 <sup>d</sup>	L-selctride	MeOH	2 d	4:1	25%
6 <sup>d</sup>	KBH <sub>4</sub>	THF	1 d	4:1	15%

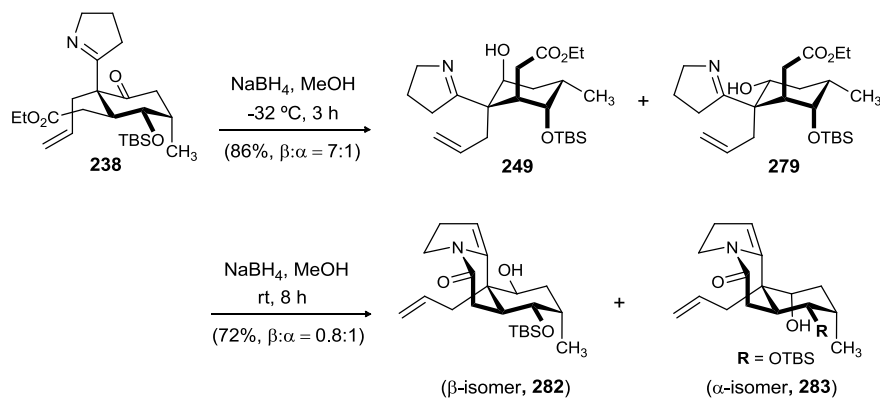
<sup>a</sup> All reactions were performed at -3 °C. <sup>b</sup> All reactions employed 1.4 equiv. of reducing agents. <sup>c</sup> The crude reaction mixture was analyzed by <sup>1</sup>H NMR. <sup>d</sup> decomposition of SM observed in the reaction.

Treatment of a solution of **238** in MeOH with NaBH<sub>4</sub> at -3 °C for 2 h afforded the  $\alpha$ -alcohol (**279**, 0.8:1 *dr*) in excellent yield. Although the diastereoselectivity of the reduction step was modest, we were pleased to find out that the undesired  $\beta$ -alcohol (**249**) isomer could be easily separated and reoxidized with almost no loss in material throughput (Scheme 74).



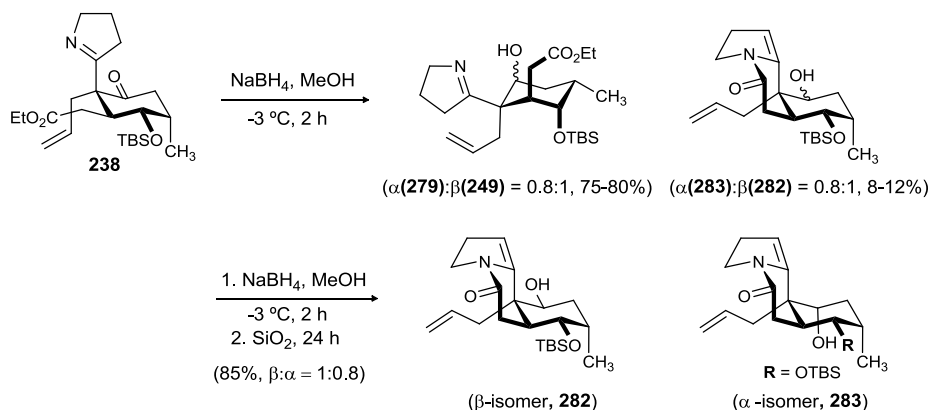
Temperature is very critical to the diastereoselective outcome of this reduction reaction. Performing the reaction at lower temperatures (< -3 °C) provided  $\alpha$ -alcohol in even poorer diastereoselection. At -35 °C,  $\beta$ -alcohol **249** could be isolated in excellent diastereoselectivity (7:1) and yield (86%). Executing the reaction at higher temperatures (> 0 °C) were found to initiate imine cyclization, following the ketone reduction step, resulting in  $\alpha$ - and  $\beta$ -enamides (**283** and **282**) (Scheme 75). Selective enamide formation was observed while running the reaction at room temperature. The NMR peaks of  $\alpha$ - and  $\beta$ -enamides (**283** and **282**) were all very broad, suggesting two interconverting chair conformations. The enamides (**283** and **282**) were found to be stable upon storage for long duration of time.

**Scheme 75.** Effect of Temperature on the Ketone (**238**) Reduction



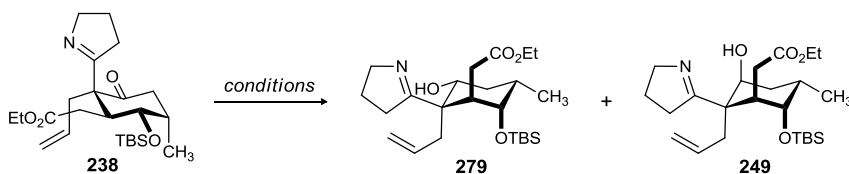
Although the reduction of ketone **238** worked well on small scale, problems were encountered upon scaling up of this reaction. Varying amounts of the undesired  $\alpha$ - and  $\beta$ -enamides (**282** and **283**) were also isolated along with alcohols (**249** and **279**) in the purification process. It was hypothesized that the undesired intramolecular lactamization was promoted by the exposure of the alcohols to  $\text{SiO}_2$ . Indeed, treatment of the crude alcohol mixture with  $\text{SiO}_2$  for 24 hours provided the individual enamides (**282** and **283**) in excellent yields upon purification (Scheme 60). Due to the poor separation of  $\alpha$ - and  $\beta$ -alcohols (**279** and **249**) on column chromatography, large scale purification process generally took a reasonable amount of time, and as a result substantial quantities (8-12%) of undesired enamides were isolated. The alcohols (**249** and **279**) were also found to undergo intramolecular lactamization upon storage for long duration of time. The intramolecular lactamization was even observed, when the alcohols were stored at low temperature ( $-78\text{ }^\circ\text{C}$ ), upon storage for long storage of time.

**Scheme 76.** Undesired Formation of Enamides **283** and **282**



In theory, the undesired  $\beta$ -alcohol (**249**) could be recycled to  $\alpha$ -alcohol **279** via efficient oxidation to ketone **238**. However, multiple purification processes (column chromatography) associated with the reduction step led to greater product loss as enamides (**282** and **283**). Subsequently, the attention was focused on improving the diastereoselectivity of the reduction step. The effect of solvents on the diastereoselective outcome of ketone **238** reduction was investigated (Table 3). Employing 1-propanol as a solvent provided the  $\alpha$ -alcohol (**279**) in good diastereoselection (3:1 *dr*), as indicated by crude NMR analysis.

**Table 3.** Solvent Screen for the Reduction of **238**

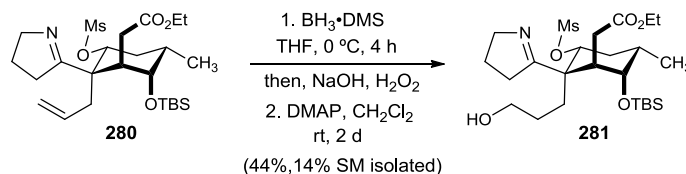


entry <sup>a</sup>	solvent	$\alpha$ : $\beta$	Conversion <sup>b</sup>
1	MeOH	0.8:1	100%
2	EtOH	1.4:1	100%
3	<b>1-propanol</b>	<b>3:1</b>	<b>100%</b>
4	sec-butanol	-	~6%

<sup>a</sup> All reactions were performed at  $-3\text{ }^\circ\text{C}$  and employed 1.4 equiv. of  $\text{NaBH}_4$  as reducing agent. <sup>b</sup> The crude reaction mixture was analyzed by  $^1\text{H}$  NMR.

After solving the issues related to the reduction of ketone **238**, the attention focused on elaboration of the terminal alkene. To this end,  $\alpha$ -alcohol **279** was converted to  $\alpha$ -mesylate **280** in quantitative yield. The  $\alpha$ -mesylate (**280**) was treated with  $\text{BH}_3 \cdot \text{DMS}$  for 4 hours at 0 °C to afford the primary alcohol (**281**) in 28% yield, along with 25% of  $\alpha$ -mesylate **280**. Surprisingly, no intramolecular cyclization products were isolated, considering the basic nature of the oxidative work-up step of the hydroboration reaction. In an attempt to increase the yield of this reaction, various reaction conditions were investigated. After some screening, the optimal conditions were found to be  $\text{BH}_3 \cdot \text{DMS}$  (2.1 equiv) in THF with stirring for 3 h (0 °C to rt), which provided primary alcohol **281** in 44% yield (with 14% of **280**, Scheme 77).

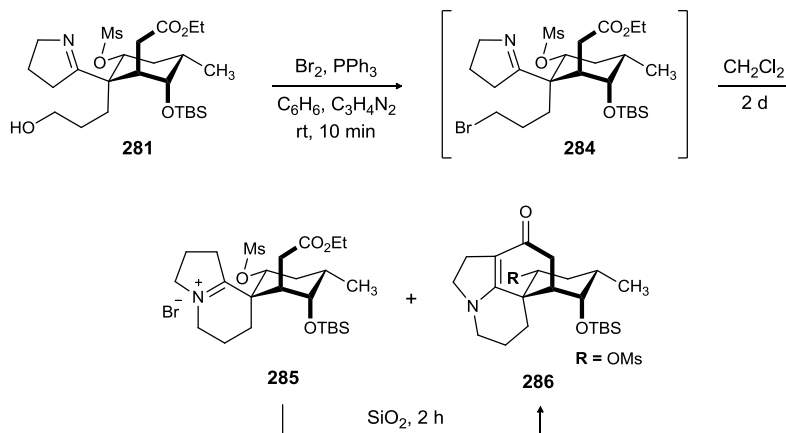
*Scheme 77.* Hydroboration of **280** under Optimized Conditions



With primary alcohol **281** in hand, efforts turned to the synthesis of piperidine ring. The alcohol was treated with bromine,  $\text{PPh}_3$  and imidazole for 10 minutes. After the subsequent work-up step, the crude reaction mixture (solution in  $\text{CH}_2\text{Cl}_2$ ) was left standing for 2 days. Surprisingly, only a trace amount of the desired iminium salt (**285**) was isolated upon purification and a side product was isolated in 60% yield. This undesired side product could be fully characterized by 2D NMR as the vinylogous amide (**286**). Investigation of the crude reaction mixture by  $^1\text{H}$  NMR analysis indicated that the relative amount of the vinylogous amide (**286**) increases over time, and that treatment with  $\text{SiO}_2$  led to the complete conversion of iminium salt **285** to **286** (Scheme 78). At this

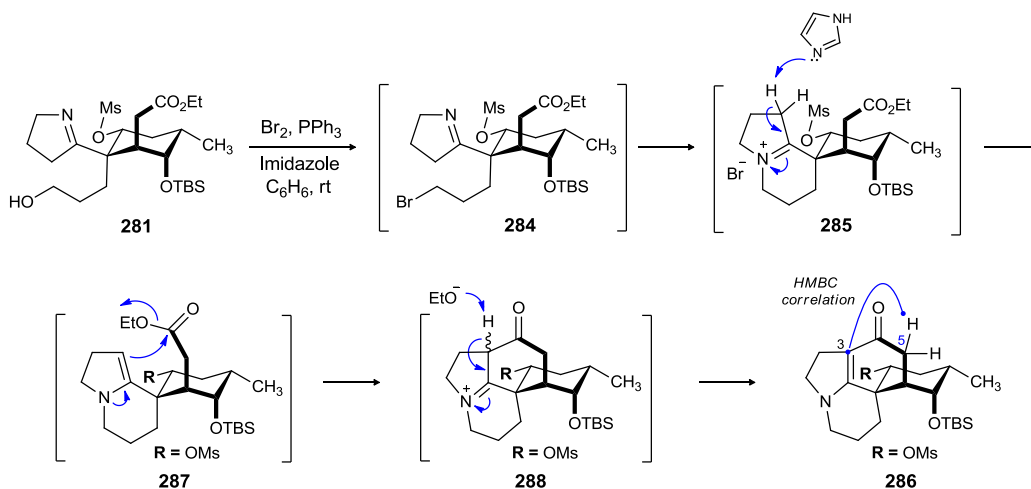
point, it was clear that the iminium salt (**285**) was getting converted to the vinylogous amide (**286**) in the reaction, as well as during the purification process ( $\text{SiO}_2$ ).

**Scheme 78.** Undesired Formation of Vinylogous Amide **190**



Based on these observations, a mechanism for this domino reaction was proposed (Scheme 79). Treatment of **281** with an excess of  $\text{Br}_2$ ,  $\text{PPh}_3$  and imidazole provides bromide **284**, which upon subsequent work-up with  $\text{H}_2\text{O}$  and satd. aq.  $\text{NH}_4\text{Cl}$  was dissolved in  $\text{CH}_2\text{Cl}_2$ . The crude bromide (**284**) cyclized slowly upon standing to provide the desired iminium salt (**285**).

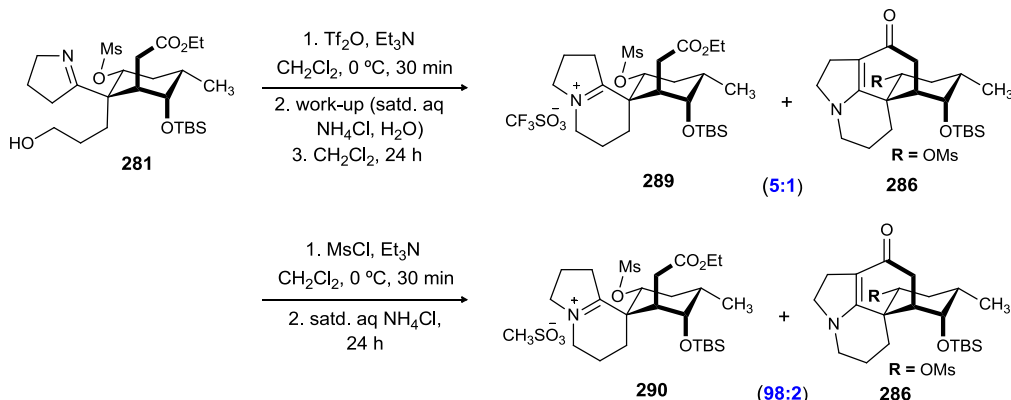
**Scheme 79.** Mechanism for the Undesired Formation of Vinylogous Amide **286**



Abstraction of the acidic 3*H* proton by residual imidazole resulted in the formation of the enamide (**287**). The enamide then underwent an efficient cyclization with the terminal ester and tautomerization of the resulting iminium ion (**288**) leads to the undesired vinylogous amide (**286**).

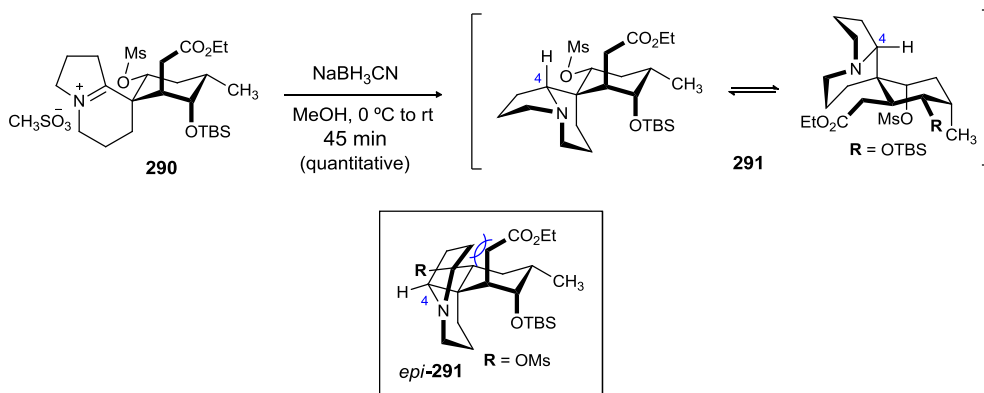
To eliminate the purification step using column chromatography (SiO<sub>2</sub>), which initiates the intramolecular cyclization, other reagents and conditions were explored. It was also postulated that using a water soluble base (aliphatic amines) could be advantageous as it can be washed away in the aqueous work-up step of the bromination reaction. The primary alcohol (**281**) was therefore treated with trifluoromethanesulfonic anhydride and triethylamine for 30 minutes at 0 °C. Upon subsequent work-up step, the crude reaction mixture was left standing for a day. The crude NMR analysis indicated that the desired iminium triflate (**289**) and the vinylogous amide (**290**) existed in a ratio of 5:1 (Scheme 80). However, the result was promising as no other impurities could be identified in the crude NMR analysis. It was reasoned that, as triflate is an excellent leaving group, the cyclization is happening before the aqueous work-up step, and the presence of the base (Et<sub>3</sub>N) in the reaction leads to the subsequent formation of the vinylogous amide (**286**). As a result, the effect of a comparatively weaker leaving group was investigated. To implement this strategy, the primary alcohol (**281**) was treated with methanesulfonyl chloride and triethylamine for 30 minutes at 0 °C. The crude reaction mixture was subsequently treated with excess of satd. aq NH<sub>4</sub>Cl, and the reaction was stirred for an additional 24 h. Gratifyingly, the crude NMR analysis indicated the quantitative formation of iminium mesylate **290** along with trace amount (~2%) of the undesired vinylogous amide (**286**) (Scheme 80).

**Scheme 80.** Leaving Group Effect on Vinylogous Amide **286** Formation



The crude iminium mesylate (**290**) was then reduced with sodium cyanoborohydride to afford the tertiary amine in quantitative yield (Scheme 81).<sup>122</sup> The NMR peaks of **291** were again all very broad, suggesting two interconverting chair conformations, and as a result 2D NMR analysis to determine the facial selectivity of the reduction step could not be conducted. Model studies indicated that the reduction most likely took place from the  $\beta$ -face, as interactions between the pyrrolidine and cyclohexane rings in **291** are considerably less than in *epi*-**291** (at C4) (Scheme 81).

**Scheme 81.** Substrate Controlled Reduction of Iminium **290**

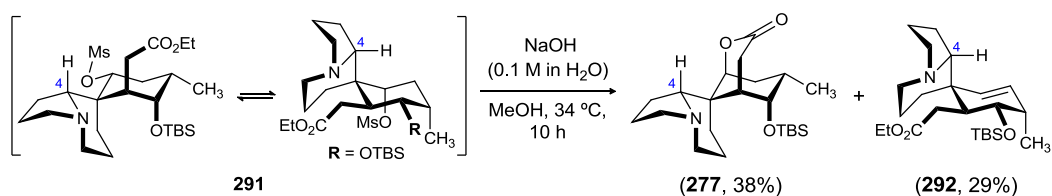


<sup>122</sup> The pure tertiary amine (**291**) was isolated in 53% yield. In addition, (**291**) was also isolated as an amine:borane complex in 44% yield. This amine borane complex could be used in the next reaction as well.



Having accessed tertiary amine **291**, efforts next focused on installing the bridged lactone by a tandem saponification/intramolecular S<sub>N</sub>2 cyclization strategy. Employing different reagents and reaction conditions including, NaOTMS,<sup>123</sup> K<sub>2</sub>CO<sub>3</sub>,<sup>124</sup> LiOH, and NaOH (1.4 equiv, rt) led to either decomposition of the material or formation of alkene **292** by facile mesylate elimination. Success was finally realized by treating **291** with NaOH (0.1 M in H<sub>2</sub>O) at 34 °C for 10 h to afford a 1.1:1 mixture of lactone **277** and alkene **292** (Scheme 82), as indicated by crude NMR analysis. Employing other bases (KOH, Ba(OH)<sub>2</sub>) to effect the saponification reaction resulted in no improvement over NaOH. Purification attempts were unsuccessful, as the lactone (**277**) and the alkene (**292**) coeluted in the column chromatography. However, subjecting the crude reaction mixture to mass directed LC purification process provided the desired lactone in 38% yield along with the alkene (**292**, 29%).<sup>125</sup> The observed ratio of lactone **277** and alkene **292** could be due to the involvement of the both chair conformations of the amine (**291**).

**Scheme 82.** Successful Lactonization of **291**



The final desilylation reaction was performed on the crude lactone as material loss was observed in the mass directed LC purification process. Treatment of the crude reaction mixture of **277** and alkene **292** with TBAF at 40 °C for 20 h led to a separable 3:2 mixture of (+)-Serratezomine A and the fused lactone (**293**) (Scheme 83). Performing

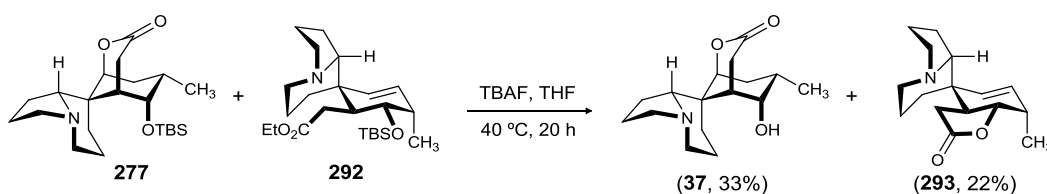
<sup>123</sup> Laganis, E. D.; Chenard, B. L. *Tetrahedron Lett.* **1984**, 25, 5831.

<sup>124</sup> Ziegler, F. E.; Klein, S. I.; Pati, U. K.; Wang, T. F. *J. Am. Chem. Soc.* **1985**, 107, 2730.

<sup>125</sup> The alkene could not be fully characterized due to impurities.

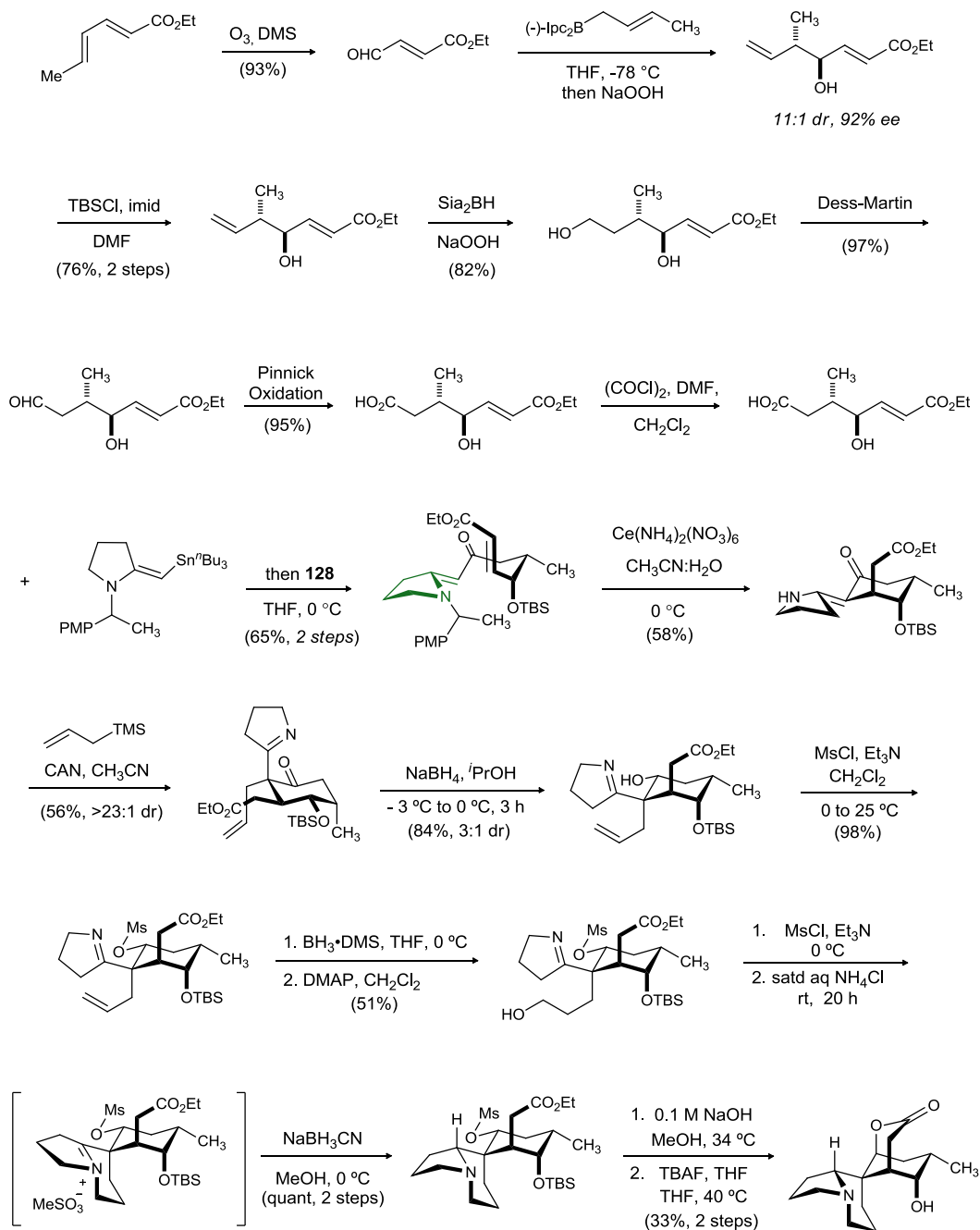
the reaction at lower or higher temperature led to the decomposition of the starting materials. Exposure of the crude mixture of **277** and alkene **292** to other fluoride sources also led to decomposition of starting materials. The spectral data ( $^1\text{H}$  NMR and  $^{13}\text{C}$  NMR and IR) and the optical rotation values [syn. ( $[\alpha]_{\text{D}} +9.5$  ( $c$  0.3, MeOH), nat. ( $[\alpha]_{\text{D}} +13.0$  ( $c$  0.5, MeOH)) for synthetic (+)-Serratezomine A were in agreement with the reported values, confirming their structural and absolute stereochemical assignments.<sup>54</sup>

**Scheme 83.** Completion of the Total Synthesis of (+)-Serratezomine A



In summary, a first total synthesis of (+)-Serratezomine A has been accomplished in 15 steps from the commercially available aldehyde (**228**) (Scheme 84). Apart from the brevity of the current synthesis, there are a number of prominent features: (a) application of the free radical-mediated vinyl amination to construct the pyrrolidine ring; (b) a highly stereoselective intramolecular Michael addition to construct the cyclohexane ring; (c) the use of an oxidative allylation promoted by cerium(IV) (CAN) to establish the all carbon quaternary chiral center with the proper configuration; (d) a tandem saponification/intramolecular  $\text{S}_{\text{N}}2$  cyclization to form the bridging lactone; and (e) minimal use of the protecting groups.

**Scheme 84.** Total Synthesis of (+)-Serratezomine A



## Chapter 3

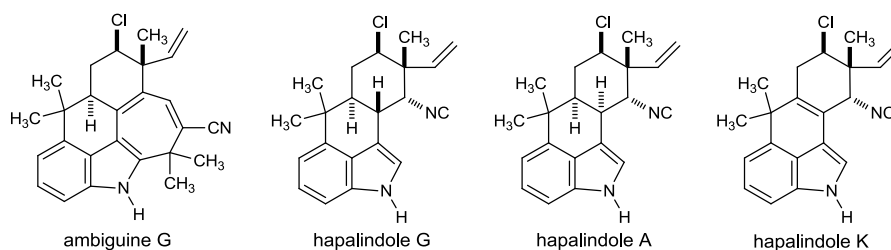
### Total Synthesis of Chlorinated Hapalindoles (K, A, G) and Progress towards the Total Synthesis of (+)-Ambiguine G Nitrile

#### 3.1. Background

##### 3.1.1. Introduction to Indole Marine Alkaloids and (+)-Ambiguine G Nitrile

The Isonitrile and nitrile indole marine alkaloids are a structurally diverse family of heterocyclic compounds. They are isolated from branched, filamentous blue green algae (cyanobacteria) belonging to *Stigonemataceae*, and are classified into four main groups: hapalindoles, fischerindoles, welwitindolinones, and ambiguines.<sup>126</sup> Ambiguine G nitrile was isolated from the cyanobacteria *H. delicatulus* in 1998 by Moore and coworkers (Figure 45).<sup>127</sup>

**Figure 45.** Structure of (+)-Ambiguine G Nitrile and Chlorinated Hapalindoles (A, G, K)



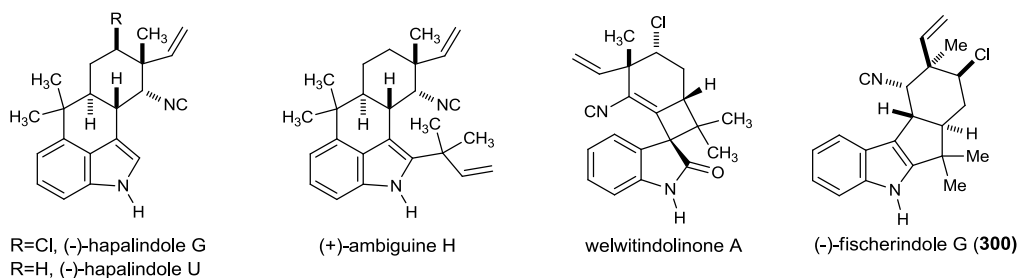
<sup>126</sup> a) Moore, R. E.; Cheuk, C.; Yang, X.-Q. G.; Patterson, G. M. L.; Bonjouklian, R.; Smitka, T. A.; Mynderse, J. S.; Foster, R. S.; Jones, N. D.; Swartzendruber, J. K.; Deeter, J. B. *J. Org. Chem.* **1987**, *52*, 1036. b) Schwartz, R. E.; Hirsch, C. F.; Springer, J. P.; Pettibone, D. J.; Zink, D. L. *J. Org. Chem.* **1987**, *52*, 3704. c) Moore, R. E.; Yang, X.-Q. G.; Patterson, G. M. L. *J. Org. Chem.* **1987**, *52*, 3773. d) Smitka, T. A.; Bonjouklian, R.; Doolin, L.; Jones, N. D.; Deeter, J. B.; Yoshida, W. Y.; Prinsep, M. R.; Moore, R. E.; Patterson, G. M. L. *J. Org. Chem.* **1992**, *57*, 857. e) Park, A.; Moore, R. E.; Patterson, G. M. L. *Tetrahedron Lett.* **1992**, *33*, 3257. f) Stratmann, K.; Moore, R. E.; Bonjouklian, R.; Deeter, J. B.; Patterson, G. M. L.; Shaffer, S.; Smith, C. D.; Smitka, T. A. *J. Am. Chem. Soc.* **1994**, *116*, 9935. g) Huber, U.; Moore, R. E.; Patterson, G. M. L. *J. Nat. Prod.* **1998**, *61*, 1304. h) Jimenez, J. I.; Huber, U.; Moore, R. E.; Patterson, G. M. L. *J. Nat. Prod.* **1999**, *62*, 569. i) Klein, D.; Daloz, D.; Braekman, J. C.; Hoffmann, L.; Demoulin, V. *J. Nat. Prod.* **1995**, *58*, 1781. j) Moore, R. E.; Yang, X.-Q. G.; Patterson, G. M. L.; Bonjouklian, R.; Smitka, T. A. *Phytochemistry* **1989**, *28*, 1565. k) Raveh, A.; Carmeli, S. *J. Nat. Prod.* **2007**, *70*, 196. l) Becher, P. G.; Keller, S.; Jung, G.; Süßmuth, R. D.; Jüttner, F. *Phytochemistry* **2007**, *68*, 2493. m) Asthana, R. K.; Srivastava, A.; Singh, A. P.; Singh, S. P.; Nath, G.; Srivastava, R.; Srivastava, B. S. *J. Appl. Phycol.* **2006**, *18*, 33. n) Mo, S.; Kronic, K.; Chlipala, G.; Orjala, J. *J. Nat. Prod.* **2009**, *72*, 894.

<sup>127</sup> Moore, R. E.; Patterson, G. M. L. *J. Nat. Prod.* **1998**, *61*, 1304.

Ambiguine G nitrile contains a pentacyclic indolo-terpenoid framework that includes a trisubstituted indole ring and a 1,3,5-cycloheptatriene ring. The molecule possesses some unique structural features that including a neopentyl chlorine atom, two geminal dimethyl groups, an all carbon quaternary center, and a nitrile group on the cycloheptatriene ring. Of the nineteen atoms that comprise the structural core, eight (42%) are involved in ring fusions.

The ambiguine class of indole alkaloids has been shown to effect many biochemical processes within cells and displays an array of activities such as hepatotoxicity, neurotoxicity, antibacterial, antifungal activity, as well as protease inhibition.<sup>128</sup> The structure of ambiguine G was determined by <sup>1</sup>H and <sup>13</sup>C NMR as well as 2D NMR techniques including COSY, HMBC and NOE correlations.

**Chart 2.** Structure of Isocyanide-Containing Indole Alkaloids



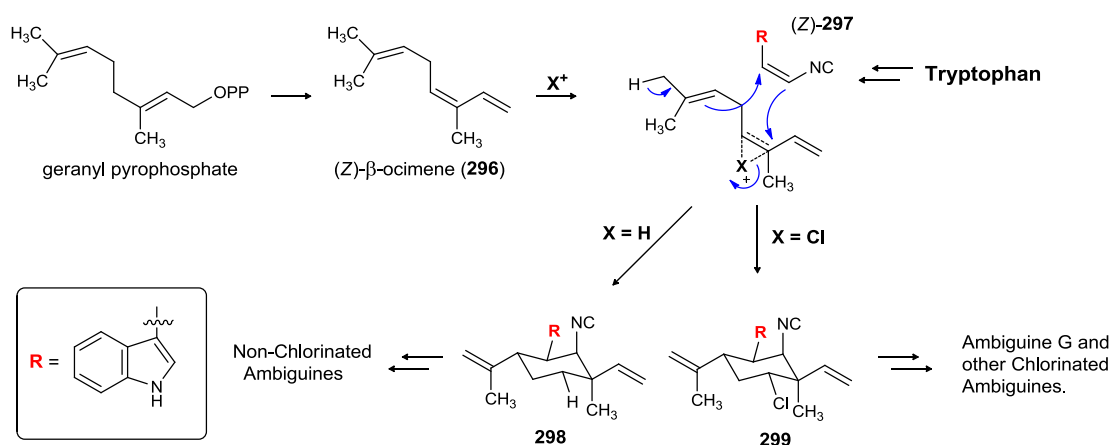
### 3.1.2. Biosynthesis of Indole Marine Alkaloids and (+)-Ambiguine G Nitrile

The co-occurrence of the non-chlorinated derivatives with the chlorinated ambiguines (Figure 45) implies some imperfection in the biosynthesis of these compounds. Moore *et al.*<sup>126,127</sup> proposed a common biogenesis of the hapalindoles, ambiguines, fischerindoles, and welwitindolinones, which may involve a chloronium ion-

<sup>128</sup> Burja, A. M.; Banaigs, B.; Abou-mansour, E.; Burgess, J. G.; Wright, P. C. *Tetrahedron*. **2001**, *57*, 9347.

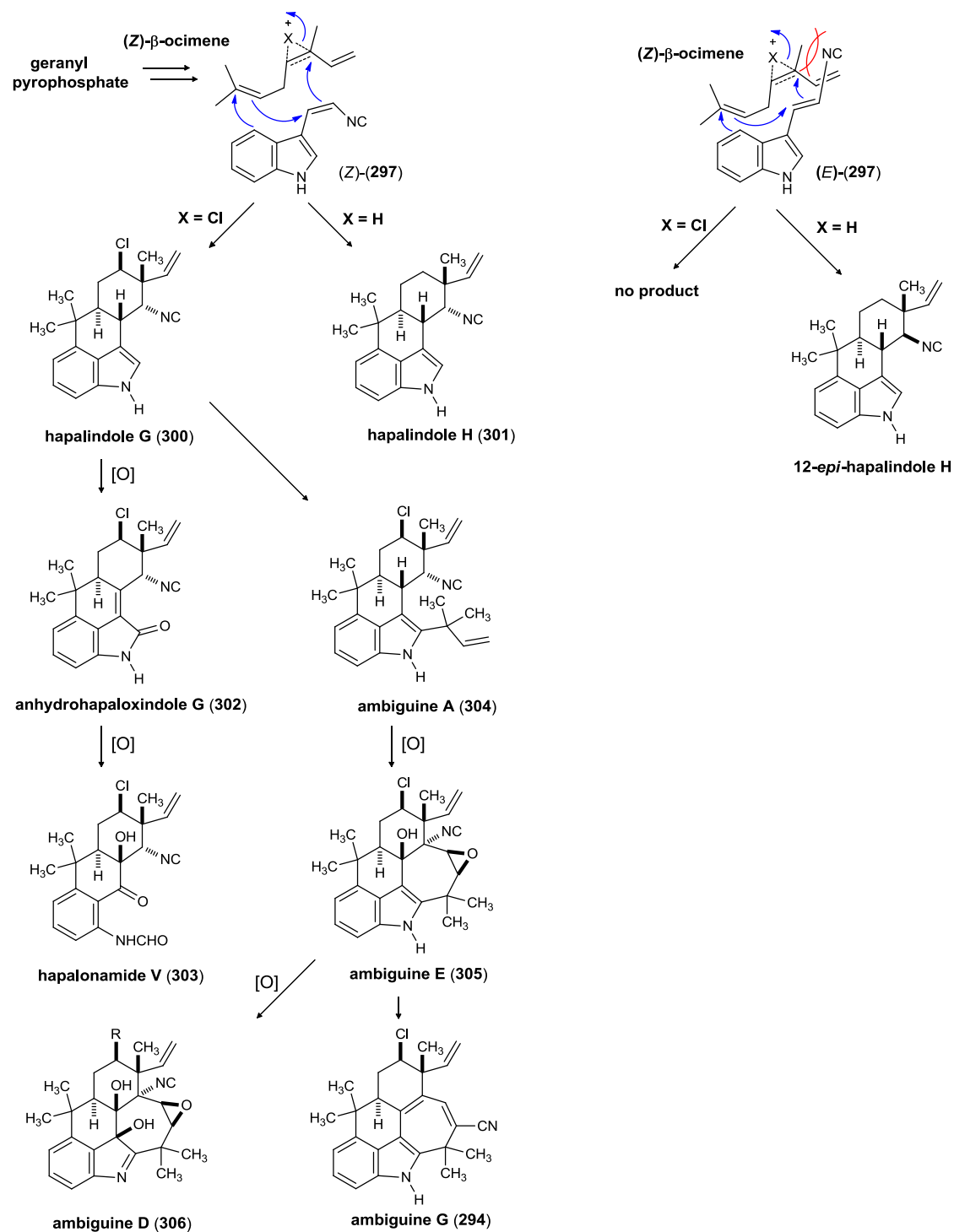
induced condensation of (*Z*)- $\beta$ -ocimene (**296**) and 3-((*Z*)-2'-isocyanoethenyl)indole ((*Z*)-**297**), leading to intermediate 3-cyclohexylindole derivatives with 10, 15-*cis*-diequatorial stereochemistry (**299**, as in the case of the ambiguines) or 10, 15-*cis*-equatorial, axial stereochemistry (**298**, as in the intermediate of hapalindole A) that are converted to the final products by additional cyclization and tailoring processes (Scheme 85).

**Scheme 85.** Proposed Biogenesis of Hapalindoles, Ambiguines, Welwitindolinones and Fischerindoles



While the chlorinated and non-chlorinated ambiguines may be derived from a competition between chloronium and proton ions in the active site of the condensation enzyme (Figure 44), the presence of 12-*epi*-hapalindole H likely represents an alternative biosynthetic manifold. Utilization of (*E*)-**297** over the 3-((*Z*)-2'-isocyanoethenyl)indole ((*Z*)-**297**) could result in a larger steric hindrance due to the bulky isonitrile group, which prevents insertion of the larger chloronium ion in the active site of the enzyme, thus resulting in the production of only 12-*epi*-hapalindole H, but not its chloro-derivative (Figure 46).

Figure 46. Proposed Biosynthesis of Hapalindoles and Ambiguines



Furthermore, the equatorial nitrile group in 12-*epi*-hapalindole H prevents its processing to ambiguiene. The presence of only *tetra*- and *pentacyclic* hapalindoles and

ambiguines in different cyanobacteria suggests that, at least in the case of the biosynthesis of ambiguines, the tetracyclic product is synthesized in one step, as illustrated in Figure 46. The hapalindoles (**300,301**) can undergo oxidation at the indole moiety, leading to oxindole containing tetracyclic framework (**302**). Oxidative cleavage of the oxindole (**302**) probably leads to hapalindole V (**303**). Alternatively, hapalindole G can undergo *tert*-prenylation at C-2 of indole, leading to tetracyclic ambiguines (ambiguine A, **304**). The *tert*-prenylated ambiguines can engage in an intramolecular cyclization process leading to the pentacyclic scaffold of ambiguines (**305,306,294**), which can then be transformed to different ambiguines through a series of oxidation and rearrangement processes (ambiguine A, D, and G).

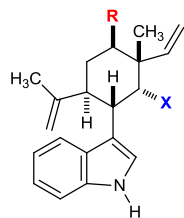
### ***3.2. Approaches towards the Synthesis of Nitrile- and Isonitrile-Containing Indole Marine Alkaloids***

#### ***3.2.1. Synthetic Studies towards Hapalindoles***

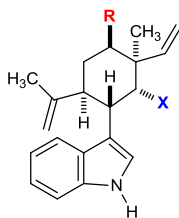
The hapalindoles are a group of 20 structurally related alkaloid natural products isolated from the terrestrial bluegreen algae *Hapalosiphon fontinalis*, an organism found to exhibit antibacterial and antimycotic activity. The hapalindole class of indole marine alkaloids contains intriguing and unprecedented molecular architectures (Figure 47). Some contain further functionalization, in the form of either unsaturation at C10 or chlorination at C13. Additionally, the tetracyclic hapalindoles have further complexity in the form of two chiral centers at C10 and C16, leading to the thermodynamically unstable *cis*-decalin system or the thermodynamically unstable *trans*-decalin ring system (Ring C and D).



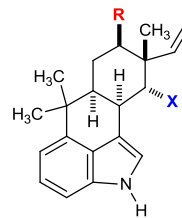
**Figure 47.** Structures of Members of Hapalindole Family of Indole Alkaloids



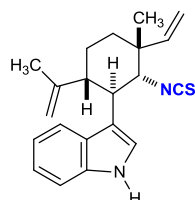
**R = H, X = NC**, hapalindole C  
**R = H, X = NCS**, hapalindole D  
**R = Cl, X = NC**, hapalindole E  
**R = Cl, X = NCS**, hapalindole F



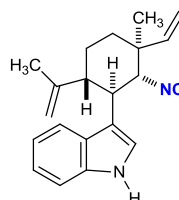
**R = H, X = NC**, 12-*epi*-hapalindole C  
**R = H, X = NCS**, 12-*epi*-hapalindole D  
**R = Cl, X = NC**, 12-*epi*-hapalindole E  
**R = Cl, X = NCS**, 12-*epi*-hapalindole F



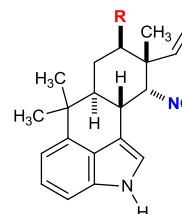
**R = H, X = NC**, hapalindole J  
**R = H, X = NCS**, hapalindole M  
**R = Cl, X = NC**, hapalindole A  
**R = Cl, X = NCS**, hapalindole B  
**R = OH, X = NCS**, hapalindole O



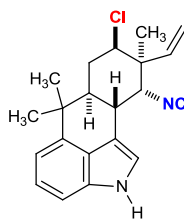
hapalindole Q



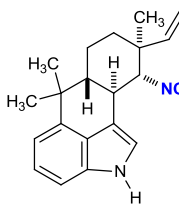
12-*epi*-hapalindole Q isonitrile



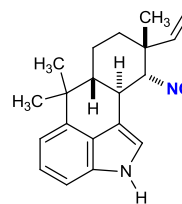
**R = H**, hapalindole U  
**R = Cl**, hapalindole G



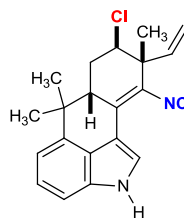
12-*epi*-hapalindole G



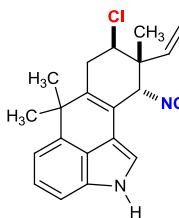
12-*epi*-hapalindole H



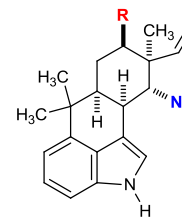
hapalindole H



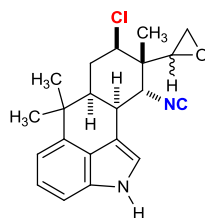
hapalindole I



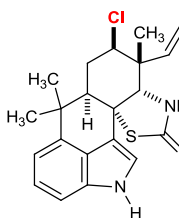
hapalindole K



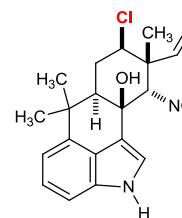
**R = H**, 12-*epi*-hapalindole J  
**R = Cl**, hapalindole L



hapalindole N/P



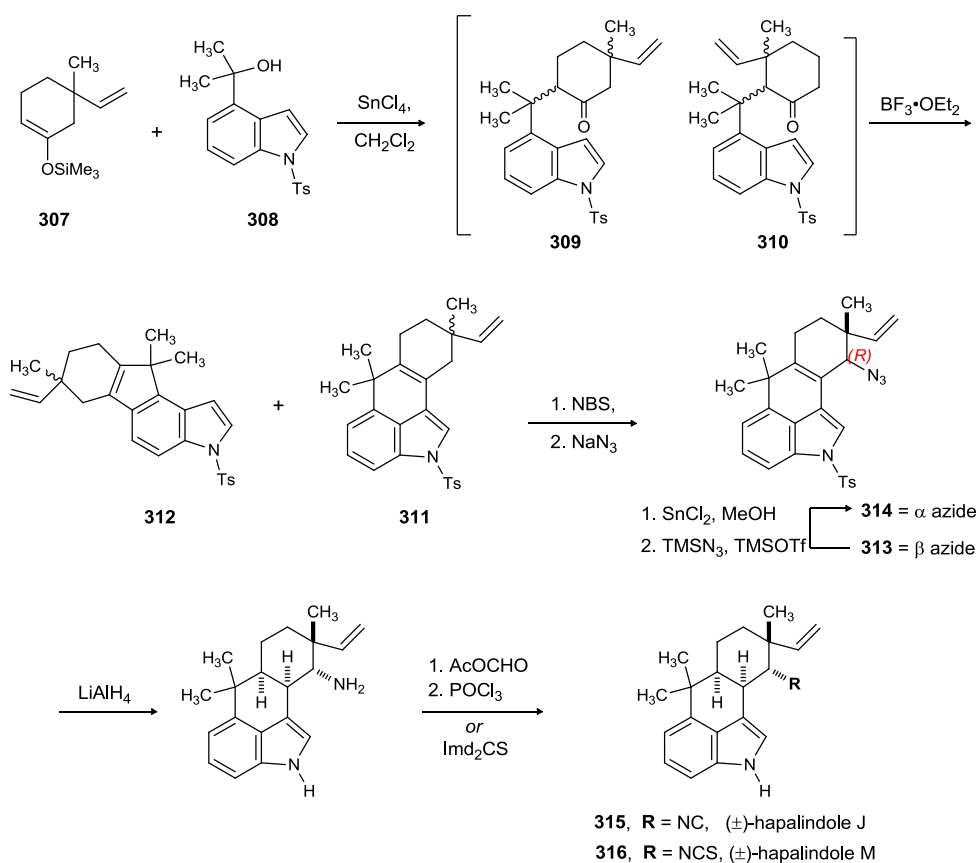
hapalindole T



hapalindole V

The complex structures and biological activity of these compounds has encouraged several syntheses of hapalindoles. The first synthesis of hapalindoles J, M, O, H, and U was accomplished by Natsume and coworkers.<sup>129</sup> Natsume's synthesis of ( $\pm$ )-hapalindole J, M commences with the coupling of trimethylsilyl enol ether **307** with the tertiary alcohol (**308**) using tin (IV) chloride as a catalyst (Scheme 86). Treatment of the adduct (**309** and **310**) with  $\text{BF}_3 \cdot \text{OEt}_2$  furnished the tetracyclic core (**311**) of ( $\pm$ )-hapalindole J, M, along with a by-product **312** in modest yield.

**Scheme 86.** Natsume's Synthesis of ( $\pm$ )-Hapalindoles J and M



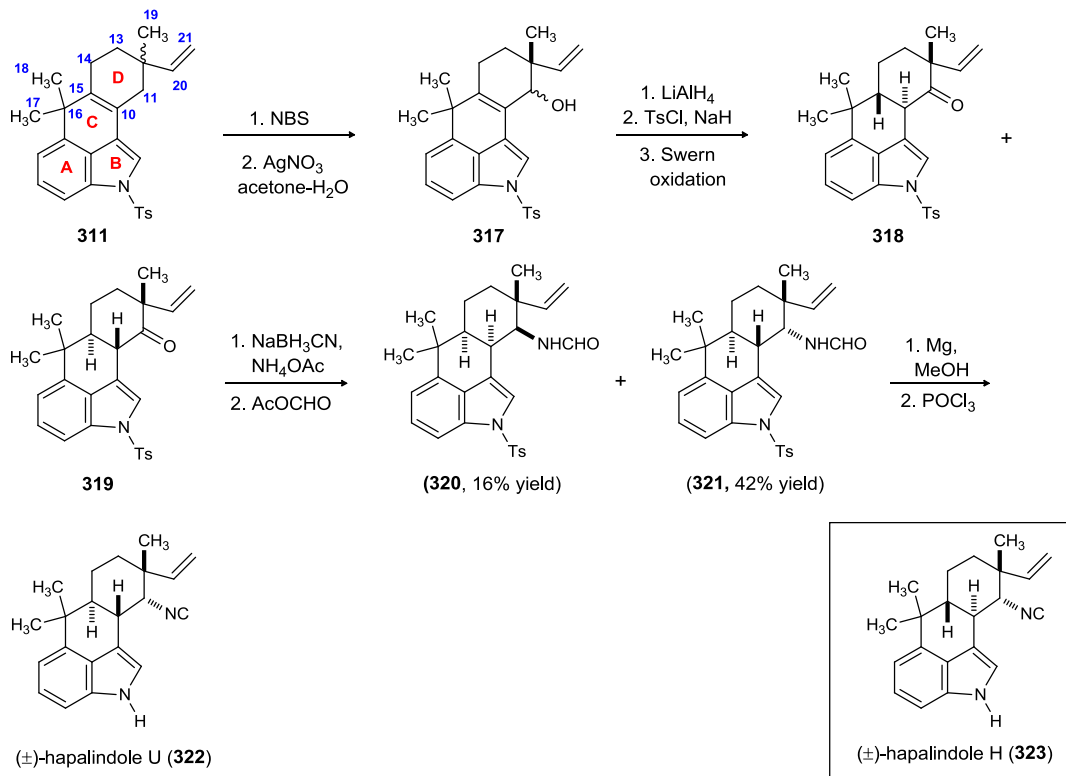
<sup>129</sup> Hapalindoles J, M, O, H, U: a) Muratake, H.; Natsume, M. *Tetrahedron* **1990**, *46*, 6331. b) Sakagami, M.; Muratake, H.; Natsume, M. *Chemical & Pharmaceutical Bulletin* **1994**, *42*, 1393. c) Muratake, H.; Kumagami, H.; Natsume, M. *Tetrahedron* **1990**, *46*, 6351. d) Muratake, H.; Natsume, M. *Tetrahedron* **1990**, *46*, 6343. e) Muratake, H.; Natsume, M. *Tetrahedron. Lett.* **1989**, *30*, 1815.

Bromination of **311** followed by the treatment of crude mixture with sodium azide afforded the two individual diastereomeric azides (**313** and **314**). The undesired  $\beta$ -azide was converted to  $\alpha$ -azide over two standard transformations.  $\text{LiAlH}_4$  reduction of the  $\alpha$ -azide and then formylation of the resulting amine followed by phosphorous oxychloride treatment afforded ( $\pm$ )-hapalindole J (**315**). Synthesis of ( $\pm$ )-hapalindole M (**316**) was achieved by reducing azide **314** with lithium aluminum hydride. This time, however, the reduction mixture was treated with 1, 1'-thiocarbonyldiimidazole to afford **316** in decent yield (Scheme 86).

Natsume's approach to the racemic synthesis of hapalindole H, U was very similar to hapalindole J, M (Scheme 87).<sup>129c</sup> Bromination of the tetracyclic indole (**311**) followed by hydroxylation furnished the alcohol as a mixture of two diastereomers (**317**). *N*-Tosylation and then Swern oxidation followed by  $\text{Et}_3\text{N}$  treatment (epimerization of *C10* proton) led to the two individual diastereomers (**318**, **319**). Stereostructure including the *trans* nature of the C/D ring juncture was established by NOE experiment. The following reductive amination to construct the isonitrile functionality proved to be challenging. Harsh reaction conditions led to the inversion of C/D ring juncture, and reduced products with *cis* juncture were obtained exclusively. Employing mild reductive amination condition (sodium cyanoborohydride in methanol in the presence of ammonium acetate) followed by formylation afforded **321** in 42% yield along with the epimerized compound (**320**, 16% yield). Tosyl deprotection followed by the treatment with phosphorous oxychloride led to the first total synthesis of ( $\pm$ )-hapalindole U (**322**).

Employing the same sequence of synthetic transformations on diastereomeric ketone **323** afforded ( $\pm$ )-hapalindole H (Scheme 87).

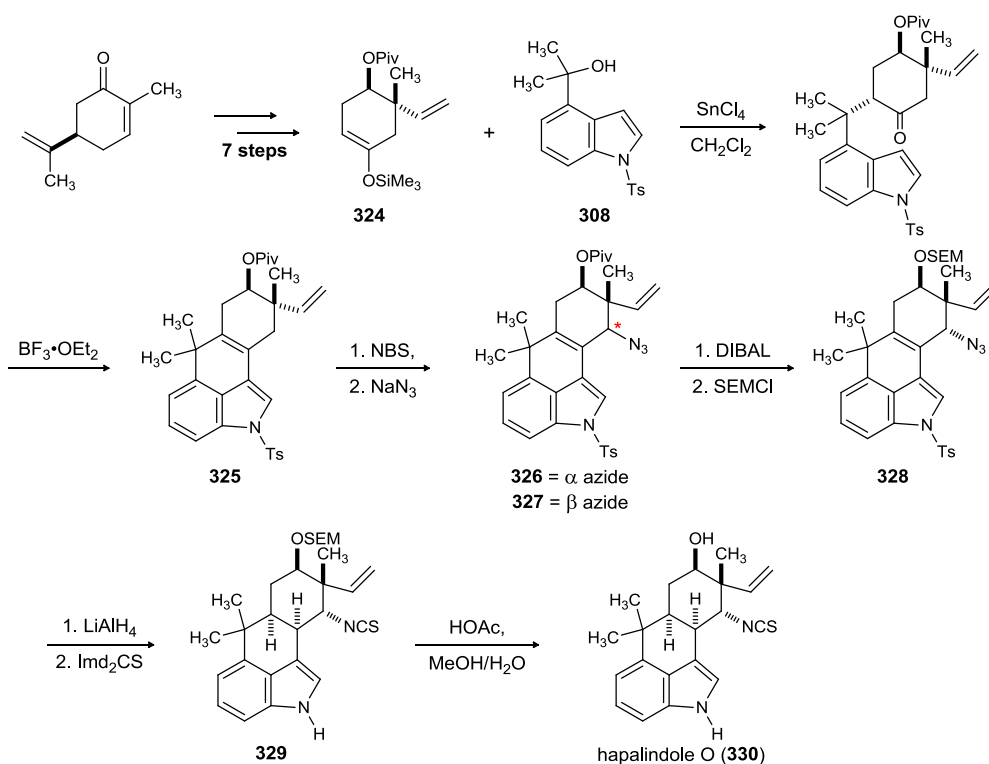
**Scheme 87.** Natsume's Synthesis of (±)-Hapalindoles U and H



In 1994, Natsume and coworkers reported the first enantioselective synthesis of Hapalindole O.<sup>129b</sup> The coupling of an enantiomerically pure trimethylsilyl enol ether **324**, synthesized in 7 steps from naturally occurring (*R*)-(-)-carvone, with indole derivative **308** to construct the tetracyclic framework of hapalindole O was effected according to their previous synthetic studies on hapalindoles J,M,H, and U (Scheme 88).<sup>129a,c</sup> The coupled product was subsequently treated with  $\text{BF}_3 \cdot \text{OEt}_2$  to furnish the cyclized compound (**325**). Bromination followed by the treatment of the crude reaction mixture with sodium azide afforded the two individual epimeric azides (**326** and **327**). The desired  $\alpha$ -azide (**326**) was treated with DIBAL to reductively remove the pivaloyl group and the resulting alcohol was protected as 2-(trimethylsilyl)ethoxymethyl (SEM) to furnish compound **328**. In an unusual reduction with  $\text{LiAlH}_4$ , the following reactions

where effected in a single operation: i) reductive cleavage of the tosyl group from the indole nitrogen carbon, ii) reduction of the azide, and iii) stereoselective ( $\alpha$ -face) reduction of the alkene conjugated with the indole nucleus. Treatment of the crude reaction mixture with 1, 1'-thiocarbonyldiimidazole led to the isothiocyanate **329**. Removal of the SEM protecting group under mild reaction conditions furnished hapalindole O (**330**) in 16 steps from (*R*)-(-)-carvone in less than 1% yield.

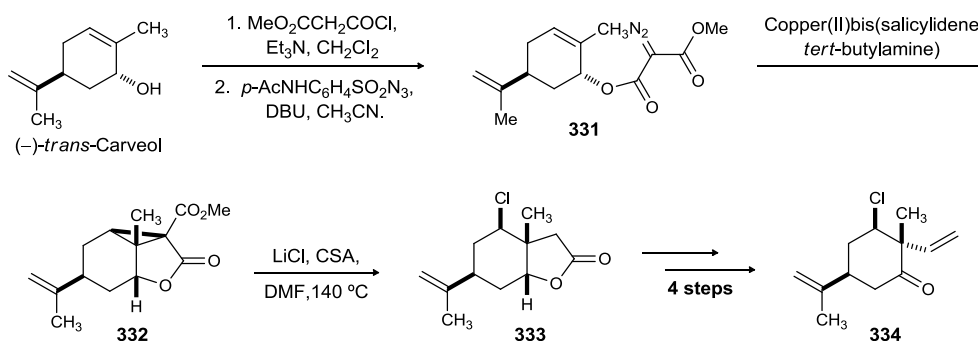
**Scheme 88.** Natsume's Enantioselective Synthesis of Hapalindole O



Though the total syntheses of racemic hapalindoles J, M, H, and U as well as the enantiospecific synthesis of hapalindole O was reported by Natsume and coworkers, the synthesis of more challenging chlorinated hapalindoles remained elusive. Fukuyama *et al.* reported the first enantiospecific total synthesis of (-)-hapalindole G (**300**), a

neopentyl chlorine-containing hapalindole.<sup>130</sup> The synthesis commences with the condensation of (-)-*trans*-Carveol with methyl (chloroformyl)acetate followed by a diazo transfer under standard conditions. The resultant diazomalonate **331** was subjected to an intramolecular cyclopropanation reaction, to provide cyclopropyl ester **332**. The stereospecific introduction of chlorine to the hindered C-13 position with concomitant decarbomethoxylation was achieved by heating the activated cyclopropane ester with lithium chloride and camphorsulfonic acid, providing lactone **333**. The lactone (**333**) was converted to the desired vinyl ketone **334** in an efficient four-step sequence (Scheme 89).

**Scheme 89.** Fukuyama's Enantioselective Synthesis of (-)-Hapalindole G



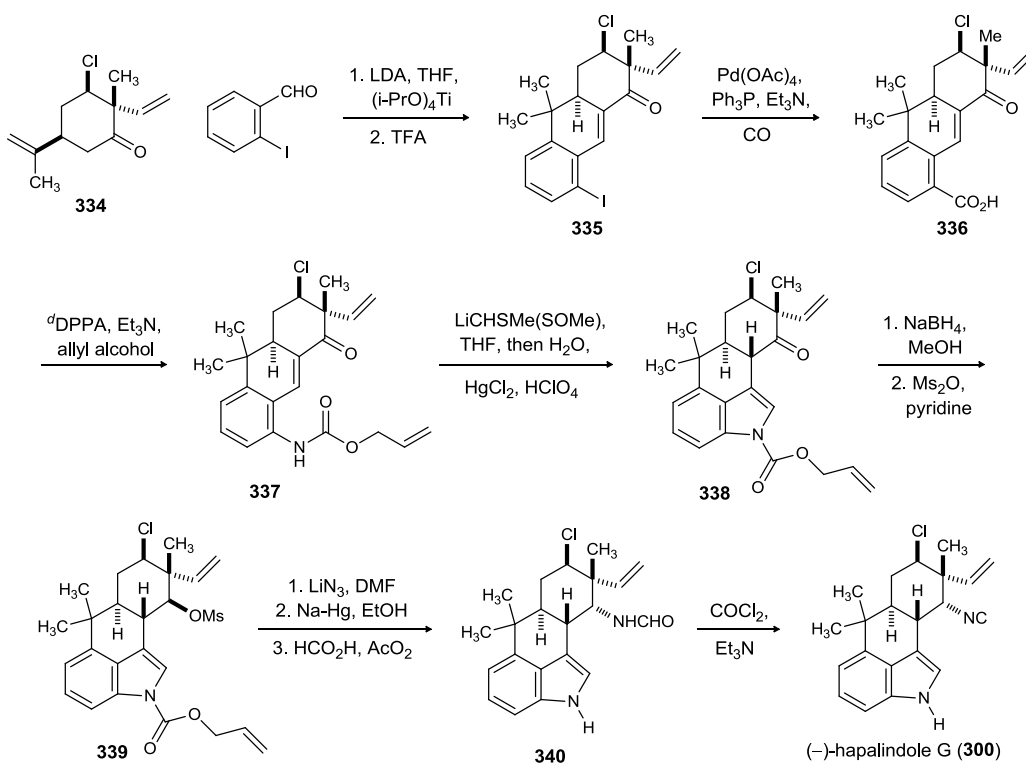
Subsequent aldol reaction of the ketone with *o*-iodobenzaldehyde followed by treatment of the crude reaction mixture with trifluoroacetic acid afforded the tricyclic enone (**335**) (Scheme 90). Construction of the requisite indole was performed by first converting the aryl iodide to the carboxylic acid (**336**) by a palladium-mediated carbonylation and then transforming **336** to the allyl urethane (**337**) according to the Shioiri-Yamada procedure.<sup>131</sup> Conjugate addition of lithiated methyl (methylthio)methyl sulfoxide to the enone (**337**) followed by acid treatment in presence of mercuric chloride

<sup>130</sup> Fukuyama, T.; Chen, X. Q. *J. Am. Chem. Soc.* **1994**, *116*, 3125.

<sup>131</sup> Shioiri, T.; Ninomiya, K.; Yamada, S. -I. *J. Am. Chem. Soc.* **1972**, *94*, 6203.

furnished the indole (**338**) as a single stereoisomer. Reduction of the ketone with NaBH<sub>4</sub> followed by mesylation of the alcohol afforded mesylate **339**. Displacement of the mesylate by an azide with concomitant deprotection of allyl urethane, and subsequent reduction of the azide followed by formylation afforded **340**. Finally, dehydration of the formamide with phosgene and triethylamine gave (-)-hapalindole G (**300**) in 21 steps from (-)-*trans*-Carveol in less than 3.5% yield. To date, this is the only synthesis of chlorinated hapalindole reported in the literature.

**Scheme 90.** Fukuyama's Enantioselective Synthesis of (-)-Hapalindole G (Completion)



Several syntheses of hapalindole Q have been reported since their discovery by Moore and coworkers. The first enantioselective synthesis of (+)-hapalindole Q was accomplished by Albizati and coworkers.<sup>132</sup> Albizati's synthesis begins with the bromide

<sup>132</sup> Vaillancourt, V.; Albizati, K. F. *J. Am. Chem. Soc.* **1993**, *115*, 3499.

(**342**) (Scheme 91).  $\alpha$ -Arylation of the 9-bromocamphor derivative (**343**) provided the desired *endo* camphor derivative (**344**). The intermediate **344** underwent fragmentation of the C1-C7 bond by treatment with sodium naphthalenide and the resulting enolate was directly alkylated with acetaldehyde to provide **345**. Mesylation of **345** followed by iodide ion promoted thermal elimination of the mesylate provided alkene **346** as a single stereoisomer. Reductive amination employing ammonium acetate and sodium cyanoborohydride was followed by treatment with 1,1'-thiocarbonyldiimidazole, which provided (+)-hapalindole Q (**341**).

**Scheme 91.** Albizati's Enantioselective Synthesis of (+)-Hapalindole Q

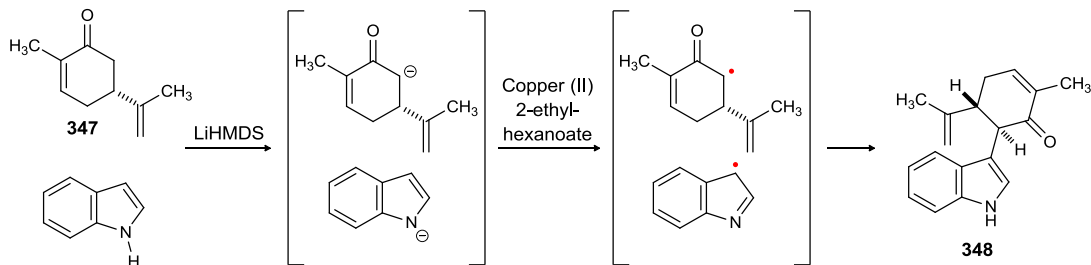


Baran and coworkers applied the direct coupling of indole with the enone (**347**) to the most concise and efficient synthesis of (+)-hapalindole Q.<sup>133</sup> The strategy utilizes an unprecedented radical coupling of indole and (*R*)-carvone fragment **347** to access the coupling adduct (**348**) as a single diastereomer. The optimum protocol emerged upon addition of LiHMDS (3.0 equiv.) to a solution of indole (2.0 equiv) and **347** (1.0 equiv.) in THF at -78 °C followed by addition of 1.5 equiv. of copper(II)2-ethylhexanoate, furnishing the coupled product (**348**) in 53% yield (Scheme 92).

<sup>133</sup> a) Baran, P. S.; Richter, J. M. *J. Am. Chem. Soc.* **2004**, *126*, 7450. b) Richter, J. M.; Ishira, Y.; Masuda, T.; Whitefield, B. W.; Llamas, T.; Pohjakallio, A.; Baran, P. S. *J. Am. Chem. Soc.* **2008**, *130*, 17938.

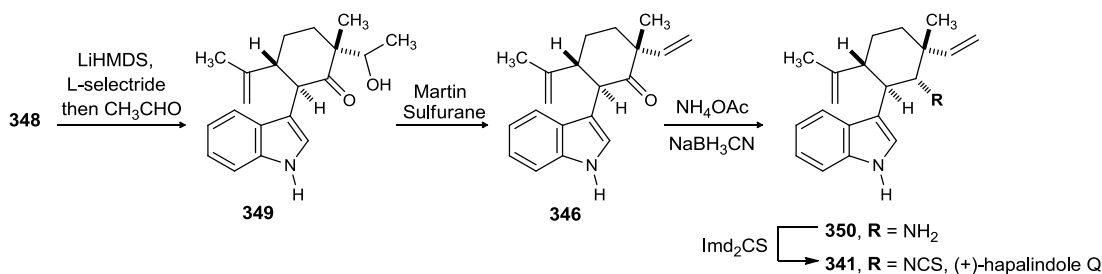


**Scheme 92.** Radical Coupling of Indole and (R)-Carvone Fragment



The completion of the total synthesis was accomplished by executing the following operations (Scheme 93): (i) deprotonation of the indole N-H of **348**, conjugate reduction and stereoselective quenching of the resulting enolate with acetaldehyde; (ii) dehydration of the crude alcohol **349** to give alkene **346**; (iii) reductive amination to furnish the amine (**350**) as a 6:1 mixture of diastereomers; and (iv) conversion to (+)-hapalindole Q (**341**) by isothiocyanate formation.

**Scheme 93.** Baran's Enantioselective Synthesis of (+)-Hapalindole Q

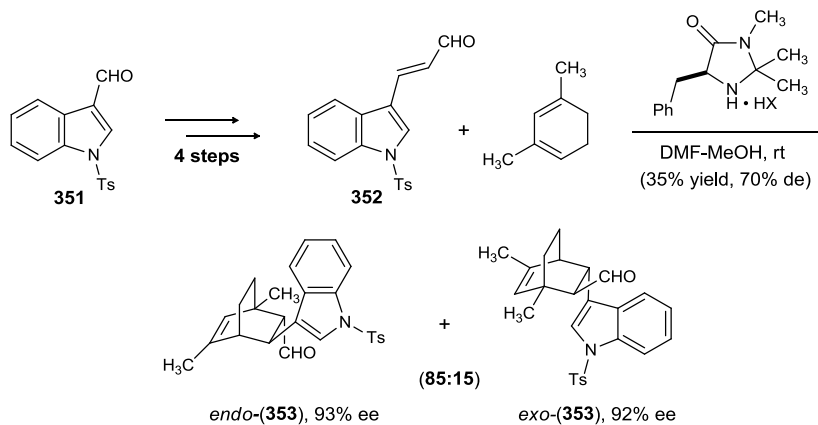


An efficient synthetic approach to (+)-hapalindole Q was demonstrated by Kerr using an organomediated Diels-Alder reaction.<sup>134</sup> The required enal dienophile **352** was prepared in four steps from the known indole **351**. Asymmetric Diels-Alder reaction

<sup>134</sup> a) Kinsman, A. C.; Kerr, M. A. *Org. Lett.* **2001**, *3*, 3189. b) Kinsman, A. C.; Kerr, M. A. *J. Am. Chem. Soc.* **2003**, *125*, 14120.

mediated by organocatalyst provided the adduct (**353**) as an 85:15 mixture of *endo:exo* isomers (Scheme 94) in 70% de.

**Scheme 94.** Organomediated Diels-Alder Reaction

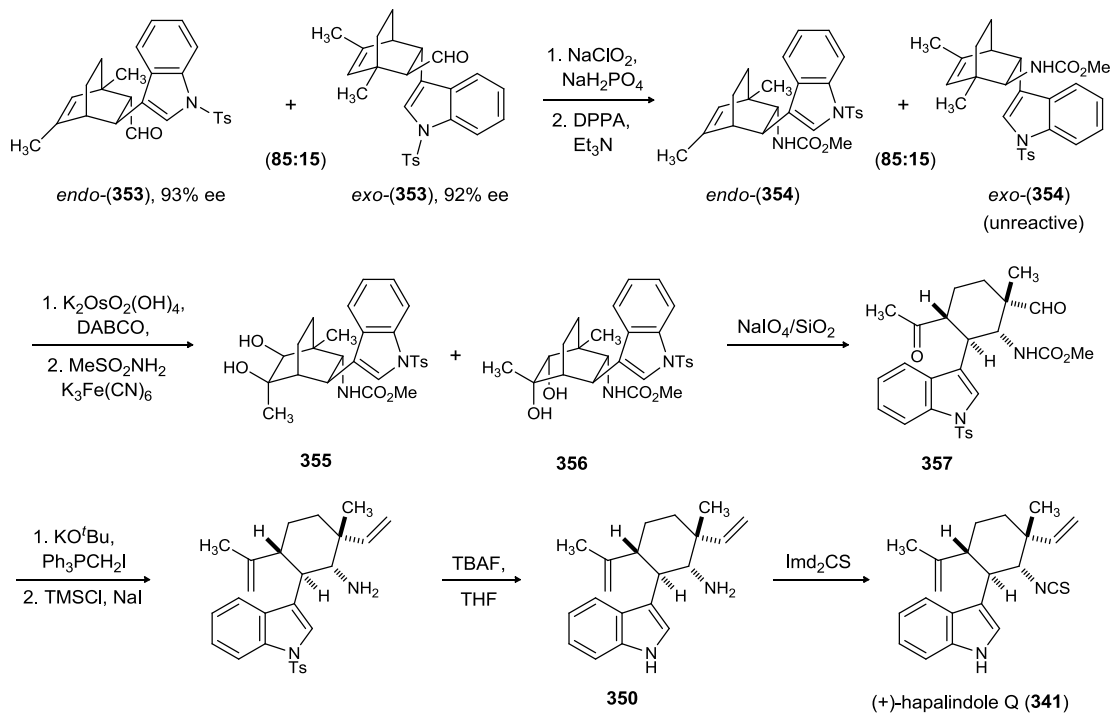


Oxidation of **353** followed by Curtius rearrangement furnished **354** as an inseparable mixture of *endo*- and *exo*-carbamates. *endo*-Carbamate **354** underwent dihydroxylation to provide mixture of diols **355** and **356** (Scheme 95). The *exo*-carbamate was unreactive to the reaction conditions and could be separated by flash chromatography. The mixture of diols could be cleanly cleaved with silica-supported  $\text{NaIO}_4$  to give keto-aldehyde **357**. Double methylenation of the keto-aldehyde by sequential Wittig reaction, and subsequent amine deprotection followed by fluoride mediated detosylation of indole provided amine **350**, intersecting with the Albizati synthesis (Scheme 95).

There are some other reported synthetic approaches, in addition to those discussed here, to the tetracyclic core of various other hapalindoles.<sup>135</sup>

<sup>135</sup> a) Brown, M. A.; Kerr, M. A. *Tetrahedron. Lett.* **2001**, 42, 983. b) Banwell, M. G.; Ma, X.; Taylor, R. M.; Willis, A. C. *Org. Lett.* **2006**, 8, 4959.

**Scheme 95.** Kerr's Enantioselective Synthesis of (+)-Hapalindole Q



### 3.2.2. Synthetic Studies towards Welwitindolinones

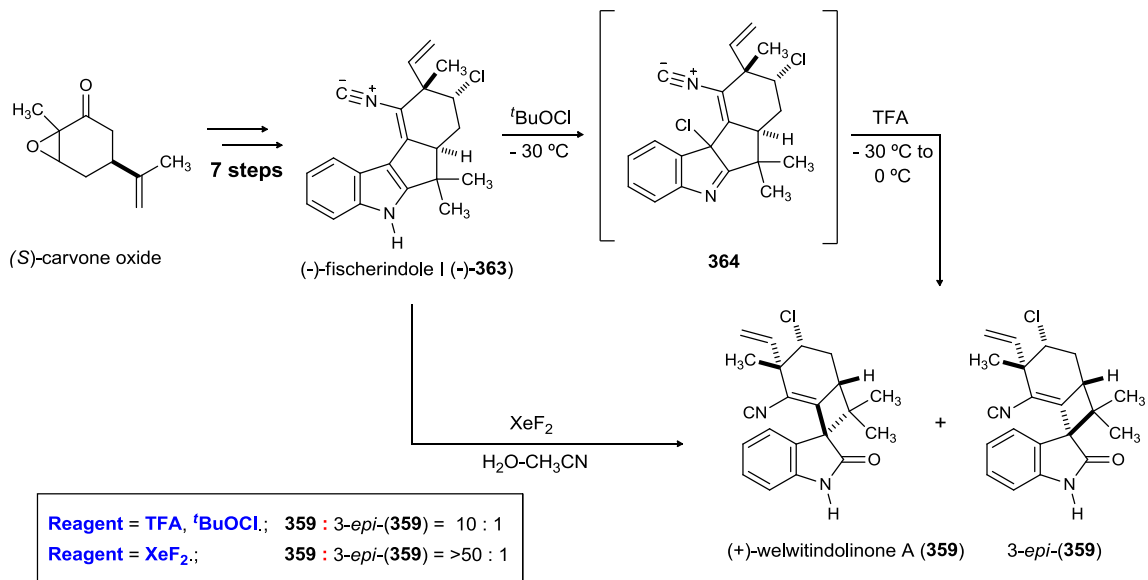
#### 3.2.2.1. Biosynthesis and Biological Properties of Welwitindolinones

It is supposed that welwitindolinones are derived from 12-*epi*-hapalindole (Scheme 96). 12-*epi*-hapalindole could be transformed to **358**, a direct precursor of the spiro-compound **359** (welwitindolinone A). Epoxidation of the central cyclohexene double bond of welwitindolinone A could lead to **360**, which after intramolecular Friedel-Crafts alkylation (arylation) may afford the tetracyclic skeleton of welwitindolinones (**361** and **362**). This intermediate can then lead to all complex welwitindolinones after a series of functionalization including oxidation, unsaturation and thiocyanation.



Due to their structural similarities, Baran *et al.* later suggested that the biosynthetic precursor of welwitindolinone A could be fischerindole. This hypothesis was supported by a chemical synthesis of (+)-welwitindolinone A and (+)-*epi*-welwitindolinone A from (-)-fischerindole I (Scheme 98). The synthesis commenced with (-)-fischerindole I, which is synthesized in seven steps from (*S*)-carvone oxide. Treatment of (-)-fischerindole I with <sup>t</sup>BuOCl at -30 °C for 1 minute provided 3-chloroindolenine (**364**). The key ring contraction occurred upon dissolving the crude 3-chloroindolenine in THF/H<sub>2</sub>O/TFA to provide a 10:1 mixture of (+)-welwitindolinone A and 3-*epi*-(+)-welwitindolinone A (**359**) in 28% yield.

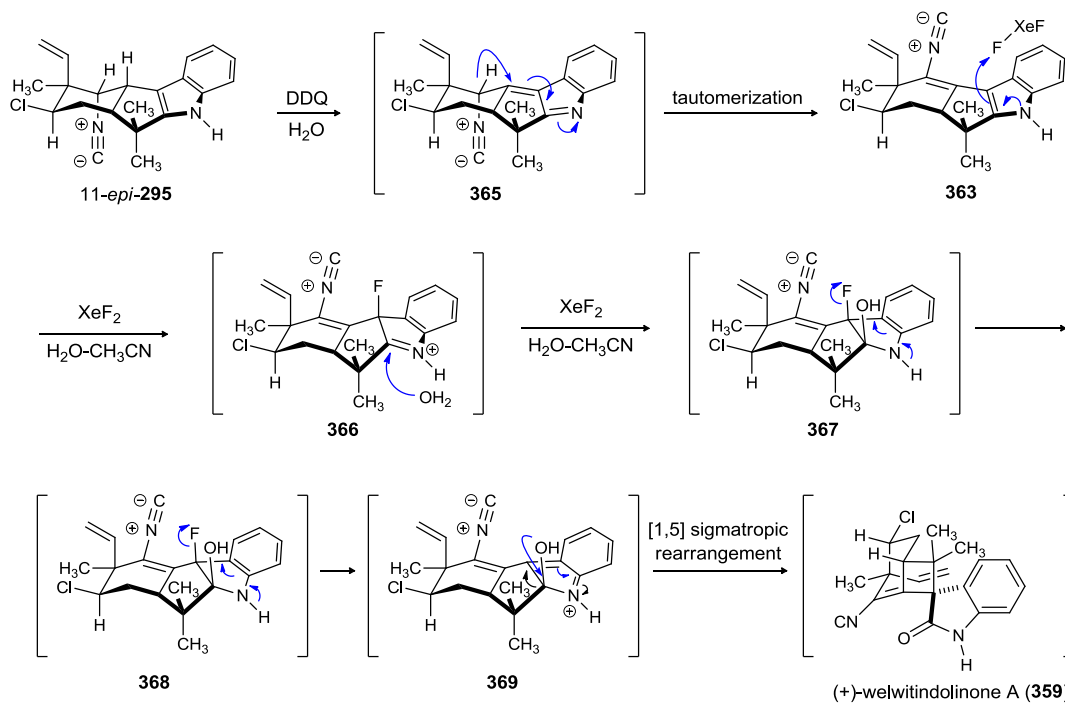
**Scheme 98.** Baran's Biomimetic Enantioselective Synthesis of (+)-Welwitindolinone A



Due to the low yield and diastereoselection in the oxidative ring contraction process leading to welwitindolinone A (Scheme 98), Baran and coworkers performed an exhaustive screen of halogen-based oxidants to circumvent this problem. Success was finally realized when the chlorohydroxylation process in this reaction was replaced with

fluorohydroxylation using XeF<sub>2</sub> (Scheme 99).<sup>137</sup> The rearranged product could be isolated in modest yield, but more importantly as a single diastereomer. This domino process commences with the fluorination of the more nucleophilic C-3 of indole followed by hydroxylation of the intermediate iminium **366**. **367** then undergoes a series of rearrangement, including a ring contraction process, to provide welwitindolinone A.

**Scheme 99.** Mechanism of Xenon Fluoride Mediated Ring Contraction Process



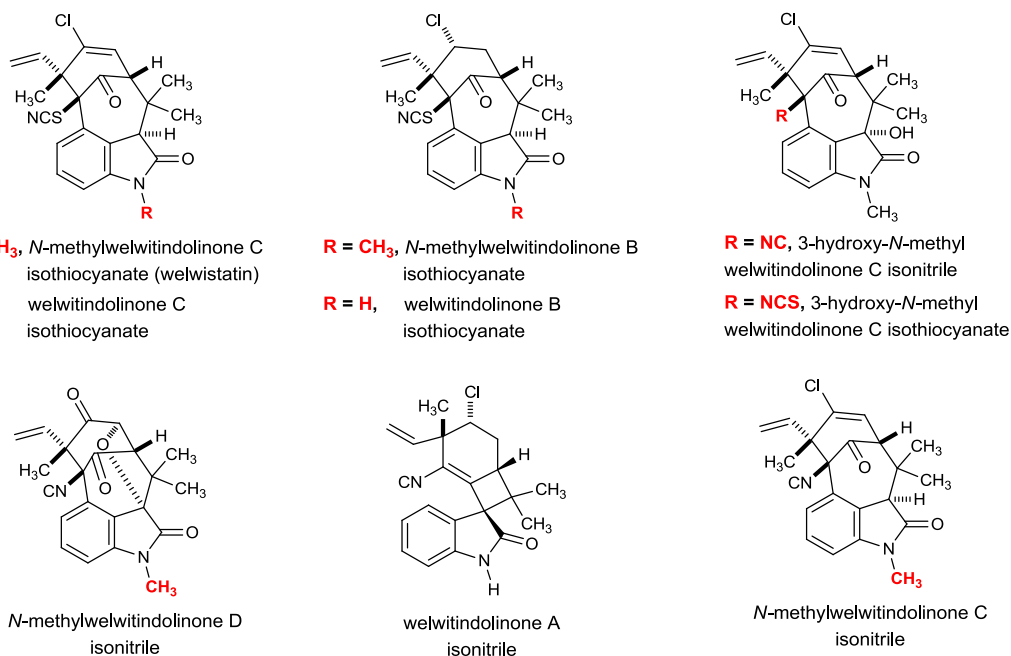
### 3.2.2.2. Synthetic Efforts towards Welwitindolinones

Welwitindolinones are a family of unusual oxindole marine alkaloids obtained from marine cyanobacteria. The first members of the group were isolated in 1994 by Moore and coworkers from the blue green algae *Hapalosiphon welwitschii*.<sup>126f</sup> Structures of the members of the welwitindolinone family are shown in Figure 48. Welwistatin (**362**) inhibits multidrug resistance (MDR) to antitumor agents. Welwistatin also inhibits

<sup>137</sup> Baran, P. S.; Maimone, T. J.; Richter, J. M. *Nature*. **2007**, *446*, 404.

cell proliferation, with reversible depletion of cellular microtubules in ovarian carcinoma cells and A-10 vascular smooth muscle cells, by inhibiting the polymerization of tubulin.<sup>138</sup>

**Figure 48.** Structures of the Members of the Welwitindolinone Family



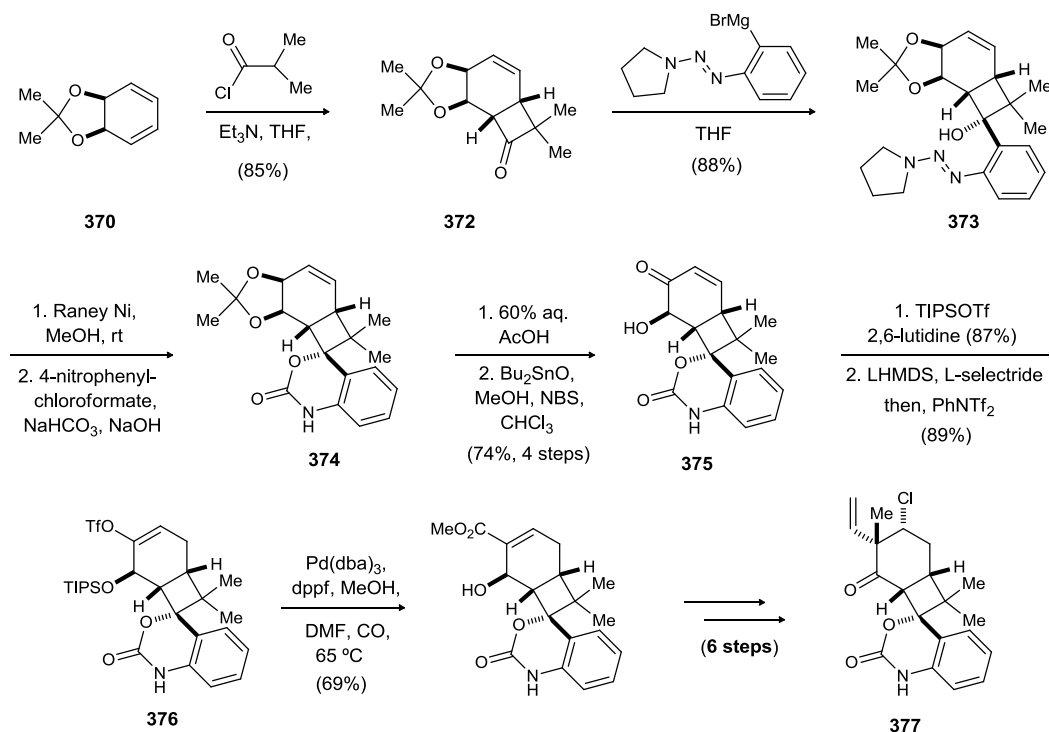
The only other synthesis of (+)-welwitindolinone A, in addition to its biomimetic syntheses by Baran *et al.*, has been reported by Wood and coworkers in 2006.<sup>139</sup> The synthesis commences with a regio- and diastereoselective [2+2] cycloaddition between cyclohexadiene acetonide (**370**) and a ketene derived from acyl chloride **371** to provide adduct **372** (Scheme 100). The required arylamine moiety was introduced by utilizing an *ortho*-metallated aniline equivalent. The triazene **373** was reduced with raney Ni, and the hydroxyl and amine functionalities in the resulting hydroxylamine were protected as a cyclic carbamate **374** upon treatment with 4-nitrophenyl chloroformate. Acid-mediated

<sup>138</sup> Zhang, X.; Smith, C. D. *Mol Pharmacol.* **1996**, *49*, 228.

<sup>139</sup> a) Reisman, S. E.; Ready, J. M.; Hasuoka, A.; Smith, C. J.; Wood, J. L. *J. Am. Chem. Soc.* **2006**, *128*, 1448. b) Reisman, S. E.; Ready, J. M.; Weiss, M. M.; Hasuoka, A.; Hirata, M.; Tamaki, K.; Ovaska, T. V.; Smith, C. J.; Wood, J. L. *J. Am. Chem. Soc.* **2008**, *130*, 2087.

unmasking of the diol in **374** was followed by selective oxidation of the allylic alcohol under mild oxidative condition to furnish **375**. The TIPS ether, derived in one step from secondary alcohol **375**, was converted to enol triflate **376** upon treatment with L-selectride and *N*-phenyltriflimide. A number of steps were required for the central cyclohexene ring functionalization, to ultimately provide the advanced intermediate **377**.

**Scheme 100.** Wood's Enantioselective Synthesis of (+)-Welwitindolinone A

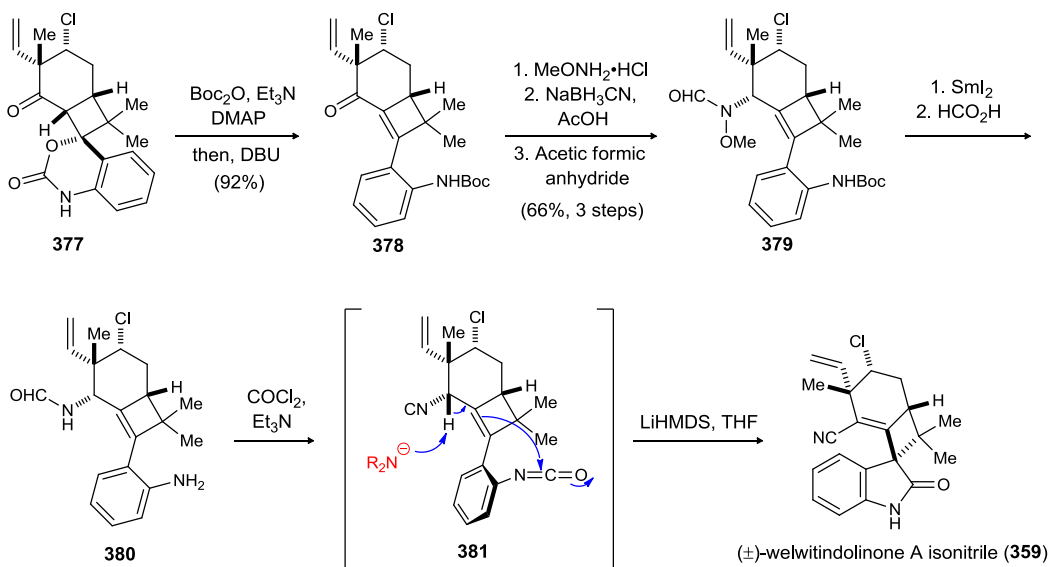


The final few steps proved to be quite challenging; and after exhaustive investigation the Wood's group finally found a successful route to the natural product (Scheme 101). To this end, carbamate **377** was transformed into **378** via a tandem decarboxylation and BOC protection. The two step substrate-controlled stereoselective reductive amination of the ketone (**378**) was followed by formylation of the resulting hydroxylamine to provide **379**. Reductive cleavage of the N–O bond mediated by samarium (II) iodide, furnished intermediate formamide, which gave **380** after acid-



catalyzed BOC deprotection. Isonitrile functionality could be incorporated in a straightforward manner by treatment with phosgene. Exposure of the crude **381** to lithium hexamethyldisilazide furnished the natural product as a single diastereoisomer.

**Scheme 101.** Wood's Enantioselective Synthesis of (+)-Welwitindolinone A (Completion)



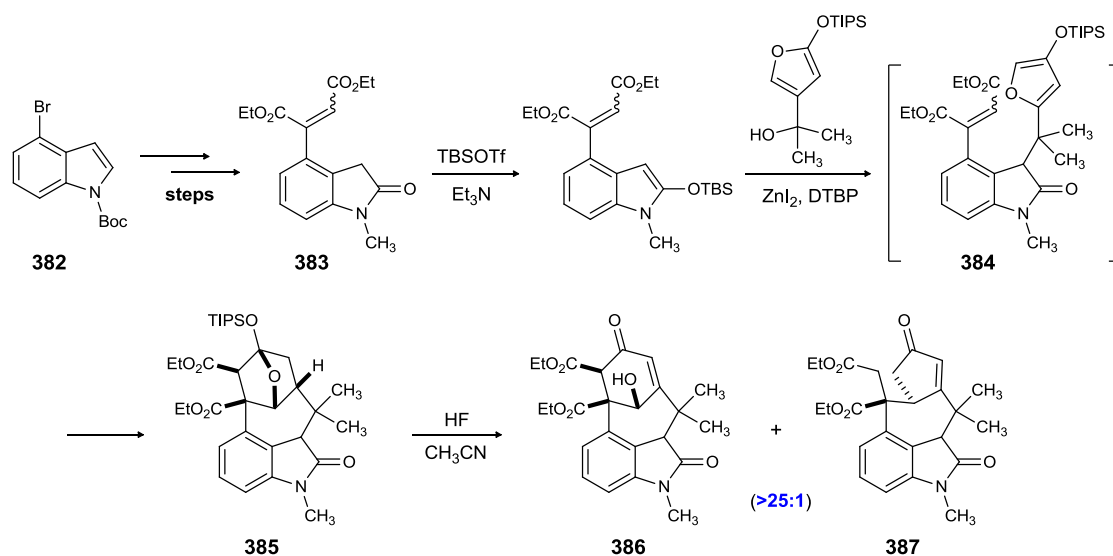
The synthesis of welwistatin (**362**), a more complex welwitindolinone, and the related welwitindolinones still remains elusive to the synthetic community (Figure 48). Over the years, a number of synthetic efforts have been reported towards these structurally complex welwitindolinones. These key reactions in all these approaches utilize either a Diels-Alder cycloaddition or palladium catalyzed arylation and C-H insertion reactions.

Two research groups have utilized the Diels-Alder cycloaddition reaction to construct the tetracyclic framework of Welwistatin.<sup>140</sup> Shea *et al.* uses the intramolecular Diels-Alder approach to construct the C and D ring in one synthetic operation.<sup>140a,b</sup> The

<sup>140</sup> a) Lauchli, R.; Shea, K. J. *Org. Lett.* **2006**, *8*, 5287. b) Brailsford, J. A.; Lauchli, R.; Shea, K. J. *Org. Lett.* **2009**, *11*, 5330. c) Trost, B. M.; McDougall, P. J. *Org. Lett.* **2009**, *11*, 3782.

precursor for this Diels-Alder reaction was synthesized from *N*-protected 4-bromo indole **382** (Scheme 102). The dienophile fragment (**383**) was derived from **382** by using a Pd-catalyzed arylation approach. Masking the oxindole oxygen as the TBS-ether was followed by a Freidel-Crafts alkylation at C-3 of indole, to provide the Diels-Alder precursor (**384**). Thermal induced intramolecular Diels-Alder cycloaddition occurred uneventfully to provide the adduct (**385**). Silyl deprotection led to the functionalized tetracyclic core of welwistatin (**386**) along with a rearranged side product (**387**).

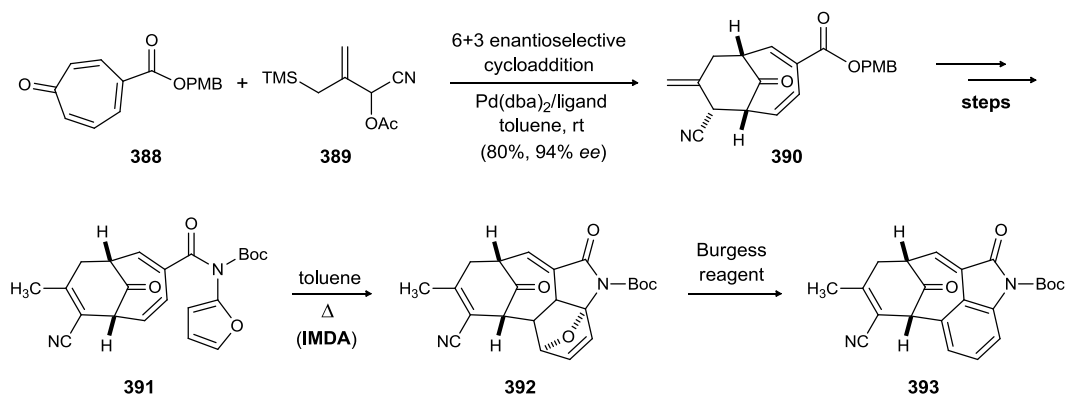
*Scheme 102.* Shea's Diels-Alder Approach towards Welwistatin



Trost and coworkers used two cycloaddition cascade reactions to synthesize the tetracyclic core in a convergent and concise manner.<sup>140c</sup> The key reaction in their synthesis utilizes a palladium catalyzed enantioselective [6+3] trimethylenemethane, derived from the cyano donor (**389**), cycloaddition onto a functionalized tropone **388** to provide bicyclo[4.3.1]decadiene **390** (Scheme 103). Elaboration of the ester side chain provided desired furan-diene **391**, thus setting the stage for the intramolecular Diels-

Alder reaction. The adduct (**392**), isolated as a single diastereomer, was exposed to the Burgess reagent-mediated dehydrative conditions to provide oxindole **393** in 48% yield.

**Scheme 103.** Trost's Diels-Alder Approach towards Welwistatin/Welwitindolinone



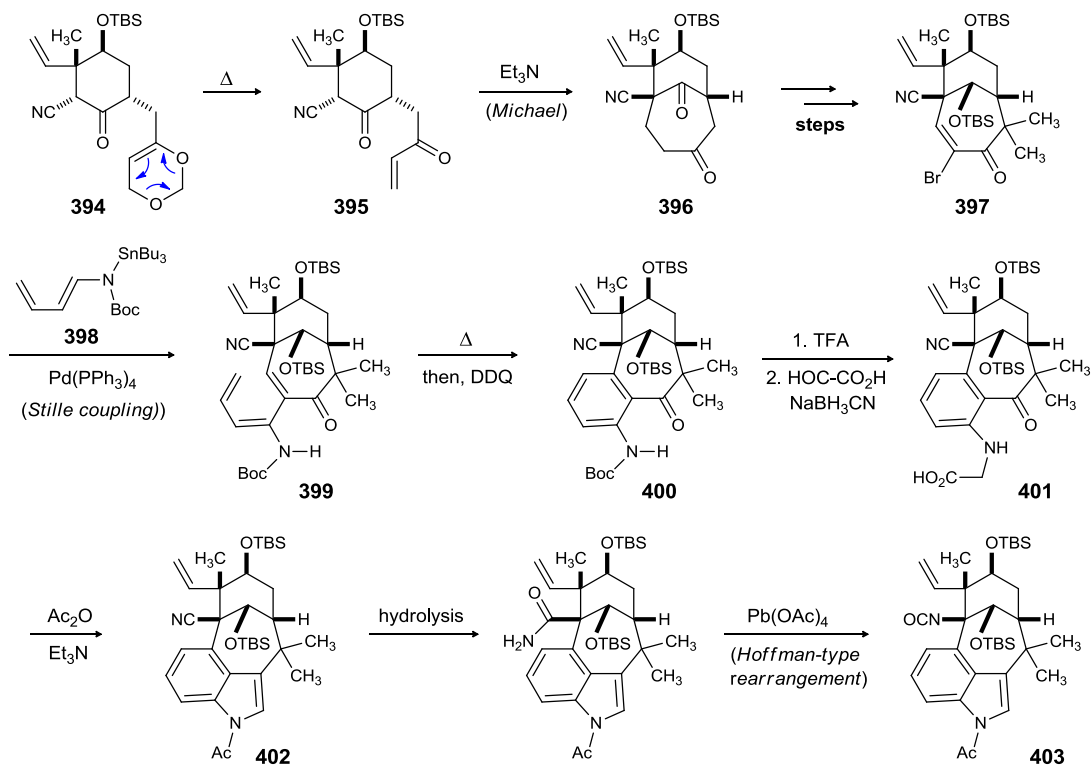
Funk and coworkers have utilized an intramolecular Diels-Alder cycloaddition to synthesize the indole core of welwistatin.<sup>141</sup> The key reaction in this work was the late-stage synthesis of the indole framework, using an in-house developed methodology.<sup>142</sup> The synthesis commences with a thermal degradation of the dioxine ring in **394**, available in few synthetic steps from 3-methylanisole, through a retro Diels-Alder pathway to reveal **395** (Scheme 104). The facile conversion of enone **395** to Michael adduct **396** was carried out under mild basic conditions. With the CD-ring system of welwistatin in place, the attention focused on appending the AB-ring system (indole core). To this end, the Michael adduct (**396**) was elaborated to provide 2-bromoenone **397**. The palladium catalyzed coupling of **397** with a known stannane **398** provided amidotriene **399**, the key precursor for the planned intramolecular Diels-Alder reaction. The electrocyclization reaction occurred uneventfully to provide the intermediate hexadiene which was oxidized *in situ* to provide the aniline derivative **400**. Functional group manipulation led to **401**,

<sup>141</sup> Greshock, T. J.; Funk, R. L. *Org Lett.* **2006**, *8*, 2643.

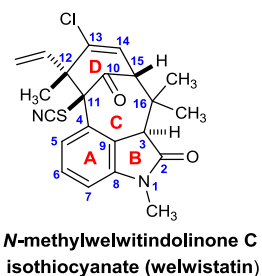
<sup>142</sup> Greshock, T. J.; Funk, R. L. *J. Am. Chem. Soc.* **2006**, *128*, 4946.

which was subsequently converted to indole **402** using the in-house developed annelation sequence. Finally, appending the isocyanate functionality at C-11 using a Hoffman-type rearrangement completed the synthesis of one of the most advanced intermediate (**403**) *en route* to welwistatin.

**Scheme 104.** Funk's Synthetic Approach towards Welwistatin/Welwitindolinone

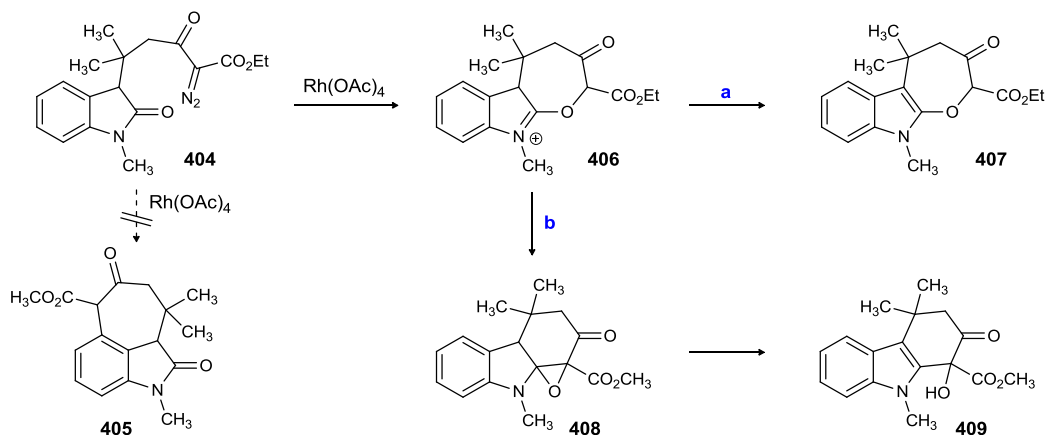


One of the most convergent approach to forge the C-ring of welwistatin is through intramolecular cyclization of 3-substituted indoles onto C-4, and one of the most lucrative ways to construct the C4-C11 bond is by applying a metal-catalyzed C-H insertion reaction. A number of groups have unsuccessfully attempted this transformation. Jung and coworkers attempted the C-H insertion reaction *via* a rhodium carbenoid



intermediate to access the tricyclic intermediate (**405**) (Scheme 105).<sup>143</sup>

**Scheme 105.** Jung's C-H Insertion Approach towards Welwistatin/Welwitindolinone

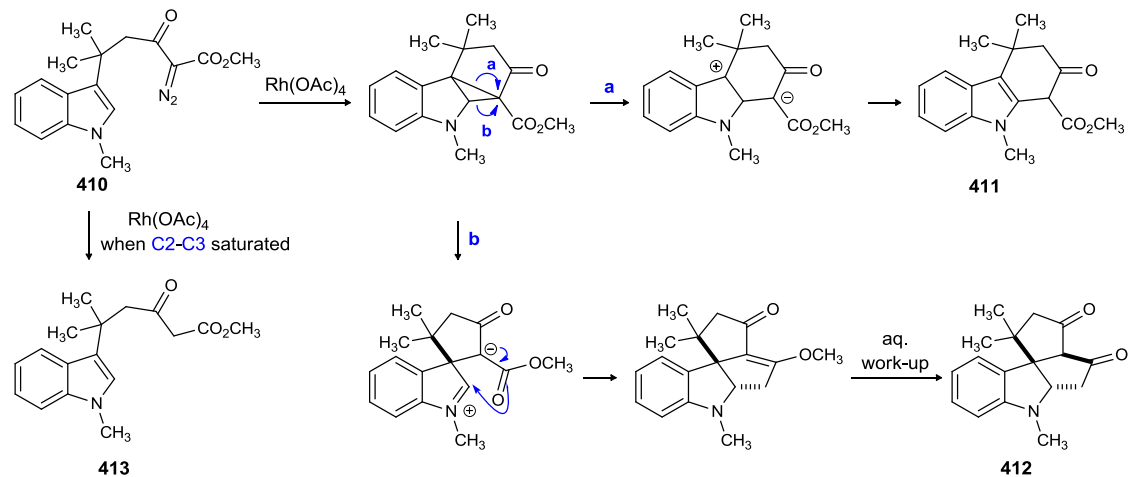


Unfortunately, **404** failed to give the desired C-H insertion to **405**. Instead **406** was formed by the intramolecular  $S_N2$  displacement of nitrogen by oxindole oxygen functionality. The zwitter ion evolved either to (a) the indolooxepine **407** via tautomerisation of iminium **406** or, to (b) epoxide **408** by an intramolecular cyclization process which undergoes rearrangement to provide **409**.

Similarly, the attempted cyclization of rhodium carbenoid **410** onto the indole C-4 position was unsuccessful, and the only observed products were compounds **411** and **412**, resulting from a cyclization/rearrangement cascade after insertion onto the indole C-2 position (Scheme 106). In an attempt to circumvent this undesired C-H insertion, the corresponding indoline was chosen as the ideal substrate. Unfortunately, exposure of indoline to  $Rh_2(OAc)_4$  gave only the intramolecular dismutation derived **413**.

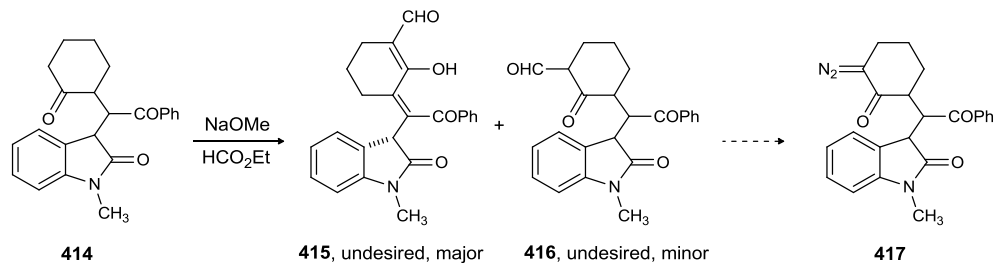
<sup>143</sup> Jung, M. E.; Slowinski, F. *Tetrahedron Lett.* **2001**, 42, 6835.

**Scheme 106.** Jung's C-H Insertion Approach towards Welwistatin/Welwitindolinone



Avendanö *et al.* attempted to forge the C4-C11 bond by a C-H insertion reaction involving the rhodium carbenoid of  $\alpha$ -diazo ketone **417**.<sup>144</sup> However, all efforts to synthesize keto-aldehyde **416**, a precursor of **417**, only resulted in the formation of **415** through the *in situ* oxidation of **414** (Scheme 107).

**Scheme 107.** Avendanö's C-H Insertion Approach

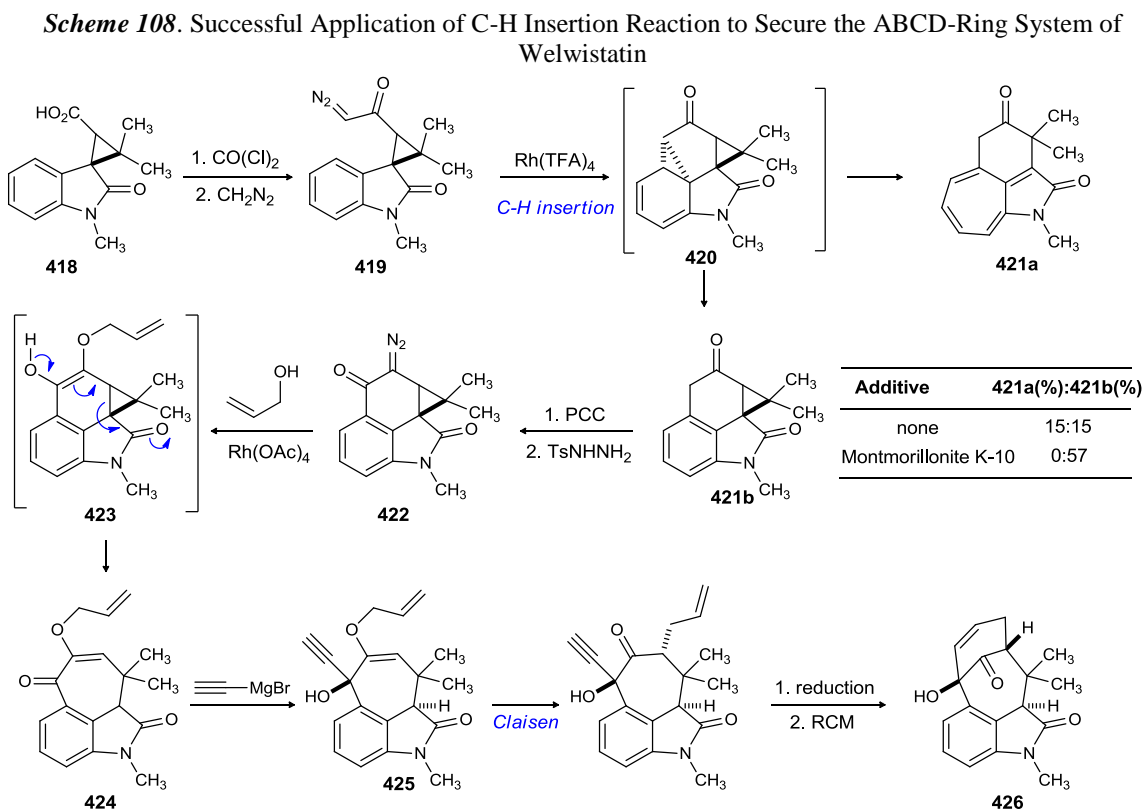


The first successful application of a C-H insertion reaction to form the ABCD ring system of welwistatin was reported by Wood and coworkers in 1999.<sup>145</sup> The troublesome seven-membered ring of the 3,4-bridged oxindole core was synthesized

<sup>144</sup> a) López-Alvarado, P.; García-Granda, S.; Álvarez-Rúa, C.; Avendanö, C. *Eur. J. Org. Chem.* **2002**, 1702. b) Avendanó, C.; Menéndez, J. C. *Curr. Org. Synth.* **2004**, *1*, 65.

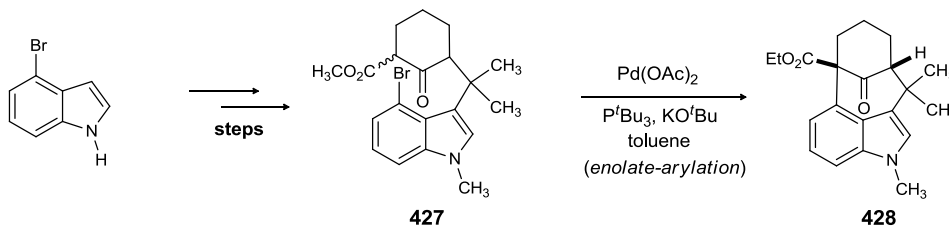
<sup>145</sup> a) Wood, J. L.; Holubec, A. A.; Stoltz, B. M.; Weiss, M. M.; Dixon, J. A.; Doan, B. D.; Shamji, M. F.; Chen, J. M.; Heffron, T. P. *J. Am. Chem. Soc.* **1999**, *121*, 6326. b) Ready, J. M.; Reisman, S. E.; Hirata, M.; Weiss, M. M.; Tamaki, K.; Ovaska, T. V.; Wood, J. L. *Angew. Chem. Int. Ed.* **2004**, *43*, 1270.

through opening of the cyclopropane ring of diazo ketone **422** (Scheme 108). **422** was synthesized from easily accessible **418** using the following synthetic operations (Scheme 108): (i) homologation of **418** to  $\alpha$ -diazo ketone **419** by treatment of the derived acid chloride with diazomethane; (ii) construction of the C-ring by a Buchner reaction (C-H insertion) followed by selective fragmentation of the norcaradiene intermediate (**420**) in the presence of montmorillonite K-10; and (iii) conversion of the resulting tricyclic system (**421b**) to the desired  $\alpha$ -diazo ketone **422** by a well-documented two-step protocol. The rhodium carbenoid, derived from **422**, was treated with allylic alcohol to give an enol intermediate **423** which, after cyclopropane ring-opening, gave the desired ABC-ring system (**424**) of welwistatin. The key reaction for the synthesis of the D-ring was a Claisen rearrangement of enol ether **425**, which resulted in migration of the allyl group to a position which resulted in the creation of ring D in **426** through a metathesis reaction.



Rawal *et al.* used a different approach to construct the C4-C11 bond of welwistatin. The strategy utilized a palladium-catalyzed intramolecular coupling of  $\beta$ -ketoester **427**, available in several steps from commercially available 4-bromo indole, to construct the tricyclic system (**428**) of welwistatin (Scheme 109).<sup>146</sup>

**Scheme 109.** Rawal's Approach to the Synthesis of ABC-Ring system of Welwistatin



In addition to the strategies discussed here, there have been a number of other synthetic reports towards Welwistatin and related welwitindolinone natural products.<sup>147</sup>

### 3.2.3. Synthetic Efforts towards Fischerindoles

The fischerindole family of indole marine alkaloids contains a tetracyclic core structures with varying degrees of complexity. The fischerindole class of marine indole alkaloids has been proposed to biosynthetically derive from tricyclic hapalindoles through the union of the indole C2 with an isopropylidene unit at C15. In the laboratory, this transformation is generally favored over the C4-C16 bond formation, as seen in hapalindole class of alkaloid synthesis. Structures of the members of this family of indole alkaloids are shown in Figure 48. Structures of some other members of this class of

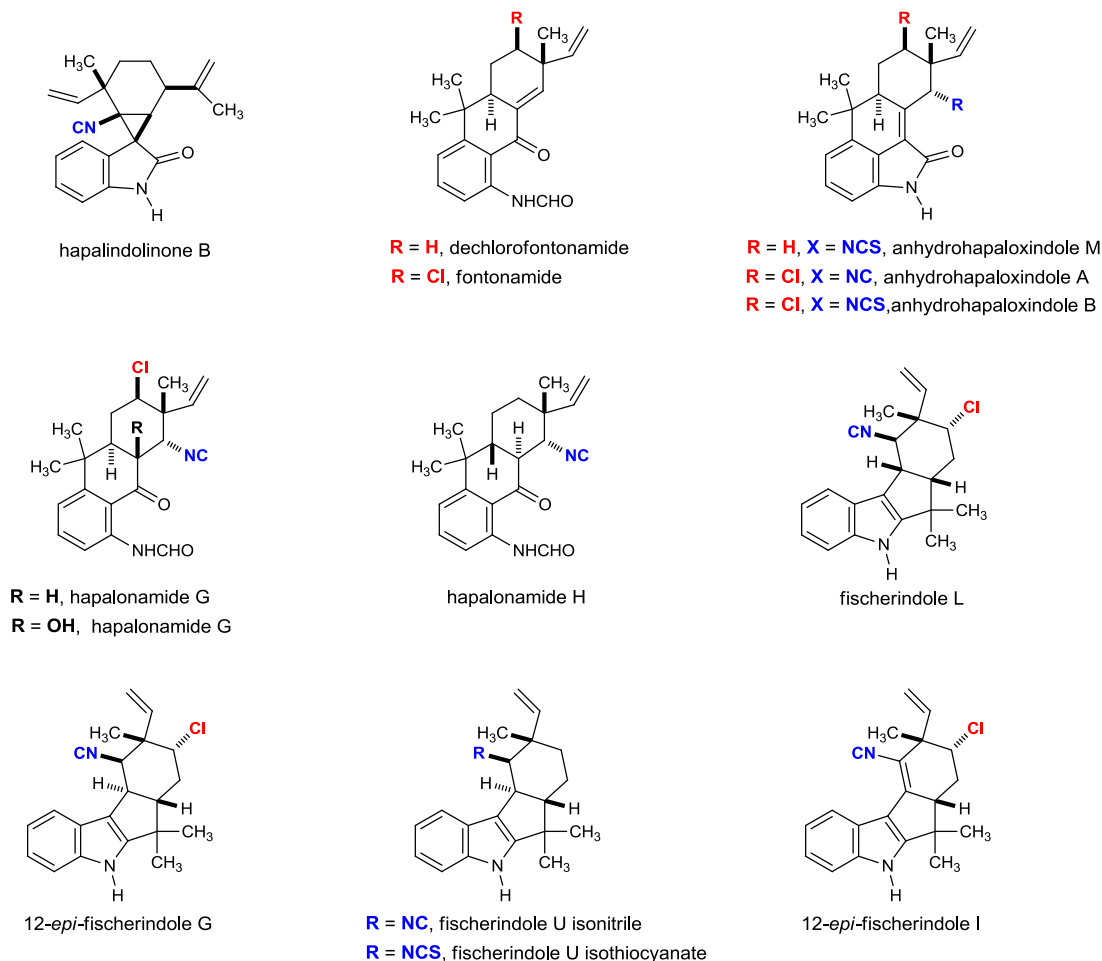
<sup>146</sup> MacKay, J. A.; Bishop, R. L.; Rawal, V. H. *Org. Lett.* **2005**, *7*, 3421.

<sup>147</sup> a) Baudoux, J.; Blake, A. J.; Simpkins, N. S. *Org. Lett.* **2005**, *7*, 4087. b) Deng, H.; Konopelski, J. P. *Org. Lett.* **2001**, *3*, 3001. c) Elliott, G. I.; Konopelski, J. P. *Tetrahedron*. **2001**, *57*, 5683. d) Konopelski, J. P.; Lin, J.; Wenzel, P.Z.; Deng, H.; Elliot, J. I.; Gerstenberger. *Org. Lett.* **2001**, *4*, 4121. e) Elliott, G. I.; Konopelski, J. P.; Olmstead, M. M. *Org. Lett.* **1999**, *1*, 1867. e) Konopelski, J. P.; Deng, H.; Schiemann, K.; Keane, J. M.; Olmstead, M. M. *Synlett*. **1998**, *4*, 1105.



marine alkaloid resulting from the oxidative manipulations of hapalindoles and fischerindoles are also depicted in Figure 49.

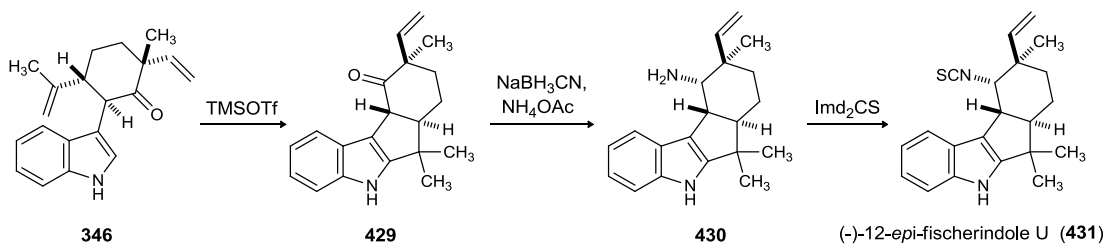
**Figure 49.** Structures of the Members of Fischerindole and Related Class of Indole Alkaloids



The only synthesis of fischerindole alkaloids have been achieved by Baran and coworkers. A highly advanced intermediate in (+)-hapalindole Q synthesis was utilized to achieve the first total synthesis of (-)-12-*epi*-fischerindole isothiocyanate (Scheme 110).<sup>133</sup> Ketone **346** available in 3 steps from naturally occurring (*R*)-carvone was converted to (-)-12-*epi*-fischerindole using the following synthetic operations (Scheme 110): (i) TMSOTf catalyzed ring closure of alkene **346** to afford tetracyclic indole **429**; (ii)  $\alpha$ -face reductive amination to furnish the amine **430** as a 10:1 mixture of

diastereomers; and (iii) conversion to (-)-12-*epi*-fischerindole by isothiocyanate formation. The total synthesis was accomplished in 3 steps from **346**.

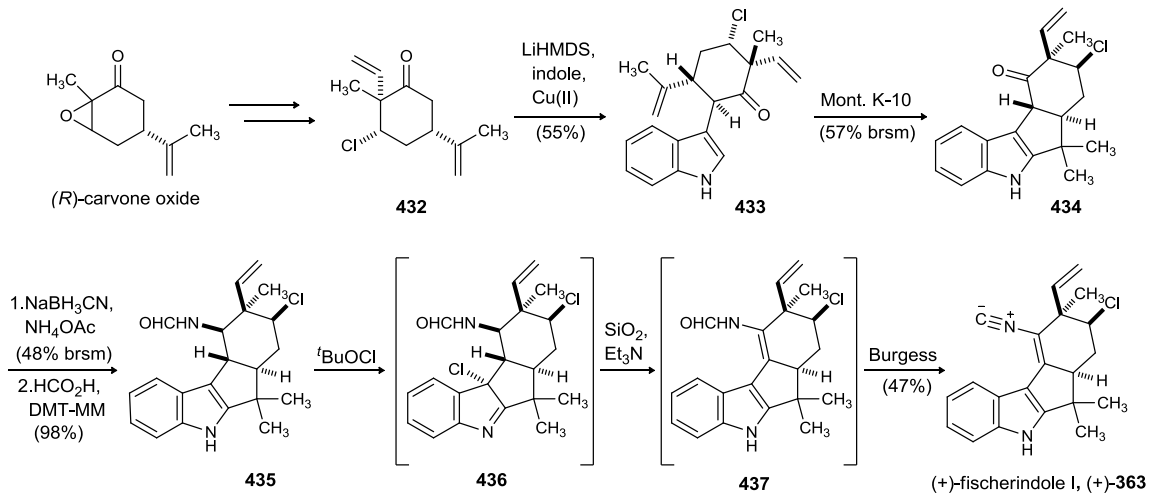
**Scheme 110.** Baran's Enantioselective Synthesis of (-)-12-*epi*-Fischerindole U



Baran and coworkers have also reported the enantioselective, protecting group free syntheses of fischerindoles I and G. The total syntheses of fischerindoles I and G also established the biogenetic relationship between these two alkaloids.<sup>148, 133b</sup> The synthesis commenced with (*R*)-carvone oxide (Scheme 111). Enolization of this compound with LiHMDS, followed by addition of vinylmagnesium bromide and chlorination of the subsequent alcohol provided the chloroketone (**432**). The radical mediated coupling of chloroketone with indole furnished the adduct **433**, as a single diastereomer. The structure of the coupling adduct was confirmed by X-ray crystallographic analysis. The key 5-*exo-trig* cyclization was effected by montmorillonite K-10 to afford the tetracyclic compound (**434**). Reductive amination of the ketone from the  $\alpha$ -face followed by formylation of the resulting amine afforded the formamide (**435**). The key C10-C11 unsaturation was installed by treatment of the formamide (**435**) with <sup>t</sup>BuOCl, followed by exposure of the resulting 3-chloroindolenine **436** to deactivated (Et<sub>3</sub>N) silica gel. Treatment of the resulting conjugated formamide **437** to Burgess reagent afforded (+)-fischerindole I ((+)-**363**).

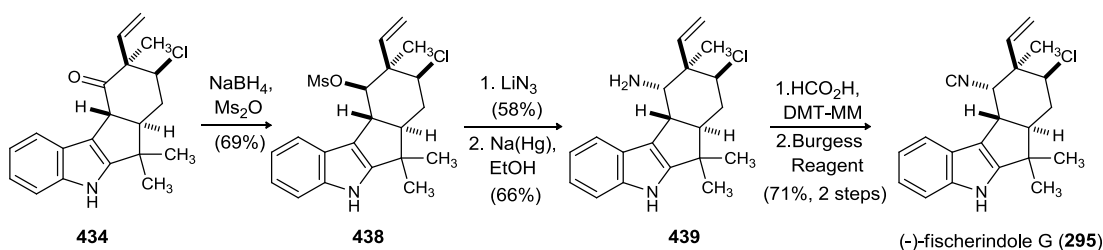
<sup>148</sup> Baran, P. S.; Richter, J. M. *J. Am. Chem. Soc.* **2005**, *127*, 15394.

**Scheme 111.** Baran's Enantioselective Synthesis of (+)-Fischerindole I



The ketone (**434**) was also transformed to (-)-fischerindole G in 5 synthetic steps.<sup>137</sup> Selective reduction of the ketone followed by mesylation of the resulting alcohol afforded mesylate **438**. Displacement of the mesylate with azide and subsequent reduction azide using sodium-mercury amalgam provided amine **439**. The amine was converted to (-)-fischerindole G (**295**) using the standard procedure for isocyanide formation (Scheme 112).

**Scheme 112.** Baran's Enantioselective Synthesis of (-)-Fischerindole G

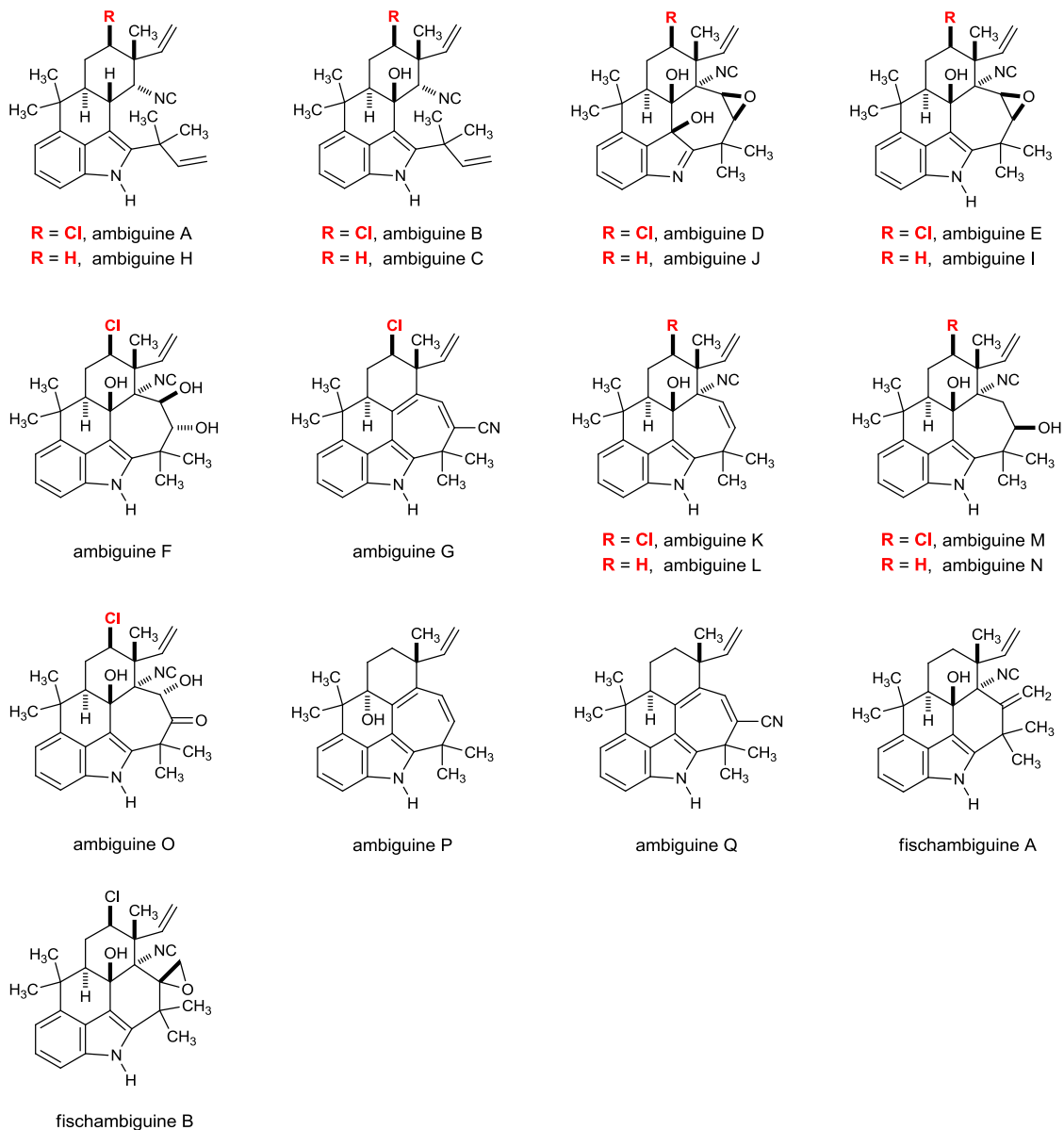


### 3.2.4. Synthetic Efforts towards Ambiguines

Ambiguines are biogenetically derived from hapalindoles, and possesses a *tert*-prenyl functionality at C2 of the indole. In some cases this *tert*-prenyl group is further

cyclized and oxidized to form strained six or seven membered rings. The structures of all the ambiguines isolated so far are depicted in Figure 50.

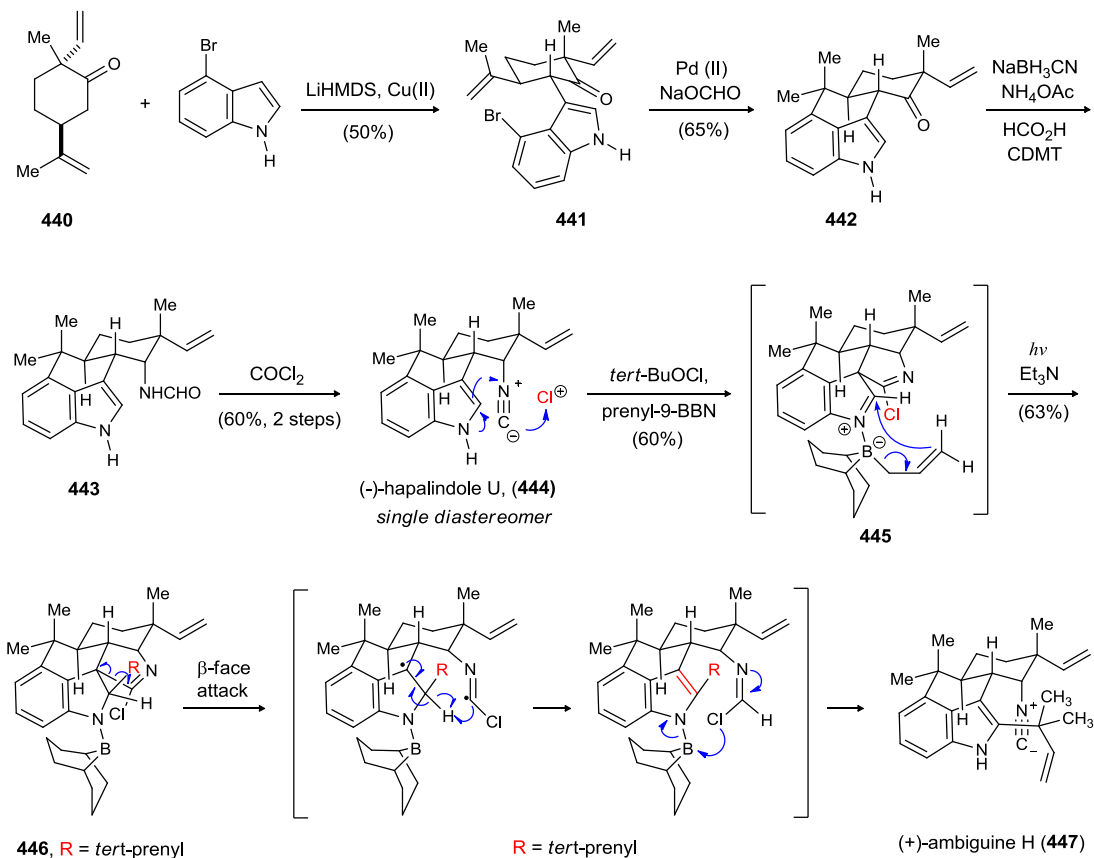
**Figure 50.** Members of the Ambiguine Family



Though a number of syntheses have been reported in this family, there is only one reported synthesis of an ambiguine. Baran's group reported the first enantioselective synthesis of (+)-ambiguine H.<sup>137</sup> The synthesis commenced with readily available terpene

**440**, which is synthesized in four steps from (-)-limonene. Radical initiated coupling of indole with **440**, a methodology developed within the group and applied to the synthesis of halapindole Q,<sup>119</sup> provides the coupling adduct (**441**) as a single diastereomer (Scheme 113).

**Scheme 113.** Baran's Protecting Group Free Synthesis of (+)-Ambiguine H and (-)-Hapalindole U



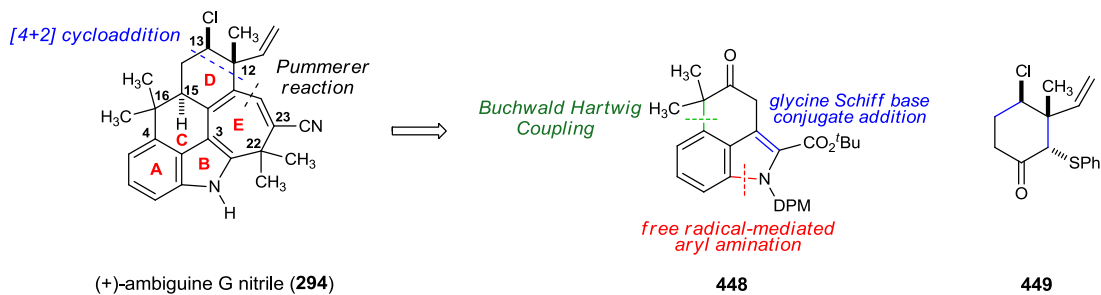
The desired 6-*exo-trig* cyclization of **441** to **442** was effected using Herrmann's catalyst. Microwave-assisted reductive amination of **442**, followed by formylation of the crude amine and dehydration of the resulting formamide provided (-)-hapalindole U in 4 steps from ketone **440**. The exposure of **444** to *t*BuOCl, followed by prenyl-9-BBN produced the pentacyclic chloroimidate (**446**). The observed stereochemistry of the *tert*-

prenyl unit at the C2 stems from its addition to the less-hindered  $\beta$ -face of the folded architecture of the imine (**445**). Irradiation of the chloroimidate (**446**) initiates a fragmentation cascade to liberate the BBN functionality, the extraneous chlorine atom, and an unwanted C–C bond to provide (+)-ambiguine H (**447**) in 10 steps from (-)-limonene without using protecting groups.

### **3.3. Retrosynthetic Analysis of Ambiguine G**

In contrast to members of the first three classes which have been synthesized, the chlorinated tetracyclic and pentacyclic members of ambiguity family have not yet succumbed to synthesis. While planning the synthetic route to Ambiguine G, several challenges were apparent. Introduction of chloride at a sterically crowded neopentyl carbon by nucleophilic substitution strategy would be difficult. Setting the stereochemistry at the C12 quaternary carbon in a predictable fashion was anticipated to be a challenge. The highly conjugated heptacyclic ring would be constructed using the Pummerer reaction. A stereoselective Diels-Alder reaction was envisioned to be the best solution for the construction of the D-ring (**449**). Functional group transformations for the construction of the diene portion would then reveal tricyclic ketone **448** as a viable precursor. The mild and regioselective radical-mediated amination process developed in our group will be employed to introduce the indole ring.<sup>46</sup> This route offers the possibility of a late stage enantioselective variant of the Diels-Alder reaction to accomplish the enantioselective synthesis of ambiguity G.

**Scheme 114.** Retrosynthetic Analysis of (+)-Ambiguine G Nitrile

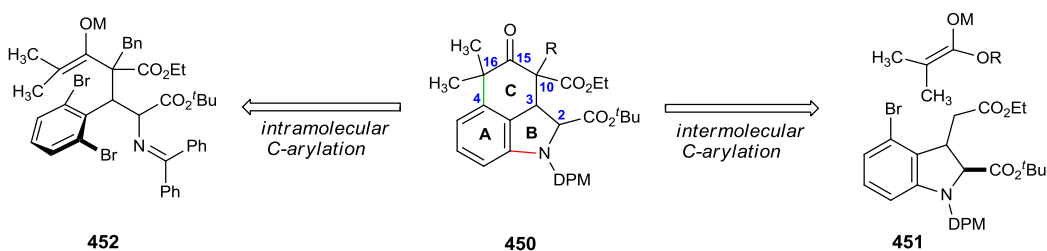


**3.4. Results and Discussion of First/Second Generation Synthetic Endeavours**

**3.4.1. C-Ring Construction through Enolate C-Arylation Attempts**<sup>149</sup>

Tricyclic indoline **450** was envisioned to be built using a transition metal-mediated enolate C-arylation. This approach could in principle be executed in two ways (Scheme 115). The first approach uses substrate **452** for an intramolecular cyclization of the enolate at C16 to C4 of the indoline. Alternatively, an intermolecular enolate arylation using substrate **451** with an appropriate ester enolate would provide the tricyclic core of ambiguity G. The investigation of these approaches towards the core of ambiguity G was performed by Viswanathan *et al.*<sup>150</sup>

**Scheme 115.** Retrosynthetic Disconnections for Tricyclic Ketone 450

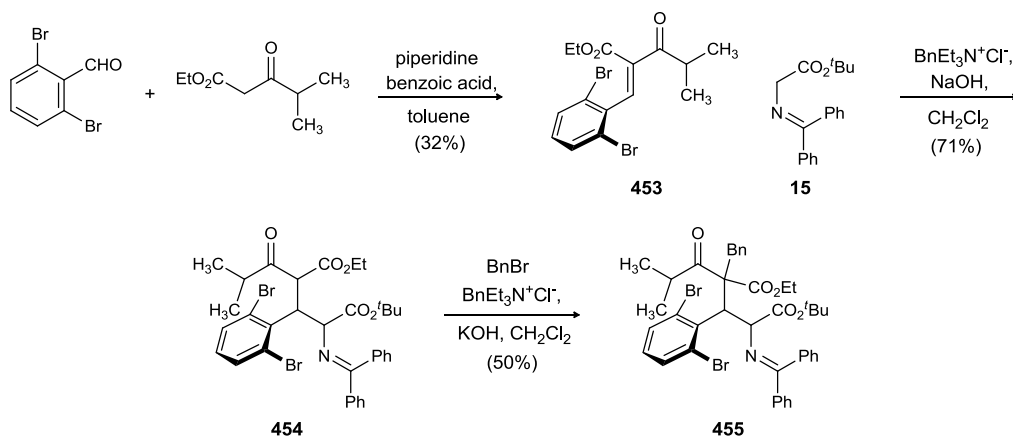


The intramolecular enolate arylation involved isopropyl containing ketone **455** and the use of palladium based catalysts. An aryl amination event would then follow this

<sup>149</sup> Viswanathan, R. Ph. D. Dissertation, Indiana University Bloomington, IN, **2005**.

arylation step, leading to the tricyclic ketone (**450**). Synthesis of **455** was pursued using the previously established protocol of Knoevenagel condensation/Michael addition/alkylation sequence (Scheme 116).<sup>150</sup> Knoevenagel condensation of 2,6-dibromobenzaldehyde with ethylisopropyl acetoacetate afforded **453**. The Michael acceptor (**453**) was subjected to standard phase transfer conditions with Schiff base **15** and the benzylation of the resulting adduct **454** at C-10 furnished the 5:1 diastereomeric mixture of desired isopropyl containing ketone **455**.

*Scheme 116.* Synthesis of Ketone-Imine **455**



Several conditions were applied on the keto-imine (**455**) in order to effect an  $\alpha$ -arylation reaction to provide the desired C-ring.<sup>151</sup> However, none of the reactions proved effective and the unreacted ketone was recovered in all the cases. The unreactivity of the ketone (**455**) could be associated with the sterically hindered aryl bromide. The strain

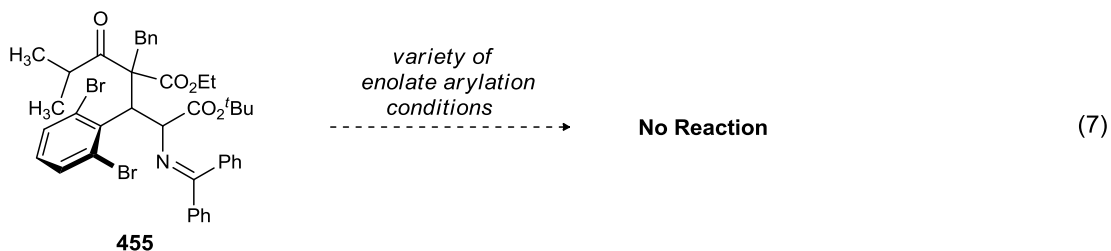
<sup>150</sup> Viswanathan, R.; Smith, C. R.; Prabhakaran, E.N. Johnston, J. N. *J. Org. Chem.* **2008**, *73*, 3040.

<sup>151</sup> Hamann, B. C.; Hartwig, J. F. *J. Am. Chem. Soc.* **1997**, *119*, 12382.; Lee, S.; Beare, N. A.; Hartwig, J. F. *J. Am. Chem. Soc.* **2001**, *123*, 8410. Jorgensen, M.; Lee, S.; Liu, X.; Wolkowski, J. P.; Hartwig, J. F. *J. Am. Chem. Soc.* **2002**, *124*, 12557. Culkin, D. A.; Hartwig, J. F. *Acc. Chem. Res.* **2003**, *36*, 234; Palucki, M.; Buchwald, S. L. *J. Am. Chem. Soc.* **1997**, *119*, 11108. Scolastico, C.; Poli, G. *Chemtracts* **1999**, *12*, 498. Viciu, M. S.; Germaneau, R. F.; Nolan, S. P. *Org. Lett.* **2002**, *4*, 4053. Muratake, H.; Nakai, H. *Tetrahedron Lett.* **1999**, *40*, 2355. Muratake, H.; Natsume, M. *Tetrahedron Lett.* **1997**, *38*, 7581.



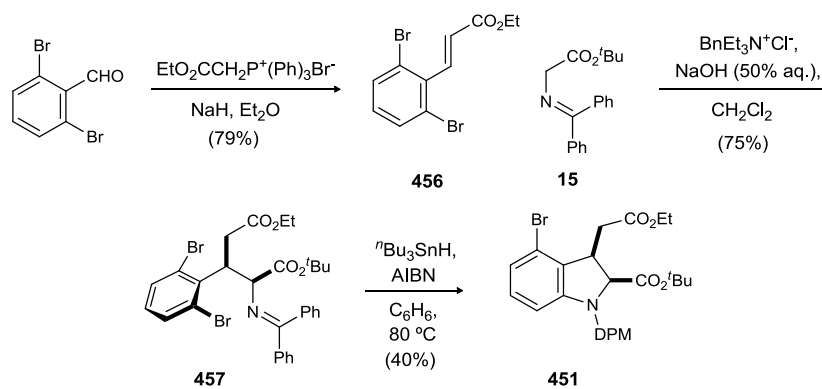
involved if such a palladacycle were to form is further cause for the low reactivity.

Therefore, an intermolecular version of the enolate arylation was attempted instead.



The indoline (**451**) was envisioned as a viable precursor for the execution of an intermolecular enolate arylation. 2,6-Dibromo benzaldehyde was converted to the desired indoline (**451**) using the following synthetic operations (Scheme 117): (i) treatment of 2,6-dibromo benzaldehyde with a stabilized ylide to furnish the *E*-cinnamate derivative (**456**) in 79% yield; (ii) phase transfer catalyzed addition of the imine (**15**) to the Michael acceptor (**456**) to afford the syn-adduct in  $\geq 20:1$  diastereomeric ratio; and (iii) conversion of the resulting Schiff base **457** to the desired indoline **451** using free radical mediated aryl amination, a process well studied in our laboratories. A single diastereomer (*cis*) was obtained from this cyclization reaction.

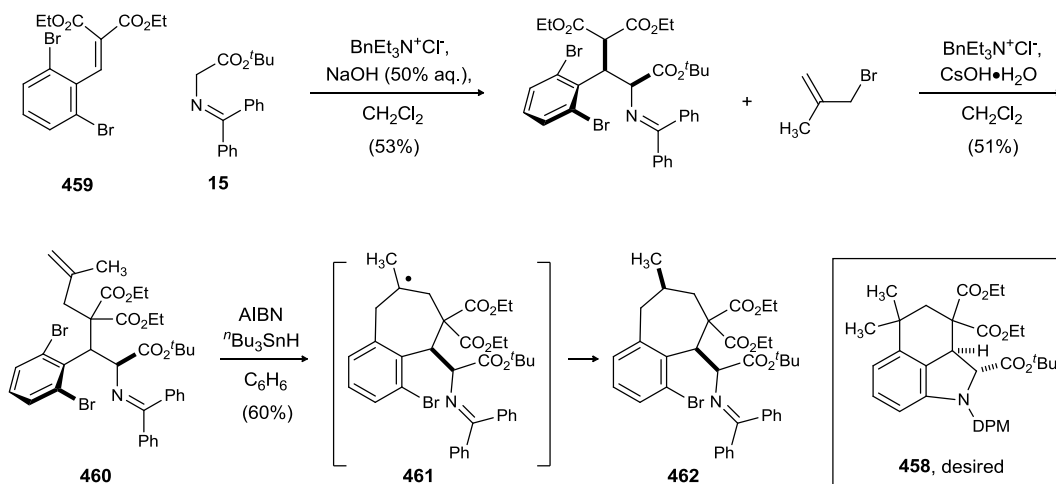
**Scheme 117.** Synthesis of the Indoline (**451**)



The indoline (**451**) was subjected to the various intermolecular Pd(0) and Ni(0)<sup>152</sup> catalyzed arylation methods. However, the only evidence of reaction was the addition of *in situ* generated nucleophiles to the highly reactive ethyl ester functionality leading to several by-products. The bromide remained intact in all of these reaction conditions.

One of the alternate strategies utilized a bis-radical cyclization reaction to form the ABC rings of ambiguine G. This key step was expected to be possible based on the prior experience with the aryl amination protocol.<sup>153</sup> A simultaneous 6-*exo-trig* cyclization was envisioned to provide the 6-membered ring (**458**). With this plan, the synthesis of an appropriate cyclization precursor was pursued (Scheme 118). To this end, Schiff base **460** was synthesized from **459** through a tandem phase transfer catalyzed alkylation/Michael reaction sequence. Unfortunately, treatment of **460** with AIBN and tributyl tinhydride under standard conditions, led only to a 7-*endo* cyclization product **462**.

**Scheme 118.** Attempted bis-Radical Cyclization



<sup>152</sup> Millard, A. A.; Rathke, M. W. *J. Am. Chem. Soc.* **1977**, *99*, 4833. Wender, P. A. Wolanin, D. J. *J. Org. Chem.* **1985**, *50*, 4418.

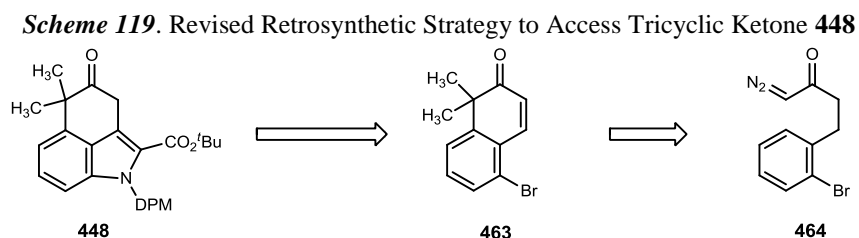
<sup>153</sup> This protocol is discussed in Chapter 1 for the synthesis of unnatural proline analog.

This result suggested that the intermediate aryl radical cyclized onto the terminal alkene generating a more stable tertiary radical (**461**), and that the *7-endo-trig* cyclization was occurring predominantly over a *5-exo-trig* cyclization onto the azomethine nitrogen.

Unable to advance indoline **451** or the Schiff base (**455** and **460**) to the tricyclic ketone (**458**) via bis-radical cyclization or intermolecular/intramolecular enolate arylation methods, we began to consider other strategies for effecting the C-ring construction.

### 3.4.2. C-Ring Construction through Rh(II) Catalyzed Intramolecular C-H Insertion Reaction

Our revised retrosynthetic strategy now called for the construction of tricyclic ketone **448** via the intermediacy of  $\beta$ -tetralone **463**. The  $\beta$ -tetralone would be accessible from an intramolecular Buchner addition of a diazoketones to an aryl ring (Scheme **119**).<sup>154</sup>

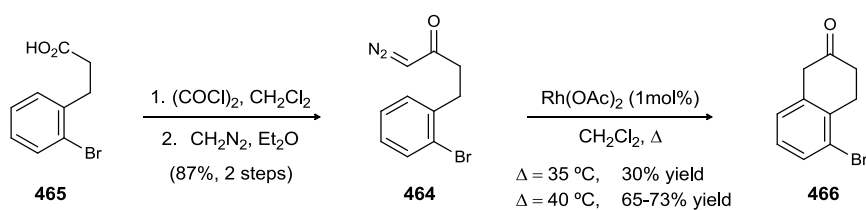


The synthesis commenced with commercially available carboxylic acid **465**. Treatment of the acid with oxalyl chloride led to the formation of acyl chloride in quantitative yield. Exposure of acyl chloride to excess diazomethane led to the formation

<sup>154</sup> Cordi, A. A. *J. Chem. Soc., Perkin Trans.* **1993**, *1*, 3. Dias, H. V. R.; Browning, R. G.; Richey, S. A.; Lovely, C. J. *Organometallics*. **2005**, *24*, 5784. Lovely, C. J.; Browning, R. G.; Badarinarayana, V.; Dias, H. V. R. *Tetrahedron Lett.* **2005**, *46*, 2453. Kennedy, M.; Mckerverve, M. A.; Maguire, A. R.; Tuladhar, S. M.; Twohig, M. F. *J. Chem. Soc., Perkin Trans I.* **1990**, 1047.

of diazoketone **464** in 87% yield (Scheme 120). The diazoketone was unstable, and was found to decompose when stored for an extended period of time. With diazoketone **464** in hand, the key C-ring formation by  $\text{Rh}_2(\text{OAc})_4$  catalyzed intramolecular Buchner reaction was attempted. Treatment of **464** with 1 mol%  $\text{Rh}_2(\text{OAc})_4$  in  $\text{CH}_2\text{Cl}_2$  at 35 °C for an hour, followed by addition of catalytic amount of trifluoroacetic acid, furnished  $\beta$ -tetralone **466**. The yield for this cyclization step was low at 30-35% even when the reaction was complete by TLC analysis. Elevating the reaction temperature to 40 °C led to better yields (65-73%) for this C-H insertion reaction.

**Scheme 120.** AC-Ring Construction Utilizing C-H Insertion Method



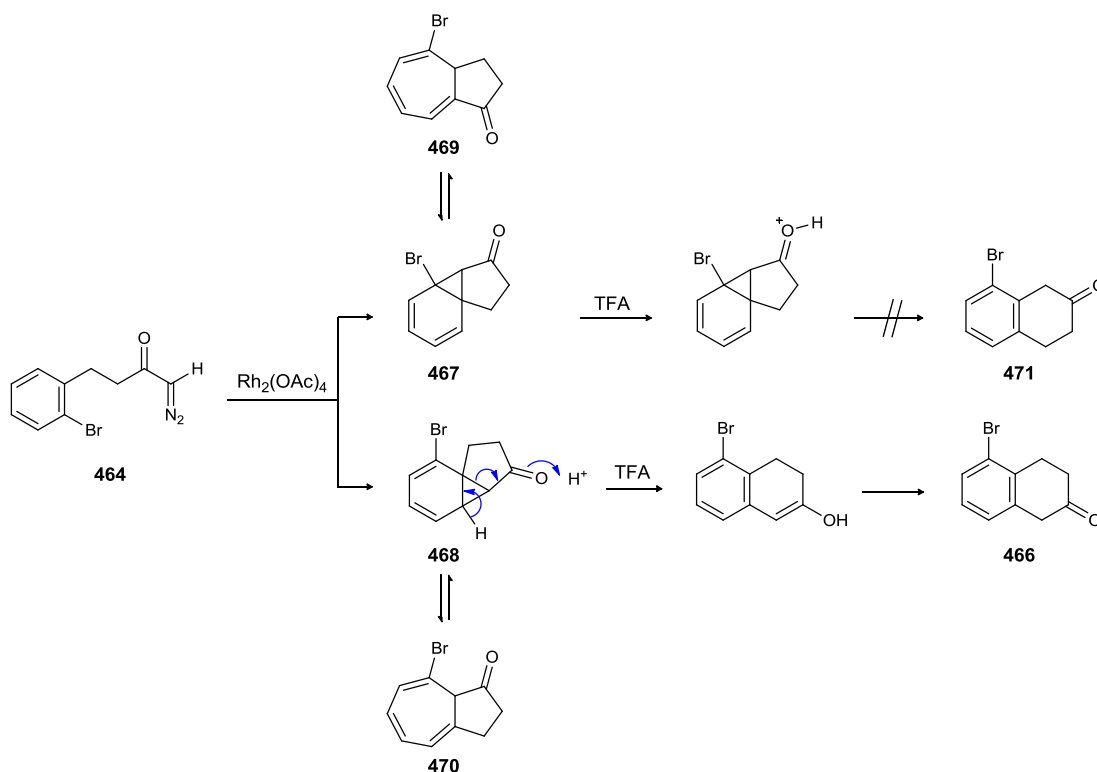
One possible reason for the low yields could be the undesired formation of the intermediates norcaradiene **467** or **468** (Scheme 121) and indeed two new spots were observed by TLC when the Buchner reaction was left standing for 4 days before TFA work up.<sup>155</sup> The mechanism of the intramolecular Buchner reaction has been reported by Cordi *et al.*<sup>155</sup> and later confirmed by Blake *et al.*<sup>156</sup> for the aryl diazoketone bearing methoxy substituents. Based on these studies, a mechanism for Rh(II) catalyzed C-H insertion reaction leading to C-ring was proposed (Scheme 121). The carbenoid resulting from addition of  $\text{Rh}_2(\text{OAc})_4$  to the diazoketone (**464**) adds to the aromatic ring to form a tricyclic norcaradienone intermediate (**467** and **468**) which, by electrocyclic ring opening

<sup>155</sup> This compound was not isolated.

<sup>156</sup> Maguire, A. J.; Blake, J. K. *J. Org. Chem.* **2001**, *66*, 7166.

and closure, is in rapid equilibrium with a bicyclic trienone (azulenones **469** and **470**). Treatment of the mixture of norcaradienes (**467** and **468**) with trifluoroacetic acid leads to the desired  $\beta$ -tetralone (**466**), derived from the kinetic product of cyclization of **464**. Mechanistically, the norcaradiene tautomer of **467** is not readily rearomatized to form the regioisomeric  $\beta$ -tetralone (**471**), as it lacks a proton on the carbon bearing the bromide. Furthermore, the desired HMBC correlation was observed between the benzylic methylene proton (H1) and aromatic methine carbon (C8) in **466**, confirming the regioselectivity of intramolecular Buchner reaction.

*Scheme 121.* Intramolecular Buchner Reaction

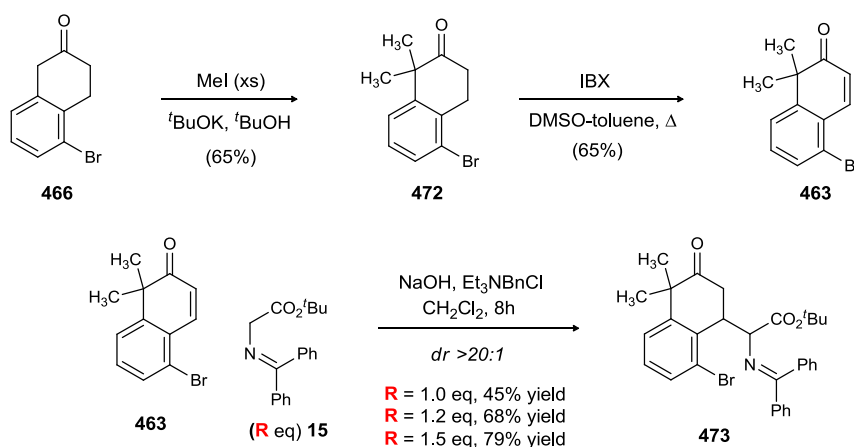


### 3.4.3. Advancement of the $\beta$ -Tetralone to Tricyclic Core of Ambiguine G

The  $\beta$ -tetralone (**466**), unstable when stored for long duration of time, was immediately subjected to the one-pot dimethylation reaction condition. The regioselective

dimethylation at the more acidic benzylic methylene was effected in 71% yield using potassium *tert*-butoxide in *tert*-butanol and methyl iodide in slight excess (Scheme 122).<sup>157</sup> Treatment of the resulting  $\beta$ -tetralone (**472**) with IBX<sup>158</sup> in a DMSO-toluene binary solvent mixture at elevated temperature led to the formation of enone **463** in 65% yield after column chromatography.

**Scheme 122.** PTC Catalyzed Alkylation



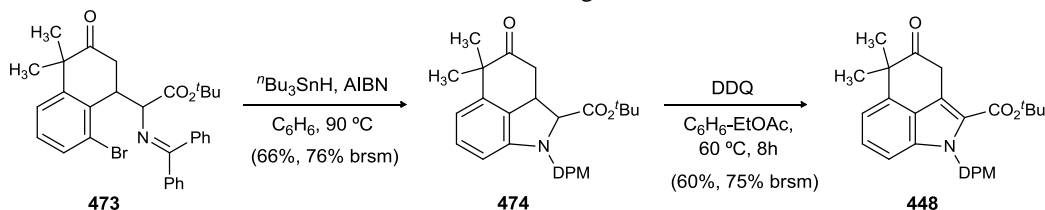
The next step was a Michael addition of the enone (**463**) with Schiff base **15** under phase transfer catalyzed conditions. Thus, treatment of 1 equivalent of the enone and the Schiff base with 20 equivalents of 50% potassium hydroxide and 20 mol% of benzyl triethylammonium chloride in methylene chloride gave the Michael adduct (**473**) in 45% yield as a single diastereomer observed by <sup>1</sup>H NMR of the crude reaction mixture (Scheme 122). The relative stereochemistry was not determined since the two chiral centers would not be preserved in the targeted intermediate. Increasing the equivalence of Schiff base in the same reaction condition led to improved yields of **473**.

<sup>157</sup> Gorka, A.; Hazai, L.; Szantay, C.; Hada, V.; Szabo, L.; Szantay, C. *Heterocycles* **2005**, *65*, 1359.

<sup>158</sup> Nicolaou, K. C.; Gray, D. L. F.; Montagnon, T.; Harrison, S. T. *Angew. Chem. Int. Ed.* **2002**, *41*, 996.

The stage was now set to examine the radical mediated aryl amination reaction to form the ABC rings of Ambiguine G. Treatment of the aryl bromide (**473**) with  $n\text{Bu}_3\text{SnH}$  and AIBN in benzene at  $90\text{ }^\circ\text{C}$  provided a 1:1 diastereomeric mixture of desired indoline **474** in 66% yield, with 13% recovery of aryl bromide **473**. Exposure of the indoline (**474**) to DDQ in EtOAc-benzene binary solvent mixture at  $60\text{ }^\circ\text{C}$  for 8 h furnished the desired indole (**448**) in 60% yield, in addition to 20% recovery of the indole (**474**).<sup>159</sup> Increasing the reaction temperature and duration had a detrimental effect on the reaction yield.

**Scheme 123.** ABC-Ring Construction



Our initial solution to the stereocontrolled construction of this D-ring utilized a Diels-Alder cycloaddition process. This initial studies in this direction was performed by Viswanathan *et al.*<sup>150</sup> To establish the feasibility of Diels-Alder approach, Cohen's diene<sup>160</sup> (**476**) emerged as an ideal substrate. Cohen *et al.* has earlier demonstrated that a sulfur substituent can direct regioselectivity in the cycloaddition process, and we hoped that this would facilitate the rather demanding cycloaddition.<sup>161</sup> As expected, the Diels-Alder cycloaddition of Cohen's diene to  $\beta$ -chloro methacrolein proceeds thermally, delivering a 44% isolated yield of the desired secondary chloride **477** after 40 hours at  $140\text{ }^\circ\text{C}$  (Scheme 124). The *cis* relationship (*endo*) was determined by NOE

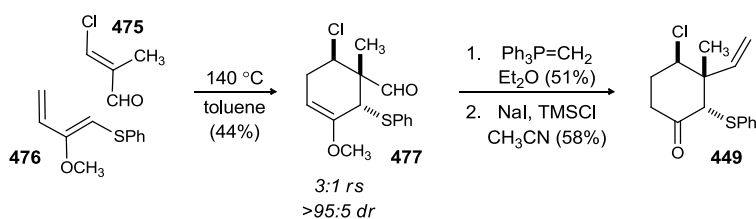
<sup>159</sup> Chandra, A.; Viswanathan, R.; Johnston, J.N. *Org. Lett.* **2007**, *9*, 5027.

<sup>160</sup> Cohen, T.; Ruffner, R. J.; Shull, D. W.; Fogel, E. R.; Falck, J. R. *Org Synth* **1988**, *50-9*, 737. Cohen, T.; Mura, A. J.; Shull, D. W.; Fogel, E. R.; Ruffner, R. J.; Falck, J. R. *J. Org. Chem.* **1976**, *41*, 3218.

<sup>161</sup> Cohen, T.; Ruffner, R. J.; Shull, D. W.; Daniewski, W. M.; Ottenbrite, R. M.; Alston, P. V. *J. Org. Chem.* **1978**, *43*, 4052.

measurements, with the methyl and allylic methine exhibiting 5% enhancement, and the aldehyde and chloromethine exhibiting a nearly 10% enhancement. The aldehyde functionality in **477** was subsequently converted to its corresponding terminal olefin by treatment with methyl phosphonium ylide and finally, cleavage of the methyl enol ether using sodium iodide/trimethyl silyl chloride<sup>162</sup> furnished the  $\alpha$ -phenylthio cyclohexanone **449** in 58% yield.

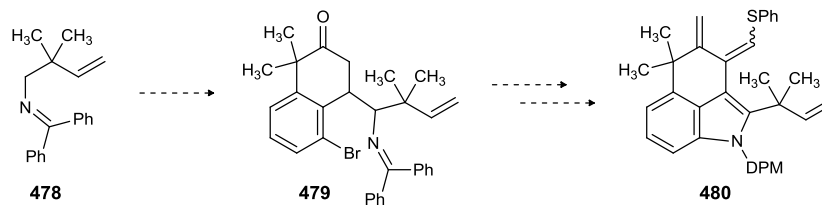
**Scheme 124.** Stereocontrolled [4+2] Cycloaddition



#### 3.4.4. Synthetic Strategy towards Prenylated Tricyclic Diene

Having established the free radical mediated aryl amination as a suitable strategy for constructing the tricyclic ketone (**448**), we began to focus our attention on the preparation of prenylated Schiff base (**478**) for advancement to diene **480** (Scheme 125).

**Scheme 125.** Outline of the Synthetic Plan towards C2 *tert*-Prenyl Tricyclic Diene **480**



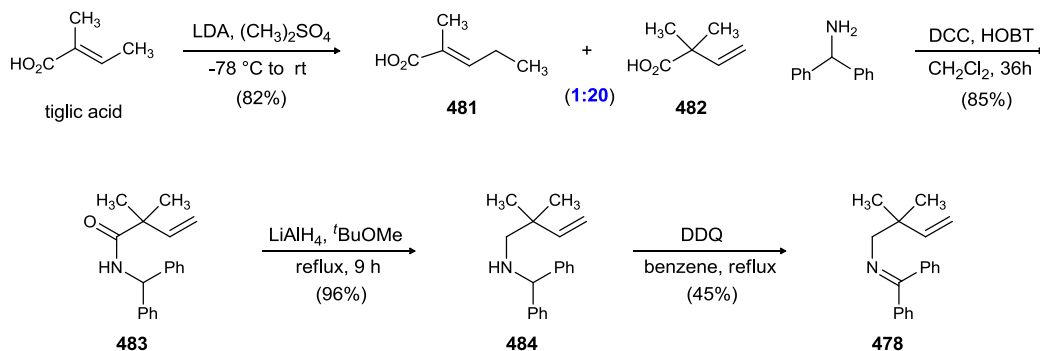
Synthesis commenced with the commercially available tiglic acid. On treatment of tiglic acid with 2.2 equivalents of LDA and subsequent quenching of the resulting  $\pi$ -

<sup>162</sup> Kosarych, Z.; Cohen, T. *Tetrahedron Lett.* **1980**, *21*, 3959. Jung, M. E.; Lyster, M. A. *J. Org. Chem.* **1977**, *42*, 3761.



conjugated enolate with dimethyl sulfate furnished the carboxylic acid **482** in 82% yield.<sup>163</sup> The carboxylic acid was characterized as an inseparable 20:1 mixture of products arising from respective  $\alpha$ - and  $\gamma$ - alkylation of the  $\pi$ -conjugated enolate (Scheme 126).

**Scheme 126.** Synthesis of *tert*-Prenylated Schiff Base **478**



The acid (**482**) was coupled with commercially available benzhydrylamine using DCC and HOBT to furnish the amide (**483**) in 85% yield. A quantitative yield of amide **483** was also achieved by using PyBrOP as a coupling reagent. Treatment of the amide (**483**) with lithium aluminum hydride in refluxing *tert*-butyl dimethylether furnished amine **484** in quantitative yield.<sup>164</sup> Using Red-Al as reducing agent led to lower yields (20-31%) of the reduction product. Use of the Honek protocol for DDQ oxidation of amine **484** to the corresponding imine provided prenylated Schiff base **478** in 45% yield.<sup>165</sup> Several attempts at increasing the yield were unsuccessful due to the hydrolysis of **478** to the corresponding amine (bp 88 °C/760 torr).

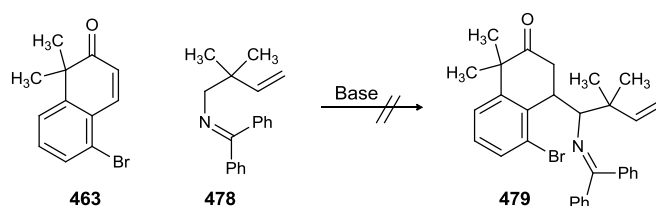
<sup>163</sup> Aurell, M. J.; Gil, S.; Mestres, R.; Parra, M.; Parra, L. *Tetrahedron*. **1998**, *54*, 4357.

<sup>164</sup> Ooi, T.; Takeuchi, M.; Kato, D.; Uematsu, Y.; Tayama, E.; Sakai, D.; Maruoka, K. *J. Am. Chem. Soc.* **1998**, *127*, 5073.

<sup>165</sup> Sampson, P. B.; Honek, J. F. *Org. Lett.* **1999**, *1*, 1395.

With prenylated Schiff base in hand, it was next desired to attempt the Michael reaction with the enone (**463**). This did not prove to be successful with a variety of bases (Scheme 127).

**Scheme 127.** Michael Addition of Enone **463** with Schiff Base **478**



entry <sup>a</sup>	Base	solvent	NMR analysis <sup>b</sup>
1 <sup>c</sup>	LDA	THF, TMEDA	No reaction
2 <sup>d</sup>	LDA	THF, HMPA	No reaction
3 <sup>e</sup>	LDA	THF, HMPA	No reaction
4 <sup>d</sup>	Lithium dimethyl amide	THF, TMEDA	No reaction
5 <sup>e</sup>	LiHMDS	THF, TMEDA	No reaction
6 <sup>c</sup>	<sup>n</sup> BuLi	THF	No reaction
7 <sup>e</sup>	<sup>n</sup> BuLi	Benzene, HMPA	side reaction <sup>f</sup>

<sup>a</sup> All reaction employed 1.5 equiv. of Schiff base, 1.1 equiv. of base, at 0.2 M in enone.

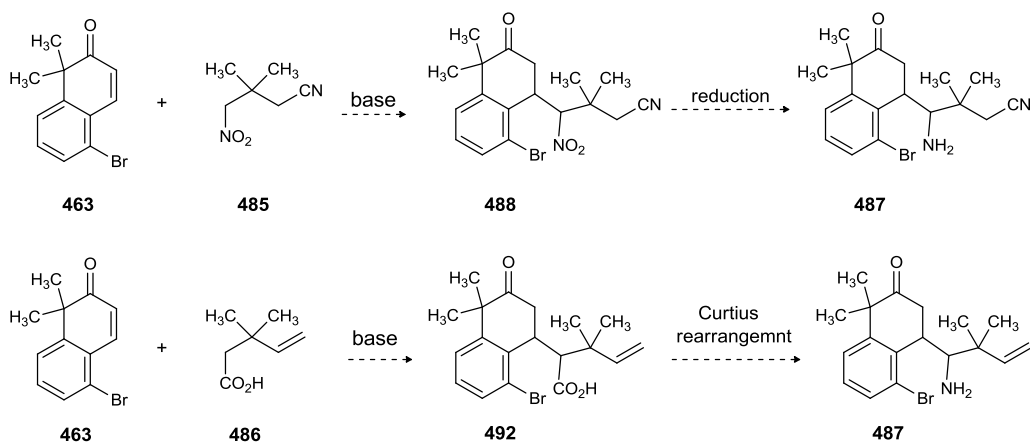
<sup>b</sup> The crude reaction mixture was analyzed by <sup>1</sup>H NMR. <sup>c</sup> The reaction was performed at -78 °C. <sup>d</sup> The reaction was performed at 0 °C. <sup>e</sup> The reaction was performed at rt. <sup>f</sup> The undesired product was not characterized.

In all cases, starting material was recovered. There could be following two reasons for it: (i) the aza-allyl anion, resulting from the treatment of prenylated Schiff base with base, is sterically hindered, or (2) the Schiff base doesnot undergo deprotonation. To test this hypothesis, Schiff base (**478**) was treated with <sup>n</sup>BuLi and subsequently quenched with D<sub>2</sub>O at 0°C. However, <sup>1</sup>H NMR analysis of the crude reaction mixture only showed the unreacted starting material. Even performing the reaction at room temperature didn't elicit the desired transformation, and the Schiff base (**478**) was recovered in all these cases. We had earlier reasoned that the formation of the 2-azaallyl anion, derived from exposure of **478** to strong bases, would be straightforward.

However, it was now clear to us that other substrates, which could be easily deprotonated, must be investigated to elicit the desired transformation.

The nitroalkane **485** and acid **486** were chosen as the model substrate to investigate this strategy. It was reasoned that the desired amine could be accessed in a few straightforward synthetic formations from the resulting adduct (Scheme 128).

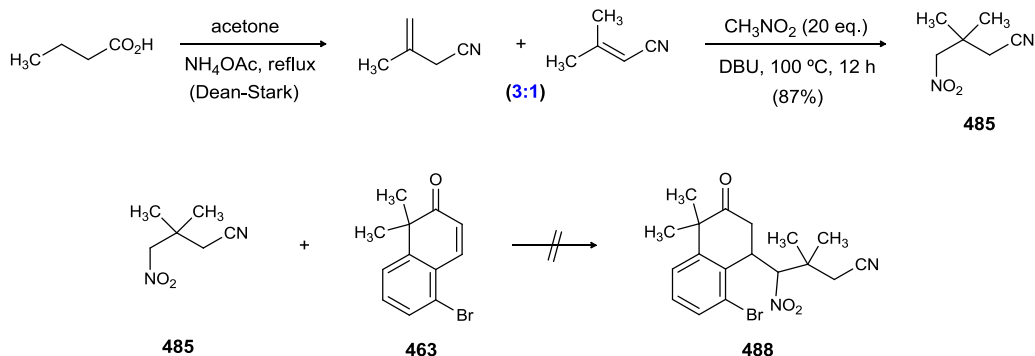
**Scheme 128.** Model Substrate to Install the C2 *tert*-Prenyl Functionality



The synthesis of nitroalkane **485** was undertaken first.<sup>166</sup> Treatment of commercially available cyanoethanoic acid and acetone with ammonium acetate provided 3,3-dimethyl acrylonitrile and its regioisomer in 54% yield (Scheme 129). Michael addition of nitromethane to the mixture of regioisomeric nitriles provided the desired nitroalkane **485**. The stage was then set for the coupling of enone **463** and nitroalkane **485**. However, exposure of this compound to a variety of bases and under different temperatures, did not provide the desired adduct, as the starting material was recovered in all these cases.

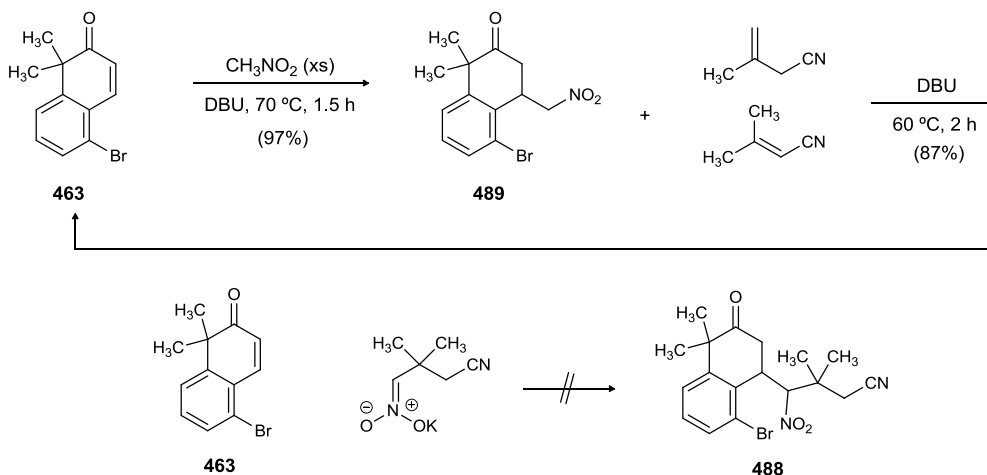
<sup>166</sup> Misuhiro, M.; Kunihiro, F. U.S. Patent 5498725, **1996**.

**Scheme 129.** Attempted Michael Addition with Nitroalkane



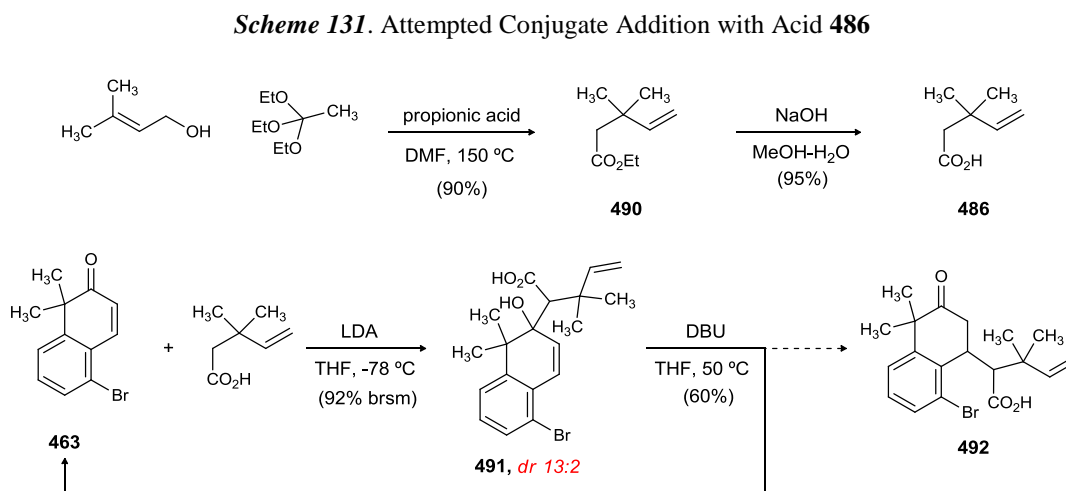
In the event, we were pleased to observe that treatment of nitromethane with enone **463** provided the adduct (**489**) (Scheme 130). With **489** in hand, Michael addition to the mixture of regioisomeric nitriles was investigated. Surprisingly, enone **463** was isolated as the sole product from this reaction. This result indicated that the Michael addition of nitroalkane to enone **463** (Scheme 129) was indeed taking place; however, presence of base in the reaction initiates a retro-Michael process leading to the sterically less congested enone **463**.

**Scheme 130.** Attempted Double Conjugate Addition Approach to Access **488**



To circumvent this problem, conjugate addition of potassium nitronate to **463** was attempted (Scheme 130). Unfortunately, the enone was unreactive under all reaction conditions investigated.

At this stage, we were hopeful that this retro-Michael process could be suppressed by using *tert*-prenylated acid **486**. Due to the higher pKa of the  $\alpha$ - carbon of this acid, the adduct (**492**) once formed, should not revert back to the starting enone. To test this hypothesis, acid **486**, prepared in two steps from 3,3-dimethyl allyl alcohol, was reacted with enone under basic conditions. However, the adduct **491** resulting from 1,2-addition to the enone was isolated as a mixture of diastomers. We believed that subjecting **491** to basic conditions for an extended period of time would lead to the thermodynamically favored 1,4 product **492**. To our disappointment, the reaction again led the starting enone (Scheme 131).

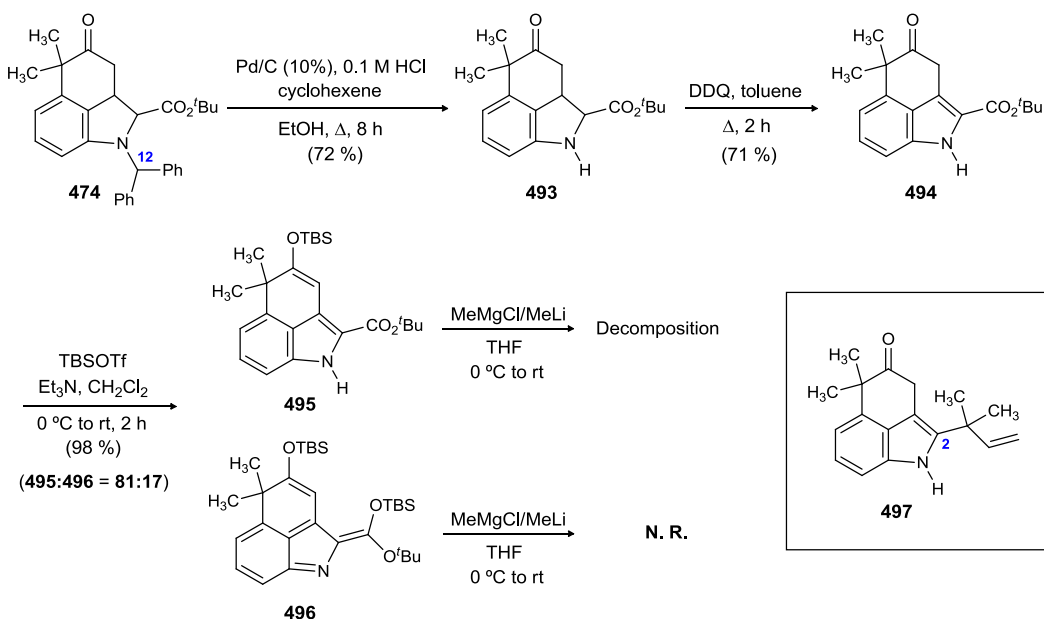


Unable to elicit the desired Michael addition between enone (**463**) with different nucleophiles (**478**, **485** and, **486**), we began to consider other strategies for installing the desired C2 *tert*-prenyl functionality.

### 3.4.5. Elaboration of the Aryl Amination Product (474)

In this new strategy, our attention focussed on using aryl amination product **474** as starting material for the production of C2 *tert*-prenylated indole **497**. With the tricyclic system in place, we anticipated that that the elaboration of the ester functionality in **474** to the *tert*-prenyl group in **497** would be straightforward. To this end, the diphenylmethyl group was removed under reductive conditions to provide **493** (Scheme 132). Treatment of indoline **493** with DDQ led to the indole (**494**). At this stage, we also attempted to directly convert the protected indoline (**474**) to indole **494** by treatment with 2.5 equiv. of DDQ. In this procedure, developed by Honek *et al.*, the oxidation of indoline to indole **448** would be followed by the formation of its corresponding iminium (N-C12) which upon hydrolysis would lead to indole **494**.<sup>165</sup> However, the one step protocol was marred by low yields.

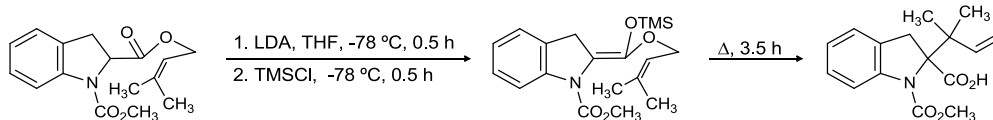
**Scheme 132.** Elaboration of the Ester Side Chain of **474**



The ketone was masked as silyl enol ether **495** upon treatment with TBSOTf. Surprisingly, low yields of a highly conjugated side product **496**, resulting from the concomitant protection of the ketone and ester functionalities, were also isolated from the reaction. **495** was then exposed to methyl magnesium halide or methyl lithium under a variety of reaction conditions and temperatures. Disappointingly, decomposition of the starting material was observed under all reaction conditions.

Failure to convert indoline **474** to indole **497** necessitated yet another synthetic evaluation. Therefore, C2 *tert*-prenylation via a Claisen-Ireland rearrangement protocol was investigated. Dunkerton *et al.* has earlier reported the application of this approach to install the *tert*-prenyl group (Scheme 133).<sup>167</sup>

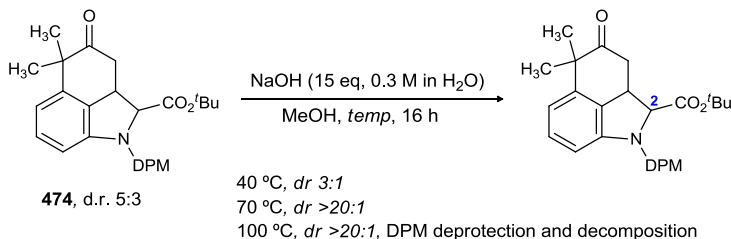
**Scheme 133.** Dunkerton's Claisen-Ireland Approach to Install C2 *tert*-Prenyl Group in Indole



Encouraged by this literature precedence, we focused our approach towards the synthesis of the Claisen-Ireland rearrangement precursor. Our plan involved a DCC coupling between acid **498** and 3,3-dimethyl allyl alcohol. To this end, the tricyclic system (**474**) was subjected to various saponification conditions group (Scheme 135). The *tert*-butyl ester group remained intact, however, DPM deprotection and epimerization of C2 carbon was observed under these harsh conditions. Hydrolysis under acidic conditions led to low product yields (Scheme 134).

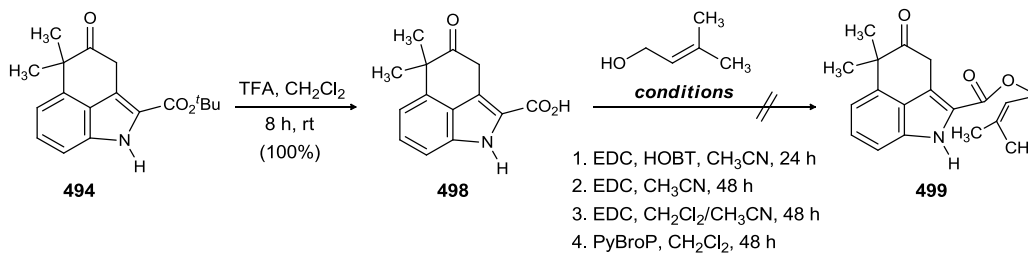
<sup>167</sup> Dunkerton, L. V.; Chen, H.; Mckillican, B. P. *Tetrahedron Lett.* **1988**, 29, 2539.

**Scheme 134.** Attempted Saponification of Indoline **474**



In the event, we were pleased to observe that exposure of **494** to TFA provided the corresponding acid (**498**) in quantitative yields (Scheme 135). The acid was found to be unstable upon treatment with SiO<sub>2</sub> or storage for a long duration of time. The acid (**498**) was subjected to a number of coupling reaction conditions, including a variety of coupling reagents. However, decomposition of the acid was observed in all cases..

**Scheme 135.** Attempted Synthesis of Claisen-Ireland Rearrangement Precursor



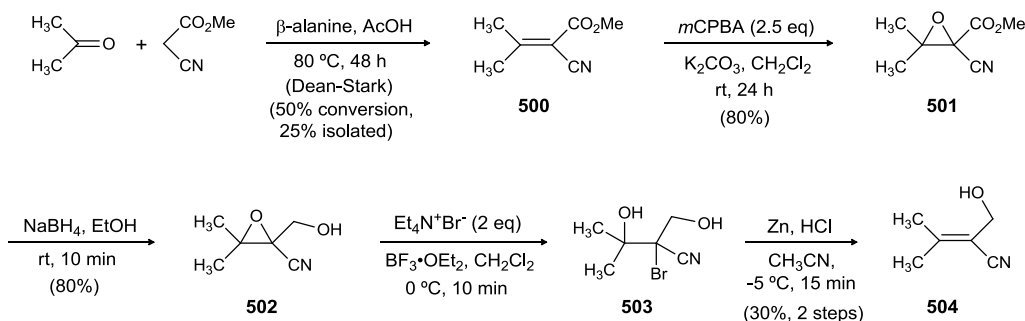
In due course, an allylic alcohol bearing the desired nitrile (**504**) was also synthesized in a known five step protocol. We anticipated that the nitrile functionality might aid in the desired Ireland-Claisen rearrangement protocol.<sup>168</sup> The synthesis of **504** commenced from known methyl cyanoacetate (Scheme 136). An aldol condensation with acetone led to acrylonitrile derivative **500**. The reactive alkene functionality in **500** was subsequently masked as an epoxide **501**. Reduction of the ester (**501**) followed by treatment of resulting epoxy alcohol **502** with tetraethylammonium bromide afforded

<sup>168</sup> Ireland, R. E.; Mueller, R. H. *J. Am. Chem. Soc.* **1972**, *94*, 5897.



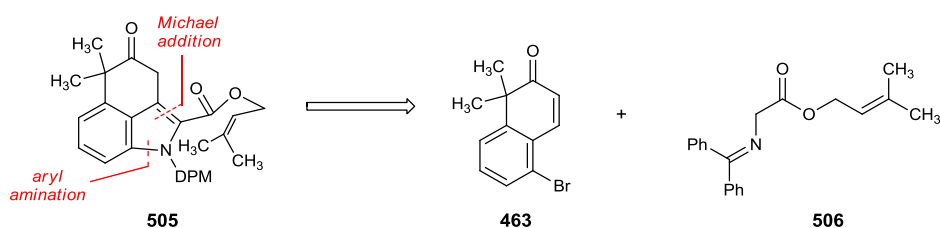
hydroxyl bromide **503**. Zinc/HCl mediated elimination provided the requisite allylic alcohol. However, we were again unable to couple the alcohol (**504**) to acid **498**. It was now clear to us that a different strategy was needed to synthesize the Ireland-Claisen rearrangement precursor (**499**).

**Scheme 136.** Synthesis of Alcohol **504**



Although non-productive, our efforts to synthesize (**499**) from **498** did illustrate the need to install the allyl ester side chain in the early stages of synthesis. This task was envisioned to arise in a straightforward manner by the coupling of enone **463** with Schiff base **506** (Scheme 137).

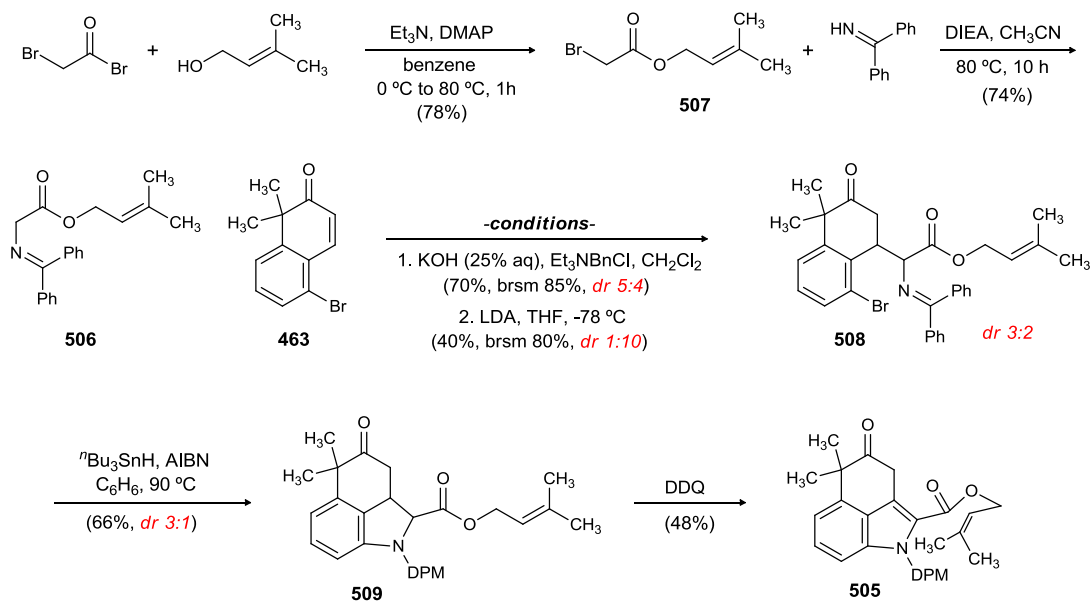
**Scheme 137.** Revised Strategy to Access Ireland-Claisen Rearrangement Precursor



The synthesis of the desired Schiff base (**506**) commenced with the commercially available bromoacetyl bromide. Base promoted coupling of bromoacetyl bromide and 3,3-dimethyl allyl alcohol provided bromoacetate derivative **507** in good yield (Scheme 138). **507** was treated with diphenyl ketimine under basic condition to provide Schiff base **506**. Surprisingly, purification of the easily hydrolysable Schiff base could be

carried out with SiO<sub>2</sub> column chromatography. The Schiff base was subsequently treated with phase transfer-catalyzed Michael reaction conditions to provide the adduct (**508**) as an inconsequential 5:4 mixture of diastereomers. Performing the reaction under kinetic conditions led to product in excellent diastereoselectivity. The Michael adduct was subsequently exposed to <sup>n</sup>Bu<sub>3</sub>SnH and AIBN to provide the desired tricyclic product **509** in good yield. There are two notable aspects of this reaction: (i) The *5-exo-trig* cyclization is favored over the highly difficult, yet possible, *8-exo-trig* cyclization to provide the product (**505**) as a single regioisomer and (ii) epimerization of C2 stereocenter by the earlier established ACCRI process was observed. The indoline (**509**) was subsequently converted to indole **505** upon treatment with DDQ.

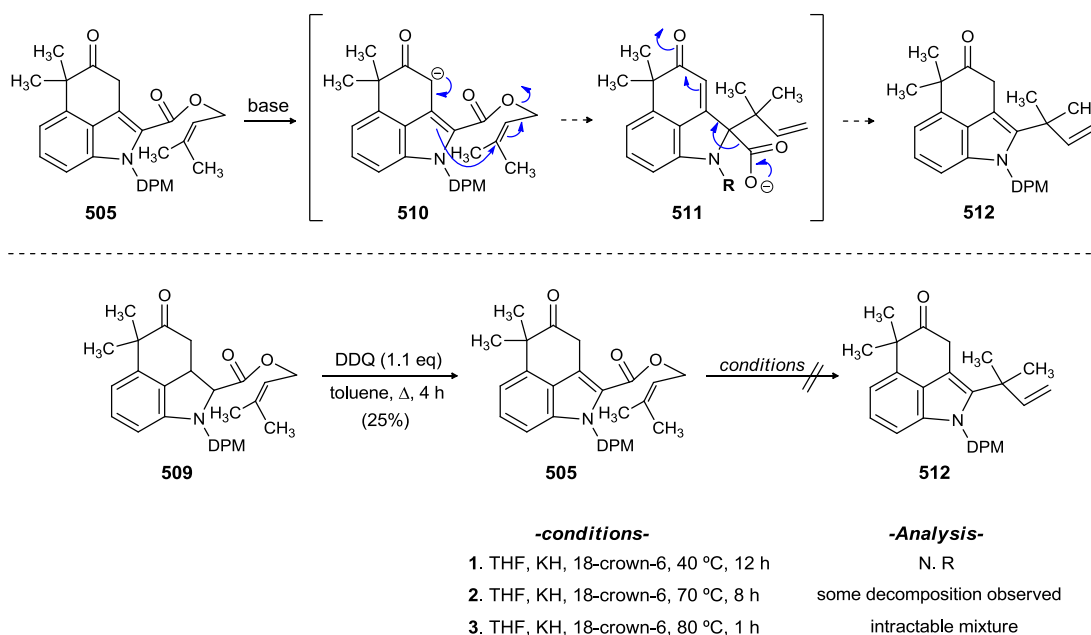
**Scheme 138.** Preparation of Ireland-Claisen Rearrangement Precursor



With indole **505** in hand, various conditions to elicit the desired Ireland-Claisen rearrangement were investigated. Although **505** lack a C2 proton, which is indispensable for this transformation, we hypothesized that the enolate **510** could involve the C2-C3

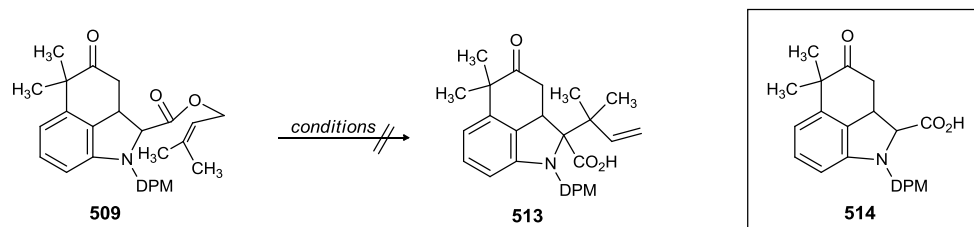
double bond of the indole leading to the required C2 anion (**511**) (Scheme 139). To test this hypothesis, the indole was treated with potassium hydride in presence of 18-crown-6. The substrate **505** remained unreactive at low temperatures; however, decomposition was observed at higher temperatures. Similar results were obtained when potassium hydride was replaced with NaH, DBU and KO<sup>t</sup>Bu as a base.

**Scheme 139.** Attempted Ireland-Claisen Rearrangement with **505**



Indoline **509** was also subjected to base mediated Ireland-Claisen rearrangement conditions. In all the conditions investigated, no product formation was observed. The starting material could be isolated as mixture of varying ratios of diastereomers as a result of C2 epimerization under basic conditions. Surprisingly, saponification of acid **509** was observed at elevated temperatures (Scheme 140).

**Scheme 140.** Attempted Ireland-Claisen Rearrangement with Indoline **509**



**-conditions-**

1. LiHMDS/LDA (3.0 eq.), 18-crown-6, THF, 30 mins, 0 °C, then  $\Delta$  (70 °C)
2. LiHMDS/LDA (3.0 eq.), 18-crown-6, toluene, 30 mins, 0 °C, then  $\Delta$  (110 °C)
3. LDA (3.0 eq.), HMPA:THF (1:6), 1 h, -78 °C, then  $\Delta$  (70 °C)

**-Analysis-**

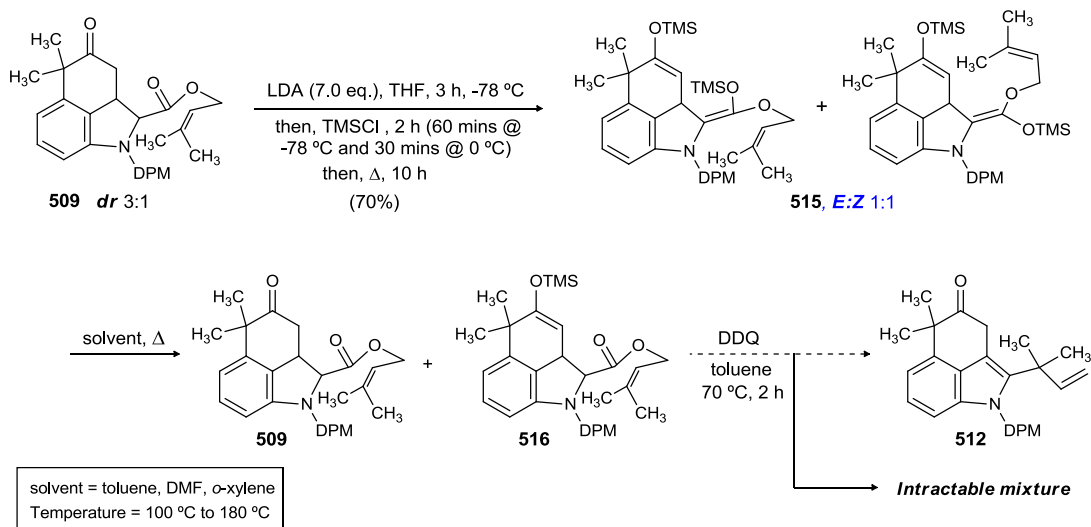
- S.M recovered, KHMDS (*dr* 10:1)  
LDA (*dr* 6:1)  
saponification (one diastereomer)  
S.M recovered ( $\sim$ *dr* 15:1)

In due course, we also analyzed the standard Ireland-Claisen rearrangement, which requires the formation of the intermediate *O*-trialkylsilylketne acetal.<sup>169</sup> Additionally, this reaction is carried out under mild conditions and involves comparatively stable *O*-trialkylsilylketne acetal. To this end, indoline was treated with an excess of LDA and the resulting enolate was trapped *in situ* to provide the desired bis-silyl enol ether **515** as a 1:1 mixture of *E:Z* isomers (Scheme 141). At this point, all our efforts to purify **515** only led to hydrolysis, and the indoline (**509**) was recovered in all these cases. As a result, the crude bis-silyl enol ether was carried onto the next step soon after its isolation. Disappointingly, bis-silyl enol ether **515** provided an inseparable mixture of hydrolysis product **509** and silyl enol ether **516**, resulting from the partial hydrolysis of bis-silyl enol ether **515**, under a variety of reaction condition which included an extensive solvent and temperature screen. Using our earlier hypothesis outlined in Scheme 141, we also investigated the possibility of an Ireland-Claisen rearrangement of indole **516**. The inseparable mixture of hydrolysis products (**509** and

<sup>169</sup> Paterson, I.; Hulme, A N. *J. Org. Chem.* **1995**, *60*, 3288.

**516**) were exposed to DDQ (Scheme 141). Unfortunately, this only led to an intractable mixture.

**Scheme 141.** Attempted Ireland-Claisen Rearrangement of bis-Silyl Enol Ether **515**

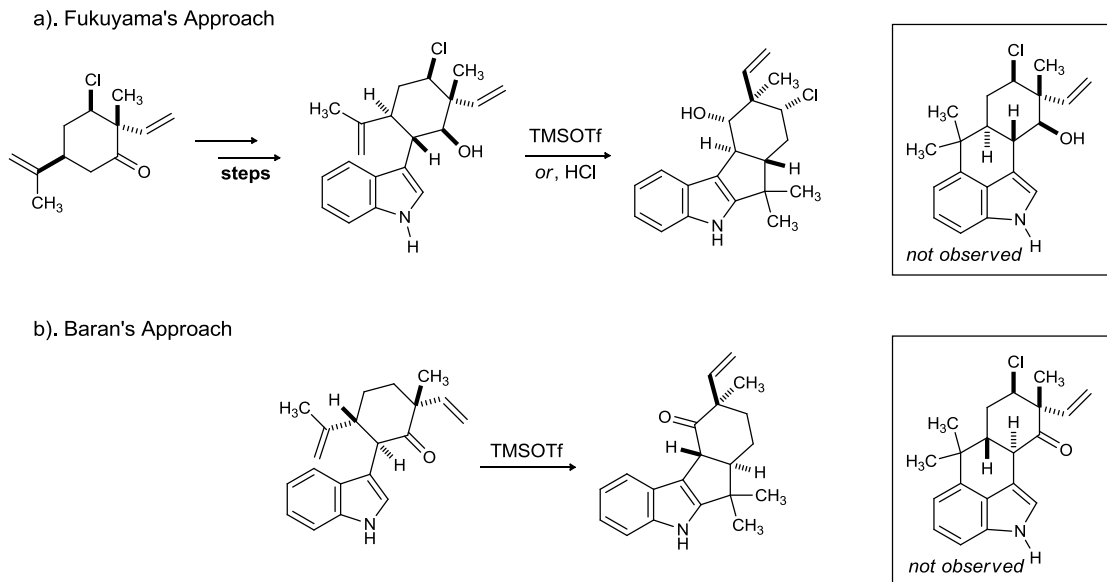


While the results of our various attempts to install the C2 *tert*-prenyl were disappointing, they did serve to demonstrate how decisive the steric factors are responsible for our inability to elicit the desired transformation. As, a result, a second generation synthesis of ambiguine G was conceived.

### 3.4.6. A tandem Friedel-Crafts Acylation/Alkylation Sequence to Access the ABC-ring System of Ambiguine G.

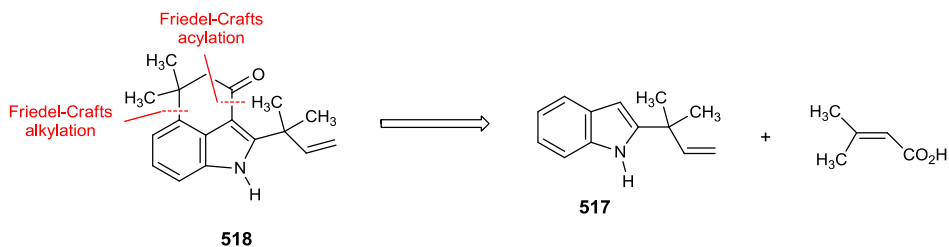
From the earlier work of Fukuyama *et al.*<sup>130</sup> and Baran *et al.*<sup>148</sup> towards the syntheses of hapalindoles and ambiguines, we were aware of the fact that the ABC-ring system of ambiguine G must be synthesized in the earlier stages of synthesis, because of the known propensity of the isopropylidene unit at C15 to undergo Lewis acid induced regioselective cyclization to C2 of indole (Scheme 142).

**Scheme 142.** Construction of Hapalindole Skeleton – A Challenge



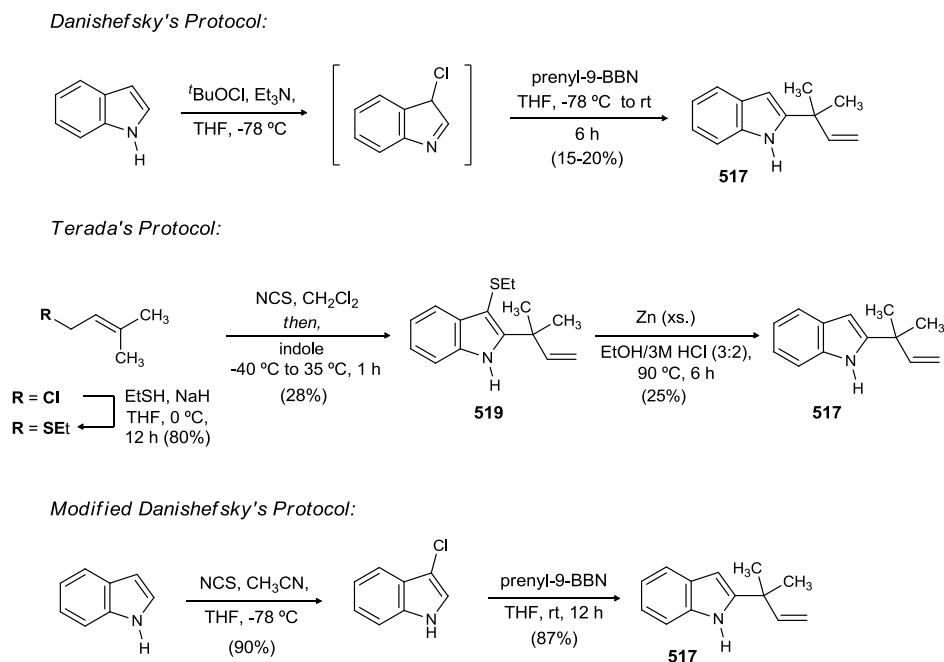
In our new synthetic plan, we proposed that the favorable cyclization, leading to the C2-C16 bond of the hapalindole skeleton, could be completely inhibited by installing substitution at the the C2 of indole. To this end, C2 *tert*-prenyl indole **517** emerged as a viable substrate to test this hypothesis. The advantage of this route was its conciseness, as well as the fact that the *tert*-prenyl group would be installed in the earlier stages of the synthesis (Scheme 142). A tandem Friedel-Crafts acylation/alkylation sequence would lead to the targeted tricycle (**518**).

**Scheme 142.** Tandem Friedel-Crafts Acylation/Alkylation Sequence to Access ABC-Ring System of Hapalindoles and Ambiguines



Synthesis of the C2 *tert*-prenyl indole was attempted using Danishefsky's protocol.<sup>170</sup> According to this procedure, indole was reacted with *tert*-butyl oxylchloride to provide 3-chloro indoline which was subsequently treated with prenyl-9-BBN to provide the desired compound (Scheme 143). The low yields of this reaction prompted us to evaluate other ways of forming **517**. To this end, treatment of indole with NCS and 3,3-dimethylallyl sulfide at  $-20\text{ }^{\circ}\text{C}$  provided the intermediate 3-sulfonium salts, which on warming to  $20\text{ }^{\circ}\text{C}$  rearranged to **517**.<sup>171</sup> Removal of the unwanted C-3 thioethyl group in **519** under reductive conditions led to the desired indole (**517**) in 7% overall yield (Scheme 143).

**Scheme 143.** Optimization of C2 *tert*-Prenyl Indole Synthesis

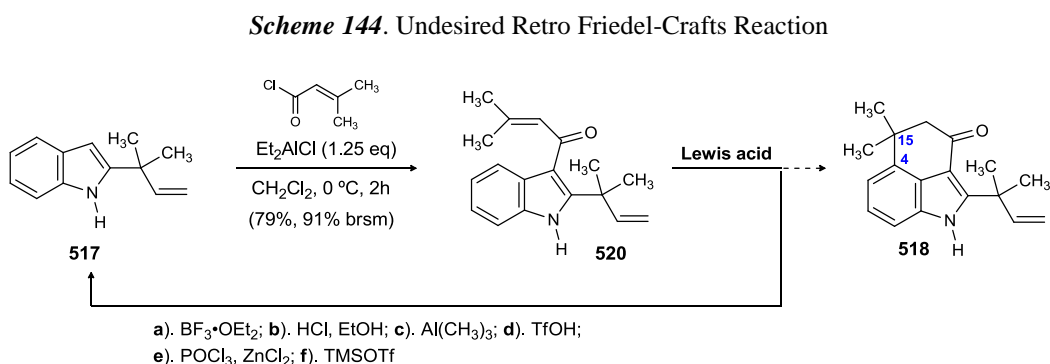


Gratifyingly, a slight modification of the Danishefsky protocol, which required a two step sequence, led to the desired product (**517**) in 79% yield. The stage was then set

<sup>170</sup> Schkeryantz, J. M.; Woo, J. C. G.; Siliphaivanh, P.; Depew, K. M.; Danishefsky, S. J. *J. Am. Chem. Soc.* **1999**, *121*, 11964.

<sup>171</sup> a) Tomita, K.; Terada, A.; Tachikawa, R. *Heterocycles*. **1976**, *4*, 729. b) Tomita, K.; Terada, A.; Tachikawa, R. *Heterocycles*. **1976**, *4*, 733.

to carry out the desired Friedel-Crafts acylation/alkylation sequence. Treatment of indole **517** with commercial available 3,3-dimethylacetyl chloride provided adduct **520** (Scheme 144).<sup>172</sup> A number of Lewis acids were screened to forge the desired C4-C16 bond. Surprisingly, under these conditions a retro Friedel-Crafts reaction, leading to the indole **517**, was observed. Evaluating different conditions, including solvents and temperatures screen, resulted in the isolation of **517** in quantitative yield. Although our inability to carry out the Friedel-Crafts alkylation was frustrating, we were hopeful that changing the steric/electronic aspect of the substrate might lead to the rapid assembly of the tricyclic core.



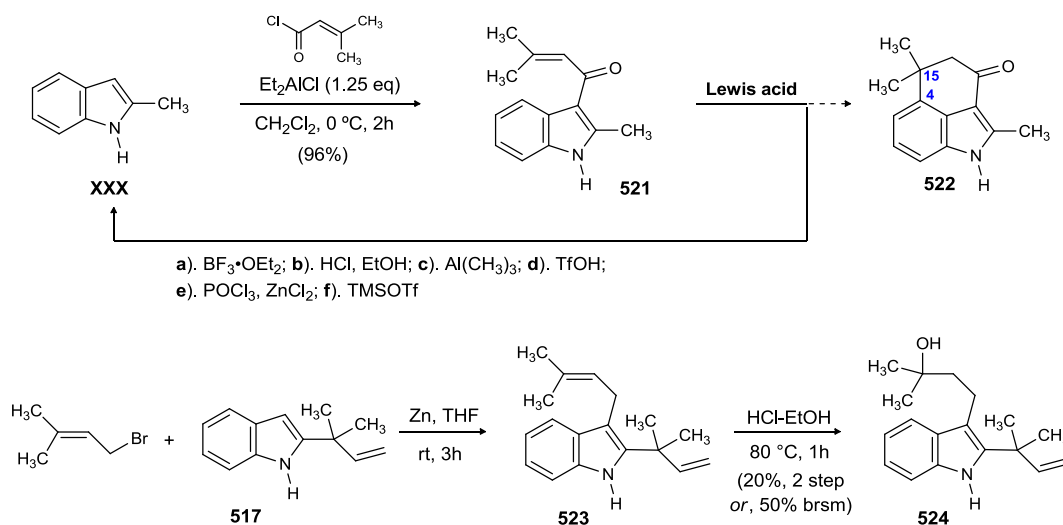
Initially, we decided to study the effect of sterics on the Friedel-Crafts alkylation step. To this end, the bulky *tert*-prenyl group was replaced with a methyl group. The commercially available 2-methyl indole was subjected to the Friedel-Crafts acylation conditions (Scheme 145). A number of Lewis acids were screened to effect the Friedel-Crafts alkylation of the adduct (**521**). Disappointingly, all these attempts led to 2-methyl indole. At this stage it was clear that the presence of a ketone in **520** or **521** was initiating the undesired retro Friedel-Crafts process. Hence, we decided to replace the ketone functionality in **521** with a methylene group to inhibit the retro Friedel-Crafts process.

<sup>172</sup> Okauchi, T.; Itonaga, M.; Minami, T.; Owa, T.; Kitoh, K.; Yoshino, H. *Org. Lett.* **2000**, *2*, 1485.



The synthesis could be achieved in one step by a zinc-mediated Barbier reaction of **517**,<sup>173</sup> and the desired alkylation adduct was isolated as an inseparable mixture with **517** (Scheme 145). While **523** was unreactive to most of the Friedel-Crafts alkylation conditions tried, it could be converted to **524** in 20% yield (50% brsm) upon treatment with boiling HCl-Et<sub>2</sub>O solution.

**Scheme 145.** Effect of Electronics and Sterics on the Friedel-Crafts Alkylation Step

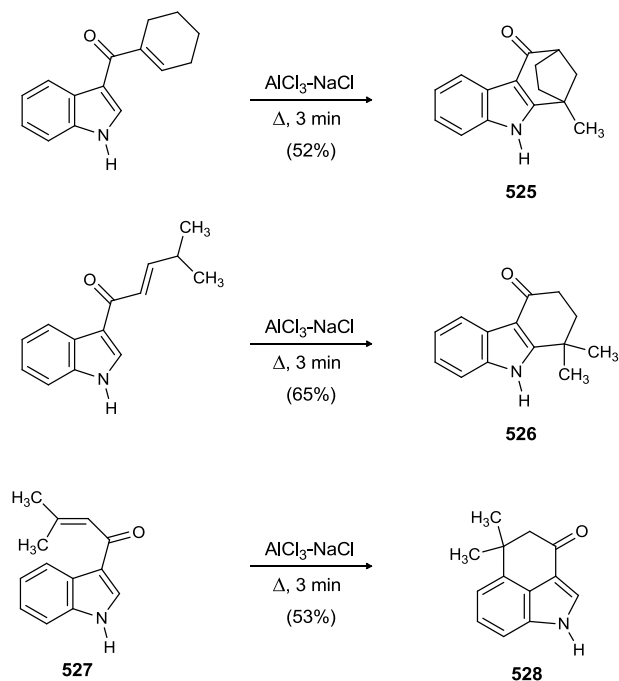


While we were trying to figure out the desired Friedel-Crafts alkylation conditions, our attention was drawn to a published report, which utilized a molten AlCl<sub>3</sub>-NaCl solution to carry out a Friedel-Crafts alkylation of a related system (Scheme 146).<sup>174</sup> Gogoll and coworkers screened a number of AlCl<sub>3</sub>-NaCl mediated cyclizations of C-3 acylindole substrates, and found that all but one substrate provided the expected C2 alkylated product (**525** and **526** are representative example). Surprisingly, subjecting **527** to the same reaction conditions provided C4 alkylated product **528** (Scheme 152).

<sup>173</sup> Yadav, J. S.; Reddy, B. V.S.; Reddy, P. M.; Srinivas, C. *Tetrahedron Lett.* **2002**, *43*, 5185.

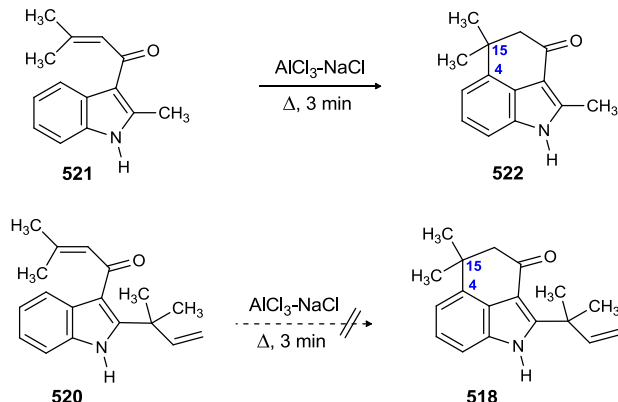
<sup>174</sup> Bergman, J.; Venemalm, L.; Gogoll, A. *Tetrahedron.* **1990**, *46*, 6067.

**Scheme 146.** Literature Precedence for a Novel Molten  $\text{AlCl}_3\text{-NaCl}$  Solution Mediated C-4 Alkylation of Indoles



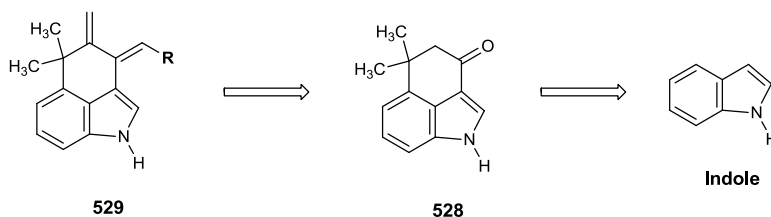
Encouraged by these results, we subjected **520** and **521** to these reaction conditions. We were pleased to find that **521** could be successfully converted to the desired tricyclic ketone **522**; however, decomposition of 2-*tert* prenyl indole derivative (**520**) was observed under these reaction conditions (Scheme 147). We reasoned that the terminal bond of the *tert*-prenyl group is also participating in the reaction, thus leading to nonselective product formation. Although we were disappointed in our failure to synthesize the 2-*tert* prenylated tricyclic indole,  $\text{AlCl}_3\text{-NaCl}$  mediated cyclization provided us a way to rapidly access the tricyclic core of hapalindoles. These results prompted us to reevaluate our synthetic plan, and we decided to install the requisite *tert*-prenyl group towards the end-stages of synthesis.

**Scheme 147.** AlCl<sub>3</sub>-NaCl Solution-Mediated C-4 Alkylation of Model Compounds



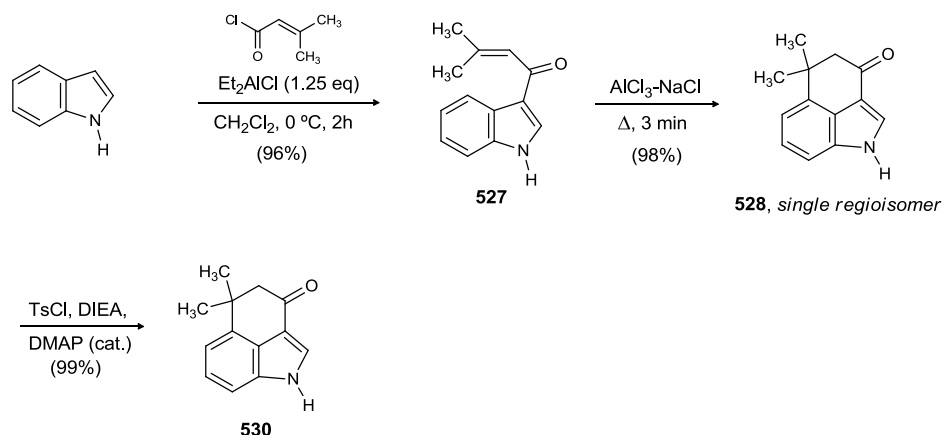
The retrosynthesis of this new approach is summarized in Scheme 148. Diene **529** would be constructed from tricyclic **528** via a series of functional group manipulations. **528** was envisioned to arise in a straightforward manner from indole, using the Friedel-Crafts acylation/alkylation sequence.

**Scheme 148.** Revised Friedel-Crafts Acylation/Alkylation Sequence to Access Diene **529**



To this end, treatment of indole with 3,3-dimethylallyl chloride in presence of Et<sub>2</sub>AlCl provided adduct **527** in excellent yield (Scheme 149). As expected, a quantitative yield and single isomer of tricyclic **528** was isolated after subjecting **527** to the Friedel-Crafts alkylation protocol. Subsequently, the indole was protected with a tosyl group to provide **530**. In practice, the conversion of indole to **530** could be performed without the involvement of any purification steps.

**Scheme 149.** Synthesis of Tricyclic Ketone **530**



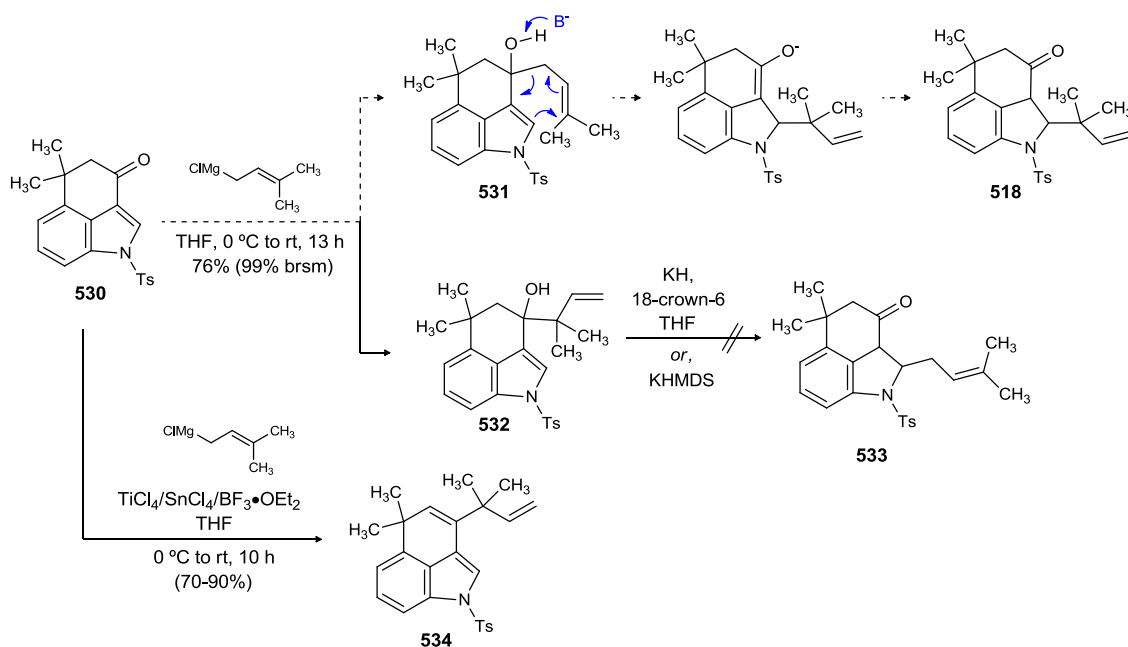
At this stage, we were tempted to explore the possibility of installing the desired *tert*-prenyl group at C2 of the indole. Although our earlier efforts in this direction were unsuccessful, we were hopeful that the presence of the ketone functionality in **530** might allow us to elicit this transformation by employing an anion-accelerated oxy-Cope rearrangement protocol.<sup>175</sup> To our utter dismay, exposing **530** to 3,3-dimethylallyl magnesium chloride provided us the undesired *tert*-prenylated product **532**. Disappointingly, attempting this reaction by employing 3,3-dimethylallylcuprate, in an attempt to inhibit this undesired transformation,<sup>176</sup> led to the same product. To test the viability of our proposed anion-accelerated oxy-Cope rearrangement protocol, **532** was treated with potassium hydride and 18-crown-6. The substrate underwent decomposition and none of the product formation (**533**) was observed. To inhibit the undesired transformation of **532**, we also attempted this reaction in the presence of different Lewis acids (Scheme 149). We reasoned that Lewis acids will bind to ketone group, in preference to magnesium, resulting in the desired product formation. However, this reaction provided the undesired dehydrated product (**534**). In a recently reported

<sup>175</sup> Benson, J. A.; Jones, M., Jr. *J. Am. Chem. Soc.* **1964**, *86*, 5019.

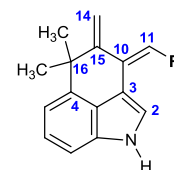
<sup>176</sup> Lipshutz, B. H.; Sengupta, S. *Org. React.* **1992**, *41*, 135.

synthesis of ambiguiene H, Baran and coworkers have installed the C2 *tert*-prenyl in the last step of synthesis.<sup>137</sup> This report, and our failure to install the C2 *tert*-prenyl group prompted us to postpone this process to the very end of synthesis.

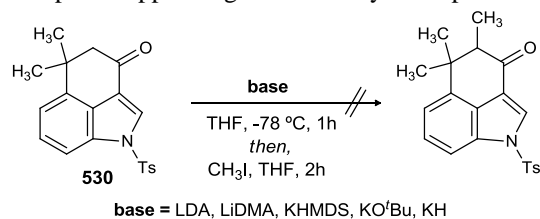
**Scheme 150.** Attempts at Appending the C-2 *tert*-Prenyl Group in Tricyclic Ketone **530** by Oxy-Cope Rearrangement Protocol



We next focused our attention on constructing diene **529**, needed for the critical Diels-Alder reaction. To this end, we subjected tricycle **530** to a variety of alkylation conditions to append the desired methyl group at C15. **530** remained unreactive under most conditions and underwent decomposition when harsher conditions were employed (Scheme 151). We were surprised by this result, as this was thought to be one of the easiest steps in the synthesis. We believe that steric hindrance imparted by the neighboring methyl groups is leading to the unreactivity of **530**. At this stage, we started to consider other ways to install C14.



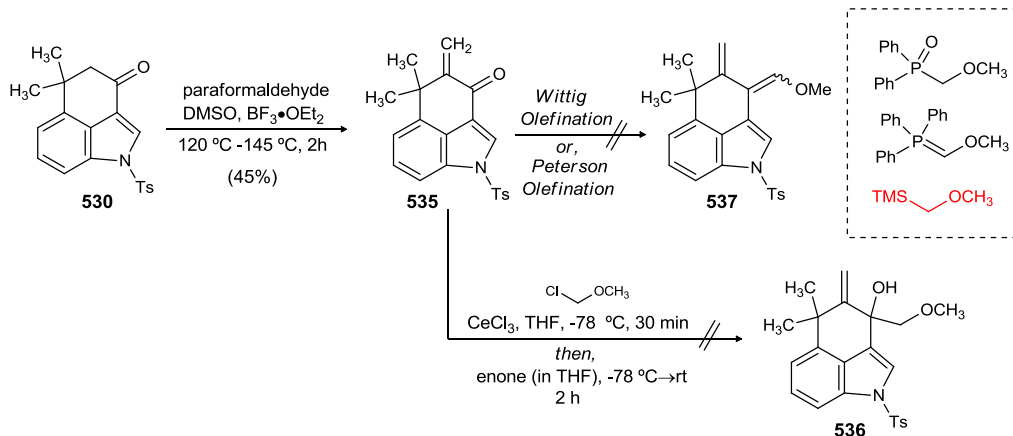
**Scheme 151.** Attempts at Appending a C14 Methyl Group in Tricyclic Ketone **530**



In the event, we came across a report published in 1965 by Lunn and coworkers.<sup>177</sup> According to this procedure, treatment of **530** with paraformaldehyde in DMSO containing BF<sub>3</sub>•OEt<sub>2</sub> at 140 °C provided enone **535** in decent yield (Scheme 152). Our efforts next turned towards appending the C10-C11 double bond by utilizing a one-carbon homologation strategy. In theory, this could be achieved in a number of ways, including Wittig or Peterson olefination. Despite considerable experimentation, exposure of enone **535** to these one carbon homologation protocols led to the formation of complex product mixtures (Scheme 152). As a result, a stepwise approach was attempted. In this approach enone **535** was treated with CeCl<sub>3</sub> and chloromethyl methyl ether. The desired hydroxyl ether **536** could be observed in the crude NMR analysis, however, all our efforts to isolate this intermediate only led to an intractable product mixture.

<sup>177</sup> Lunn, W. H. W. *J. Org. Chem.* **1965**, *30*, 2925.

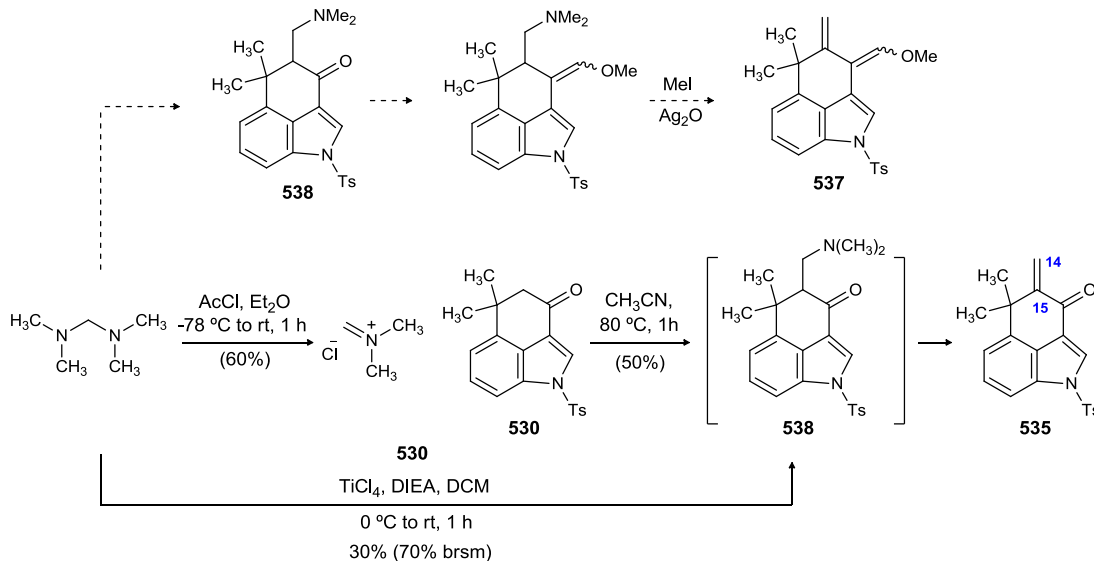
**Scheme 152.** Construction of Enone **535**



These results suggested that the nucleophiles in the above cases might be undergoing Michael addition to **532**. Additionally, we were also concerned with the stability of diene **537** under these reaction conditions. With these issues in mind, we decided to mask the C14-C15 double bond and unveil it in the later stages of the synthesis. According to the published procedure,<sup>178</sup> **530** was treated with Eschenmoser's salt (Scheme 153). However, none of the desired dimethyl amine adduct **538** was obtained; instead, enone **535** was obtained in a quantitative yield, via elimination of the dimethylamine group in **538**. Similar results were obtained when **530** was reacted with methylene-bis-dimethylamine in the presence of  $\text{TiCl}_4$  (Scheme 153). At this stage, it was clear that the desired product undergoes an elimination reaction to relieve the steric strain exerted by the neighbouring methyl groups.

<sup>178</sup> Schreiber, J.; Maag, H.; Hashimoto, N.; Eschenmoser, A. *Angew. Chem. Int. Ed.* **1971**, *10*, 330.

**Scheme 153.** Unsuccessful Attempts at Masking the C14-C15 Double Bond of Enone **535**



We then turned to an alternate strategy that would involve the installment of the C10-C11 double bond prior to the formation of the C14-15 terminal alkene. To this end, **530** was subjected to Wittig and Peterson olefination protocols; however, only an intractable reaction mixture was isolated in all these cases. In the event, we were pleased to observe that **530** could be quantitatively converted to TMS-protected cyanohydrin **539** upon treatment with TMSCN and a catalytic amount of LiOMe (Scheme 154).<sup>179</sup> **539** could be subsequently treated with TBAF and POCl<sub>3</sub> to provide **540** in decent yield. **540** could also be synthesized from **530** in an alternate 2-step sequence as shown in Scheme 154.<sup>180</sup> With the  $\alpha,\beta$ -unsaturated nitrile in hand, our attention then focused on appending C14 in **540**, utilizing Michael addition reaction conditions. **540** was treated with a variety of Grignard and alkyl lithium reagents. Unfortunately, **540** remained unreactive under all these conditions and underwent decomposition under harsher conditions (Scheme 154).

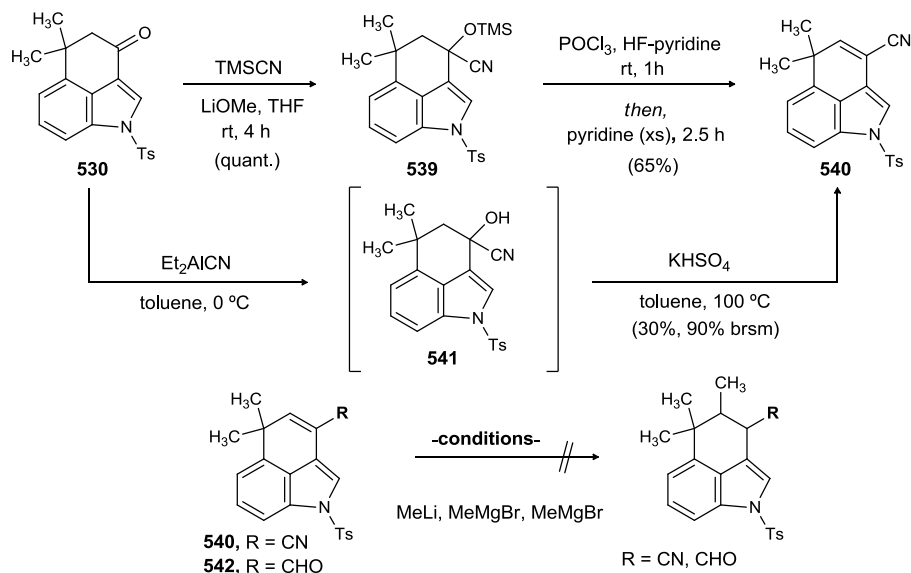
<sup>179</sup> Wilkinson, H. S.; Grover, P.T.; Vandenbossche, C. P.; Bakale, R. P.; Bhongle, N. N.; Wald, S. A.; Senanayake, C. H. *Org. Lett.* **2001**, *3*, 553.

<sup>180</sup> Harrak, Y.; Daidone, G.; Plescia, S.; Schillaci, D.; Pujol, M. D. *Bioorg. Med. Chem.* **2007**, *15*, 4876.



Enal **542**, obtained from **540** upon treatment with DIBAL-H, underwent undesired 1,2-addition under these reaction conditions.

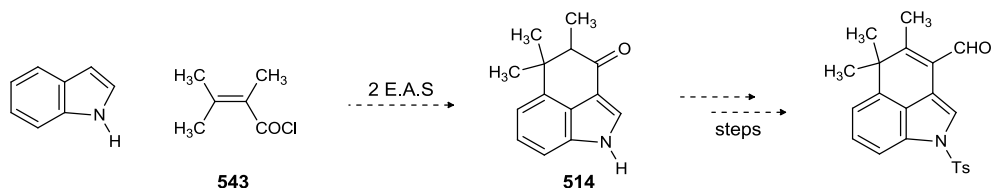
**Scheme 154.** Synthesis of the  $\alpha,\beta$ -Unsaturated Nitrile



### 3.4.7. Friedel-Crafts Acylation Utilizing 2,3,3-Trimethylacrylic Acid

Unable to append the C14 methyl group in our previous synthetic route, presumably due to the steric factors, we turned our attention to an alternate strategy wherein the required methyl group, necessary for the construction of diene, would be accessed from **544**. The tricyclic framework (**544**) was envisioned to arise in a straightforward manner by effecting a tandem Friedel-Crafts acylation/alkylation sequence of indole with 2,3,3-trimethylacryloyl chloride **543** (Scheme 155).

**Scheme 155.** Tandem Friedel-Crafts Acylation/Alkylation Using 2,3,3-Trimethylacryloyl Chloride



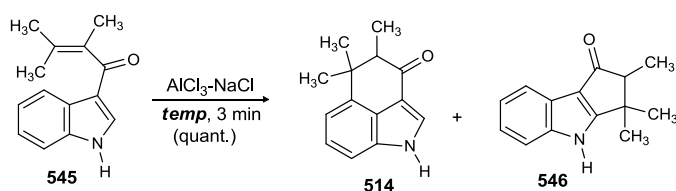
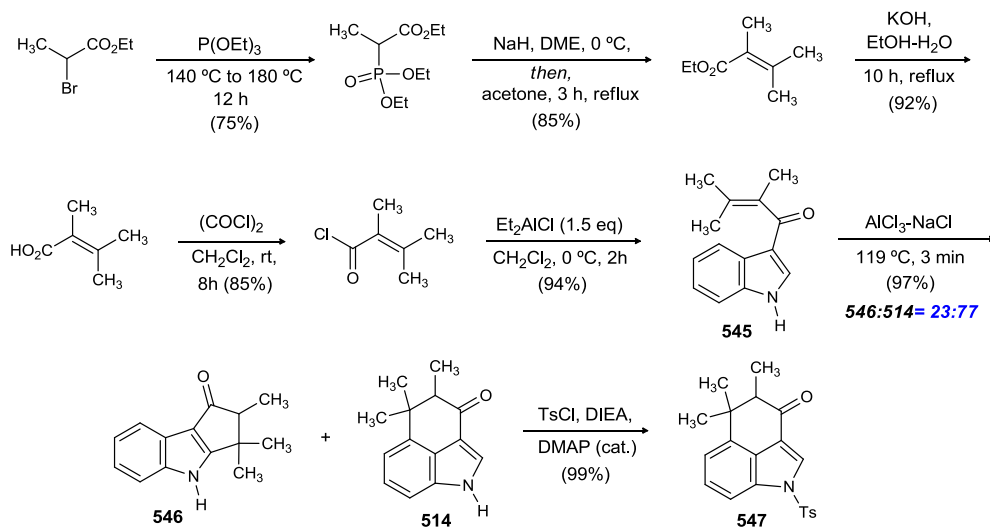
The desired 2,3,3-trimethylacryloyl chloride was prepared from ethyl-2-bromopropionate according to a known procedure (Scheme 156).<sup>181</sup> Ethyl-2-bromopropionate was subjected to Michaelis-Arbuzov reaction conditions<sup>182</sup> to provide the corresponding phosphonate. Wittig-Horner reaction of the intermediate phosphonate with acetone provided ethyl 2,3,3-trimethylacrylate in good yield. This 3-step sequence could be conveniently performed on a 20-100 g scale (Scheme 156). Subsequently, synthesis of 2,3,3-trimethylacryloyl chloride was accomplished in a straightforward two-step sequence. With 2,3,3-trimethylacryloyl chloride in hand, efforts turned to the construction of the ABC-ring system of hapalindole skeleton. Et<sub>2</sub>AlCl mediated Friedel-Crafts acylation of indole with 2,3,3-trimethylacryloyl chloride provided adduct **545** in excellent yield. **545** was subsequently treated with molten AlCl<sub>3</sub>-NaCl solution at 160 °C. Surprisingly, the desired tricyclic ketone (**514**) was isolated along with the undesired regioisomer (**546**), possessing the fischerindole skeleton. Temperature is very critical to the regioselective outcome of this cyclization step. Performing the reaction at lower temperatures (117-120 °C) provided **514** as the major product, but elevated temperature led to undesired **546** as the major product. Due to the difficulties encountered in purification, the crude product of the Friedel-Crafts alkylation was subjected to tosyl protection. The resulting masked indole **547** could be easily purified, as the undesired regioisomer **546** remained unreactive under these reaction conditions

---

<sup>181</sup> Borszky, T.; Mallet, T.; Baiker, A. *Tetrahedron: Asymmetry*. **1997**, 8, 3745.

<sup>182</sup> Michaelis, A.; Kaehne, R. *Chem. Ber.* **1898**, 31, 1048.

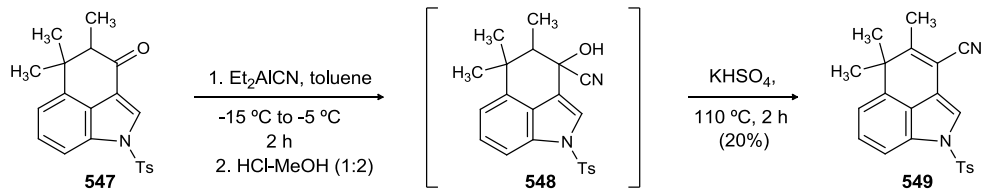
**Scheme 156. Synthesis of Tricyclic Ketone 547**



temp	AlCl <sub>3</sub> :NaCl	(514):546
160 °C	1:0.85	40:60
135 °C	1:0.85	70:30
130 °C	2:1	75:25

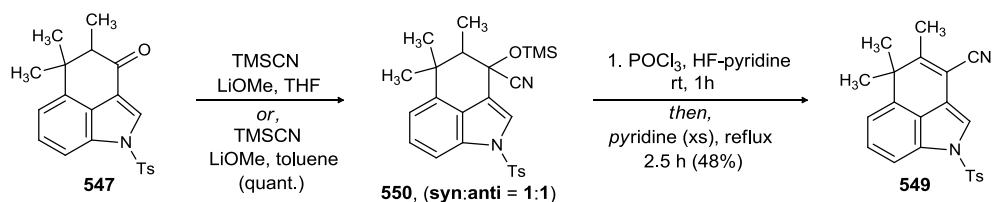
Having solved the issues related to C14 installation, synthetic strategies for constructing C10-C11 double bond by utilizing one-carbon homologation protocols were evaluated next. Ketone **547** was treated with Et<sub>2</sub>AlCN to provide the highly unstable **548** (Scheme 157). The cyanohydrin was immediately subjected to a KHSO<sub>4</sub>-mediated elimination step. Unfortunately, a very low yield of the desired product (**549**) was isolated, as **548** hydrolyzed under these reaction conditions to provide ketone **547**.

**Scheme 157.** Synthesis of  $\alpha,\beta$ -Unsaturated Nitrile **549** Using  $\text{Et}_2\text{AlCN}$



Alternatively, **547** could be quantitatively converted to TMS-protected cyanohydrin (**550**), upon treatment with TMSCN and a catalytic amount of LiOMe (Scheme 158). **550** could be subsequently treated with TBAF and  $\text{POCl}_3$  to provide **549** in a modest yield, after multiple purification steps. The low yield of  $\alpha,\beta$ -unsaturated nitrile **549** could result from the inability of *anti*-**550** to undergo elimination reaction.

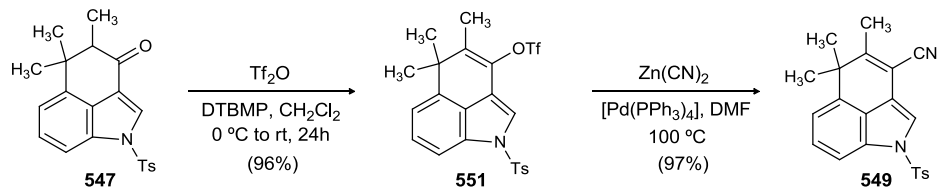
**Scheme 158.** Synthesis of  $\alpha,\beta$ -Unsaturated Nitrile **549** Using TMSCN



In an effort to optimize the synthesis of  $\alpha,\beta$ -unsaturated nitrile **549**, several other ways of appending the C10-C11 double bond by utilizing one carbon homologation strategy were evaluated next. In the event, we were glad to observe that **547** could be converted to its enol triflate **551**,<sup>183</sup> which upon treatment with  $\text{Zn}(\text{CN})_2$ , in the presence of catalytic amount of  $\text{Pd}(\text{PPh}_3)_4$ , provided nitrile **549** in excellent yield (Scheme 159). This two-step sequence could be performed on a multigram scale

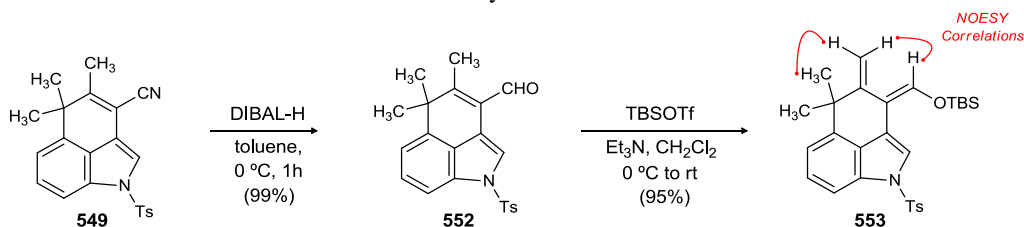
<sup>183</sup> Padwa, A.; Bur, S. K.; Zhang, H. *J. Org. Chem.* **2005**, *70*, 6833.

**Scheme 159.** Optimized Conditions for the Synthesis of  $\alpha,\beta$ -Unsaturated Nitrile **549**



Reduction of **547** with DIBAL-H provided enal (**552**) in quantitative yield. Treatment of the enal (**552**) with TBSOTf in presence of  $\text{Et}_3\text{N}$  furnished the requisite diene (**553**) with the desired diene geometry. The diene geometry was confirmed by a NOESY experiment. (Scheme 160).

**Scheme 160.** Synthesis of Diene **553**



### 3.4.8. Dienophile Synthesis

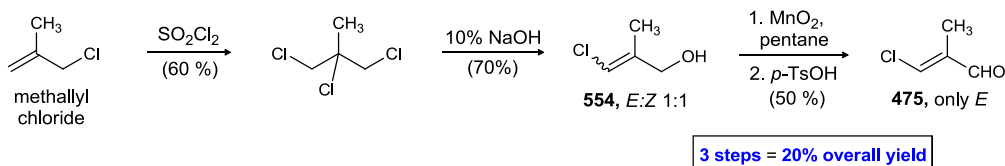
The synthesis of dienophile **475** commences with the perchlorination of commercially available methallyl chloride, using sulfuryl chloride, to give the meso trichloride in quantitative yield (Scheme 161). Slow addition of methallyl chloride was necessary as accumulation of sulfur dioxide could trigger a highly exothermic reaction. A straightforward base wash furnished the desired chloride in quantitative yield. Hydroxide-mediated elimination and nucleophilic displacement proceeded smoothly to give chloro-allylic alcohol **554** as a 1:1 mixture of *E* and *Z* stereoisomers. Though Williard<sup>184</sup> was able to separate the isomers using spinning band distillation, it proved

<sup>184</sup> Williard, P. G.; Grab, L. A.; de Laszlo, S. E. *J. Org. Chem.* **1983**, *48*, 1123.

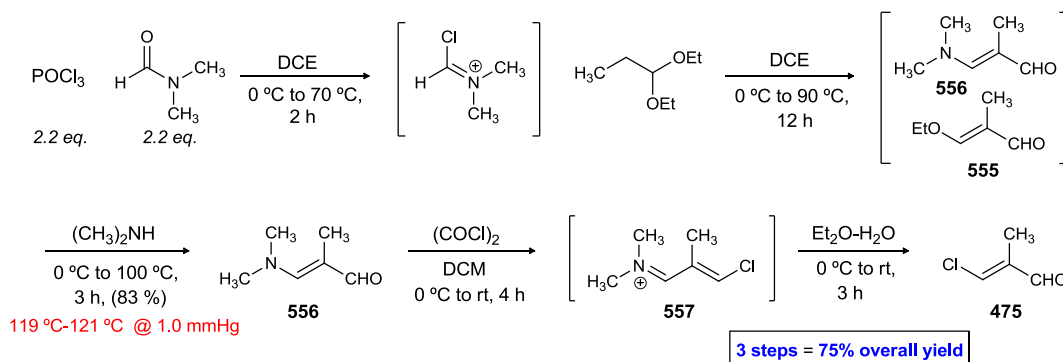
difficult in our hands. Therefore, this 1:1 mixture was oxidized to the corresponding aldehyde using commercially available manganese dioxide (activated). In order to isomerize *Z*-**475** to the corresponding *E*-isomer, a catalytic amount of *p*-toluenesulfonic acid was added to the crude mixture before removal of the pentane by distillation. Thus pure *E*-**475** was produced in 50% yield. The aldehyde was not very stable, and long term storage even at low temperature (0 °C) resulted in decomposition. In summary, the desired  $\beta$ -chloro- $\alpha$ -methyl acrolein **475** was synthesized in 20% overall yield. Various efforts directed towards increasing the yield of this sequence were unsuccessful, probably because of the low boiling point of intermediate compounds.

**Scheme 161.** Synthesis of  $\beta$ -Chloro- $\alpha$ -Methyl Acrolein **475**

**Williard's Protocol**



**Arnold's Protocol (Vilsmeier-Haack)**



In an effort to increase the overall yield of  $\beta$ -chloro- $\alpha$ -methyl acrolein synthesis, an alternate strategy developed by Arnold<sup>185</sup> was attempted next (Scheme 161) The Vilsmeier salt was formed at 0 °C in dichloroethane, using phosphorous oxytrichloride

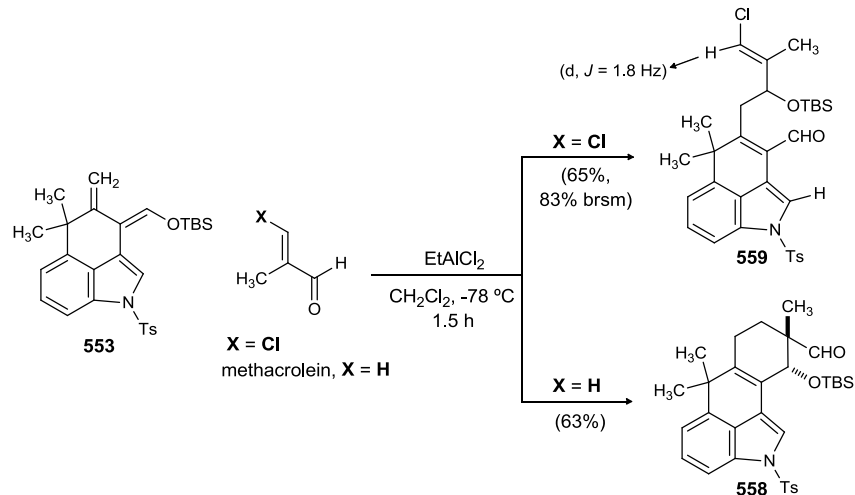
<sup>185</sup> Arnold, T.; Zemkicka, J. *J Collect Chem Comm* **1959**, 2385.

and *N,N*-dimethyl formamide. Propionaldehyde diethyl acetal was then added, and the mixture was heated to 100 °C to give vinylogous amide **556** contaminated with vinylogous ester **555**. **555** was converted to the vinylogous amide (**556**) under excess dimethylamine and heat. Treatment of the crude vinylogous amide **556**, with oxalyl chloride in chloroform resulted in formation of the iminium salt **557** in high purity. Hydrolysis of the iminium salt provided  $\beta$ -Chloro- $\alpha$ -methyl acrolein **475** which could be purified by distillation. There are two advantages of using Arnold's sequence for the synthesis of  $\beta$ -Chloro- $\alpha$ -methyl acrolein. This sequence stereoselectively produces the *E*-isomer of aldehyde **475** in a 75% overall yield from propionaldehyde diethyl acetal. In addition, this sequence was performed on a 20-100 gram scale without a significant drop in the yield of  $\beta$ -chloro- $\alpha$ -methyl acrolein.

#### ***3.4.9. Attempted Diels-Alder Reaction With $\beta$ -Chloro- $\alpha$ -Methyl Acrolein***

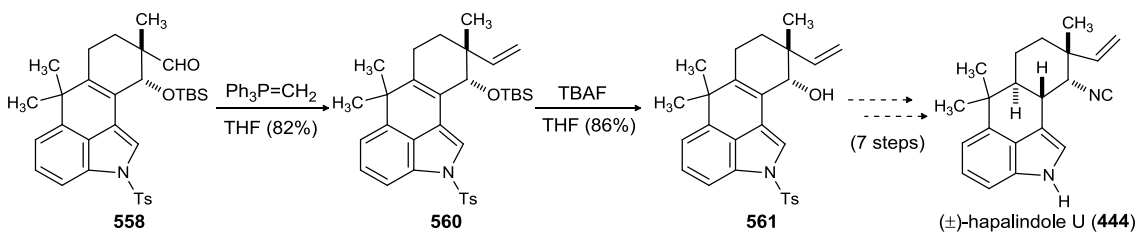
Having synthesized the diene (**553**) and the dienophile (aldehyde **475**) components, our attention focused on the execution of the Diels-Alder reaction. One of the major obstacles in this demanding cycloaddition was the instability of  $\beta$ -chloro- $\alpha$ -methyl acrolein. Efforts to carry out the Diels-Alder cycloaddition under thermal conditions led to desilylation of **553**, providing the corresponding enal **552**. Parallel to the thermal conditions for the cycloaddition, the use of Lewis acids was also explored (Scheme 162). In addition to the use of dienophile **475**, the Diels-Alder cycloadditions of **553** with  $\alpha$ -methyl acrolein were also explored. The formation of a normal Diels-Alder adduct with methacrolein and a Mukaiyama aldol product with chloro aldehyde **475** suggests that substitution at the  $\beta$ -carbon of the dienophile dictates the course of the reaction.

**Scheme 162.** Diels-Alder Cycloadditions of **553** with  $\alpha$ -Methyl Acrolein and  $\beta$ -Chloro- $\alpha$ -Methyl Acrolein



The Diels-Alder adduct **558** could be elaborated to the alcohol **561** in two synthetic operations, thus intersecting with Natsume's intermediate in the synthesis of ( $\pm$ )-hapalindole U (**444**) (Scheme 163). Treatment of aldehyde **558** with a Wittig reagent provided alkene **560** in good yield. TBAF mediated desilylation of **560** led to the allylic alcohol **561**. A further 7 steps were required by Natsume and coworkers to finish the synthesis of hapalindole U.

**Scheme 163.** Formal Synthesis of ( $\pm$ )-Hapalindole U



At this stage, we were faced with two major factors that posed an initial challenge to the execution of the Diels-Alder reaction. First, the aldehyde was not thermally stable, and a significant amount of decomposition was observed upon standing for an extended

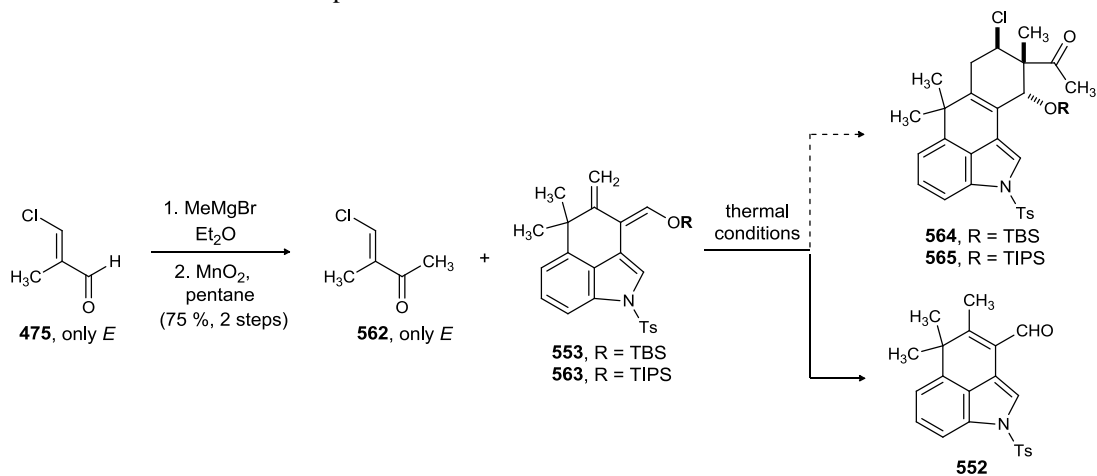


period of time. Second, the attempted Diels-Alder cycloaddition with  $\beta$ -chloro- $\alpha$ -methyl acrolein provided the undesired Mukaiyama aldol adduct.

### 3.4.10. Towards the Synthesis and Attempted Diels-Alder Reaction with Various Dienophiles under Thermal Conditions.

To eliminate the undesired formation of the Mukaiyama aldol adduct, by employing  $\beta$ -chloro- $\alpha$ -methyl acrolein as the dienophile, we started considering other dienophiles which could effect this demanding cycloaddition. It was postulated that substituting the aldehyde functionality in  $\beta$ -chloro- $\alpha$ -methyl acrolein with a ketone or ester functionality might limit the formation of **559**.

**Scheme 164.** Attempted Diels-Alder Reaction with **562** under Thermal Conditions



To this end, ketone **562** was considered as a viable substitute for  $\beta$ -chloro- $\alpha$ -methyl acrolein. **562** was synthesized from **475** by employing two straightforward synthetic operations. **475** was treated with methyl magnesium bromide at 0 °C to give an allylic alcohol, which was subjected to manganese dioxide mediated oxidation to produce methyl ketone **562** in 75% yield over two steps (Scheme 164). **562** could be stored for

months without decomposition. The ketone was subsequently subjected to a Diels-Alder reaction under thermal conditions. Unfortunately, desilylation of the diene was observed under a variety of conditions, including various temperatures and solvents, to provide the corresponding enal (**552**). It was realized that the Diels-Alder reaction under thermal conditions would not be straightforward. It became obvious that a more stable protecting group than TBS group was required to carry out this demanding cycloaddition. Subsequently, the syntheses of a number of stable dienes were undertaken.

At first, we turned our attention towards the synthesis of dienol acetate **566**. The synthesis commences with **553**. Treatment of this compound with phenylacetyl fluoride in the presence of catalytic amount of TBAF provided **566** in a modest yield (Scheme 165). Dienol acetate was stable upon storage for an extended period of time. Surprisingly, treatment of **566** with dienophile **562** under thermal conditions led to enal **552**. It was hypothesized that the dienol acetate was undergoing saponification in the reaction work up.

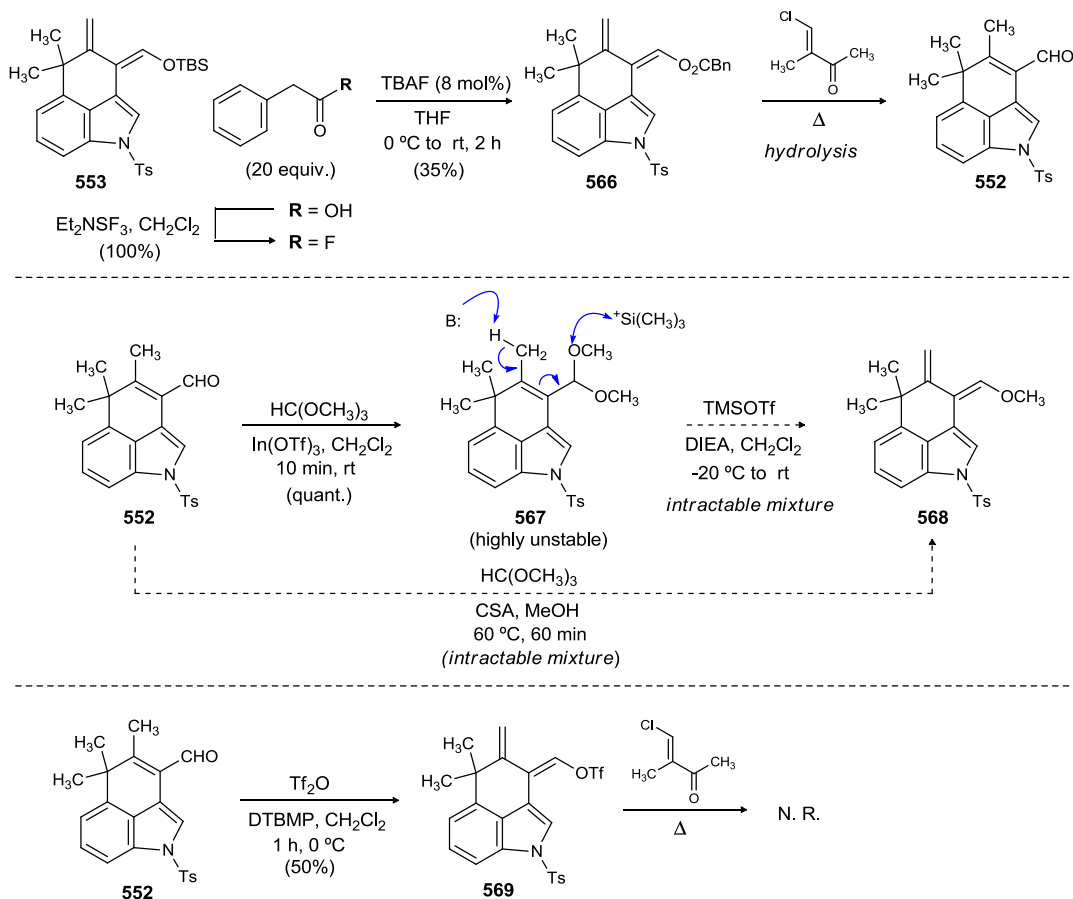
Another dienophile considered was methyl dienol ether **568**. Treatment of enal **552** with methyl orthoformate in the presence of catalytic amount of indium triflate provided the highly unstable acetal **567** in quantitative yield, which was immediately treated with TMSOTf. It was hoped that this would lead to the elimination of MeOH, to provide the desired **568**. However, decomposition of the starting material was observed under these reaction conditions. Screening a variety of Lewis acids to effect the desired transformation was unsuccessful as well. Efforts to carry out the one pot synthesis of **568**, utilizing trimethyl orthoformate and *p*-TsOH, were equally unsuccessful.<sup>186</sup>

---

<sup>186</sup> Harmata, M.; Bohnert, G.; Kurti, L.; Barnes, C. L. *Tetrahedron Lett.* **2002**, *43*, 2347.

The attempted Diels-Alder reaction with dienol triflate **569**, available in one step from **552**, led only to the isolation of unreacted starting materials

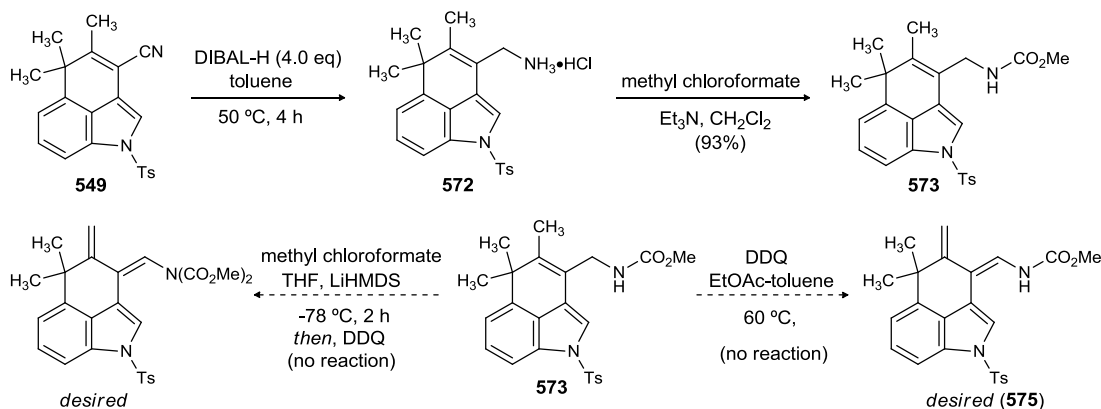
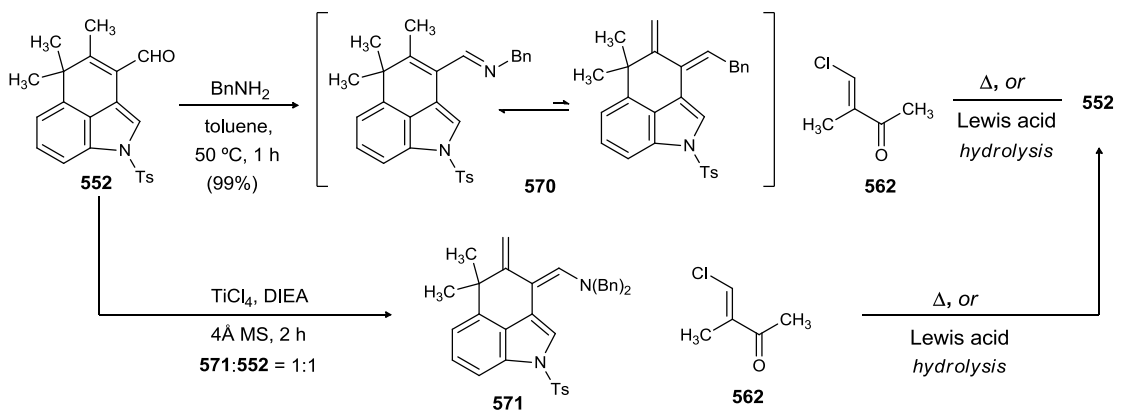
**Scheme 165.** Attempted Diels-Alder with Dienol Ether **568**, Dienol Acetate **566** and Dienol Triflate **569**



At this stage, the synthesis of comparatively more stable dienamines was also investigated. Treatment of enal **552** with benzyl amine provided imine **570**, which was subsequently subjected to the Diels-Alder reaction conditions (Scheme 166). It was hoped that under these conditions, an equilibrium between **570** and the corresponding dienamine might exist, leading to the formation of desired Diels-Alder adduct. However, the only product observed in the crude NMR analysis was enal **552**. After some experimentation we were able to synthesize dibenzyl dienamine **571**, upon treatment of

**552** with  $\text{TiCl}_4$ , as a 1:1 inseparable mixture with **552**. Unfortunately, hydrolysis of **571** was observed upon treatment with **562** under thermal conditions.

**Scheme 166.** Attempted Synthesis of Various Dienamines



The synthesis of these dienamines proved to be more challenging than anticipated. In one of our last attempts to access dienamine **575**, we considered a slightly different approach. To this end, treatment of  $\alpha,\beta$ -unsaturated nitrile **549** with excess DIBAL-H provided amine **572** (Scheme 166). Treatment of **572** with methyl chloroformate in presence of triethyl amine provided carbamate **573**. It was believed that the treatment of **573** with DDQ would lead to the formation of corresponding enamine which would isomerise to provide thermodynamically more stable dienamine **575**. To our disappointment, carbamate **573** remained unreactive under a variety of DDQ-mediated

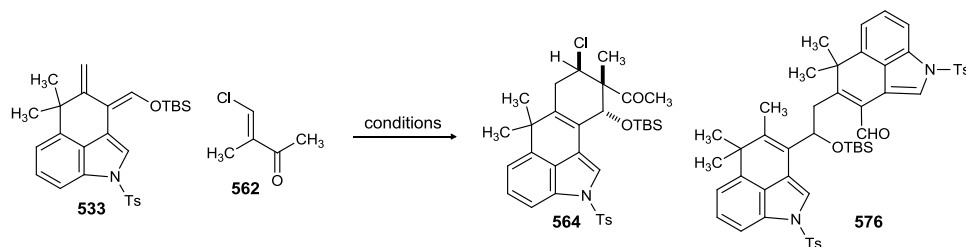
oxidative conditions. Treatment of **573** with methyl carbamate was also unsuccessful, as starting materials were isolated in all these cases. Employing harsh conditions to carry out these transformations only led to an intractable mixture.

#### ***3.4.11. Lewis Acid Mediated Diels-Alder Reaction of Silyldienol Ether 553 with 562***

At this juncture it was realized and accepted that a Diels-Alder reaction under thermal conditions was not likely feasible. In search of milder conditions to carry out this transformation, our attention focused on evaluating Lewis acids for this purpose. Subsequently, a variety of Lewis acids were screened to carry out the Diels-Alder reaction (Table 4). At the outset, our efforts took a major setback when Et<sub>2</sub>AlCl, Me<sub>3</sub>Al and Ti(<sup>i</sup>OPr)<sub>4</sub> all provided the earlier observed hydrolyzed enal **552** at 0 °C (entry 9, 10, 15). Hydrolysis of the diene was also observed when strong acids were employed in this reaction (entries 12, 13, 14). In the event, we were pleased to observe that the desired Diels-Alder adduct **564** could be isolated in 18% yield by employing TMSOTf as the Lewis acid (entry 1). Replacing TMSOTf with TBSOTf as the Lewis acid in this reaction didn't provide any observable improvement (entries 2-4). Although encouraging, TMSOTf and TBSOTf mediated reactions led to a substantial decomposition of the starting diene (**553**). In an effort to increase the yield of the Diels-Alder reaction, some other Lewis acids were attempted. Gratifyingly, the Diels-Alder reaction with TiCl<sub>4</sub> and SnCl<sub>4</sub> led to an improvement of the Diels-Alder adduct yield (entries 5-7). Varying amount of Mukaiyama aldol side product **576** was also isolated, along with the hydrolyzed enal (**552**), under these reaction conditions. After some experimentation, we were pleased to find out that that the Mukaiyama aldol side product **576** could be recycled to enal **552** upon treatment with TiCl<sub>4</sub>, with almost no loss in material

throughput. The isolation of Mukaiyama aldol side product **576** was more prominent in entries 16-19. The Diels-Alder reaction was finally optimized when EtAlCl<sub>2</sub> was utilized as the Lewis acid (entry 22).

**Table 4.** Lewis Acid Screen to Effect the Diels-Alder Reaction



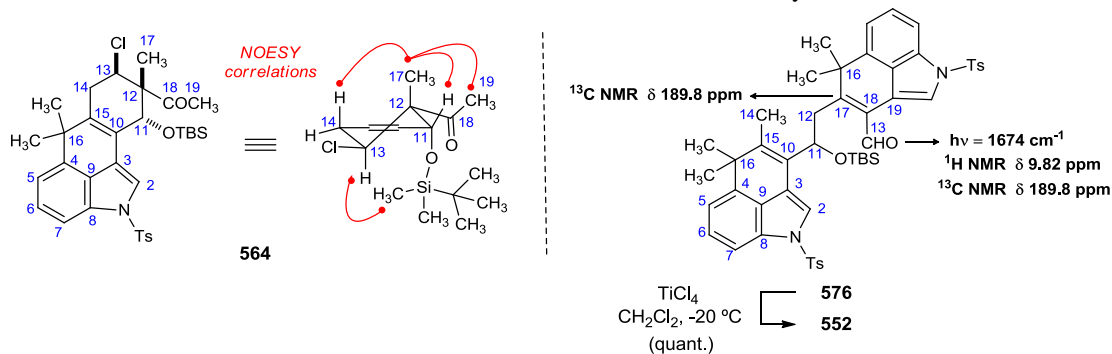
entry	lewis acid	condition	time (h)	<b>564:576:562<sup>a</sup></b>	yield <sup>b</sup>
1	TMSOTf	CH <sub>2</sub> Cl <sub>2</sub> , -78 °C	2	1:0:1	18%
2	TBSOTf	CH <sub>2</sub> Cl <sub>2</sub> , -78 °C to -20 °C	2	1:0:0	14%
3	TBSOTf	CH <sub>2</sub> Cl <sub>2</sub> , -20 °C	0.5	1:0:0	10%
4	TBSOTf	CH <sub>2</sub> Cl <sub>2</sub> , -78 °C	1	1:0:0	20%
5	TiCl <sub>4</sub>	CH <sub>2</sub> Cl <sub>2</sub> , -20 °C	0.5	1:3:1 <sup>c</sup>	90% (24%) <sup>e</sup>
6	TiCl <sub>4</sub>	CH <sub>2</sub> Cl <sub>2</sub> , -78 °C	3	2:1:1 <sup>c</sup>	75% (34%) <sup>e</sup>
7	SnCl <sub>4</sub>	CH <sub>2</sub> Cl <sub>2</sub> , -78 °C	3	2:8:1 <sup>c</sup>	85% (20%) <sup>e</sup>
8	Ti( <sup>i</sup> OPr) <sub>4</sub>	CH <sub>2</sub> Cl <sub>2</sub> , -78 °C	4	0:0:0	N.R.
9	Ti( <sup>i</sup> OPr) <sub>4</sub>	CH <sub>2</sub> Cl <sub>2</sub> , 0 °C	12	0:0:1	quant. <sup>d</sup>
10	Et <sub>2</sub> AlCl	CH <sub>2</sub> Cl <sub>2</sub> , -78 °C	N.R.	0:0:0	N.R.
11	Et <sub>2</sub> AlCl	CH <sub>2</sub> Cl <sub>2</sub> , -78 °C	12	0:0:1	quant. <sup>d</sup>
12	TfOH	CH <sub>2</sub> Cl <sub>2</sub> , -78 °C	0.5	0:0:1	quant. <sup>d</sup>
13	<i>p</i> -TsOH	CH <sub>2</sub> Cl <sub>2</sub> , -78 °C	1	0:0:1	quant. <sup>d</sup>
14	MsOH	CH <sub>2</sub> Cl <sub>2</sub> , -78 °C	10	0:0:1	quant. <sup>d</sup>
15	(CH <sub>3</sub> ) <sub>3</sub> Al	CH <sub>2</sub> Cl <sub>2</sub> , 0 °C	6	0:0:1	quant. <sup>d</sup>
16	Sc(OTf) <sub>3</sub>	CH <sub>2</sub> Cl <sub>2</sub> , -78 °C	2	1:5:0	80% (12%) <sup>e</sup>
17	Cu(OTf) <sub>2</sub>	CH <sub>2</sub> Cl <sub>2</sub> , -20 °C	3	0:2:5	85%
18	Ce(OTf) <sub>3</sub>	CH <sub>2</sub> Cl <sub>2</sub> , -20 °C	3	0:1:10	80% (8%) <sup>e</sup>
19	Al(OTf) <sub>3</sub>	CH <sub>2</sub> Cl <sub>2</sub> , -20 °C	3	1:7:0	60% (12%) <sup>e</sup>
20	EtAlCl <sub>2</sub>	CH <sub>2</sub> Cl <sub>2</sub> , -78 °C	4	5:1:1	70% (48%) <sup>e</sup>
21	Et <sub>2</sub> AlCl <sub>2</sub>	CH <sub>2</sub> Cl <sub>2</sub> , -20 °C	1	3:1:0	55% (36%) <sup>e</sup>
22	<b>Et<sub>2</sub>AlCl<sub>2</sub></b>	<b>CH<sub>2</sub>Cl<sub>2</sub>, -78 °C to -20 °C</b>	<b>2.5</b>	<b>13:1:1</b>	<b>74% (59%)</b>

<sup>a</sup> determined by crude NMR analysis. <sup>b</sup> combined yield of three products are reported. <sup>c</sup> the yield of the reactions were very inconsistent, as a result average yield and of three runs are reported. <sup>d</sup> determined by crude NMR analysis. <sup>e</sup> yield of the isolated Diels-Alder adduct (**564**)

The desired Diels-Alder adduct (**564**) (*single diastereomer*) could be isolated in 59% yield (70% brsm), along with a trace amount of the Mukaiyama aldol side product (**576**) and hydrolyzed enal. This successful Diels-Alder reaction led to the construction of the ABCD-ring system with the strategically placed functional group for further manipulation of cyclohexene ring.

A complete 2D NMR analysis was carried out to elucidate the structure of Diels-Alder adduct **564** (Scheme 167). NOESY correlations from both H11 to H17 and H11 to C19, and the absence of NOESY correlations between H11 to either H13 or H14, suggested that the H11 proton was equatorial. Additionally, a NOESY correlation between TBS-methyl protons and H13 $\alpha$  indicated that the -OTBS was in the axial position, thus confirming the stereochemistry at C11. These observations support the assignment of the Diels-Alder adduct as depicted.

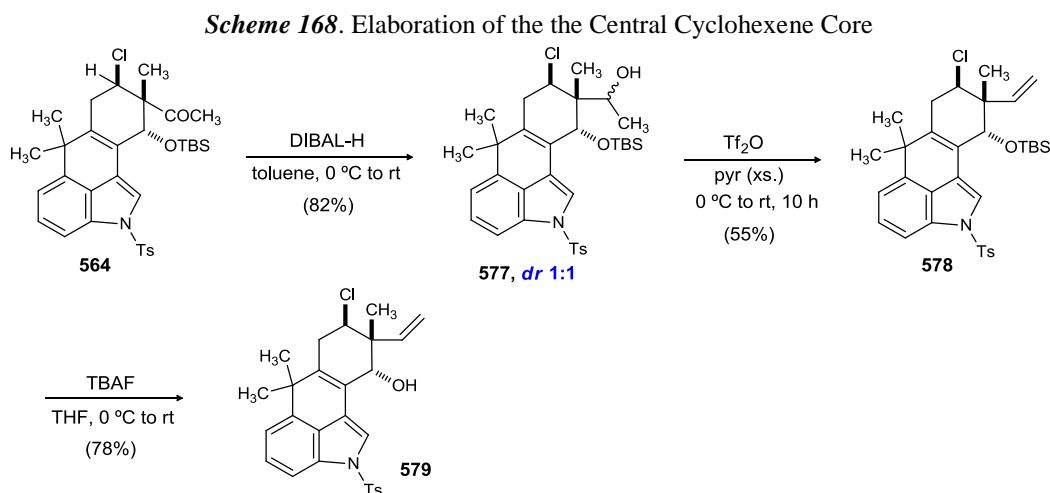
**Scheme 167.** Structure Elucidation of Diels-Alder and Mukaiyama Aldol Adduct



$^1\text{H}$  NMR and  $^{13}\text{C}$  NMR analysis was utilized to elucidate the structure of Mukaiyama side product **576** (Scheme 167). The  $^1\text{H}$  NMR analysis showed one well resolved dd pattern at 4.95, in addition to two poorly resolved patterns at 3.30 and 2.25, which can be assigned as the methine (C11) and methylene (C12) adjacent to each other. A weak IR stretch at  $1675 \text{ cm}^{-1}$ , and the presence of  $^1\text{H}$  NMR and  $^{13}\text{C}$  NMR peaks at 9.82 and 189.8 ppm indicated the presence of an  $\alpha,\beta$ -unsaturated aldehyde. The presence of an enal was confirmed by the downfield shift of C17 in the  $^{13}\text{C}$  NMR spectrum (159.0 ppm).

### 3.4.12. Cyclohexene Ring Functionalization

With the tetracyclic core of the hapalindoles in place, elaboration of the cyclohexene ring was carried out next. To this end, treatment of **564** with DIBAL-H provided the alcohol as an inconsequential mixture of diastereomers (**577**, 1:1 ratio of diastereomers) (Scheme 168). Surprisingly, the ketone (**564**) was inert to sodium borohydride and lithium borohydride mediated reduction conditions. This unreactivity could be attributed to the sterically shielded nature of ketone group. With alcohol **577** in hand, different strategies were evaluated to elicit the desired elimination process to provide **578**.

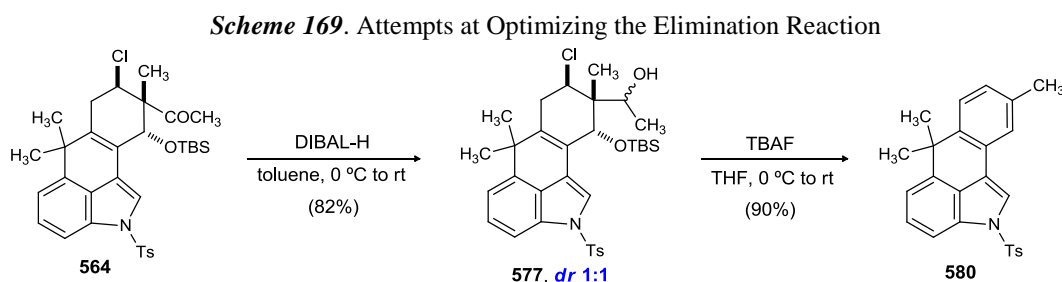


Treatment of **577** with martin sulfurane led to the desired product as an inseparable mixture with the starting material. In another set of experiments, alcohol **577** was converted cleanly to the corresponding triflate upon treatment with triflic anhydride. However, purification of the intermediate triflate proved challenging due to its facile conversion to **578** on  $\text{SiO}_2$  or upon standing for a long duration of time. Subsequently, a one pot tandem alcohol triflation/elimination sequence was carried out by exposing the diastereomeric alcohols to  $\text{Tf}_2\text{O}$  and excess of pyridine. The desired elimination product

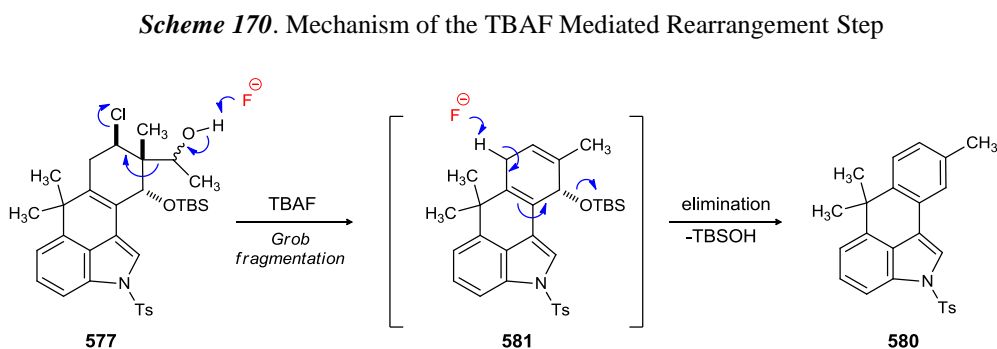


(**578**) was isolated in a modest yield. Deprotection of the TBS group, upon treatment with TBAF, provided alcohol **579**.

In an effort to increase the yield of elimination step, a different synthetic approach was considered. It was believed that the bulky silyl group was shielding one of the alcohol diastereomers (**577**) and thus leading to lower yields of elimination product **578**. In this new approach, we considered unmasking the alcohol functionalization before the elimination step. To this end, the alcohol diastereomers (**577**) were treated with TBAF at 0 °C. To our surprise, a conjugated tetracycle **580**, instead of the desired desilylation product, was isolated from the reaction (Scheme 169).

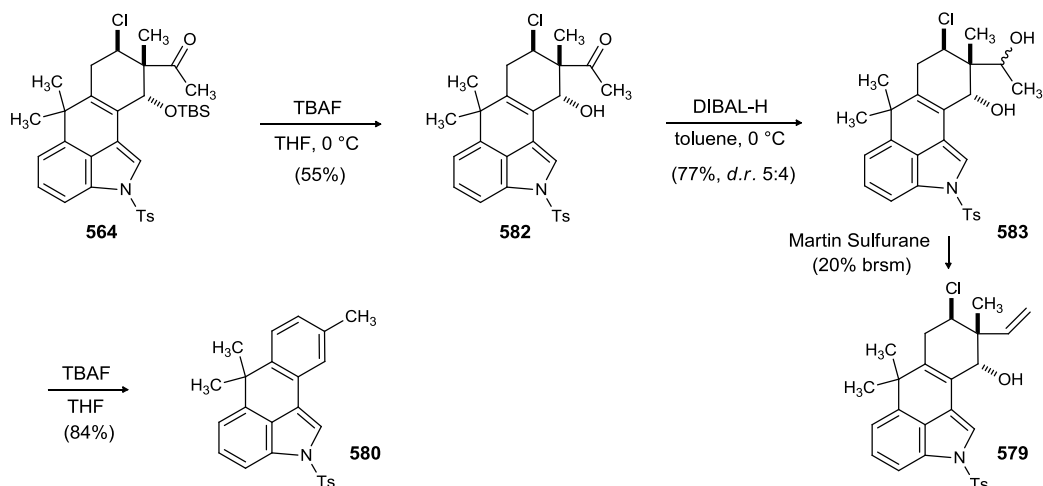


A mechanism for the undesired formation of **578** has been proposed. Treatment of alcohols with TBAF provides the intermediate **581** via a Grob fragmentation process. Subsequent aromatization of the D-ring by elimination of TBSOH provides the known tetracycle (**580**).



To circumvent the undesired Grob fragmentation pathway, we slightly modified our previous strategy. The silyl deprotection was carried out on the Diels-Alder adduct to provide keto-alcohol **582**. Treatment of **582** with DIBAL-H provided the diol as an inconsequential mixture of diastereomers (**583**, 5:4 ratio of diastereomers) (Scheme 169). Treatment of diols **571** with Martin sulfurane led to a very low yield of desired product **579**. Other conditions evaluated didn't provide any improvement over our previous established protocol (Scheme 171). Additionally, the diols (**583**) were found to be unstable and could be easily converted to the tetracycle upon treatment with TBAF or upon standing for few days at room temperature.

**Scheme 171.** Alternate Attempted Strategy to Circumvent the Formation of Undesired Tetracycle **580**

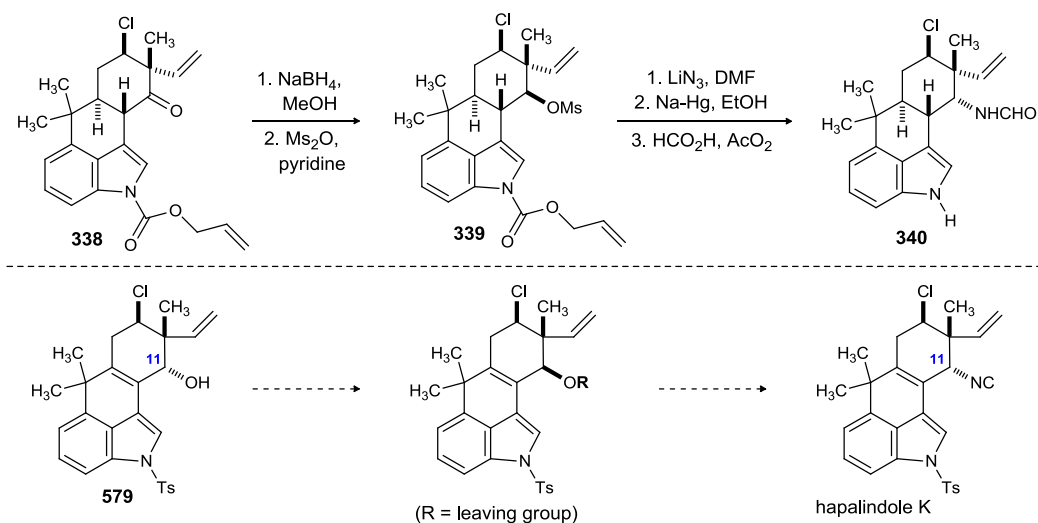


### 3.4.13. Appending the C11-N Bond Using an Established $S_N2$ Reaction Protocol

At this stage, allylic alcohol **579** was thought of as a late-stage intermediate that could be used to access ( $\pm$ )-hapalindole K. The only task that remained to achieve the total synthesis was the installation of the C11-N bond. In his synthesis of hapalindole G, Fukuyama *et al.* has demonstrated a 5 step protocol to achieve this task from ketone

(Scheme 172).<sup>130</sup> The synthetic sequence included the reduction of the ketone with NaBH<sub>4</sub>, followed by mesylation of the resulting alcohol to afford mesylate **339**. Displacement of the mesylate by an azide with concomitant deprotection of allyl urethane, and subsequent reduction of the azide followed by formylation afforded **340**. Our first generation synthetic strategy employed Fukuyama's protocol to forge the C11-N bond, which was necessary to append the desired isocyanide functionality of hapalindole K (Scheme 172).

*Scheme 172.* First Generation Synthetic Strategy towards Hapalindole K

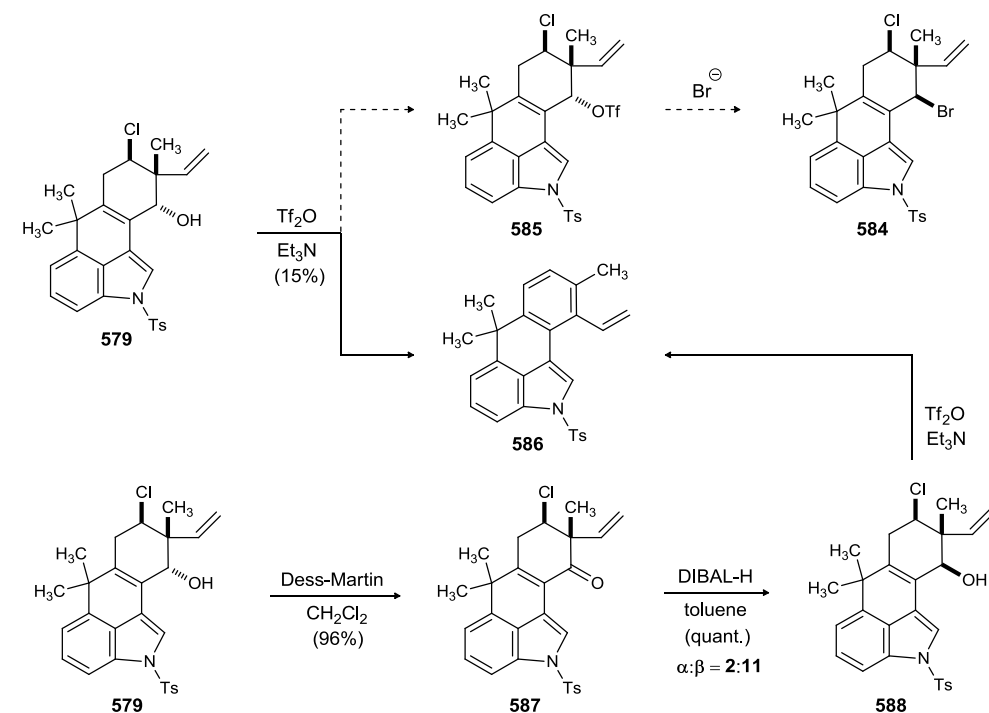


Our synthetic plan to access the desired intermediate **584** (Scheme 173) was through the nucleophilic substitution of  $\alpha$ -triflate **585** with bromide anion. To this end, **579** was treated with triflic anhydride and triethyl amine at 0 °C. To our surprise, the starting material underwent decomposition under these reaction conditions. The decomposition was perhaps influenced by the presence of the chloride and C10-C15 unsaturation. The only isolable product from this reaction was the rearranged tetracycle **586**.

Failure to synthesize the desired intermediate through a intermolecular nucleophilic substitution reaction, prompted us to follow Fukuyama's established synthetic route. To

this end, the  $\alpha$ -alcohol was converted to enone **587** upon treatment with Dess-Martin periodinane (Scheme 173). Exposure of **587** to DIBAL-H provided the alcohol as an inseparable mixture of diastereomers (**588**, 11:1  $\beta$ : $\alpha$ ). Disappointingly, treatment of alcohol with either  $\text{Tf}_2\text{O}$  or  $\text{Ms}_2\text{O}$  led to the decomposition of starting material. A trace amount of tetracycle **586** was also isolated under these reaction conditions.

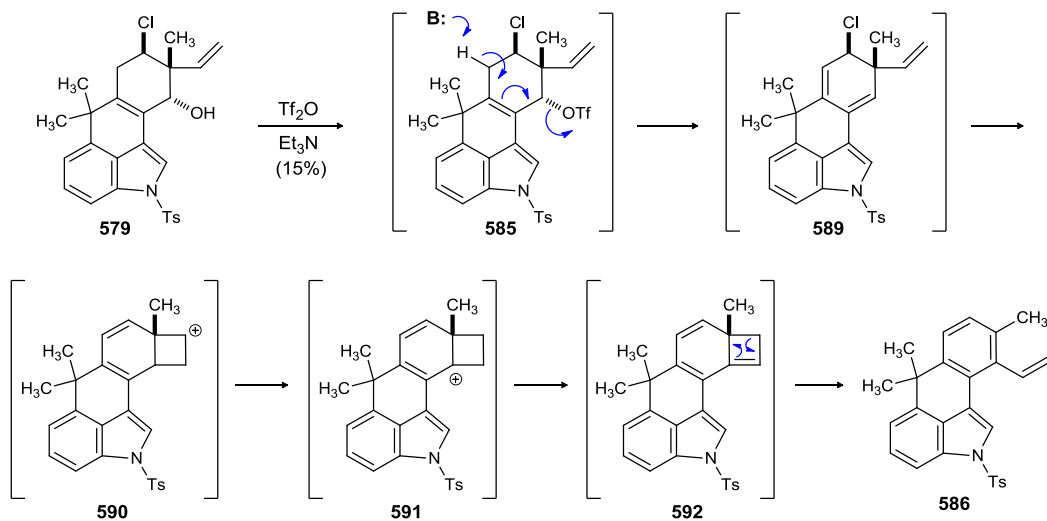
**Scheme 173.** First Generation Synthetic Strategy towards Hapalindole K



Based on these results, a mechanism for this domino reaction was proposed (Scheme 174). Treatment of **567** with  $\text{Tf}_2\text{O}$  and  $\text{Et}_3\text{N}$  provides triflate **585**, which *in situ* underwent a base promoted elimination step to provide **589**. Formation of cyclobutyl carbocation with concomitant elimination of the neopentyl chloride provides **590**. The secondary carbocation in **590** was converted to a more stable tertiary carbocation **579**, which subsequently underwent a base promoted elimination step to provide pentacycle

**580.** To relieve the strain in **592**, the cyclobutene ring undergoes a pericyclic ring opening reaction to provide the conjugated tetracycle (**586**).

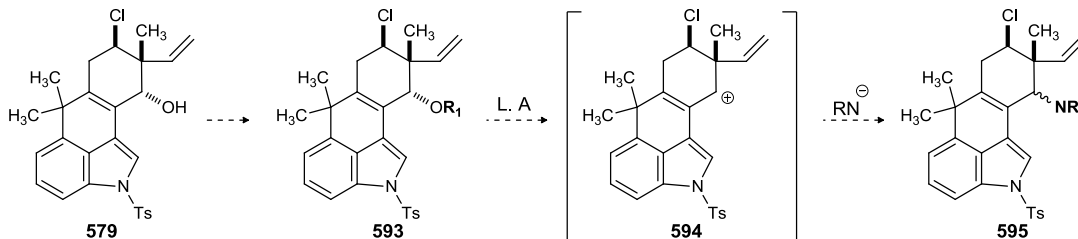
**Scheme 174.** Proposed Mechanism of Elimination/Rearrangement Reaction Side Product



#### 3.4.14. Total Synthesis of Hapalindole K

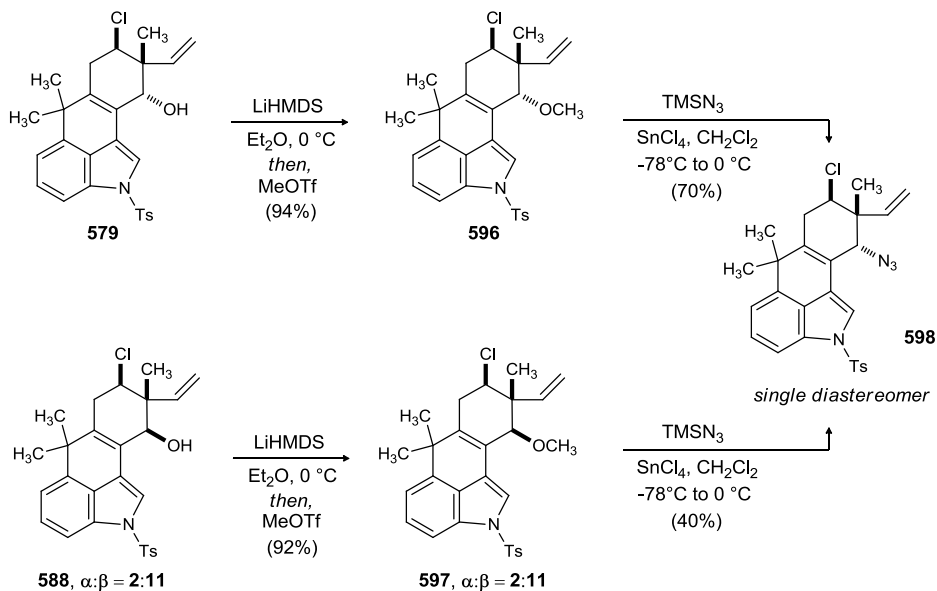
Failure to append the desired C11-N bond using an established five step protocol necessitated yet another synthetic re-evaluation. Therefore, C11-N bond construction via an  $S_N1$  process was investigated. In this strategy, we hypothesized that treatment of an allyl ether species like **593** (R = OCOMe, OMe) with a Lewis acid would lead to a stable secondary allylic carbocation **594** (Scheme 175). Trapping the carbocation with an amine source would lead to **595**. Although the approach was promising, we were concerned with the diastereoselective outcome of this reaction.

**Scheme 175.** Second Generation Synthetic Strategy towards Hapalindole K



The synthesis of methyl allyl ethers (**596** and **597**) were undertaken first (Scheme 176). To this end treatment of **579** or **588** with LiHMDS and MeOTf provided the corresponding ethers in excellent yields. Due to the instability of the related systems in our previous route, the use of an  $S_N1$  process to construct the desired C11-N bond was approached with some trepidation. However, these fears proved to be unfounded as treatment of  $\alpha$ -methyl ether **596** with  $TMSN_3$  and  $SnCl_4$  provided  $\alpha$ -azide **598** in modest yield, but more importantly as a *single diastereomer*. To our delight, 2D NMR analysis revealed the desired  $\alpha$ -diastereoselection

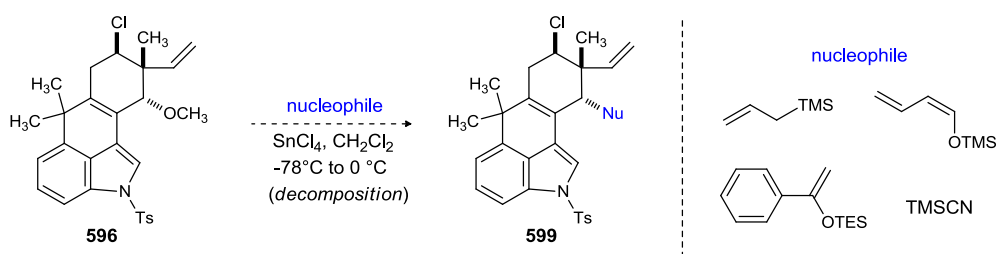
**Scheme 176.** Application of an  $S_N1$  Process to Construct the Desired C11-N Bond



Subjecting the  $\beta$ -isomer (**597**) to these reaction conditions also provided the desired  $\alpha$ -azide **598** albeit in slightly lower yield.

Encouraged by this result, we explored the possibility of using other nucleophiles in this reaction. A number of carbon based nucleophiles were screened under the same reaction conditions (Scheme 177). However, only the decomposition of the starting materials were observed under these reaction conditions

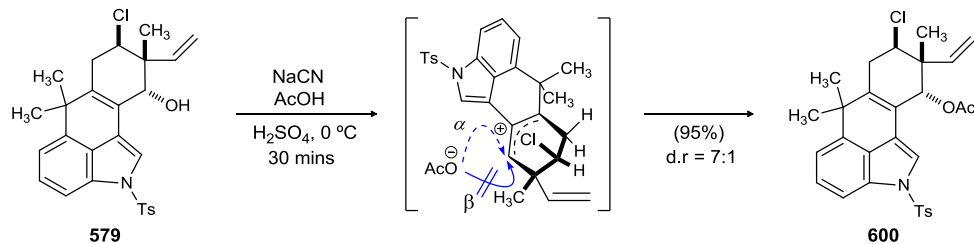
**Scheme 177.** Unsuccessful Attempt at Using a Carbon Nucleophile to Trap the Intermediate Carbocation **594**



At this stage, we also considered the viability of a Ritter reaction to elicit the desired C11-N bond formation. In the event, treatment of alcohol **579** with NaCN in an AcOH-H<sub>2</sub>SO<sub>4</sub> solvent system provided the acetate **600** in excellent yield and good diastereoselection (d.r = 7:1) (Scheme 178). That retention of configuration was observed suggested that the reaction proceeded via a stabilized allylic carbocation. At the outset, this result was surprising because the expected product of this reaction was the corresponding  $\alpha$ -formamide. We hypothesized that the formation of solvolysis product (acetate **600**) occurred due to the decomposition of NaCN in the AcOH-H<sub>2</sub>SO<sub>4</sub> solvent system.<sup>187</sup> The solvolysis product (**600**) was also formed when **579** was exposed to AcOH-H<sub>2</sub>SO<sub>4</sub> solvent system

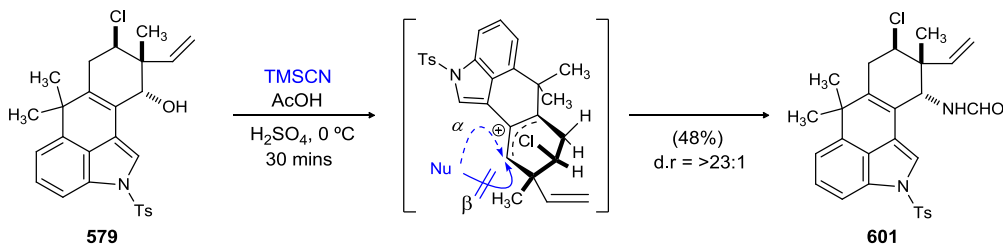
<sup>187</sup> Jirgensons, A.; Kauss, V.; Mishnev, A. F.; Kalvish, I. *J. Chem. Soc., Perkin Trans. 1*, **1999**, 3527.

**Scheme 178.** A Solvolysis product with Acetic Acid as the Nucleophile



Although non-productive, our efforts to convert alcohol **579** to the desired formamide **601** did illustrate the need for exploring other nucleophilic nitrogen sources to forge the desired C11-N bond. In the event, performing the Ritter reaction using TMSCN as a nitrogen source provided formamide **601** in a modest yield and as a *single diastereomer* (Scheme 179). Due to the bulky nature of the trimethylsilyl group, the nucleophile approaches from the less hindered α-face. The formamide (**601**) was isolated as an inseparable mixture of *cis*- and *trans*-rotamers.

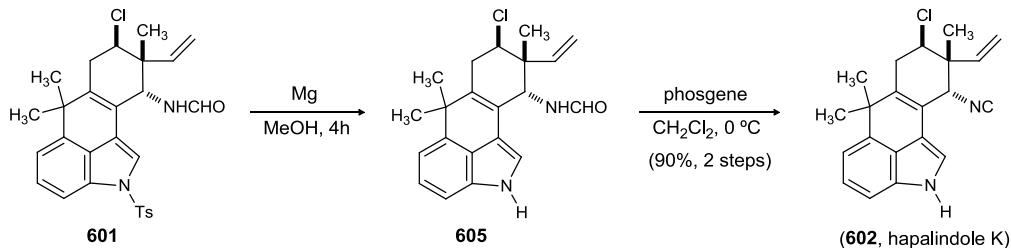
**Scheme 179.** A Ritter Reaction with TMSCN as the Nucleophile



Subsequently, the synthesis of hapalindole K was completed in two straightforward synthetic operations (Scheme 180). Tosyl deprotection was achieved by treatment with magnesium and methanol. The crude formamide (**605**) was treated with phosgene and Et<sub>3</sub>N at 0 °C to provide (±)-hapalindole K (**602**) in 90% yield over two steps.



**Scheme 180.** Total Synthesis of Hapalindole K (Completion)

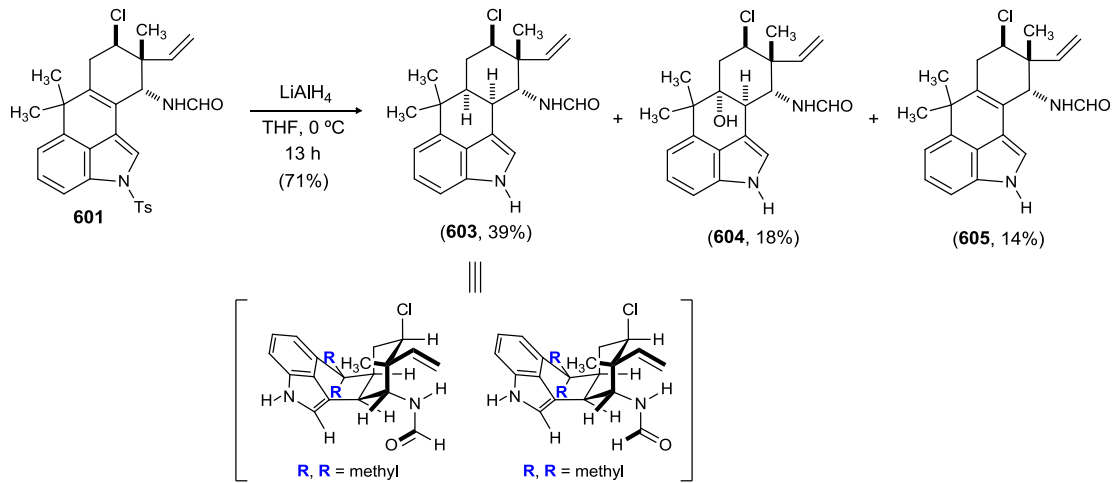


### 3.4.15. Total Synthesis of Hapalindole A

Hapalindole A exhibits two additional chiral centers at C15 and C10 in the perhaps higher energy *cis*-decalin ring system (rings **C** and **D**). Our initial strategy to solve this problem involved an alcohol directed metal catalyzed diastereoselective reduction of the allylic alcohol **579**. In due course, we came across the earlier work of Natsume *et al.* which involved a  $\text{LiAlH}_4$  mediated diastereoselective reduction of an allylic alcohol/formamide with the concomitant tosyl deprotection of a non-chlorinated tetracyclic hapalindole skeleton to provide the *cis*- fused CD-ring system.<sup>188</sup> However, we were concerned that this elegant transformation might not work in our case due to the presence of the neopentyl chloride. To our surprise, the troublesome neopentyl chloride is compatible with these reaction conditions. Exposure of formamide **601** to lithium aluminum hydride provided the desired formamide **603** (Scheme 181). Additionally, alcohol **604** and the detosylated indole **605** could be isolated as minor products. The optimization of this reaction, to limit the formation of the undesired side product, was not carried out.

<sup>188</sup> Muratake, H.; Natsume, M. *Tetrahedron* **1990**, *46*, 6343.

**Scheme 181.** Appending the *cis*-Decalin Ring System of Hapalindole A



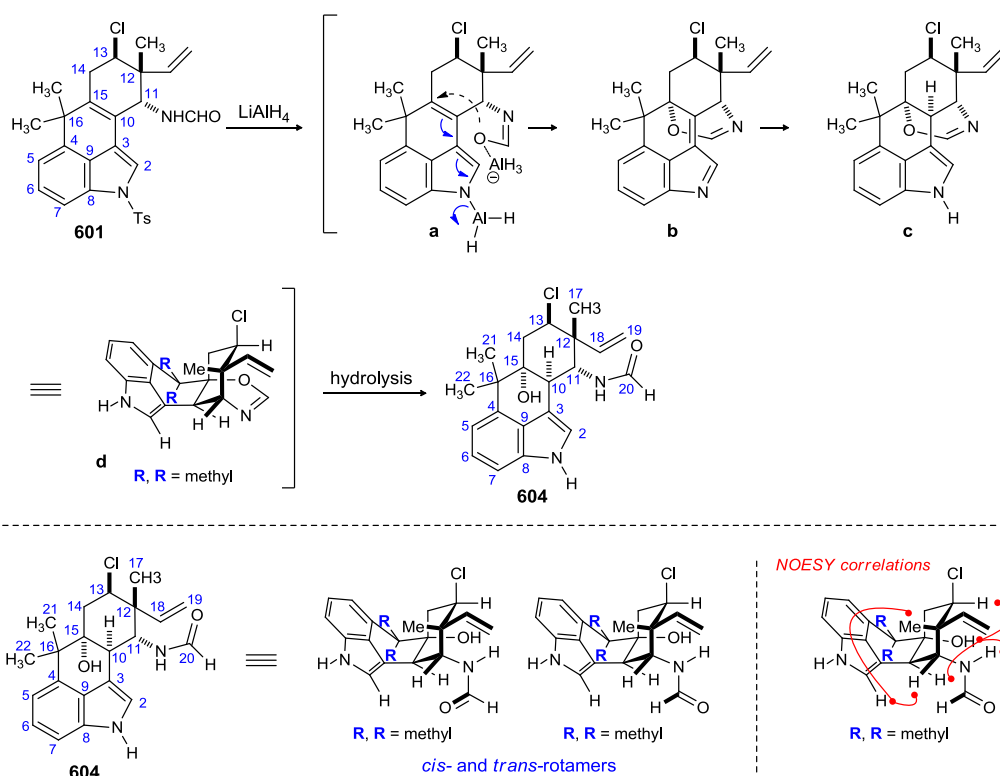
In this elegant transformation, formation of two new chiral centers and detosylation takes place in one synthetic operation. Formamide **603** was isolated as an inseparable mixture of *cis*- and *trans*-rotamers.

A mechanism for the formation of **603** was proposed by Natsume *et al.* Treatment of **601** with  $\text{LiAlH}_4$  led to the reductive cleavage of the tosyl group thus forming a 1-indolylaluminium derivative **a**, with an aluminum-chelated formamide oxygen at C11 (Scheme 182). The formamide oxygen attacks C15 in a conjugate fashion and the resulting anion at C10 aids the liberation of the lithium aluminum anion to yield  $\alpha,\beta$ -unsaturated indolenine derivative **b** having a dihydro-1,3-oxazine ring. The subsequent hydride attack at C10 by  $\text{LiAlH}_4$ , probably chelated to the formamide oxygen, may produce an intermediate **c** which is hydrolyzed during the work-up to form the C15 hydroxylated product **604**.

The structure of **604** was confirmed by 2D NMR analysis (Scheme 182). The  $^1\text{H}$  NMR analysis indicated a 5:1 mixture of *cis*- and *trans*-rotamers and, as a result, the NMR peaks in general were broadened. First, HSQC was used to assign the formamide –

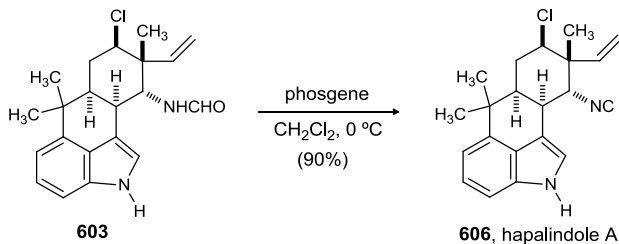
NH and –OH protons and then NOESY correlations were used to assign the stereochemistry of the newly formed quaternary center (C15). The alcohol proton shows strong correlations to the formamide –NH, H13, and H10. As previously elucidated, the formamide functionality is  $\alpha$  which indicates that the newly formed quaternary center has an  $\alpha$ -OH. Additionally, the formamide –NH was observed to shift downfield ( $\delta$  7.37 ppm) which also suggests the possibility of hydrogen bonding with  $\alpha$ -OH. The presence of a NOESY correlation between H2, H11 and H2, H17 also supports the assigned chair conformation of the cyclohexane core.

**Scheme 182.** Structural Elucidation and Proposed Mechanism for the Formation of Formamide **604**



Finally, treatment of formamide **603** with phosgene provided hapalindole A in excellent yield (Scheme 183).

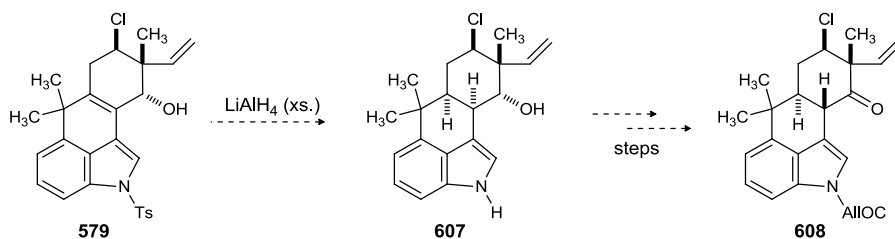
**Scheme 183.** Total Synthesis of Hapalindole A



**3.4.16. Formal Synthesis of hapalindole G**

The synthetic strategy, to access hapalindoles A and K could also be extended to the thermodynamically stable *trans*-decalin (rings **C** and **D**) containing hapalindoles. In this modified synthetic route, we planned on utilizing Nastsume's hydroalumination approach to access tetracycle **607** (Scheme 184).<sup>190</sup> We were hopeful that **607** could be subsequently converted to **608** in a few steps.

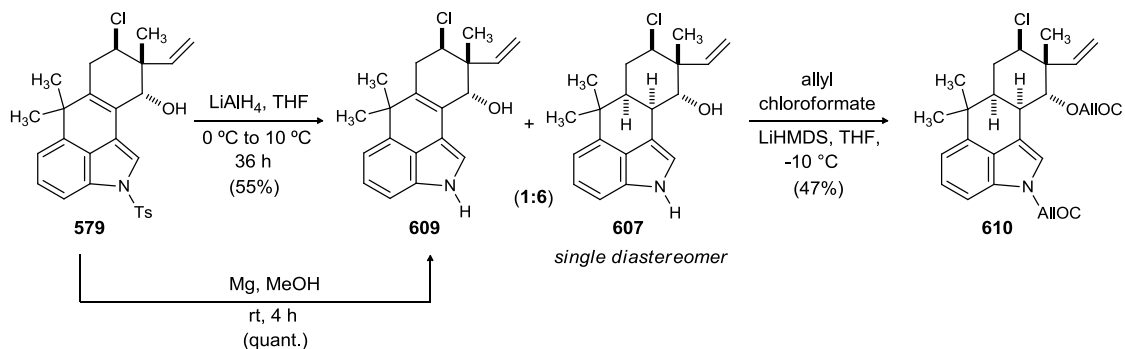
**Scheme 184.** Synthetic Strategy towards the Formal Synthesis of Hapalindole G



Gratifyingly, treatment of allylic alcohol **579** with  $\text{LiAlH}_4$  provided the the desired tetracycle **607** in modest yield. The reaction was sluggish, but could be driven to completion by performing it at higher temperature and for an extended period of time. Additionally, alcohol **609** could be isolated as minor product. **609** could also be accessed by treatment of alcohol **609** with Mg and MeOH. At this stage, all our efforts to selectively protect the indole nitrogen in presence of the C11-alcohol turned out to be

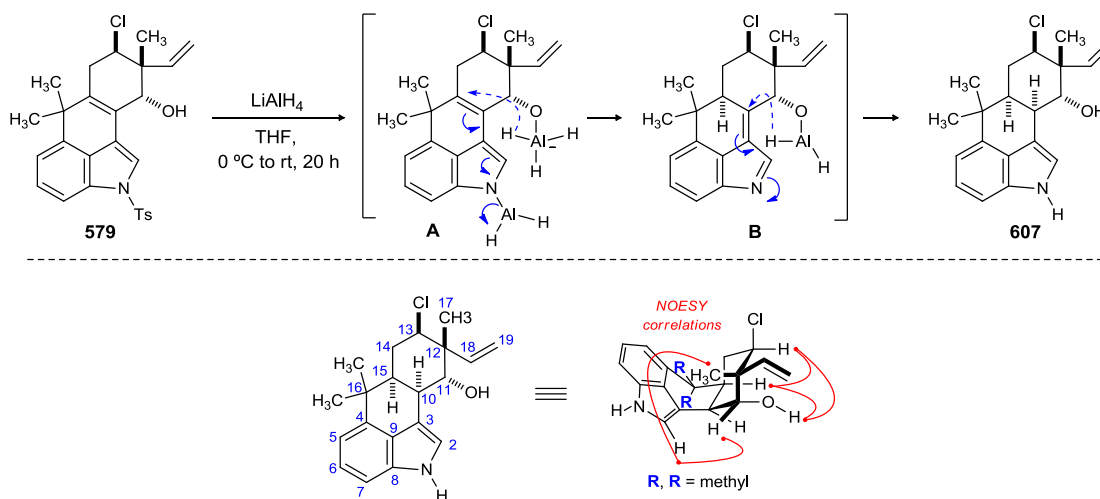
unsuccessful. Treatment of **607** with allyl chloroformate led to bis-protected tetracycle **610** (Scheme 185).

**Scheme 185.** LiAlH<sub>4</sub>-Mediated Diastereoselective Reduction of Allylic Alcohol **579**



The mechanism of the LiAlH<sub>4</sub> reduction in this case is reminiscent of the one used before in the synthesis of hapalindole A.

**Scheme 186.** Proposed Mechanism of LiAlH<sub>4</sub> Mediated Diastereoselective Reduction of **579**

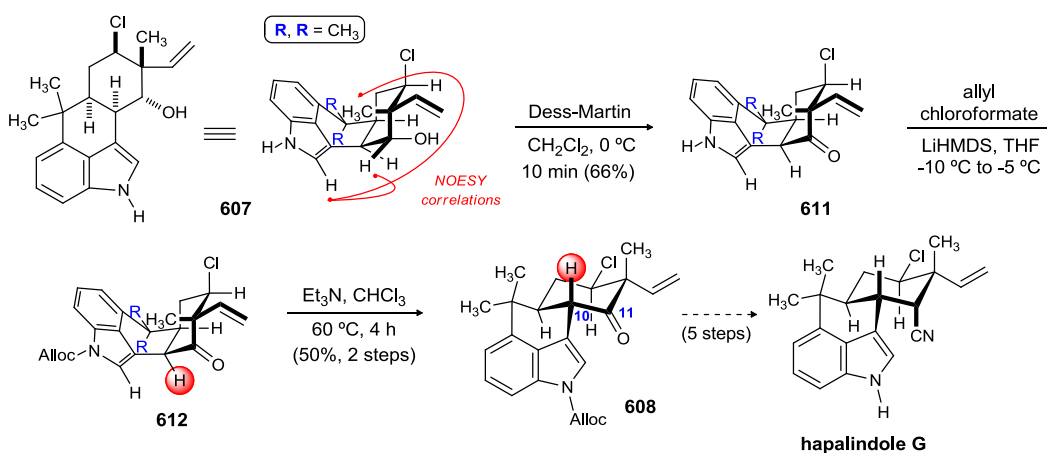


Formation of indolylaluminum derivative **A** was followed by the addition of the aluminum-chelated C15 oxygen to C15 in a conjugate fashion. The resulting anion at C10 aids in the liberation of the lithium aluminum hydride anion to yield  $\alpha,\beta$ -unsaturated indolenine derivative **B**. The subsequent hydride attack at C10 by LiAlH<sub>4</sub>, probably

chelated to the C11 oxygen, provides **607**. 2D NMR analysis confirmed the assigned structure of **607**.

Our inability to selectively protect the indole nitrogen in **607** prompted us to consider other ways to elicit this task. We hoped that this problem could be solved by oxidizing the C11 alcohol **607** to the C11 ketone **611**. To this end, alcohol **607** was treated with Dess-Martin periodinane to provide ketone **611** (Scheme 187).

**Scheme 187.** Formal Synthesis of Hapalindole G



At this stage, we were concerned that the higher acidity of the C10 proton in **611** might lead to the facile base-promoted conversion to its corresponding enol tautomer, which could then react with allyl chloroformate in the subsequent step. To our delight, treatment of **611** with allyl chloroformate under basic conditions led to the selective protection of indole nitrogen as an allyl carbamate **612**. Finally, epimerization at C10a was effected by triethylamine, leading to the thermodynamically more stable *trans*-decalin **608**. This intermediate was prepared by Fukuyama in his total synthesis of (-)-hapalindole G.<sup>130</sup>

### 3.4.17. Summary

In summary, we have accomplished the first total synthesis of hapalindoles A and K, and a formal synthesis of hapalindole G. Each case highlights the value of a key progenitor – neopentyl chloride **564** – within a convergent, stereocontrolled approach. At present, ethyl aluminum dichloride is uniquely effective in its ability to deliver the cycloadduct, perhaps reflective of this rather demanding intermolecular Diels-Alder reaction. A second new development in this overall approach was the use of a Ritter reaction to establish the C11–N bond stereoselectively. This aspect was particularly key to maintaining the brevity of each synthesis.

**Scheme 188.** Total Synthesis of Hapalindole A and K

